# INFORMATION TO USERS

This manuscript has been reproduced from the microfilm master. UMI films the text directly from the original or copy submitted. Thus, some thesis and dissertation copies are in typewriter face, while others may be from any type of computer printer.

**The quality of this reproduction is dependent upon the quality of the copy submitted.** Broken or indistinct print, colored or poor quality illustrations and photographs, print bleedthrough, substandard margins, and improper alignment can adversely affect reproduction.

In the unlikely event that the author did not send UMI a complete manuscript and there are missing pages, these will be noted. Also, if unauthorized copyright material had to be removed, a note will indicate the deletion.

Oversize materials (e.g., maps, drawings, charts) are reproduced by sectioning the original, beginning at the upper left-hand corner and continuing from left to right in equal sections with small overlaps.

Photographs included in the original manuscript have been reproduced xerographically in this copy. Higher quality 6" x 9" black and white photographic prints are available for any photographs or illustrations appearing in this copy for an additional charge. Contact UMI directly to order.

UMI®

# NOTE TO USERS

Page(s) not included in the original manuscript and are unavailable from the author or university. The manuscript was microfilmed as received.

70, 73, 75, 79, 81, 83, 84, 91, 143, 144, 149, 167, and 254 – 259

Text not included in the original manuscript and is unavailable from the author or university. The manuscript was microfilmed as received.

96 (Map Partial)

This reproduction is the best copy available.

# STRATIGRAPHY AND SEDIMENTOLOGY OF THE LOWER TRIASSIC

# MONTNEY FORMATION, PEACE RIVER ARCH AREA

BY

JIN-HYUNG LEE, B.SC., M.SC.

A Thesis

Submitted to the School of Graduate Studies

in Partial Fulfilment of the Requirements

for the Degree

Doctor of philosophy

McMaster University

1999

# STRATIGRAPHY AND SEDIMENTOLOGY OF THE LOWER TRIASSIC

# MONTNEY FORMATION, PEACE RIVER ARCH AREA

DOCTOR OF PHILOSOPHY (1999)      McMASTER UNIVERSITY
(Geology)      Hamilton, Ontario

Title: Stratigraphy and Sedimentology of the Lower Triassic Montney Formation,

     Peace River Arch area

AUTHOR: Jin-Hyung Lee, B.Sc. (Kyungpook National University, Korea); M.Sc.

     (Kyungpook National University, Korea)

SUPERVISOR: Dr. Roger G. Walker

NUMBER OF PAGES: xv, 289

# ABSTRACT

The Lower Triassic Montney Formation in the Peace River Arch area forms a sedimentary wedge up to 350 m thick, deposited on the craton margin. This study, based on 127 cores and about 1300 well logs, shows that the Montney Formation is characterized by overall southwesterly-dipping clinoform deposits with a maximum dip of about 0.3°. Based on prominent well log markers, the Montney Formation has been divided into seven depositional units lettered A through G.

Deposition of the Montney Formation was strongly influenced by tectonic activity, and two major basin reorganizations occurred: one between Unit A and Unit B and the other between Unit F and Unit G. The overall sediment source for the Montney Formation was to the northeast, but at least for Unit B and Unit C, the main source was to the southeast.

In the deeper part of the basin (southwest), the Montney Formation commonly contains turbidite deposits. Two styles of turbidite depositional systems developed: an unchannelized sheet-like system and a channel-related system. Unchannelized sheet-like turbidite systems occur in several stratigraphic units and constitutes the bulk of turbidite sedimentation, whereas the channel-related turbidite system developed only in Unit C. Here, an incised channel cuts down as much as 40 m into underlying sediment. It is relatively straight, trending southeast to northwest for a distance of 70 km. At the distal end of the channel, it turns sharply

to the southwest, following a downthrown fault block. Upslope, the width of the channel is about 1 km, but farther downslope (northwestward) it widens to 3-5 km. The turbidites are mostly thick and structureless fine-grained sandstones. Upslope the sandstones are completely confined within the incised channel, but farther downslope they spread out of the incised channel for a distance of about 10 km. Synsedimentary faulting controlled the thickness of accumulated sediment and sediment facies. Thick accumulations of sand occur in downthrown fault blocks whereas thinner and/or muddier sediments were deposited in uplifted blocks.

The turbidite systems of the Montney Formation were developed in relatively shallow environments, not deeper than a few hundred meters. The development of the Montney turbidite systems may not have been related to global sea level fluctuations, but local tectonic activity.

# ACKNOWLEDGEMENTS

# TABLE OF CONTENTS

# LIST OF FIGURES

# CHAPTER 1: INTRODUCTION

## 1.1 The Geological Problem

Cratons are characterized by uniform paleoslopes that change little through time, and cratonic platforms usually have a thin sedimentary cover, mainly carbonates and quartz arenites, and only small amounts of shale. Evidence of stability of the North American craton lies in the dominance of carbonate, paucity of clastic materials and the maturity of the sand produced. For much of its history, the Western Canada Sedimentary Basin was a broad flat platform characterized by carbonate and evaporite sedimentation. From early Cambrian to middle Jurassic time, the Western Canada Sedimentary Basin had the characteristics of a passive margin (Stott and Aitken, 1993; Edwards et al., 1994; Shannon and Naylor, 1989).

In the Western United States, deformation of the western margin of the North American Plate occurred in late Devonian to Mississippian time due to volcanic arc-continent contraction (Antler Orogeny). In late Permian to early Mesozoic time, the Western margin of the proto United States changed from passive margin conditions to an active margin setting due to its collision with volcanic island arcs (Sonoma Orogeny). However, the Western Canada Sedimentary Basin lay north of the active tectonic zone. From early Cambrian to early Jurassic time, there was no known western provenance on the cratonic margin of the Western Canada Sedimentary Basin. Although volcanic island arc-subduction complexes are preserved in British

Columbia and the Yukon Territory, they are present only in allochthonous terranes that accreted to the continent in Jurassic time.

In detail, however, some aspects of the Western Canada Sedimentary Basin are not well understood. For example, from the late Paleozoic to the Triassic, the Western Canada Sedimentary Basin records a fundamental change from carbonate-dominant facies to siliciclastic-dominant facies. Devonian and Lower Carboniferous successions in the Western Canada Sedimentary Basin are composed mainly of carbonates and evaporites. However, Upper Carboniferous and Permian successions lack the extensive carbonate development and are characterized by siliciclastics including chert and some carbonates. Early Triassic successions consist mainly of clastic materials containing well rounded quartz grains, with only small amounts of carbonate facies. However, what caused the fundamental changes in sedimentary facies is not well understood.

Furthermore, lower Triassic strata in the Western Canada Sedimentary Basin contain widespread turbidites deposited on the craton margin (Gibson and Poulton, 1994; Edwards et al., 1994; Moslow and Davies, 1996, 1997; Davies, 1997), but their origin and significance is not well understood. During the entire history of the Western Canada Sedimentary Basin, turbidite sedimentation is very uncommon. Although turbidite sedimentation was widespread during late Precambrian time, the turbidites were not deposited in a mature passive margin environment, but in a rift setting (Aitken, 1993). Another example of turbidite sedimentation in the Western Canada Sedimentary Basin occurs in the Jurassic

Passage Beds (Hamblin and Walker, 1979). However, these turbidites were derived from the Cordillera during convergent margin tectonism.

In the Western Canada Sedimentary Basin, widespread turbidite sedimentation in the passive margin phase occurs only in the Triassic. Although Triassic turbidites are widespread over a large area of the Western Canada Basin (Gibson and Poulton, 1994; Edwards et al., 1994), detailed sedimentological studies have been published only recently (Moslow and Davies, 1996, 1997). It is not well known what caused turbidite sedimentation on the cratonic margin during the Triassic. Furthermore, the source of the Triassic clastic turbidites is problematic because during the Paleozoic, much of the Canadian Shield of North America was mostly covered by carbonate and evaporites.

A detailed sedimentological analysis will provide some insight in understanding the evolution of the Western Canada Sedimentary Basin. The main purpose of this thesis is (1) to describe in detail the turbidite deposits in the Triassic Montney Formation, (2) to reconstruct Triassic basin history in the Western Canada Sedimentary Basin, (3) to relate depositional systems to tectonics.

The Montney Formation was chosen for the research because it contains relatively abundant well logs and cores of such turbidites. Another important criterion for the selection of the Montney Formation is that it is bearing hydrocarbon and is currently an important exploration target.

## 1.2 The Study Area

The study area is located in northwestern Alberta (Fig. 1-1). It covers Townships 64 to 77, Ranges 19W5M to 13W6M, an area of approximately 30,000 km². The study area is located on the southern rim of the Peace River Arch. The western limit of the study area almost coincides with the Provincial Boundary between Alberta and British Columbia. The southwestern edge of the study area is close to the eastern limit of the Cordilleran Deformation Belt and is approximately 50 km away from the closest outcrop belt. The study area covers several Triassic oil and gas fields including Valhalla, La Glace, Manir, Glacier, Hythe, Knopcik, Wembley and Sturgeon Lake.

## 1.3 Data Base and Study Methods

About 2000 geophysical well logs are currently available within the study area and about 1300 of them were used in this study (Fig. 1-2). Well log spacing varies between 500 m and 30 km. Most of wells have several kinds of logs including gamma-ray, resistivity, spontaneous potential, and porosity logs, except for some relatively old wells. About 150 wells are cored in the Montney within the study area, and 127 of these cores were logged in detail (Fig. 1-2). Cumulative core length examined is more than 2000 m. Most of the cores available are from the lower and middle part of the Montney Formation and only a few cores are available from the upper part. Cores are commonly concentrated in particular areas and commonly there is little or no core control in between. In most wells, core

T77

T74

T70

T67

T64

R19

R22

W5

R25

R1

6th MERIDIAN

R4

W6

R7

R10

R13
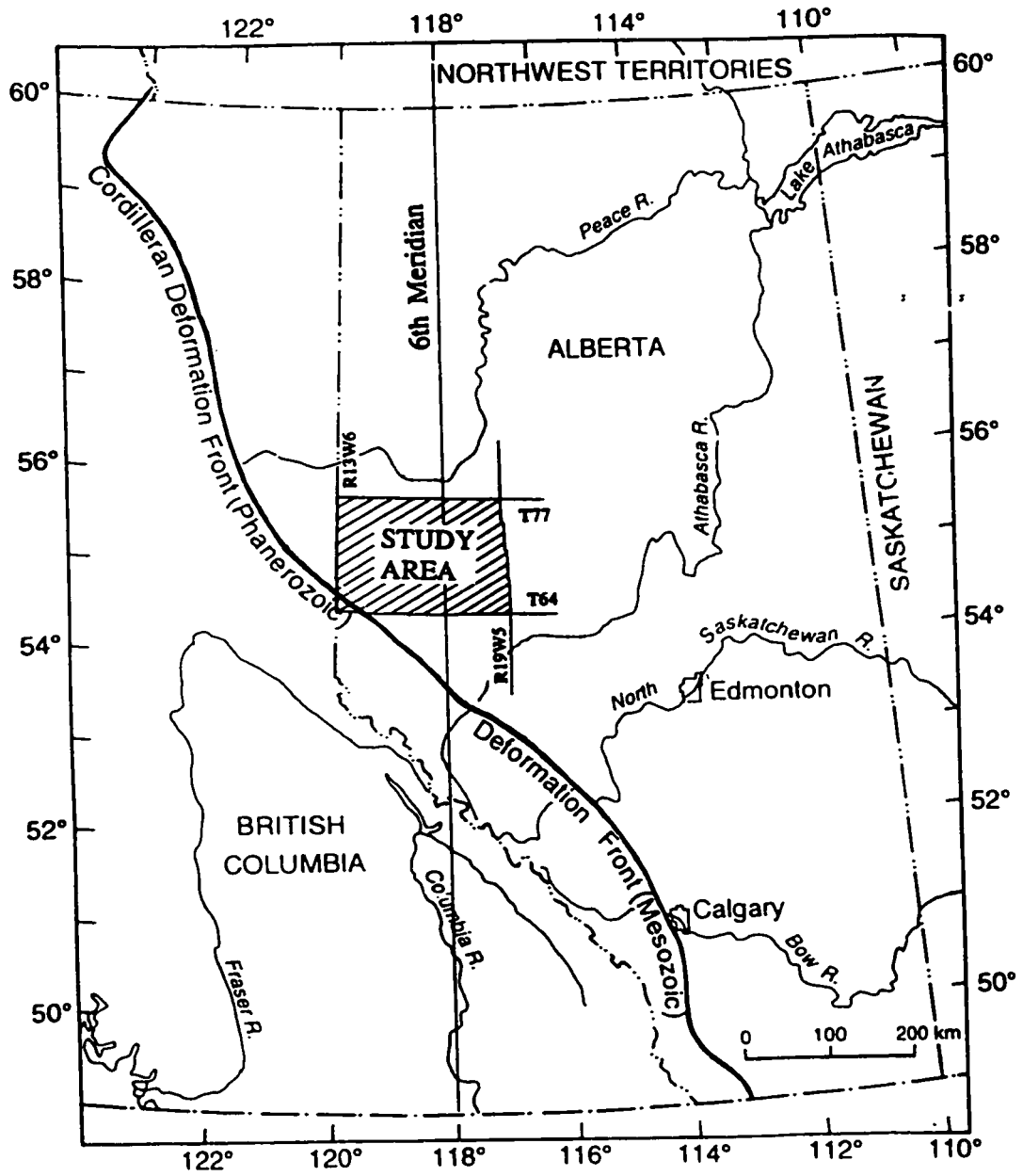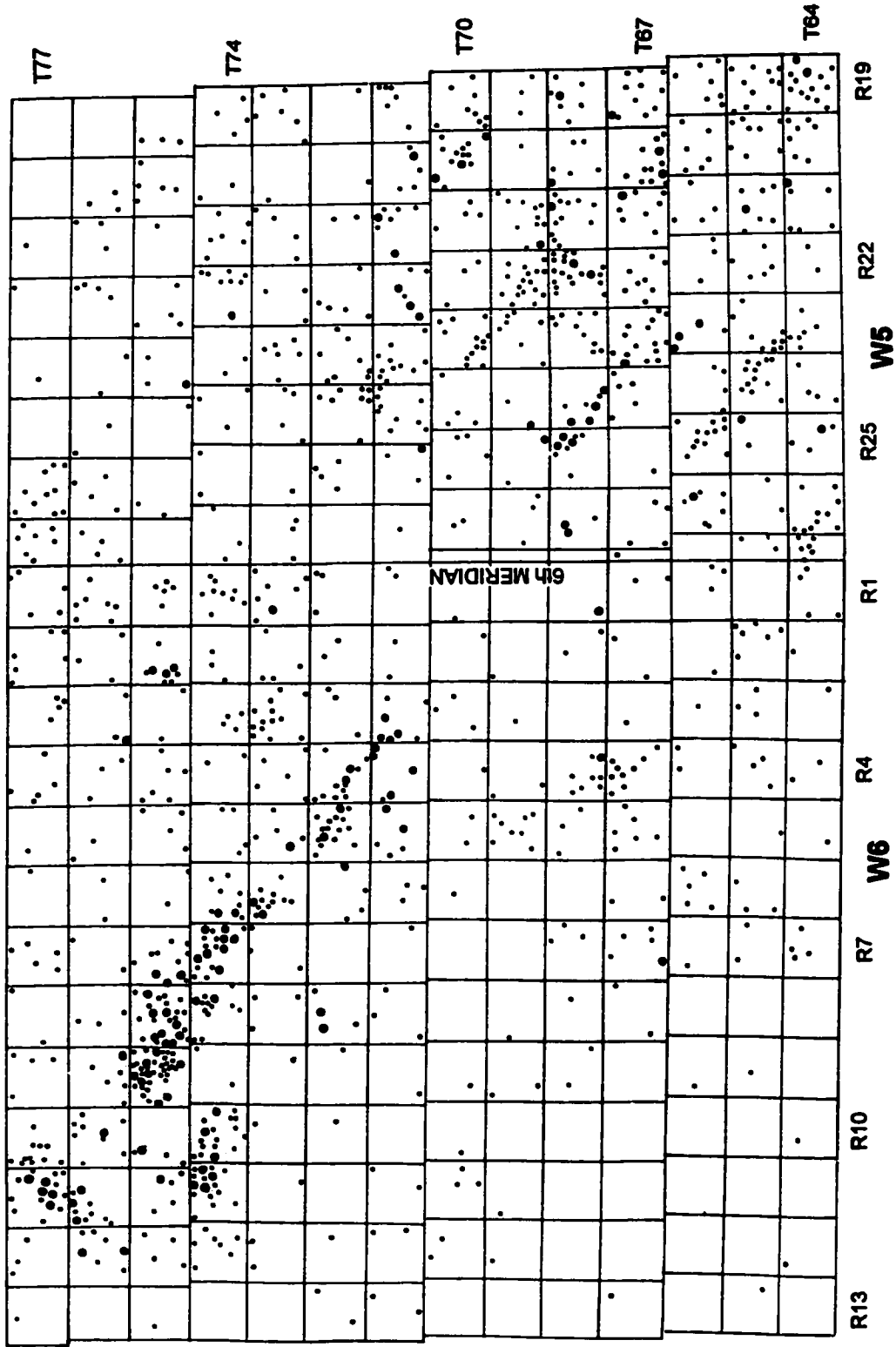
length ranges from 10 to 20 m, but some cores approach or exceed 50 m in length. In most cores, recovery is close to 100 %.

All cores were examined at the Alberta Energy and Utilities Board (AEUB) Core Research Centre in Calgary in the summers of 1994 to 1997. Each core was studied in detail and subdivided into different facies based on grain size, grain size trends, sedimentary structures and bed contacts. Cores were examined with well logs to check core recovery, log response, and to match cores with logs.

Photographs were taken of entire core boxes for most of the cores. Numerous close-up photographs of individual facies were also taken to illustrate each facies and vertical facies changes.

Before the construction of cross sections, log responses were calibrated to core control. For some intervals, the gamma-ray log in the Montney Formation is not very effective for correlation because of significant potassium feldspar content in the Montney Formation sandstones. The best log type for correlation of the Montney Formation is the induction log. However, some induction logs show unusually low values of resistivity for some massive sandstones due to salt-water saturation. This problem can be partially resolved by examining deep induction logs because whenever an unusual log deflection occurs, the deep phase of the induction curves deflects more than the shallow phase, implying that salt water saturation greatly affected log responses in induction logs (Fig. 1-3).

Other types of logs such as the spontaneous potential log and porosity logs (density porosity and neutron porosity) are not very sensitive. However, for

Density Porosity

Induction

Shallow Phase

Deep Phase

Gamma-Ray

2190

2230

SP
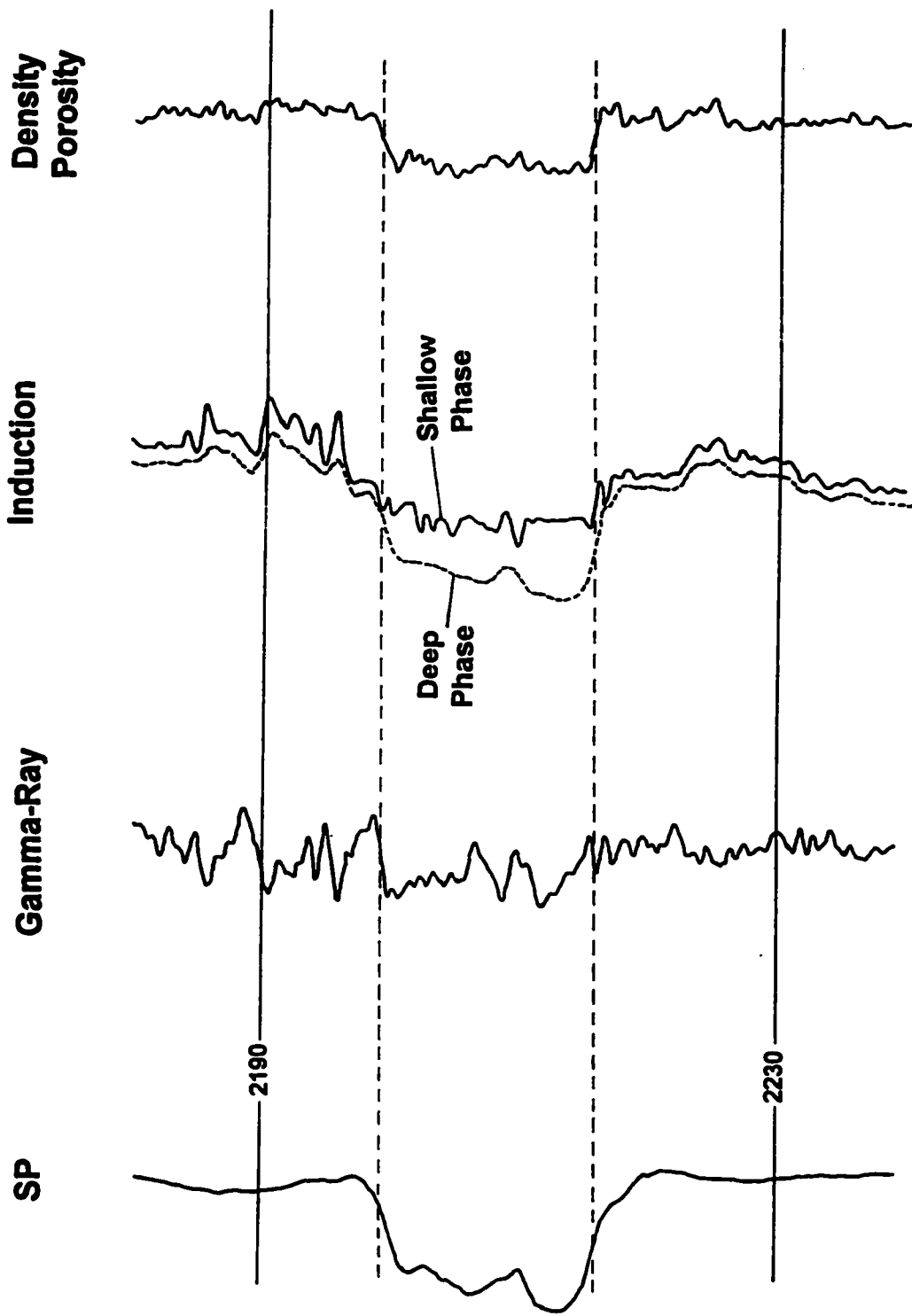
massive sandstone intervals, these logs, particularly the density logs, show a blocky response, and have a supplementary role in deciding the base and top of massive sandstone intervals. Overall, the combination of the gamma-ray and induction logs provides the best tool for correlation because over the large area, it has a sufficiently high resolution for correlation. To make correlations, all well logs were traced, and the tracings were superimposed on adjacent logs in order to correlate log markers and log trends between markers.

# CHAPTER 2: STRATIGRAPHY AND REGIONAL SETTING

## 2.1 Introduction

Early studies on the Triassic strata of the Western Canada Sedimentary Basin focused on the Rocky Mountain Foothills (McLearn, 1921, 1930, 1940, 1941, 1945, 1946, 1947; Kindle, 1944; McLearn and Kindle, 1950). These early outcrop studies were mainly paleontological and stratigraphic, and provided a basic Triassic stratigraphic framework.

Most of subsequent works on the outcrops were made by Pelletier (1960,1961, 1963, 1964, 1965), Tozer (1961, 1963, 1967) and Gibson (1968a, 1968b, 1969, 1971a, 1971b, 1972, 1974, 1975). Their works modified and refined the stratigraphy and paleontology of the Triassic strata, but did not cover sedimentological aspects of the rocks.

The gas and oil discoveries in the Peace River Region sparked subsurface studies. Hunt and Ratcliffe (1959) first published a paper on subsurface Triassic rocks in the Fort St. John and adjacent areas. Armitage (1962) suggested new stratigraphic divisions of the subsurface Triassic strata.

The first synthesis of surface and surface information for the Triassic strata in the Western Canada Sedimentary Basin was published by Barss et al. (1964). More recent syntheses of Triassic strata in the Western Canada Sedimentary Basin have been published by Gibson and Edwards (1990a, 1990b), Gibson and Barclay

(1989) and Edwards et al. (1994). Recently, Davies (1997) published a paper about Triassic tectonic and stratigraphic framework, paleogeography and paleoclimate in the Western Canada Sedimentary Basin.

The first sedimentological study on the early Triassic Montney Formation was done by Miall (1976). More detailed sedimentological studies on the Montney Formation have only recently been published (Moslow and Davies, 1996, 1997; Davies et al., 1997; Davies and Sherwin, 1997).

## 2.2 Stratigraphy

### 2.2.1 Introduction

The Triassic stratigraphic framework of the Western Canada Sedimentary Basin has been established by outcrop mapping and subsurface work over several decades. Most of present knowledge of the Triassic in outcrop is from Gibson's work (1968a, 1868b, 1971a, 1971b, 1972, 1974, 1975). Edwards et al. (1994) have published the most recent synthesis of the Triassic of the Western Canada Sedimentary Basin.

Three main nomenclatural systems have been used for Triassic strata in the Western Canada Sedimentary Basin (Fig. 2-1). Stratigraphic subdivision in subsurface is based mainly on geophysical well logs, and for many stratigraphic intervals they have different terminology. Even in the outcrop belt of British Columbia and Alberta, two stratigraphic nomenclatures have been used, one between the United States Border and the Pine-Sukunka River area of northeastern

| PERIOD/ EPOCH /AGE | | | OUTCROP Liard-Pine River Area, British Columbia | SUBSURFACE British Columbia- West-Central Alberta | OUTCROP Banff, Jasper and Cadomin Areas, Alberta |
|---|---|---|---|---|---|
| JURASSIC | | | FERNIE FM | FERNIE FM | FERNIE FM |
| TRIASSIC | Late | NORIAN | BOCOCK FM | | |
| | | | PARDONET FM | PARDONET FM | |
| | | CARNIAN | BALDONNEL FM / Ducette Mbr | BALDONNEL FM | Winnifred / BREWSTER LIMESTONE MBR  Mbr |
| | | | CHARLIE LAKE FM | CHARLIE LAKE FM | Starlight Evaporite Member |
| | | | | HALFWAY FM | |
| | Middle | LADINIAN | LIARD FM | | Llama Member |
| | | ANISIAN | TOAD FM | DOIG FM | |
| | | | | | Whistler Mbr |
| | Early | SPATHIAN | | | Vega Siltstone Member |
| | | SMITHIAN | | MONTNEY FM | |
| | | DIENERIAN | GRAYLING FM | | Phroso Siltstone Member |
| | | GRIESBACHIAN | | | |
| PERMIAN | | | | ISHBEL GROUP | |

(Ludington Fm — Schooler Creek Gp / Daiber Group — Spray River Group / Whitehorse Fm, Sulphur Mountain Fm)

British Columbia, and the other in the remaining outcrop belt to the north (Fig. 2-1).

Rapid changes in lithology and thickness and the scarcity of fossils make detailed correlation difficult. Caution is required, especially in correlation between outcrop and subsurface because biostratigraphic dating is based mainly on outcrop sections and almost no datable fossils have been found in the subsurface. In this chapter, the present knowledge of the Triassic stratigraphy and related problems will be outlined. Detailed descriptions will be focused mainly on the Montney equivalent interval.

## 2.2.2 Foothills and Front Ranges

Triassic rocks of the southern Rocky Mountain Foothills and Front Ranges are assigned to the Spray River Group. This has been divided into two distinct and contrasting units, the Sulphur Mountain Formation and the overlying Whitehorse Formation (Fig. 2-1). Each formation is further subdivided into several members. The Spray River Group commonly disconformably overlies the Permian Ishbel Group but in parts of the eastern Foothills it rests disconformably on the Mississippian Rundle Group. The Spray River Group is disconformably overlain by the Jurassic Fernie Formation (Gibson, 1968a, 1968b, 1969, 1974).

In most areas, the Sulphur Mountain Formation is subdivided into four members, the Phroso Siltstone, Vega Siltstone, Whistler and Llama Members (Fig. 2-1). The Phroso Siltstone Member consists of recessive, shaly to flaggy weathering, grey to dark grey siltstone and shale and less commonly very fine

grained sandstone. The thickness of the Phroso Siltstone Member ranges from 60 to 240 m. The Phroso Siltstone Member contains few fossils but the occurrence of the index fossil *Claraia stachei* indicates an Early Triassic, Griesbachian age (Tozer, 1967, 1984). The overlying Vega Siltstone Member consists of greyish to rusty brown weathering calcareous siltstone, silty limestone and shale. The Vega Siltstone Member reaches a maximum thickness of 360 m. In some areas, it contains a distinctive dolomitic lithofacies, named the Mackenzie Dolomite Lentil. This lentil consists of yellowish grey, silty to sandy dolostone and dolomitized coquina, and ranges from a depositional pinch-out to a maximum of 50 m in thickness. The Vega Siltstone member is abruptly overlain by either the Whistler Member or the Llama Member. Although fossils are rare, the ammonite *Euflemingites cf. cirratus* suggests that the Vega Siltstone Member is early Triassic (Smithian) in age.

In the Pine Pass - Smoky River area, subdivision of the Phroso-Vega Siltstone Members is impractical because no well-defined contact exists between the two facies and they interfinger over a few hundred meters (Gibson, 1972, 1975). The Phroso-Vega Siltstone Member contains ammonites indicating ages from Griesbachian to Spathian.

The Whistler Member (0-85 m thick) consists of dark grey to black weathering, calcareous silty dolostone, dolomitic siltstone, silty and fossiliferous limestone, silty shale, and locally phosphatic sandstones, quartz sandstone and phosphatic pebble conglomerate. A widely occurring basal phosphatic pebble

conglomerate and abrupt lithological change from the underlying strata may suggest a minor unconformity or diastem (Gibson, 1972, 1975). The occurrence of the fossil *Beyrichtes gymnotoceras* indicates a middle Triassic (Anisian) age (Tozer, 1967, 1984).

The Llama Member comprises cliff-forming, thin to thick bedded, dolomitic siltstone, silty to sandy dolostone, silty and bioclastic limestone. It ranges in thickness from 3 to a maximum of 365 m.

The Whitehorse Formation is typically divisible into three members, the Starlight Evaporite Member, the Brewster Limestone Member and the Winnifred Member. It reaches a maximum thickness of 500 m (Gibson, 1972, 1975).

In the northern Rocky Mountain Foothills and Front Ranges, the Triassic succession differs from that to the south and is divided into eight formations, the Grayling, Toad, Liard, Charlie Lake, Ludington, Baldonnel, Pardonet and Bocock Formations (Gibson, 1971a, 1975).

The Grayling Formation comprises shaly to dolomitic siltstone, silty shale, and lesser calcareous siltstone, silty limestone, dolostone and very fine-grained sandstone. Its thickness ranges from 35 to 395 m. The unit disconformably overlies the Permian Fantasque Formation. The Grayling Formation is early Triassic in age and correlates with the Phroso Siltstone Member of the Sulphur Mountain Formation in the south. The upper contact with the Toad Formation is gradational, and is defined mainly by a change in carbonate composition. The contact is placed where the cement of the Grayling siltstone changes upward from

a dominance of dolomite to a dominance of calcite (Gibson, 1971a, 1975). The Grayling Formation is generally more thinly bedded and more recessively weathered than the Toad Formation.

The Toad Formation consists of dark grey, thin to medium bedded, shaly to flaggy weathering very calcareous siltstone, silty shale and minor amounts of silty dolostone and calcareous sandstone. The formation is fossiliferous and contains well preserved ammonites ranging from early Triassic (Smithian) to middle Triassic (Ladinian) in age (Tozer,1967,1984). It reaches a maximum thickness of 825 m. The upper contact with the Liard Formation is gradational or sharp.

The Liard Formation consists of resistant, commonly cliff-forming dolomitic to calcareous, fine to coarse sandstone, calcareous and dolomite siltstone, and lesser amounts of silty to sandy dolostone. The thickness of the Liard Formation ranges from an erosional and non depositional edge to a maximum of 420 m. The fossils from the Liard Formation indicate late middle to early late Triassic ages (Tozer, 1967, 1984).

## 2.2.3 Subsurface, Western Interior Plains

The Triassic succession in the Western Interior Plains forms part of the same regional stratigraphic package as described above for exposures in the Foothills and Front Ranges. However, the lower part of the succession has a different nomenclature (Fig. 2-1). The Triassic succession in the Western Interior Plains is divided into two groups, the lower Daiber Group and upper Schooler Creek Group.

The succession reaches a maximum thickness of 1000 m and is divided into six formations, the Montney, Doig, Halfway, Charlie Lake, Baldonnel and Pardonet Formations. The succession unconformably overlies the Permian Belloy Formation and is unconformably overlain by the Jurassic Fernie Formation (Gibson and Barclay, 1989; Edwards et al., 1994).

The Daiber Group is divided into two formations, the Montney Formation (below) and the Doig Formation (above) based on an abrupt increase in gamma-ray values in the basal part of the Doig Formation (Armitage, 1962; Fig. 2-2A). The abrupt gamma-ray deflection to very high API values (commonly much greater than 150 API, and maximum value of 450 - 500 API) indicates phosphatic shales in the basal part of the Doig Formation and the contact between the Montney and Doig formations is easily recognized over a large area in British Columbia and Alberta. However, in oil industries, a different stratigraphic horizon (ES3 in Fig. 2-2) has been used as the boundary between the Montney and Doig (i.e., Alberta Energy, 1999). Althouth both definitions for the top of the Montney are accetable, the definition of Armitage (1962; Fig. 2-2) was used in this study because the Armitage's definition has been used in most publications (i.e., Edwards et al., 1994; Embry, 1997; Gibson and Barclay, 1989; Gibson and Edwards, 1990a, 1990b; Gibson, 1975; Barss, 1964).

Figure 2-3 shows the distribution of the Montney Formation in the subsurface. Although its original distribution was more widespread to the east and northeast, sub-Jurassic and intra-Triassic unconformities truncate progressively

**B**

6-9-85-19W6

Sonic

Density

← ES3

Gamma-ray

Dolg Fm

Montney Fm

Permian

metres

1600

1700

1800

1900

SP

**A**

Texaco N.F.A. Buick Creek #7
6-26-87-21W6

Density

← ES3

Gamma-ray

feet

5500

5600

5700

5800

5900

6000

6100

6200

6300

6400

6500

Dolg Fm

Montney Fm

Permian
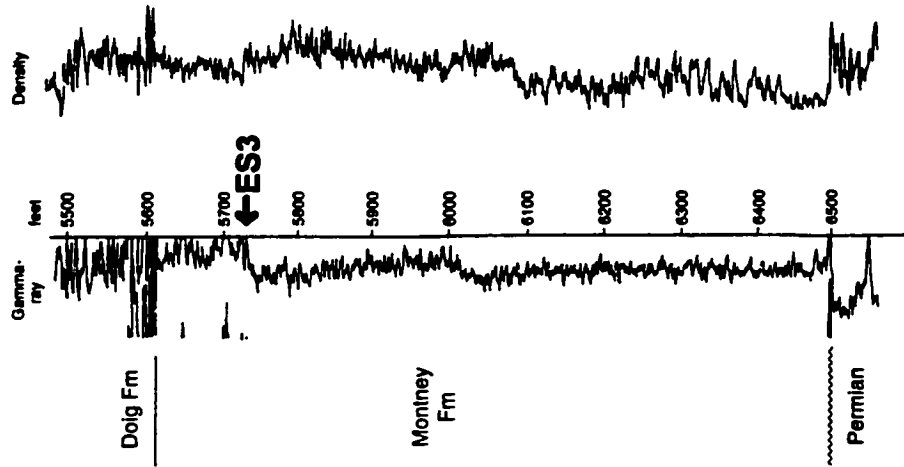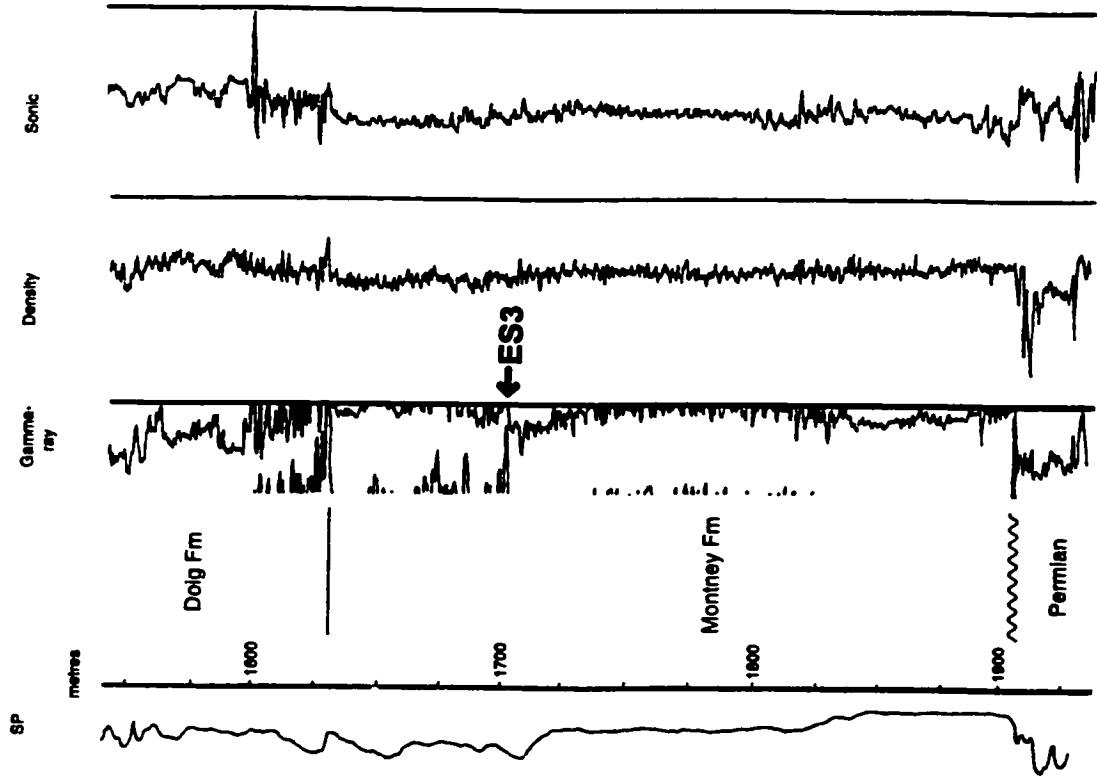
older strata of the Montney to the east and northeast. The subcrop edge of the Montney in the subsurface has an arcuate trend from about Township 113 to Township 48, and the preserved Montney has an elongate distribution in length 700 km long with a maximum width of about 250 km. The prominent thinning trend to the east and northeast in Figure 2-3 was the result of progressively deeper erosion of the Montney in that direction. The subcrop boundary of the depositional top of the Montney is approximately coincide with the "eastern" 200 m isopach in the map.

It should be noted that the isopachs in Figure 2-3, particularly in the deeper part of the basin (Township 74 to Township 84, Range 14M6 to the deformed belt), are largely misleading. Detailed information presented in this thesis suggests that the isopachs in the map do not represent the real thickness values of the entire Montney succession. The uppermost depositional unit G (of this thesis) of the Montney was not included in the isopach values in Figure 2-3. Unit G is relatively thin (less than 20 m) in the northeast (most parts of Alberta and the northern part of British Columbia). However, it thickens to the southwest, and is commonly greater than 130 m in the deeper part of the basin (see Figure 5-14). Thus, the Montney in the deeper part of the basin is much thicker than the isopach values depicted in Figure 2-3, and is commonly thicker than 300 m (see Figure 5-17). Thus, the overall southwestward thinning trend (depicted in Figure 2-3) of the Montney toward the deformed belt does not occur.

The Montney Formation consists of dark grey calcareous and dolomitic siltstone and shale and less commonly very fine grained sandstone. Along the
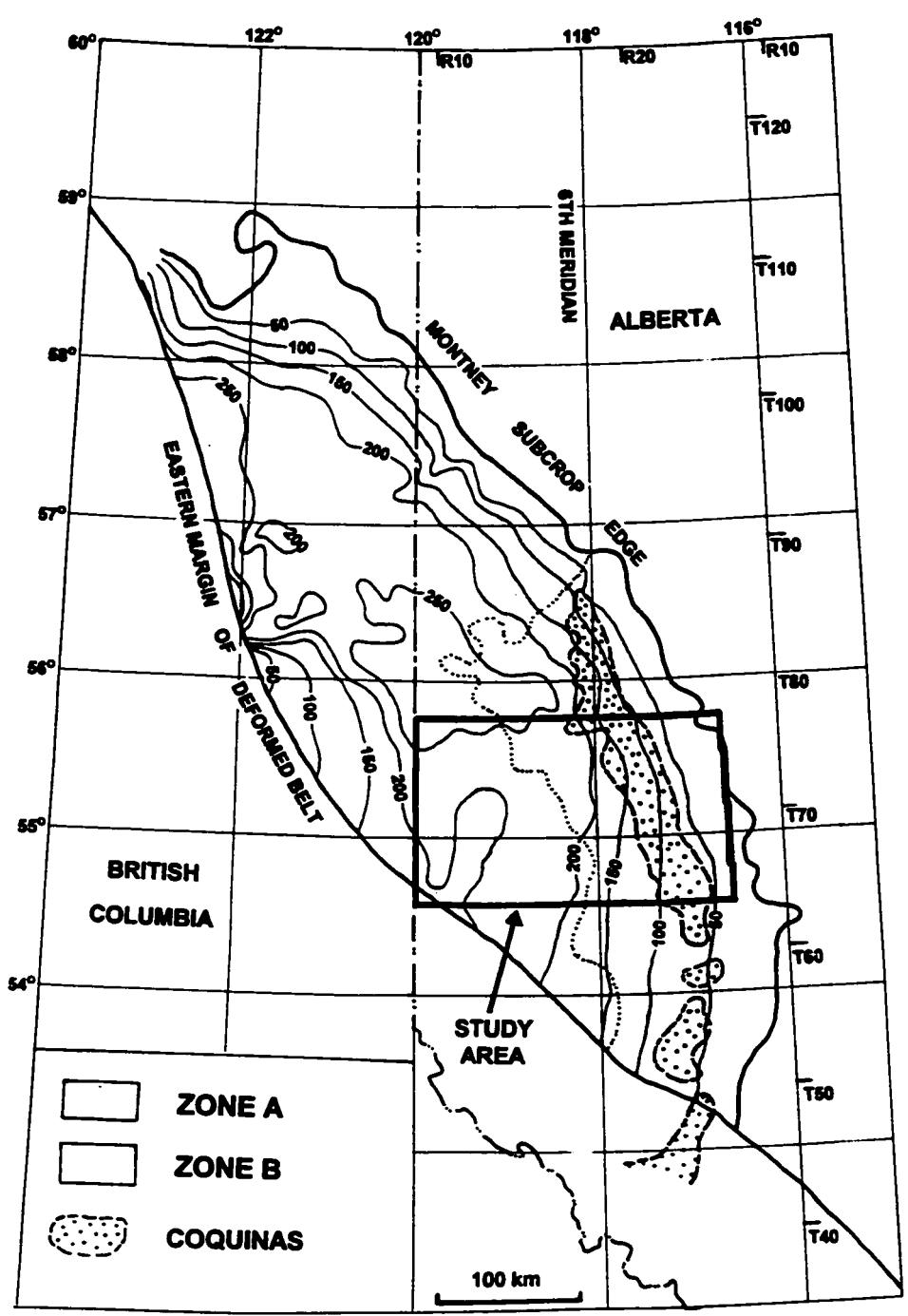
eastern depositional margin, however, the Montney Formation is characterized by additional sandstone and dolomitized coquina sandstone (Fig. 2-3)(Miall, 1976; Davies et al., 1997). The volume percentage of sandstone in the east is about 30 %, whereas it is about 10 % in the west, suggesting an eastern source of the Montney. Near the eastern margin, dolomitized coquinas also occur at several stratigraphic positions, and the most extensive is outlined in Figure 2-3. The overall distribution of the dolomitized coquina parallel to the subcrop boundary suggests that the subcrop boundary approximately reflects the original depositional trend (Davies et al., 1997).

Recently, Davies et al. (1997) have divided the Montney Formation into three members: the Lower Member, the Coquinal Dolomite Middle Member, and the Upper Member. The Lower and Upper Members have been further divided into a number of smaller scale units (Figs. 2-4, 2-5). Based on palynological analysis, they dated the Lower Member as Griesbachian-Dienerian, the Coquinal Dolomite Middle Member as mixed Dienerian and Smithian, and the Upper Member as Smithian-Spathian.

The Montney Formation is overlain by phosphatic shale of the basal part of the Doig Formation. The Doig Formation consists of dark grey siltstone and dark shale with thin to thick intervals of very fine grained sandstone and dolomitized coquinas along the eastern margin of deposition. In some areas, the upper Doig contains large, isolated sandstone units from 30 to 55 m in thickness. The maximum thickness of the Doig Formation is 790 m, thinning to an eastern

| PERIOD / EPOCH / AGE | FOOTHILLS / FRONT RANGES | | PLAINS | PLAINS |
| | SIKANNI CHIEF-PINE RIVERS (GIBSON, 1974, 1975) | SUKUNKA-BOW RIVERS (GIBSON, 1974, 1975) | PEACE RIVER SUBSURFACE (GIBSON & BARCLAY, 1989) | PEACE RIVER SUBSURFACE, AB,BC (THIS PAPER) |
|---|---|---|---|---|
| TRIASSIC — MIDDLE — ANISIAN | TOAD FM. | Whistler Mbr. | DOIG FM. | DOIG FM. |
| TRIASSIC — EARLY — SPATHIAN | | Vega Slt. Mbr. / Phroso Slt. Mbr. | | (GORDONDALE SST) D3 D4 MONTNEY UPPER MEM. |
| TRIASSIC — EARLY — SMITHIAN | * MACKENZIE DOLOMITE LENTIL | Vega-Phroso Slt. Mbr. | MONTNEY FM. | D2 D1 MONTNEY LOWER MEM. C B A |
| TRIASSIC — EARLY — DIENERIAN | GRAYLING FM. | | | |
| TRIASSIC — EARLY — GRIESBACHIAN | | | | |
| PERM — LATE — TATARIAN | ISHBEL GROUP | | | * COQUINAL DOLOMITE MIDDLE MEMBER |

SULPHUR MOUNTAIN FM. · SPRAY RIVER GROUP · DIABER GROUP
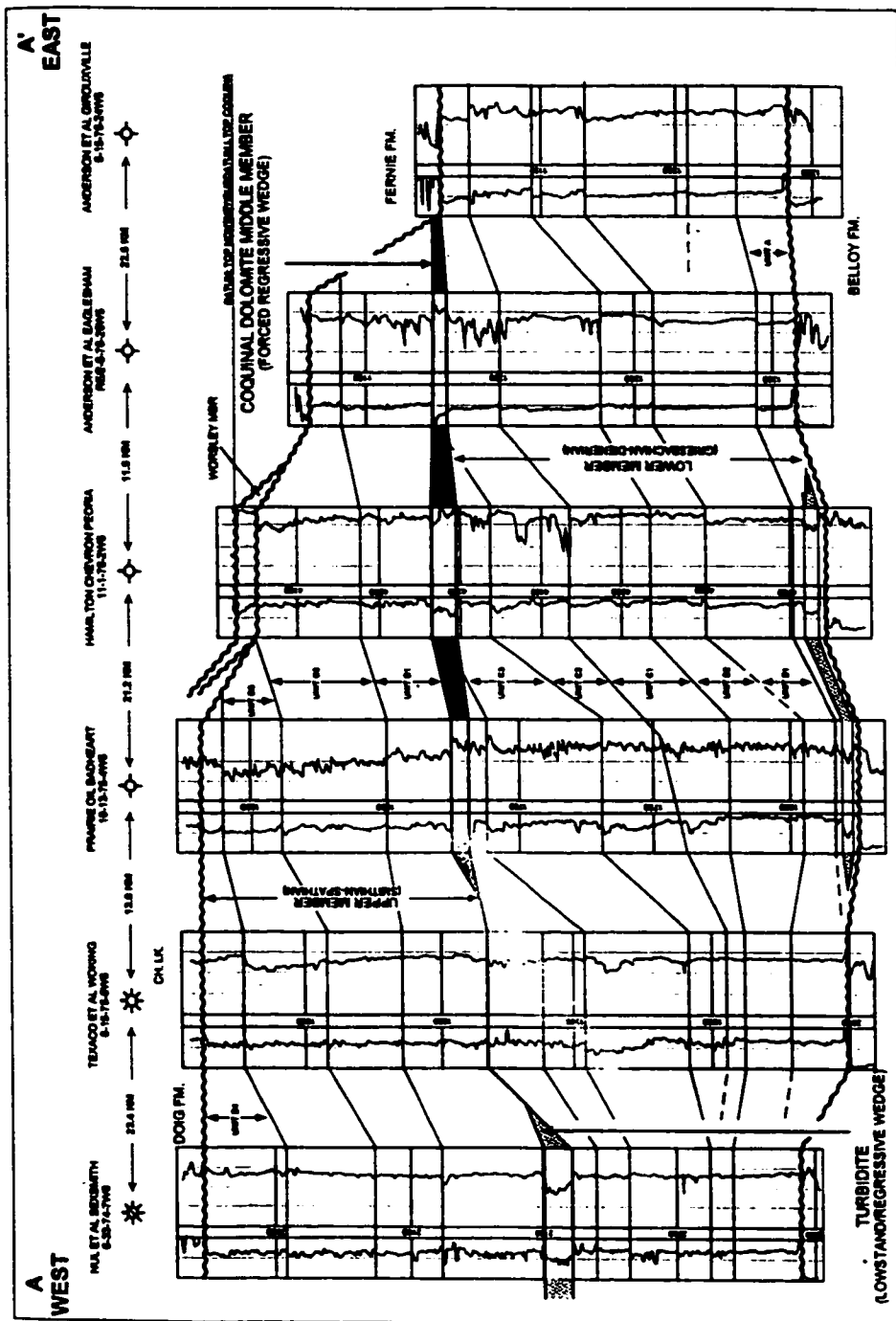
erosional pinch-out. The Doig Formation is overlain by the Halfway Formation. The contact with the overlying Halfway Formation is gradational or unconformable.

## 2.2.4 Correlation

The various stratigraphic terminologies for Triassic strata in the Western Canada Sedimentary Bain are shown in Figures 2-1 and 2-4. The correlations have been based mainly on lithologic similarities, and to a lesser degree on fossil content. However, in detail, exact correlation is very difficult because of rapid changes in lithology and thickness, and the scarcity of fossils. In some areas, differentiation of the Phroso and Vega Siltstones is almost impossible because of lateral facies changes. The same problem occurs with respect to the Grayling and Toad Formations. The rapid facies change is exemplified in the diachronous Toad - Liard boundary. In the eastern outcrop belts, the Toad - Liard boundary is between the Anisian and Ladinian stages, but in the western outcrop belts, the boundary is as young as late Ladinian.

The biggest problem occurs in correlation between the outcrop belt and subsurface because almost no datable fossils have been found in the subsurface. Gibson (1975) correlated the phosphatic pebbles at the base of the Whistler Member with the phosphatic shale interval at the base of the Doig Formation. However, phosphatic intervals occur at several horizons between the upper part of the Montney Formation and the lower part of the Halfway Formation (see gamma-ray log in Fig. 2-2). Thus the correlation between the outcrop belt and subsurface

still remains speculative. An anomalous thickness near the outcrop belt in an isopach map of the Montney Formation (see Fig. 2-3) was caused by mispicking the top of the Montney Formation. In that isopach map, the minimum thickness value is approximately 50 m to 100 m, whereas the real thickness values commonly exceed 300 m. Correlations developed in this study suggest that the phosphatic pebble interval at the base of the Whistler Member should be correlated not with the basal phosphatic shale interval of the Doig Formation but with a phosphatic shale interval within the Montney Formation. A detailed explanation of the new correlations will be discussed in a later chapter.

## 2.3 Tectonic Setting

### 2.3.1 General Setting

Two main tectonic stages in the development of the Western Canada Sedimentary Basin can be recognized by striking changes in provenance of the clastic sediment preserved within the supracrustal wedges (Bally et al., 1966; Price and Mountjoy, 1970). The first tectonic unit comprises a miogeoclinal platform stage (late Proterozoic to middle Jurassic), and the second comprises a foreland basin stage (late Jurassic to early Eocene).

In the late Precambrian, the western margin of North America underwent rifting and a passive continental margin was formed (Stewart, 1972; Monger and Price, 1979). With continental separation, a thick continental terrace wedge began to accumulate on the margin. The main source of the sediment was from the

present North America Craton. It is generally believed that the continental margin was roughly parallel to the Cordilleran Belt, but the exact shape is poorly known because of later tectonism. From the stratigraphic record of the Western Canada Sedimentary Basin, it would appear that a passive margin style of sedimentation continued for 400 Ma from the late Cambrian to the middle Jurassic.

A major problem is the extraordinarily prolonged passive margin phase of sedimentation as compared with the currently prevailing Atlantic Margin Model. Monger and Price (1979) have proposed that for at least part of this 400 Ma, the continental margin was actually a back arc basin. In the United States, in late Devonian to Mississippian time, deformation (Antler Orogeny) of the western margin of the North America Plate occurred as a result of volcanic arc-continent contraction (Fig. 2-6). The arc-continent contraction was due to the collision of the southern to southeastern margin of the North American Plate with Gondwanaland, pushing the North American Plate westward to northwestward into subducting volcanic island arcs (Davies, 1997). To the south in the United States, a foreland basin formed during the Antler Orogeny at the end of the Devonian (Burchfiel and Davis, 1975). Richards (1989) has proposed that the late Devonian and Carboniferous Prophet Trough in the Western Canada was a northern extension of the Antler Foreland Basin in United States. The Prophet Trough extended from southeastern British Columbia to the Yukon Fold Belt. However, the Antler Orogeny did not markedly affect the continental margin in Canada because no major amount of sediment was transported eastward from the orogenic belt.

## 2.3.2 Triassic Setting

In Triassic time, the Western Canada Sedimentary basin was located on the northwestern margin of the Pangea supercontinent (Fig. 2-6). During the Triassic, the northwestern continental margin was relatively stable and no major tectonic events have been recognized in Canada. However, in late Permian to early Mesozoic time, the western margin of the United States part of the supercontinent collided with a volcanic arc system (Sonoma Orogeny). Although the Western Canada Sedimentary Basin in Triassic time was relatively tectonically quiescent, some large scale tectonic events (for example, the episodic reactivation of the Dawson Creek Graben Complex and associated faults, the origin of the Coplin Unconformity, Sukunka Uplift, and other elements) might be linked to the southern tectonic event (Davies, 1997).

During the Triassic, the offshore area west of the craton margin consisted of volcanic island arcs, archipelagos, shoals and carbonate banks with intervening deep water basins and troughs. These rocks now constitute the exotic terranes of the central and western Cordillera (Tozer,1982). Evidence of western volcanic land masses immediately offshore from the craton margin is lacking, and it seems that the volcanic land masses were separated from the craton margin by a marine embayment or open ocean. Tozer (1982) has suggested that the Triassic sedimentary and volcanic rocks in exotic terranes accumulated in volcanic archipelagos as much as 5,000 km away from the Triassic continental shelf of western Canada, indicating that the continental margin faced an open ocean.
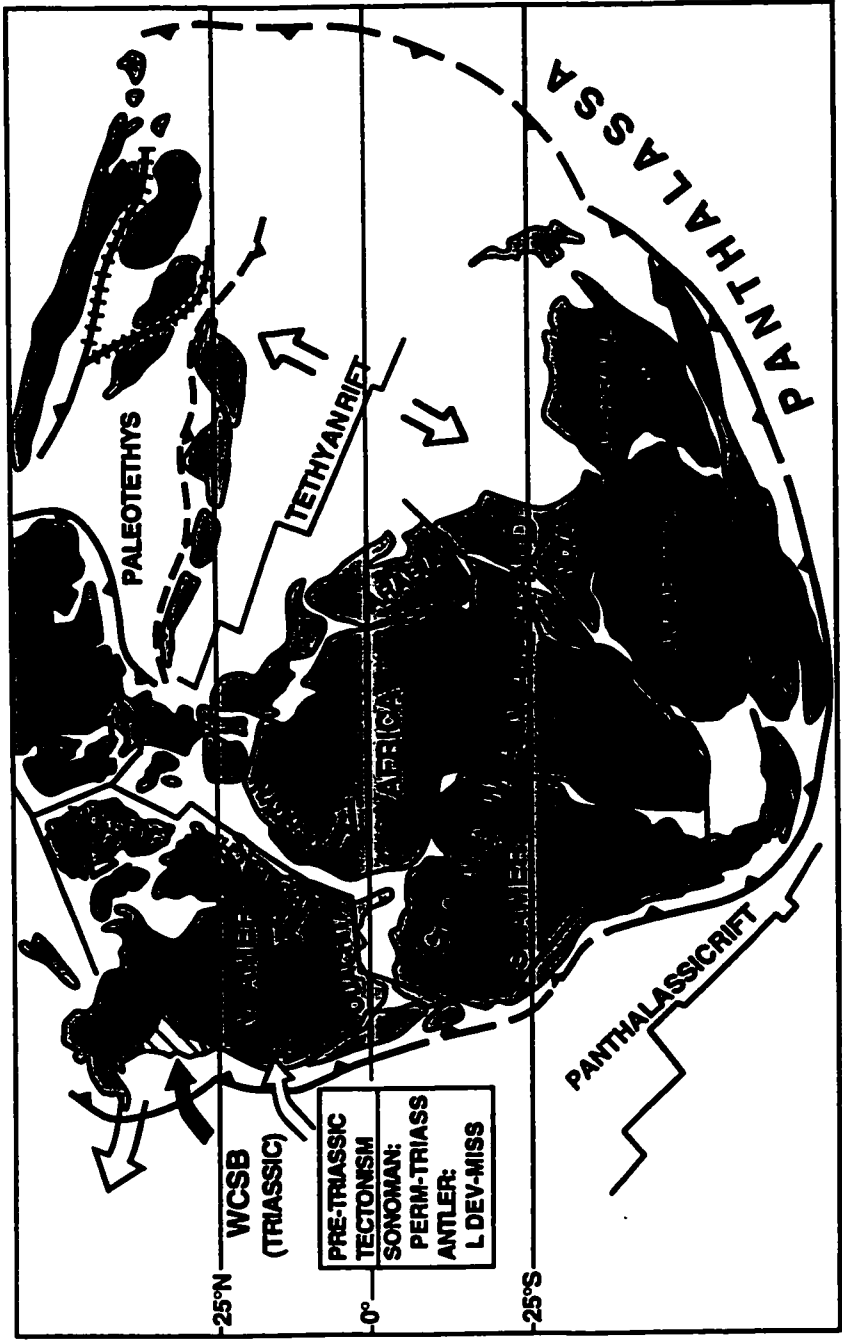
The onset of convergent tectonism in middle to late Jurassic time changed the tectonic setting of the Western Canada Sedimentary Basin. Accretion of allochthonous terraces resulted in thrust faulting, tectonic shortening and lithospheric loading, with the formation of a foreland basin (Monger and Price, 1979; Price, 1981; Beaumont,1981).

## 2.4 Peace River Arch and Dawson Creek Graben Complex

The Peace River Arch, located in northwestern Alberta and northeastern British Columbia, is a large cratonic uplift. It is an elongate structure trending in an east-northeast to west-southwest direction and its total preserved length is approximately 750 km. The structural fabric of the basement rocks of the Peace River Arch has two dominent orientations, northwest-southeast and northeast-southwest (Fig. 2-7). The arch is a complex structure consisting of an upper Proterozoic to Devonian Arch and lower Carboniferous Graben Complex (Fig. 2-8). Near the Alberta/British Columbia boundary, the granitic basement of the arch area stands approximately 1000 m above its regional elevation (Cant, 1988). The arch is perpendicular to the passive continental margin of the Noth American Plate and the arch configuration is asymmetrical, with greater subsidence to the north of the structure compared with the south.

The first positive tectonic feature of the Peace River Arch appears in the latest Proterozoic, as suggested by outcrops in the Rocky Mountains. Facies changes and thinning trends of the upper Proterozoic Windermere Supergroup

## Peace River Arch

| Stratigraphy | History (Cant, 1988) |
|---|---|

MYBP

| | | | |
|---|---|---|---|
| | | Peace River Fm. | 97 |
| Cretaceous | | | |
| | Mannville Gp. | Upper | |
| | | Lower | |
| | | Nikanassin Fm. | |
| Jurassic | | Fernie Gp. | 208 |
| | | Baldonnel Fm. | |
| | | Charlie Lake Fm. | |
| Triassic | | Halfway Fm. | |
| | | Doig Fm. | |
| | | Montney Fm. | |
| Permian | | Belloy Fm. | |
| | | | 320 |
| | Stoddart Gp. | T. Flat Fm. | |
| | | Kiskatinaw Fm. | |
| Carboniferous | | Golata Fm. | |
| | Rundle Gp. | Debolt Fm. | |
| | | Shunda Fm. | |
| | | Pekisko Fm. | |
| | Banff Fm. | | 360 |
| | Wabamun Gp. | | |
| | Winterburn Gp. | | |
| Devonian | Woodbend Gp. | Ireton Fm. | |
| | | Leduc Fm. | |
| | Beaverhill Lake Gp. | | |
| | Elk Point Gp. | | 395 |
| Cambrian | (Mid Cambrian) | | |
| Precambrian | | | |

Deep basin

**Downwarp**

Upper
Paleozoic
Embayment

**Collapse**

Lower
Paleozoic
Arch

**Uplift**

indicate that the arch had a positive expression in the latest Proterozoic (McMechan, 1990). A more evident indication of relative uplift of the Peace River Arch is indicated in the lower and middle Cambrian, with relatively abrupt thickness and facies changes along the southern boundary of the arch (McMechan, 1990). There is no information concerning the Peace River Arch from Ordovician to Silurian time because strata of these ages in the Peace River Arch area and most of the surrounding areas were eroded or never deposited before the Devonian (Cant, 1988; O'Connell, 1994).

The isopach map of the Granite Wash (which underlies the middle Devonian and has not been dated) shows that the arch consisted of a number of east-west trending horsts and grabens. Cant (1988) interpreted these horsts and grabens as extensional responses to the uplift of the arch. The middle and upper Devonian strata in the vicinity of the Peace River Arch onlapped and almost completely buried the arch. Major uplift of the arch did not occur and the arch was in a passive stage after the middle Devonian (O'Connell et al., 1990).

During the early Carboniferous, the Peace River Arch was completely buried and a broad depression known as the Peace River Embayment was established. During deposition of the Banff Formation and the lower part of the Rundle Group, the maximum subsidence occurred north of the crest of the previous arch. The upper part of Rundle Group and the Stoddart Group show maximum thicknesses over the central axis of the previous arch, centred on the Dawson Creek Graben Complex (O'Connel et al., 1990). An anomalously thick Carboniferous and Permian

succession is preserved within the Dawson Creek Graben Complex (Fig. 2-9). The thickness trends of the Taylor Flat Formation indicate reduced subsidence of the graben complex, with continued differential subsidence of smaller graben and horst blocks. The lower Permian Belloy Formation shows subtle thickening over the graben complex and records the end of significant differential subsidence (Barclay et al., 1990).

During the Mesozoic, no major movements were observed, but some readjustment of minor structures did occur. Episodic movement of horst and graben fault blocks subtly influenced local sedimentation and thickness trends, such that Triassic sediments shows their thickest development in the Peace River Arch area (Gibson and Edwards, 1990b). Triassic sediments in the Wembley area show common synsedimentary deformation representing small amounts of movement on basement structures (Cant, 1986). Davies (1997) has proposed that lobate isopach thicks in the Montney Formation, facies changes in the upper Triassic Baldonnel and Pardonet Formations, and localization of turbidite facies in the Montney Formation were controlled or influenced by reactivated fault structures of the Dawson Creek Graben Complex. Some thickness anomalies and localization of facies of the Jurassic and Cretaceous succession are related to the renewed subsidence of the Dawson Creek Graben Complex (Poulton et al., 1990; Gibson, 1992; Leckie, 1986; Hart and Plint,1990; Donaldson et al., 1998).

Although various theories for the origin of the Peace River Arch have been proposed, no one theory satisfies all the major aspects of the arch development.

**A**



**B**
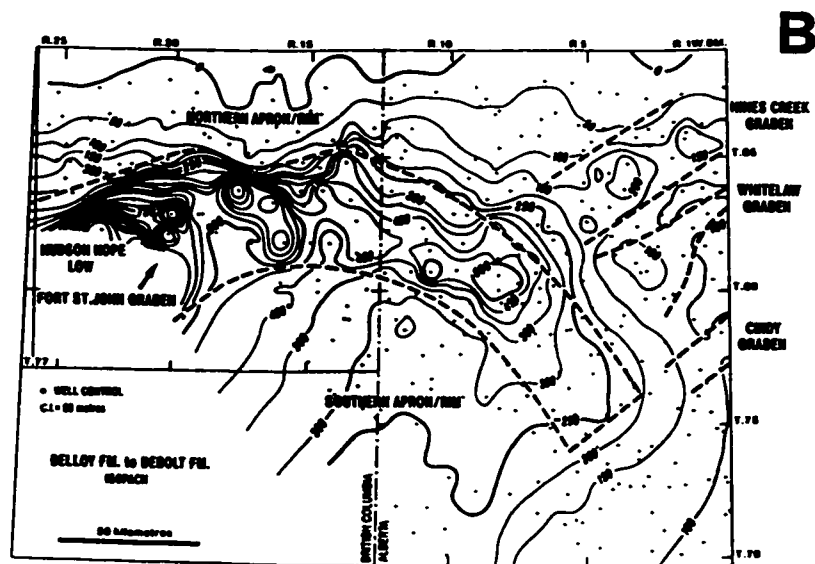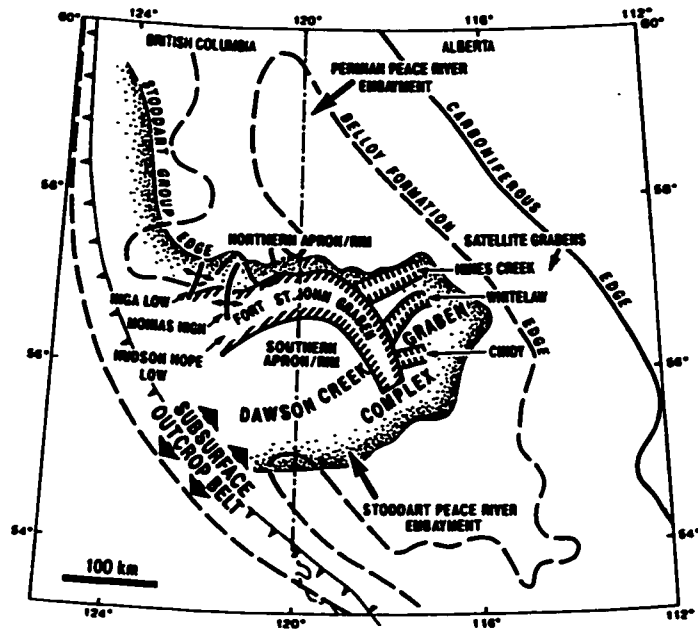
Ross (1990) divided the crystalline basement of the Alberta Basin into a series of Archean and Proterozoic tectonic domains, based on the interpretation of aeromagnetic data and U-Pb geochronology (Fig. 2-10). The basement of the area is characterized by N-S trending, curvilinear tectonic domains. Ross (1990) suggested that these tectonic elements accereted on the western edge of the Canadian Shield, and the juxtaposition of these tectonic domains was the result of collisions that occurred between 2.3 and 1.85 Ga.

The crystalline basement in the Peace River Arch area is composed mainly of four distinct basement domains; the Buffalo Head Terrane, the Chinchaga Low, the Ksituan High, and the Kiskatinaw Low. The N-S curvilinear trends of the basement tectonic domains do not coincide with the trend of the Peace River Arch (Fig. 2-10); indeed, they are nearly perpendicular to the trend of the arch. In addition, the arch does not coincide with any single tectonic zones of the basement, but is much greater than the width of any basement tectonic domains. This suggests that there is no direct relationship between the tectonic domains of the basement and the development of the Peace River Arch.

However, a spacial coincidence between the structural contacts of the basement domains and various Phanerozoic structural and sedimentary trends in the Peace River Arch area has been demonstrated (O'Connell et al., 1990; Wright et al., 1994; O'Connell, 1994). The 88 km long Dunvegan Fault (Fig. 7-8) has a northwest-southeast orientation, and it was active primarily in Late Mississippian, Pennsylvanian and possibly Permian time. The fault is approximately coincident

59° 124°   120°   114° 59°

B.C.
ALTA.

Hay River Fault

Utikuma
Belt

Buffalo
Head
High

Cordilleran deformation front

STUDY
AREA

B.C. ALTA.

54°   120°   54° 114°

54

Nahanni Terrane
age unknown

Fort Simpson High
1.85 Ga

Hottah Terrane
1.95-1.91 Ga

Nova Domain
2.00-1.99 Ga

Kiskatinaw Low
1.96-1.90 Ga

Ksituan High
1.96-1.90 Ga

Chinchaga Low
2.08-2.17 Ga

Buffalo Head Terrane
1.99-2.32 Ga

Wabamun High
2.32 Ga (?)

Arch boundaries

kilometres
0    50    100    150

0            50           100
miles

with the boundary between two Precambrian tectonic domains, the Ksituan High and the Chinchaga Low, suggesting a possibility of the rejuvenation of Precambrian fault zones (Wright et al., 1994).

O'Connell et al (1990) documented the spatial correspondence between the Ksituan-Chinchaga basement contact and Phanerozoic structural and sedimentary trends. First, they noted that the trend of the graben-filling Granite Wash sediments roughly parallels the Ksituan-Chinchaga basement contact, and the sediments deposited predominantly within the Chinchaga Low (Fig. 2-11A). Secondly, they noted that the distribution of the dolomite in the Wabamun Formation corresponds closely to the Ksituan-Chinchaga basement contact, and the sediments emplaced within the Ksituan High (Fig. 2-11 B). Third, they noted that the southeasterly structural offset of the Fort St. John Graben coincides with the Ksituan-Chinchaga basement contact (Fig. 2-8A). Finally, it appears that the Low Cretaceous Fox Creek Escarpment is collinear with the basement contact between the Ksituan High and the Chinchaga Low (Fig. 2-11C). These examples do not prove a direct cause-effect relationship, but they may indicate the rejuvenation of Precambrian basement faults.

Burwash and Krupicka (1969, 1970) have proposed simple isostatic basement uplift caused by potassium enrichment within the crust of the arch area. Stephenson et al. (1989), however, conclude that there is no geophysical evidence to confirm that theory. Cant (1988) proposed that the arch originated as an uplift over an incipient rift extending into the continent. However, O'Connell et al. (1990)
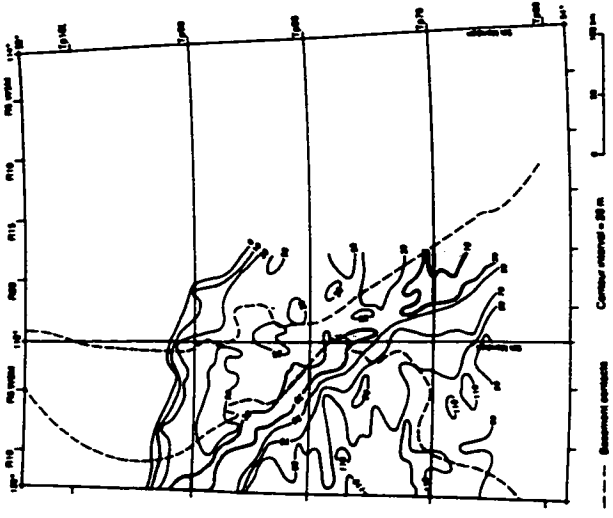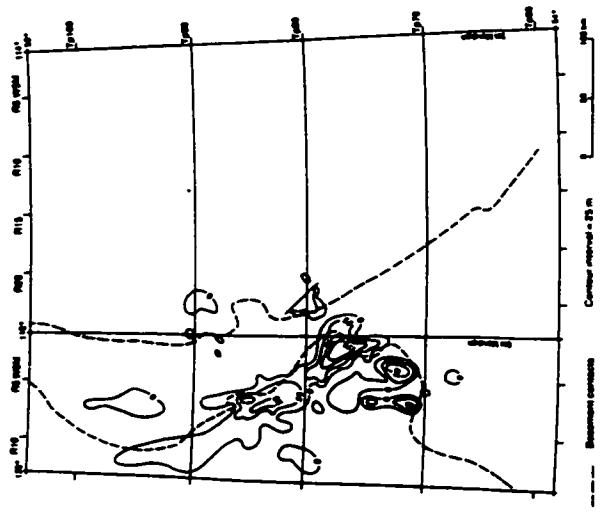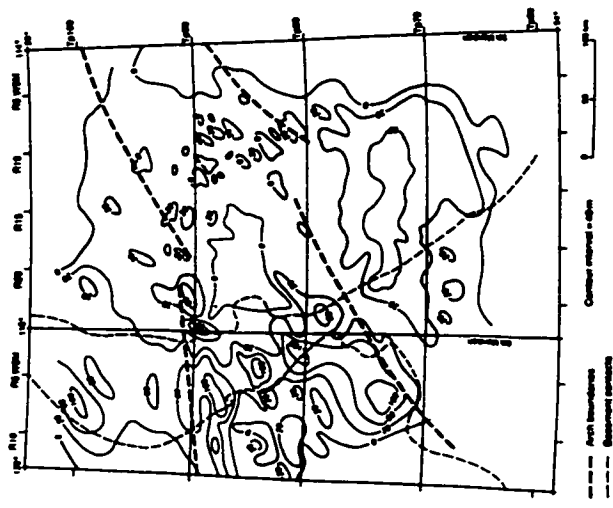
have concluded that the failed-rift scenario is difficult to explain because of the long duration of the arch and its asymmetrical configuration. O'Connell et al. (1990) have proposed that the arch was possibly formed by uplift related to the continental extension of an oceanic fracture zone. Cant (1988) has stated that the history of the Peace River Arch cannot be properly understood until there is much greater understanding of the tectonic events of the whole basin.

Cant (1988) postulated that the formation of the Dawson Creek Graben Complex may be related to a later phase of rifting. However, Barclay et al. (1990) recognized that the geometry and tectonic trends of the Dawson Creek Graben Complex were different from the underlying Peace River Arch and therefore suggested that the origin of the Dawson Creek Graben Complex is essentially unrelated to that of the Peace River Arch. Barclay et al. (1990) and O'Connell et al. (1990) have proposed that although the tectonic origin is not well understood, the Dawson Creek Graben Complex is the result of crustal extension that was coupled with strike-slip motion and related compressional and rotational movement. Barclay et al. (1990) have suggested that the Antler Orogeny was a possible driving force for this movement. The origin of the Peace River Arch and Dawson Creek Graben Complex still remains problematic, and a better understanding their origin depends on the acquisition of new data (O'Connell, 1994).

## 2.5 Sedimentology and Depositional Environments

Triassic sediments were deposited mainly as a broad, northeasterly-tapering

sediment wedge on a west facing, stable continental shelf that formed part of the interior Platform along the western passive margin of the North America Craton (Gibson, 1975; Gibson and Barclay, 1989; Gibson and Edwards, 1990a, 1990b; Cant, 1988; Edwards et al., 1994). In the early Triassic, the Western Canada Sedimentary Basin appears to have been situated around 30° N paleolatitude (Dilek, 1994). Deposition occurred in an arid mid-temperate to sub-tropical climatic setting (Gibson and Barclay, 1989). Davies (1997) suggested that at least seasonal aridity would have influenced fluvial discharge and that the aridity caused syndepositional to very early diagenetic dolomitization in the Triassic strata. Davies (1997) further suggested that under an inferred arid Triassic climatic setting, aeolian transport into the Western Canada Sedimentary Basin may have been an important contributor to Triassic sedimentation.

Gibson and Barclay (1989), and Gibson and Edwards (1990b) have interpreted the entire Triassic succession as comprising three transgressive-regressive cycles. The first cycle comprises the early Triassic Grayling, Toad and Montney Formations. The second cycle consists of middle to early late Triassic Liard, Doig and Charlie Lake Formations, and the last cycle is composed of late Triassic Baldonnel, Pardonet and Bocock Formations. Each cycle contains rocks deposited in a marine shelf setting ranging from distal deep shelf waters to proximal shoreline. Embry (1988) has recognized nine regional transgressive-regressive cycles in the Arctic Canada during the Triassic, and has shown that during the early Triassic, the widespread transgressive boundary surfaces can be dated as early

Griesbachian, late Dienerian and late Smithian. Embry (1997) also has suggested that most of these boundaries appear to correlate in the Western Canada Sedimentary Basin. However, because of the lack of precise biostratigraphic data in the subsurface and the possible miscorrelation between outcrop and subsurface as suggested in Chapter 2.2.4, the proposed correlations and ages of T-R sequence boundaries (Fig. 2-12) in the subsurface Triassic strata remain ambiguous. Triassic rocks in the Peace River Arch area of British Columbia show a wide range of depositional environments. Deep water shelf-platform siltstone, shale and carbonate occur at the base (Grayling, Toad and Montney Formations), grading upward into shallower water shelf and shoreline siltstone, shale, sandstone and carbonate (Liard and Doig Formation), followed by deposition of shallow water marine to coastal and barrier, tidal inlet carbonate, siltstone, sandstone and evaporite (Halfway and Charlie Lake Formations) (Gibson and Edwards, 1990b; Edwards et al., 1994).

Few detailed sedimentological studies have been done on the Montney Formation (Miall, 1976; Davies et al., 1997; Davies and Sherwin, 1997; Moslow and Davies, 1996,1997). Miall (1976) suggested that the coarser grained siltstone, sandstone and coquina facies close to the eastern depositional margin were deposited in a shallow water, deltaic environment. Davies et al. (1997) suggested that sedimentation in the Montney Formation in the Peace River area occurred within a broad, west facing embayment structurally influenced by reactivation of the Dawson Creek Graben. They also suggested that offshore shelves were dominated
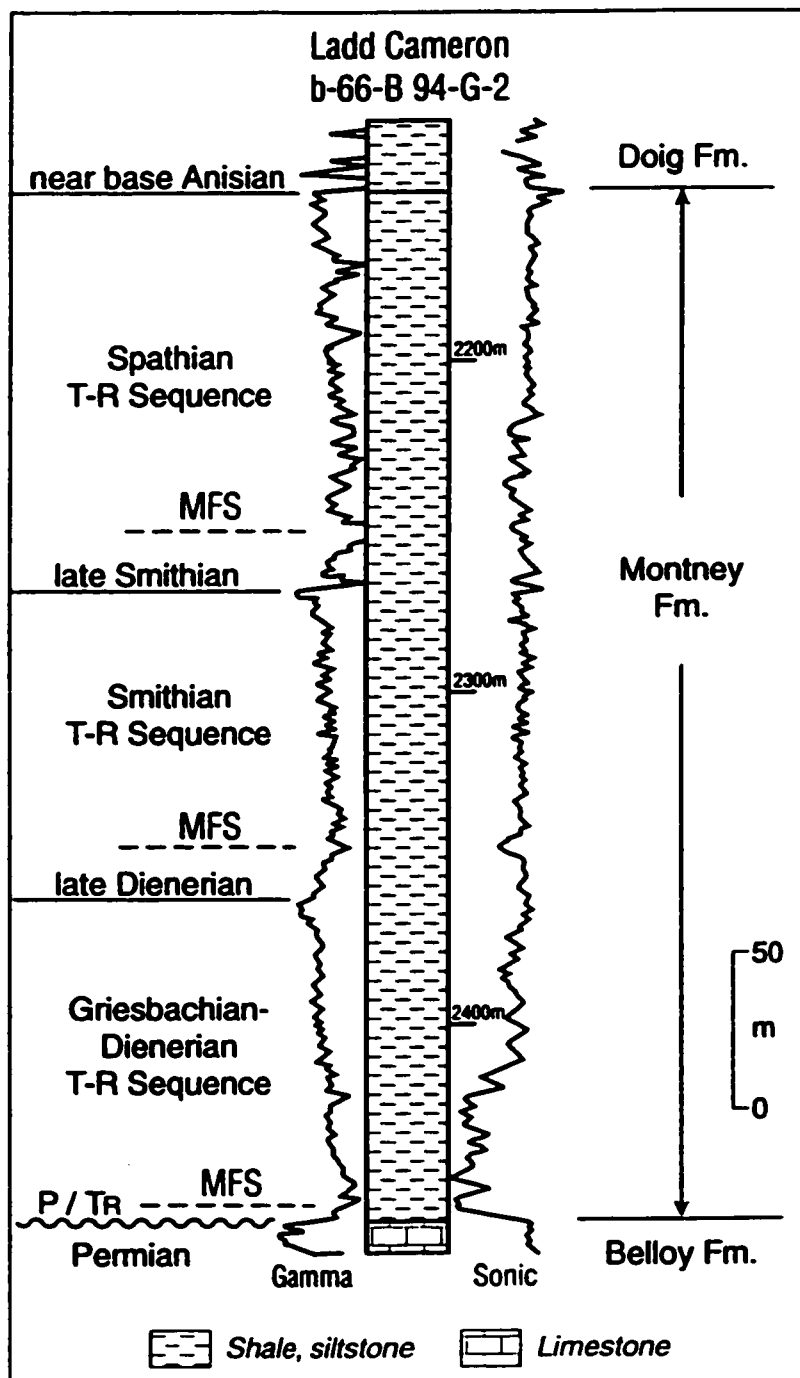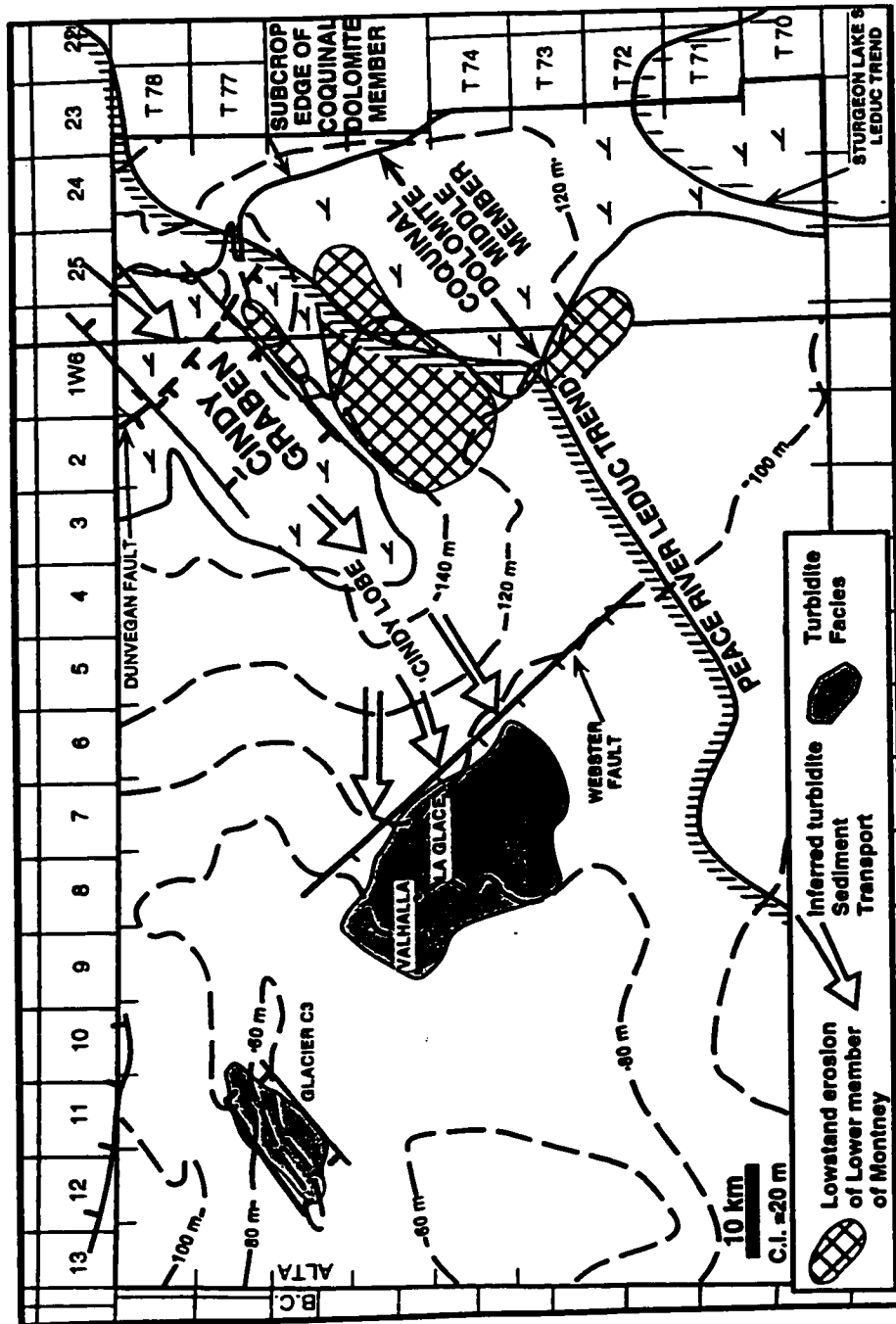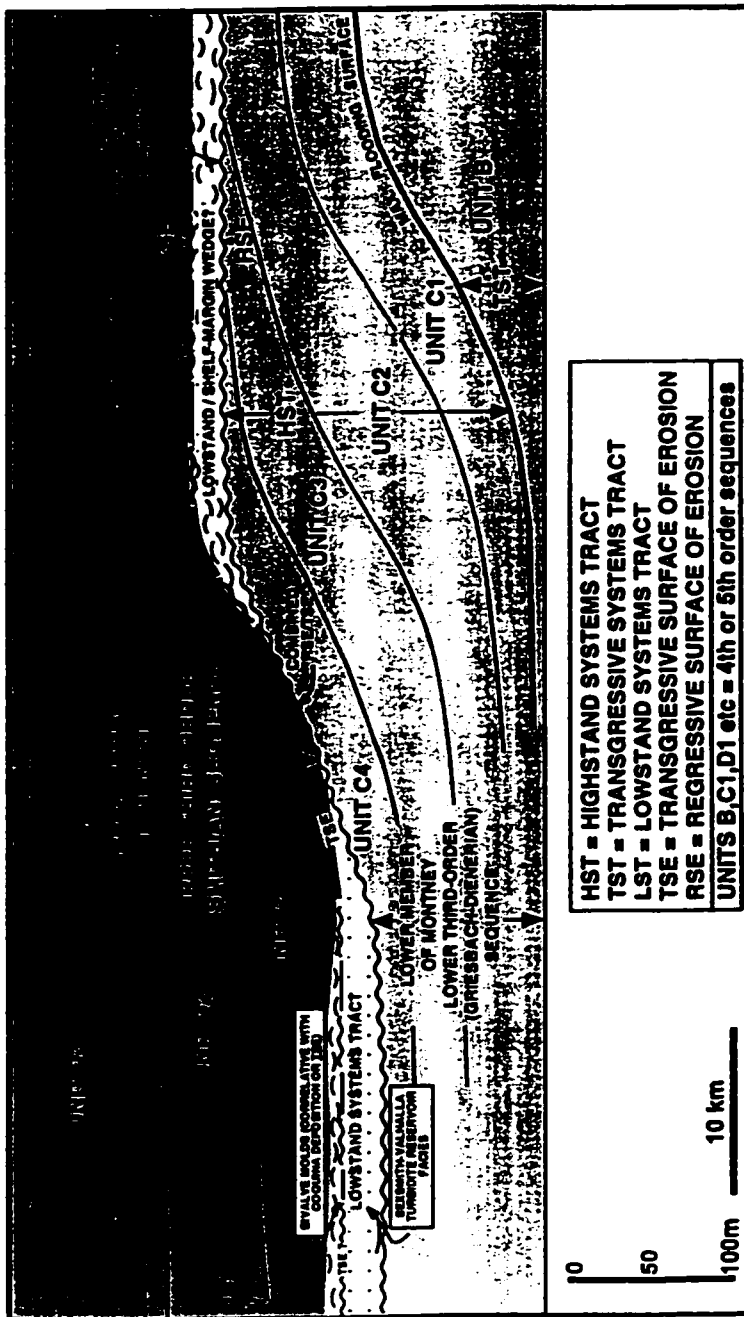
**Ladd Cameron**
**b-66-B 94-G-2**

near base Anisian

Doig Fm.

Spathian
T-R Sequence

2200m

MFS

late Smithian

Montney
Fm.

Smithian
T-R Sequence

2300m

MFS

late Dienerian

50

m

Griesbachian-
Dienerian
T-R Sequence

2400m

0

MFS

P / TR

Permian

Belloy Fm.

Gamma                 Sonic

Shale, siltstone        Limestone

HST = HIGHSTAND SYSTEMS TRACT
TST = TRANSGRESSIVE SYSTEMS TRACT
LST = LOWSTAND SYSTEMS TRACT
TSE = TRANSGRESSIVE SURFACE OF EROSION
RSE = REGRESSIVE SURFACE OF EROSION
UNITS B,C1,D1 etc = 4th or 5th order sequences

by storm processes and that turbidites accumulated in a structurally controlled downslope or toe of slope setting with northeast-southwest trending channels (Fig. 2-13). Moslow and Davies (1996, 1997) suggested that a sea level drop enhanced mass-wasting processes and generated the sediment gravity flows responsible for the deposition of turbidites. They sugggested that turbidite deposition took place at the toe of slope with contemporaneous deposition of coquina beds on the shoreface during a progressive fall in sea level and/or at a lowstand of sea level. This implies a genetic relation between the turbidite deposition and coquina beds (Fig. 2-14). However, several aspects of their work are difficult to reconcile with the results presented in this study. Detailed discussions will be provided in later chapters.

# CHAPTER 3:   FACIES DESCRIPTIONS

## 3.1 Introduction

Ten facies are defined on the basis of lithology, sedimentary structures and bioturbation. Several facies are gradational between one another as grain size and sand/mud ratio gradually change.

Generally the western part of the study area has deeper water facies than the eastern part, with finer facies and resedimented facies in the west, and coarser rocks without resedimented facies in the east. Most of sandstones and siltstones in the western part of the study area are interpreted as turbidites. Although complete Bouma Sequences (1962) are rare, the sharp bases, common occurrences of sole marks, the structureless or graded nature of the sandstones and siltstones, and absence of shallow water indicators suggest deposition from turbidity currents.

Generally the Montney sediments are characterized by rare bioturbation, perhaps because of a delayed recovery after the mass extinction at the end of Permian, and a condition of worldwide oceanic anoxia in the early Triassic (Hallam,1994).

After each facies description, a preliminary interpretation is given. Full interpretations will be developed in Chapter 7.

## 3.2 Facies 1: Dark Mudstone

Facies 1 includes a wide range of mudstones from black mudstone with almost no silty laminations to various proportions of silty laminations. It can be divided into three subfacies, dark to black mudstone with almost no silty laminations (Subfacies 1a), dark to grey mudstone with various proportions of silty laminations (Subfacies 1b) and distinctive color banded layers of thin black mud and lighter colored mud (subfacies 1c).

In Subfacies 1a (Fig. 3-1A), the only recognizable texture is very delicate color changes within laminations. The delicate, darker and lighter mm scale color contrast makes this facies appear fairly well laminated. The lamination is absolutely parallel and is the cause of fissility. The paler laminations are silty, but the silt content does not exceed 5 % of the volume of the facies. As the silt proportion increases, Subfacies 1a grades into Subfacies 1b.

In Subfacies 1b (Fig. 3-1B), the laminae consist of alternations of lighter and darker colors due to grain size differences between the very dark laminae (clay) and the greyish-white laminae (silt). The thickness of an individual silty lamination is commonly about 1 mm, and rarely exceeds 5 mm. The laminae are parallel.

Figure 3-1C shows very distinctive color banded layers (Subfacies 1c). Here, the rock consists of several black mud layers 1 to 2 cm thick, interbedded with lighter colored mudstones 1 to 7 cm thick. This facies occurs at only one stratigraphic interval, and is characterized by a distinctive low resistivity log value. It can be easily traced over a large area, and constitutes the base of stratigraphic
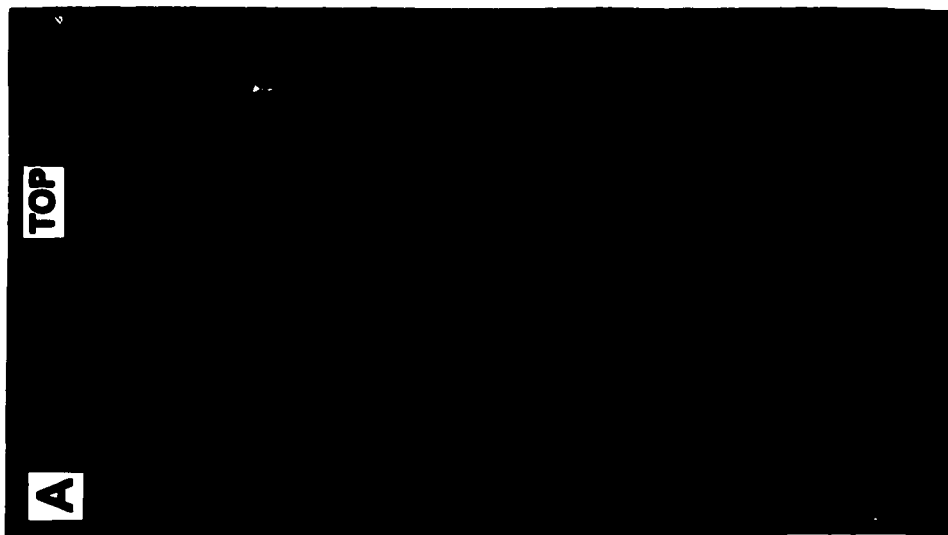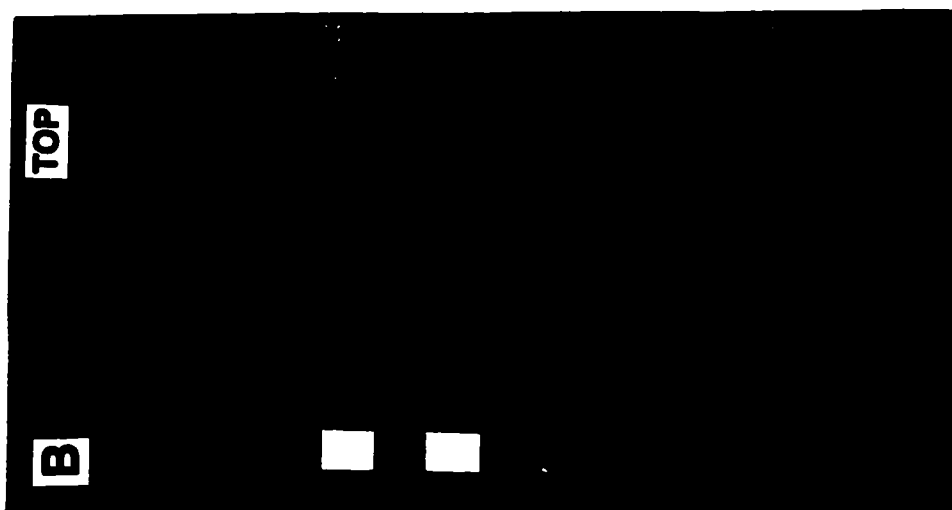
Unit C.

Subfacies 1a and 1b commonly alternate vertically and they occur in various thicknesses from 1 cm to several tens of meters. Facies 1 is commonly very thick and abundant in the western part of the study area and thinner and less abundant in the eastern part. In the well 7-5-67-7W6M, the 18 m thick core consists entirely of Facies 1. Well log responses show that in the western study area, the lowest 30 to 80 m of the succession consist entirely of Facies 1.

Trace fossils are almost absent and only very few *Planolites* have been recognized.

*Preliminary Interpretation*

Facies 1a and 1b are interpreted to have been deposited in deep, quiet water in an offshore basinal environment that was well below storm wave base. The color grading within silty laminations is attributed to episodic, very weak waning flows.

### 3.3 Facies 2: Alternation of Siltstones and Mudstones

Facies 2 is gradational from Facies 1 and consists of alternations of mudstones and siltstones with various mud-silt ratios (Fig. 3-2 ). Individual siltstone beds are commonly 1 to 5 cm thick and rarely exceed 10 cm. The bases of the siltstone beds are commonly sharp or slightly erosive on the underlying mudstone bed (Fig. 3-2A). Some thick siltstone beds contain small mud clasts in the lower
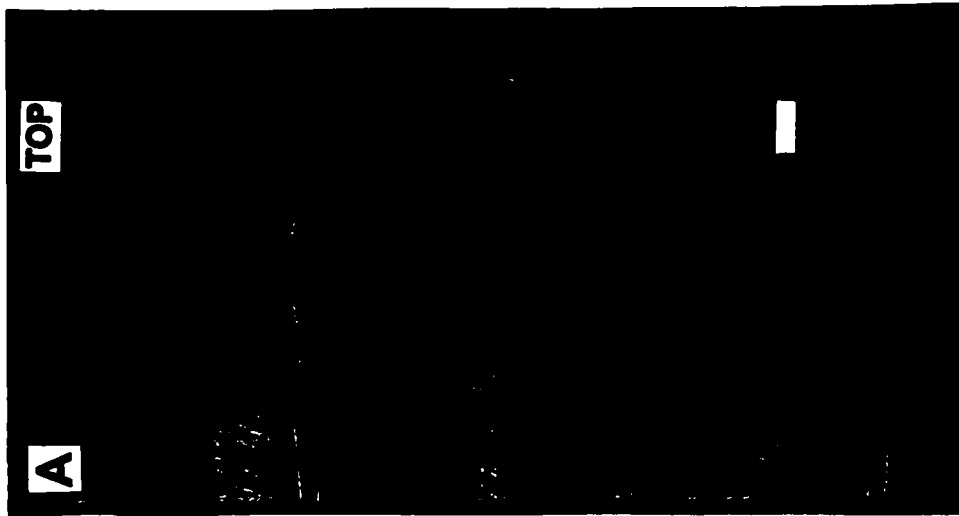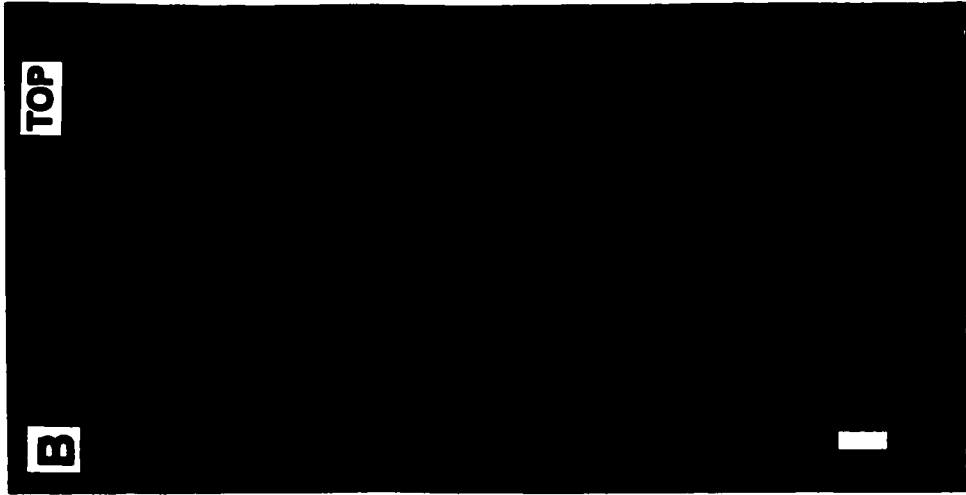
part of the beds. Some thin siltstone beds are lenticular or isolated in the surrounding mudstones. The beds contain well developed parallel, undulating or cross-laminations (Fig. 3-2B).

The upper part of individual siltstone beds commonly grades into dark mudstone (Fig. 3-2A), but a very sharp boundary with the overlying mudstone is also common. Interbedded dark mudstones are commonly less than 3 cm thick, and rarely exceed 10 cm. Convoluted beds are commonly observed in Facies 2. Bioturbation is almost absent.

*Preliminary Interpretation*

The sharp or erosive bases, small mud clasts in the lower part of the siltstone beds, and the commonly graded nature of the upper part of the siltstone beds suggest that the siltstones in Facies 2 were deposited mainly from turbidity currents (Dzulynski and Walton, 1965; Walker, 1965; Bouma, 1962). The thinness of individual siltstone beds, fine grain size, and abundant interbedded mudstones indicate a distal, basinal depositional environment, or deposition on channel levees. Some convoluted beds may represent soft sediment deformation on channel levees.

### 3.4 Facies 3: Bioturbated Silty Mudstones to Muddy Siltstones

Facies 3 occurs only in the eastern part of the study area. It consists of alternating bioturbated thin mudstone and siltstone layers with various mud-silt ratios. Facies 3 is gradational from Facies 1. The main distinction of the two facies

is bioturbation. Most of the beds in Facies 3 are slightly to moderately bioturbated by *Planolites* and *Lingulichnus*, but some intervals are intensively bioturbated (Fig. 3-3). Other criteria for distinction of Facies 3 from Facies 1 are the generally coarser nature of Facies 3, the thicker silty layers and the presence of more undulating laminations in Facies 3 (Fig. 3-3A). The thickness of silty layers in Facies 1 is 1 to 5 mm, but in Facies 3 the thickness commonly exceeds 5 mm. Facies 3 commonly constitutes the basal part of a coarsening upward succession in the eastern part of the study area.

*Preliminary Interpretation*

The dominance of mudstones in Facies 3 suggests this facies was deposited in deep, quiet water in an offshore setting below storm wave base. In some intervals, the high intensity of bioturbation associated with very low diversity of ichnospecies (mainly *Lingulichnus*) may represent deposition in a stressed environment.

## 3.5 Facies 4: Sharply Based Thin-bedded Sandstones and Siltstones

Facies 4 consists of sharply based, thin-bedded, very fine grained sandstones or coarse siltstones (Fig. 3-4). The thickness of individual sandstone or siltstone beds is commonly 5 to 40 cm and rarely exceeds 50 cm. The bases of the sandstone or siltstone beds are very sharp and commonly show tool marks (particularly prod marks) and scour marks (particularly rill marks) (Fig. 3-4 D and

A **TOP**

B **TOP**

C **TOP**

D

E
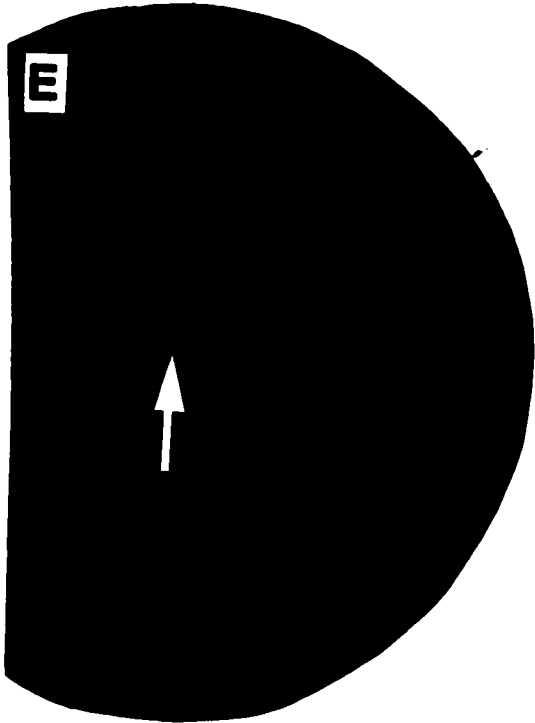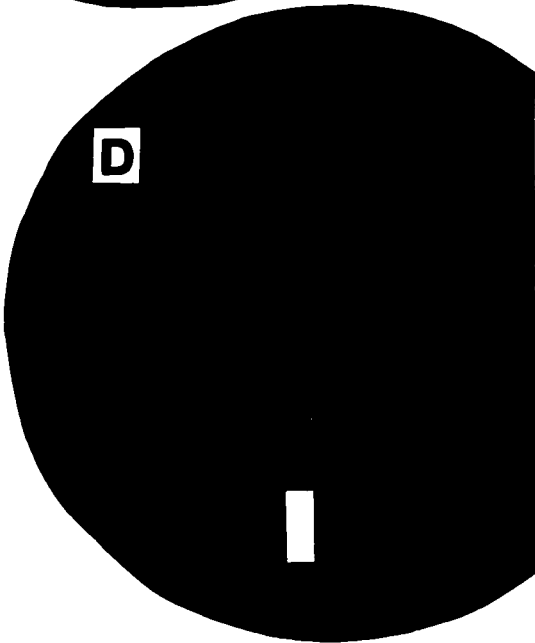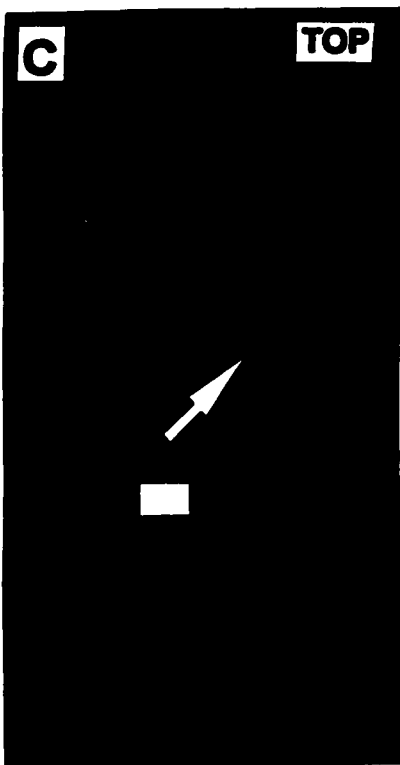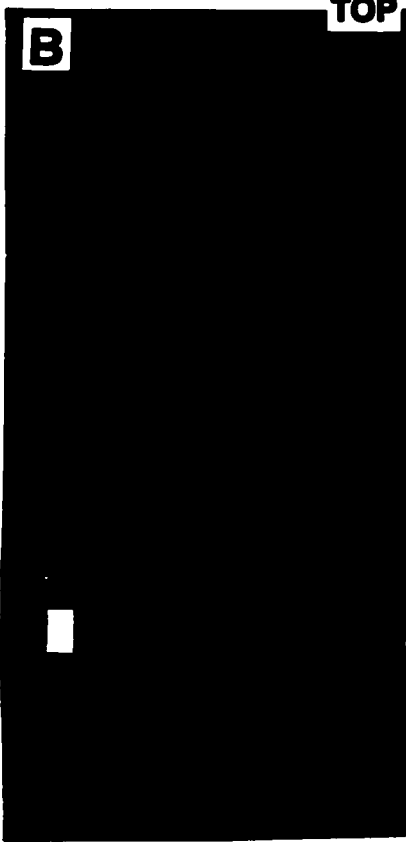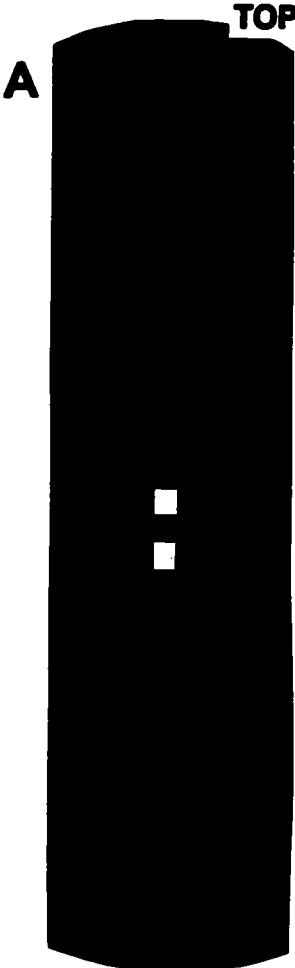
E). The lower parts of the sandstone / siltstone beds are commonly structureless or very weakly horizontally-laminated. The upper parts of the individual sandstone / siltstone beds are commonly structureless, horizontally laminated or ripple cross-laminated (Fig. 3-4 A and B). However, around T72 R6M5, the upper parts of some sandstone and siltstone beds are wave rippled. The upper boundaries of the sandstone / siltstone beds commonly grade into dark mudstone, but very sharp boundaries with the overlying thin mudstone layers are also common. The complete Bouma (1962) Sequence is very rare. Facies 4 is most common in Unit C, but limited cores suggest that this facies is also common in Units B and D. Bioturbation is absent.

*Preliminary Interpretation*

The sharp bases, common occurrences of sole marks and the structureless or graded nature of the beds in Facies 4 suggest deposition from turbidity currents (Dzulynski and Walton, 1965; Walker, 1965; Bouma, 1962). The common occurrence of structureless beds can be interpreted in terms of very rapid deposition of suspended sediments from a turbulent flow (Lowe, 1988). The common sharp upper boundary may represent truncation by a subsequent turbidity current, or may represent bypass of the late stage of the turbidity current. However, some occurrences of wave ripples in the upper parts of sandstones and siltstones suggest turbidite deposition within reach of storm waves.

## 3.6 Facies 5: Thick, Structureless Sandstones

Facies 5 consists of thick, structureless sandstones with very thin very dark mudstone layers. The thickness of sandstone beds ranges from about 0.5 to 7 m. Some of the thick beds may possibly be amalgamated. Most sandstones are structureless (Fig. 3-5 A and B), and some beds or some parts of beds are faintly laminated. Fluid escape structures are very rare.

The bases of the sandstone beds are very sharp or erosive. In some cores, the basal 1 to 4 m of the massive sandstone succession contains abundant large mud clasts wider than the core diameter (Fig. 3-5C). The tops of the sandstone beds are commonly very sharp and only rarely grade into mudstones. Interbedded mudstone layers are usually less than 10 cm thick, but a few mudstone layers are close to 1 m. In well 9-28-72-5W6M, the entire 36 m of core consists of thick, structureless sandstones with thin (<10 cm) mudstone layers. The thick, structureless sandstone succession is easily recognized by a blocky response in well logs. In some wells (7-31-72-5W6M, 9-24-73-7W6M and 16-28-74-8W6M), the overall succession of thick, structureless sandstones exceeds 40 m in thickness.

*Preliminary Interpretation*

Facies 5 is characterized by its structureless nature (commonly described as "massive"). Structureless sandstones commonly lack internal sedimentary structures even in X-radiographs of slabs (personal communication with T. Moslow, 1996), indicating complete absence of internal structure.
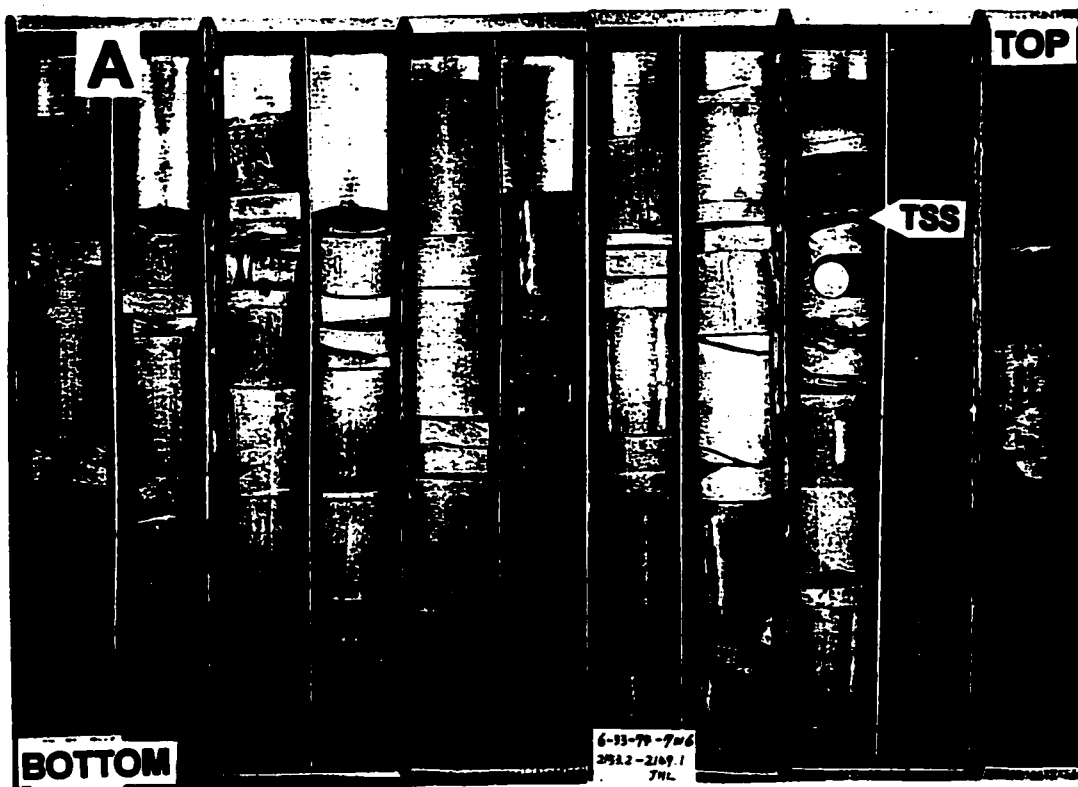
Structureless sandstones may form by a variety of processes: (1) by rapid deposition from suspension, no equilibrium bedforms developed (Lowe, 1988), (2) original physical sedimentary structures destroyed by fluid escape (Blatt et al., 1980), and (3) original physical sedimentary structures destroyed by bioturation (i.e. Bhattacharya and Walker, 1991). No evidence of bioturbation and very rare occurrences of fluid escape structures suggest that structureless sandstones were produced by rapid deposition from suspension. Therefore, structureless sandstones are interpreted as deposits from turbidity currents.

### 3.7 Facies 6: Mud-Laminated or Mud-Interbedded Sandstones and Siltstones

Facies 6 consists of a thick succession of coarse siltstones or very fine grained sandstones with various proportions of very thin mud beds or mud laminations (Fig. 3-6). Facies 6 is gradational from Facies 3, but the mudstone layers are less abundant in Facies 6. The proportion of mud in Facies 3 commonly exceeds 40 %, but ranges from 5 to 40 % in Facies 6.

Facies 6 is characterized by undulating to flat, continuous or discontinuous muddy laminations or layers. Based on the mud proportion and characteristics of laminations, Facies 6 can be divided into three subfacies. In Subfacies 6a, the mud ratio is relatively high, muddy laminations are more or less continuous, and the silty to sandy layers are commonly lenticular (Fig. 3-6A). In contrast Subfacies 6b is dominated by sand or silt layers, and the muddy laminations or layers are subtle and more discontinuous (Fig. 3-6B). In both subfacies 6a and 6b, internal

A TOP

B TOP

C TOP

D TOP
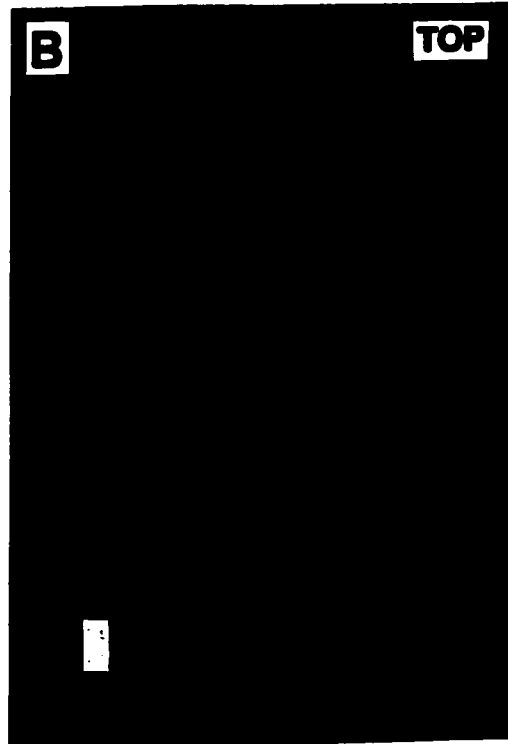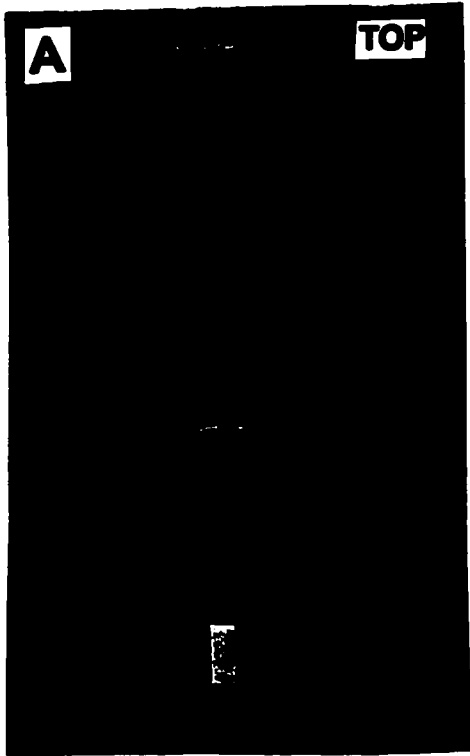
laminations are undulating. In Subfacies 6c, the inter-laminated or interbedded muds are relatively flat and continuous, forming distinctive sand-mud couplets (Fig. 3-6 C and D).

Facies 6 commonly occurs in successions several meters thick with coarsening upward trends. The core 6-32-67-19W5M is a good example of a coarsening upward succession. There, the basal part of the coarsening upward succession is characterized by Subfacies 6a. This gradually changes upward into Subfacies 6b.

Bioturbation is rare. However, some intervals are slightly to moderately bioturbated by *Planolites* and *Lingulichnus*.

*Preliminary Interpretation*

The alternations of thin, mud, silt/sand layers in Subfacies 6 represent alternating periods of slower and more rapid deposition. The dominance of the delicate undulating laminations in Facies 6 may indicate deposition close to storm wave base. In Subfacies 6a and 6b, the undulating laminations are thought to represent small scale wave ripples. The common occurrence of coarsening upward successions may represent gradual shallowing or may simply represent sediment supply changes.

### 3.8 Facies 7: Sandstones and Siltstones Associated with HCS Beds

Facies 7 generally consists of fairly well laminated, very fine grained
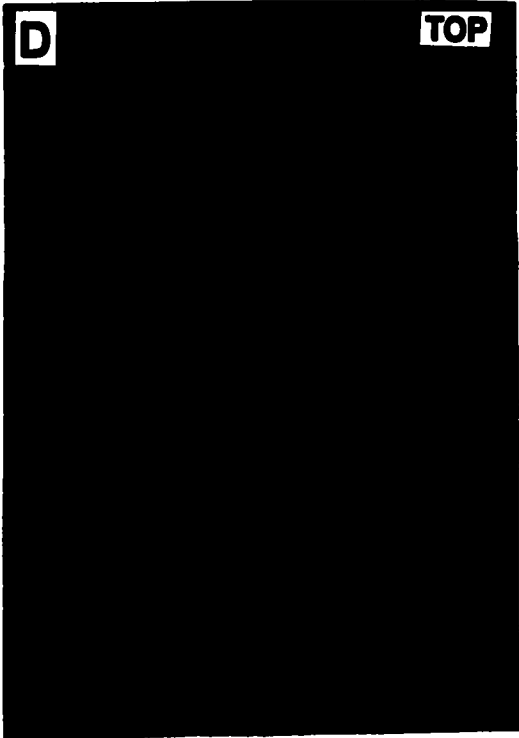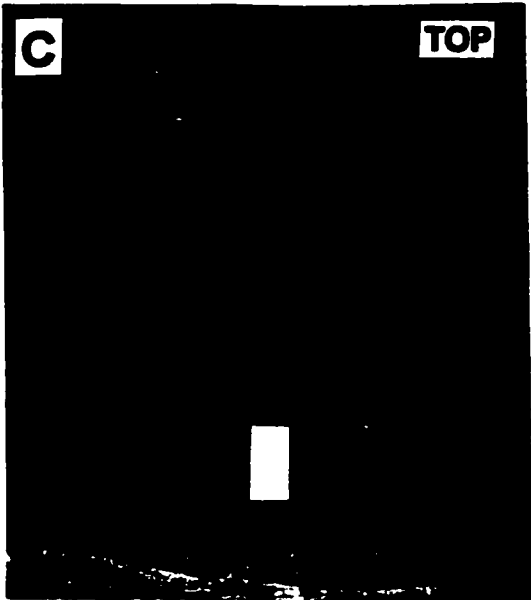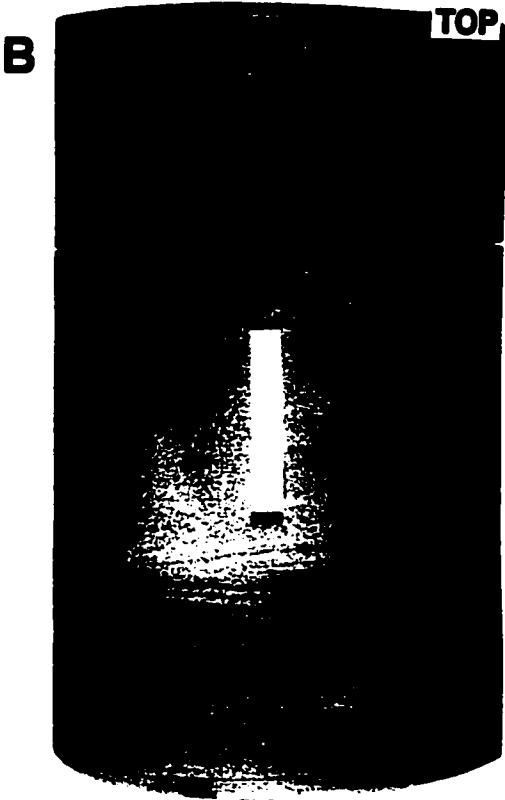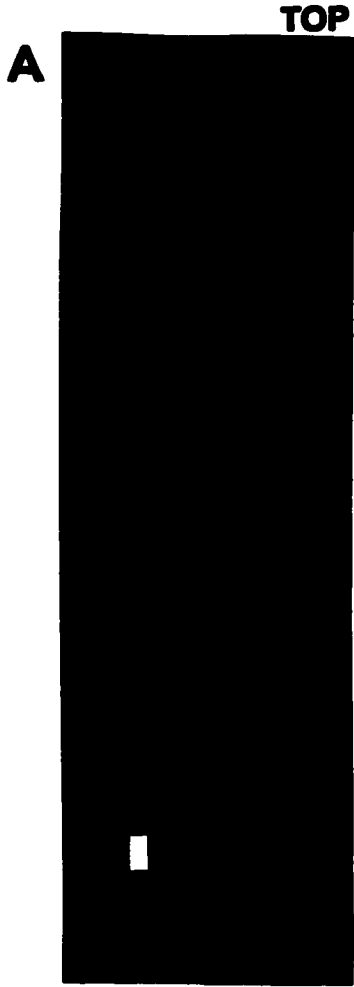
sandstones or coarse siltstones, commonly showing low angle inclined intersecting laminations or wave ripples (Fig. 3-7). Structureless siltstones and sandstones are also common. The thickness of individual beds varies from 1 to 70 cm. The bases of individual beds are commonly sharp and some beds contain small mud clasts in the lower part of the beds. The tops of the beds commonly grade into mudstone but sharp upper boundaries with the overlying thin mudstone layers are also common.

In thicker beds (>15 cm), horizontal lamination is most common, along with horizontal to subhorizontal parallel lamination characterized by low angle inclined intersecting surfaces (Fig. 3-7 A and B). The dip of the lamination changes slightly upwards through the bed, with or without distinct low angle truncation surfaces. This stratification is interpreted to be hummocky cross stratification (HCS). The upper parts of sandstone beds are commonly wave rippled (Fig. 3-7D).

Thinner beds (<10 cm) are commonly wavy laminated at least in some portions and some beds commonly show a well developed vertical succession of features (Fig. 3-7C). The bases of the beds are very sharp and the lower part of the beds consists of structureless or very weakly laminated sandstone or siltstone. The lower part is overlain by a cross-laminated interval commonly showing climbing ripples. The cross-laminated interval grades upward into dark mudstone in the upper part of the beds.

Structureless beds occur throughout the succession with thicknesses of a few cm to several tens of cm. Facies 7 commonly shows an overall thickening- and coarsening-upward succession over several meters. Bioturbation is very rare but

a few *Planolites* and *Skolithos* are observed.

*Preliminary Interpretation*

The sharp or erosional bases, grading, and common occurrence of hummocky cross stratification suggest that Facies 7 contains suddenly-emplaced storm influenced beds (Harms et al., 1975; Duke, 1985). The succession of thicker beds with HCS is interpreted as storm-generated deposits which occur below fairweather wave base but above storm wave base. The succession of thinner beds and the commonly associated graded beds are interpreted to have been deposited in a more distal setting than the succession of the thicker beds. Some of thinner beds characterized by graded nature (Fig. 7C) may suggest deposition from turbidity currents.

## 3.9 Facies 8: Flat-Laminated to Structureless Sandstones

Facies 8 consists of thick, flat-laminated to structureless sandstones. In flat-laminated sandstones (Fig. 3-8), internal laminations are commonly weakly developed, and well-developed laminations are rare. As stratification becomes vague, flat-laminated sandstones grade into structureless sandstones. This facies commonly occurs above Facies 6 (mud-laminated or -interbeded sandstones and siltstones) in overall coarsening upward successions. The succession of this facies commonly ranges from 5 to 15 m. Facies 8 occurs only in very limited areas near the subcrop edge.
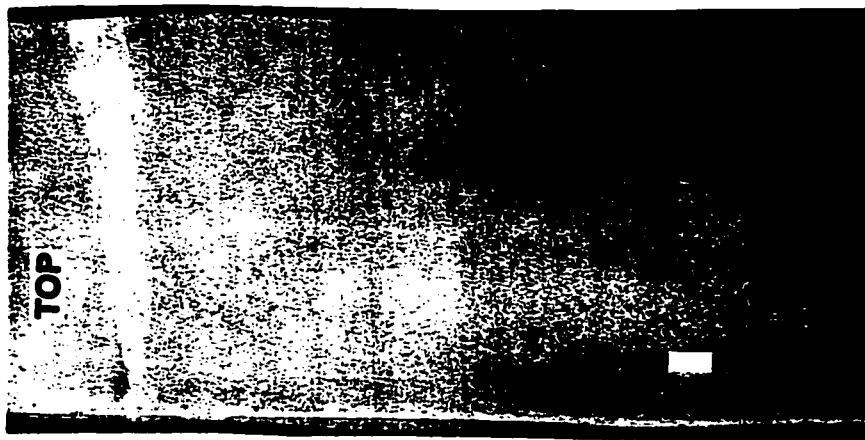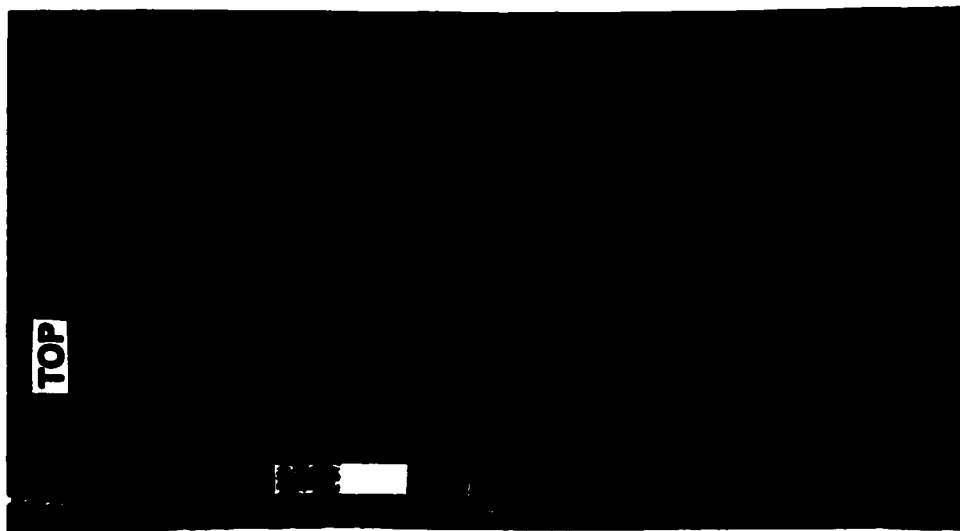
*Preliminary Interpretation*

The common occurrence of this facies above Facies 6 in coarsening upward successions suggests that this facies formed in shallower environments than Facies 6. Weak laminations and the structureless nature are attributed to a high degree of sediment sorting.

## 3.10 Facies 9: Dolomitic Coquina Beds

Facies 9 consists of dolomitic sandstones and bivalve coquinas with various proportions of shell fragments. Most coquina beds contain small shell fragments but a few cores show complete internal molds of shells (Fig. 3-9). Although severe dolomitization makes identification of components of the coquinas difficult, the remaining textures suggest that the coquinas mainly consist of *Unionites* and *Claraia* (Davies and Sherwin, 1997). Pervasive dolomitization also destroyed original sedimentary structures and formed structureless beds, but some preserved textures suggest that orginal structures of individual coquina beds commonly included cross stratification or horizontal lamination (see Fig. 6-4).

Successions of dolomitic coquina beds occur in several stratigraphic intervals. In most cases, Facies 9 overlies Facies 8 (flat-laminated to structureless sandstones), and occurs at the uppermost part of coarsening upward successions except the coquina beds in the uppermost part of Unit A. .

The thickest and most extensive succession of dolomitic coquina beds occurs in the uppermost part of Unit A and the succession ranges from zero m (at
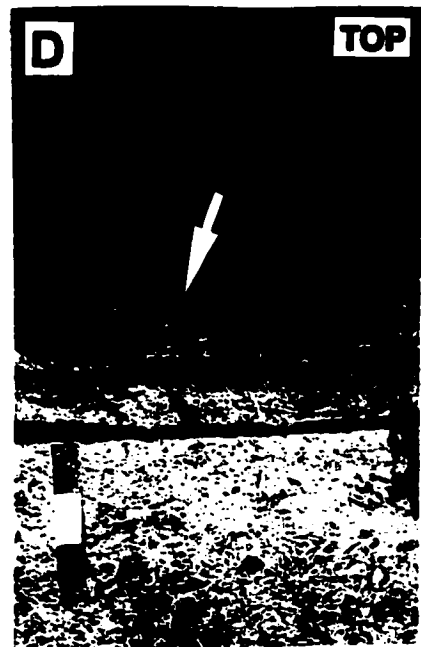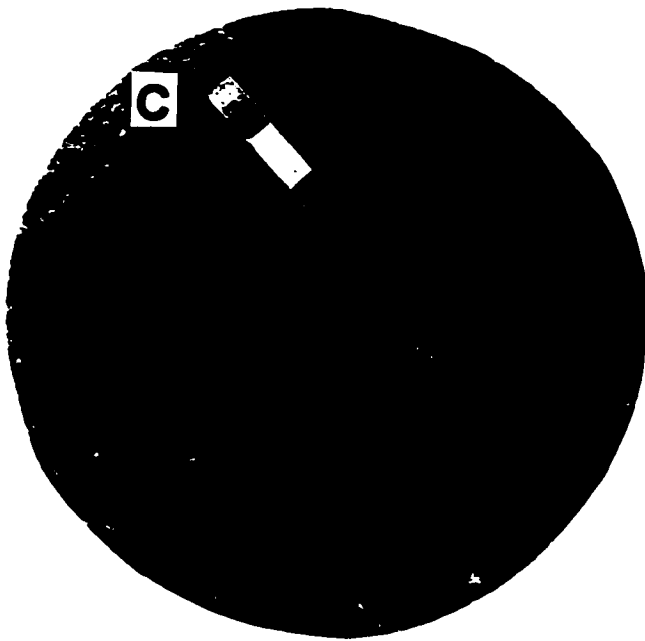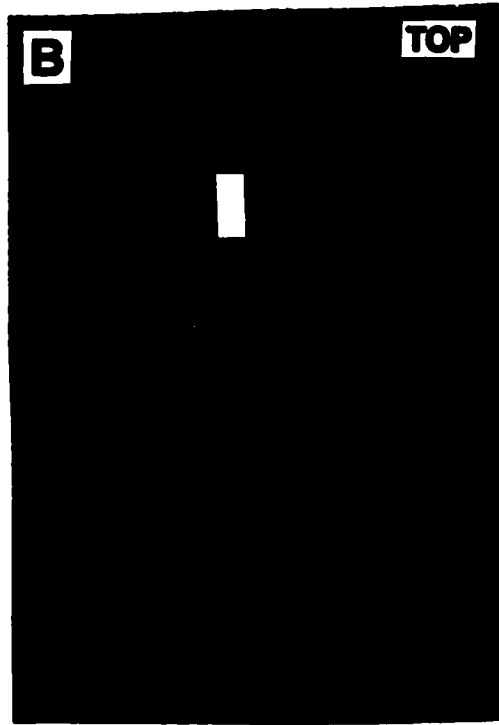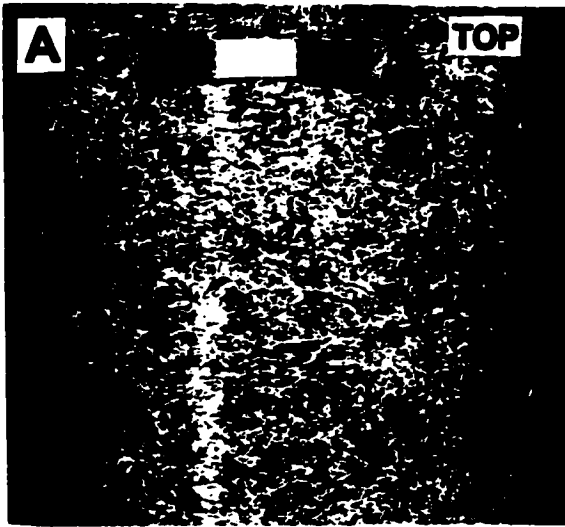
depositional pinch-out) to 20 m. The lower part of the succession consists of fine dolomitic sandstones with a few very small shell fragments, and it abruptly overlies silty mudstones (Facies 3). Individual dolomitic sandstone beds range from 10 to 30 cm in thickness and the proportion of sandstone beds gradually increases upward. The upper part of the succession contains abundant shell fragments and cavities. Individual beds are commonly thicker than 50 cm and interbedded mudstones are very rare. The succession of coquina beds is sharply overlain by dark mudstones (Fig. 3-9D).

Bioturbation is not common, but some intervals are slightly to moderately bioturbated mainly by *Lingulichnus*.

*Preliminary Interpretation*

The common occurrence of this facies overlying Facies 8 (as the uppermost part of coarsening upward succession) suggests that this facies formed in a shallower environment than Facies 8. The rare preservation of cross stratification (poorly preserved due to dolomitization), some large shell fragments, and rare mudstone interbeds suggest that the dolomitic coquina beds were deposited in fairly shallow environments.

Davies and Sherwin (1987) suggested *Claraia* facies indicates a shallow subtidal sandflat environment. They also described brecciated fabrics and rounded coarse sand grains in the matrix of some coquina beds, and suggested subaerial exposure of some of the coquina beds.

### 3.11 Facies 10: Slumped Deposits

Facies 10 consists of slumped facies. Sedimentary structures are severely distorted, or completely destroyed, resulting in structureless beds or isolated sandballs (Fig. 3-10). Individual thickness of the slumped beds varies from a few cm to a few m. Some successions of slumped beds are up to 9 m in thickness. The wells containing thick succession of slumped beds include 15-25-65-25W5M, 16-31-66-23W5M, 7-32-66-23W5M, 12-1-66-25W5M, 16-22-66-26W5M, 7-3-68-24W5M, 16-23-68-25W5M, 5-25-68-25W5M, 13-5-68-1W6M, 14-6-69-21W5M and 10-11-71-20W5M. The location of most of these wells is closely related to the western margin of the dolomitic coquina beds.

*Preliminary Interpretation*

Slumped sediments commonly reflect rapid deposition on an unstable slope. Sedimentary overloading can cause sediment failure, and slumping can be also triggered by earthquakes.

63
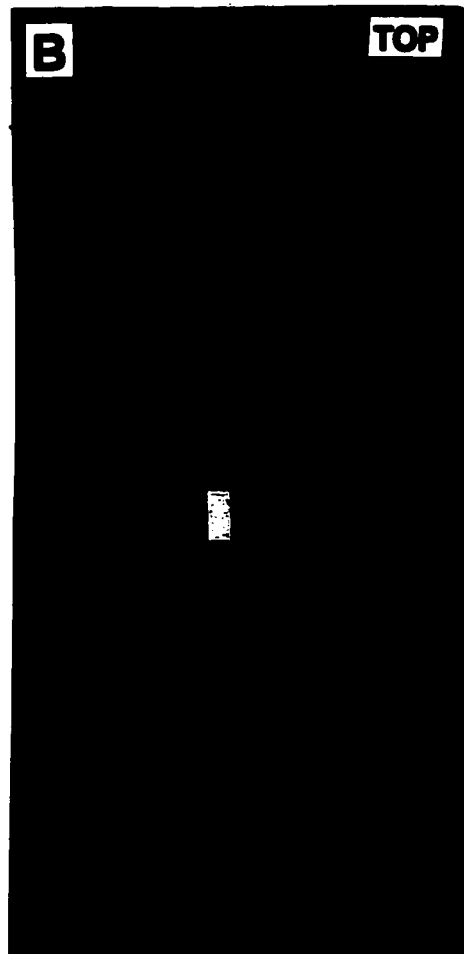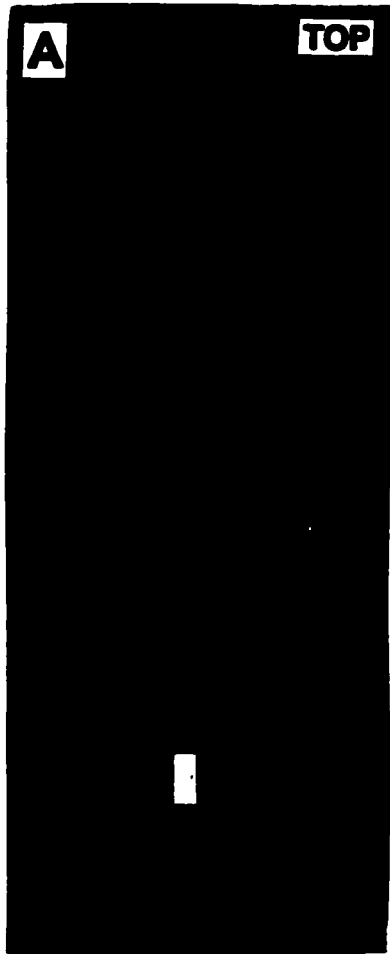
# CHAPTER 4:   WELL LOG CROSS SECTIONS

## 4.1 Introduction

The purpose of this chapter is to examine the lateral distribution of the Montney depositional units and facies in the study area.   To date, detailed correlations of units within the Montney Formation have not been published, except for those of Davies et al. (1997; see Fig. 2-5).   However, their correlations include only one cross section with 6 wells, and the large spacing between wells (10 to 24 km) makes exact correlations difficult.   Therefore, this study represents the first detailed correlation of the Montney Formation on a local and regional scale.

Correlations were based upon well log signatures and comparisons of sedimentary facies between cores.   Correlations were done by tracing and overlaying each and every adjacent well log so that individual log deflections and overall log shapes have been matched to minimize errors.   In matching, one log was overlayed on the next, and then moved up and down until the best fit was obtained.   The most prominent deflections (peaks and troughs) on individual logs have been numbered for the purpose of regional correlations.   Most of the more prominent log markers were established in the western part of the study area, and they have been traced laterally to the east.   Most of the log markers can be easily recognized in the western part of the study area, but they   become gradually weaker to the east.

The base of the Montney Formation (BM) is very easily recognized by a strong gamma-ray peak (high API values) throughout the entire study area where the Montney Formation exists (Appendix B). In cores, BM consists of dark mudstones with thin poorly sorted conglomerates at the base, abruptly overlying Paleozoic sediments. Marker 1 (M1) is defined on logs by a leftward (negative) kick on the induction logs and as a small rightward (positive) peak on the gamma-ray logs. Its strong signature is most prominent in the central part of the study area (see Fig. 4-4). It gradually becomes weaker toward the east and west, but the general shape of M1 is preserved over most of the study area. M1 is correlated with the basal mudstone (Facies 1) overlying the dolomitized coquina beds in the eastern part of the study area. Erosional surface 1 (ES1) is a regional truncation surface at the base of the dolomitized coquina beds in the eastern part of the study area. It is characterized by a sharp leftward deflection on gamma-ray logs (lower API values) and a sharp rightward deflection on induction logs (see Fig. 4-4). Marker 2 (M2) is defined as a leftward kick on the induction logs and is easily recognizable over most of the study area. Marker 3 (M3) is defined as the top of a leftward deflection on the induction logs. Marker 4 (M4) is defined as a prominent leftward kick on the induction logs and a small rightward kick (high API values) on the gamma-ray logs. In cores, M4 is very distinctive and consists of several black mudstone layers 1 to 2 cm thick, interbedded with lighter-colored mudstone layers 1 to 7 cm thick (Subfacies 1c). Erosional Surface 2 (ES2) cuts deeply into the underlying sediment (Appendix B). It is most easily recognizable in the density

porosity logs as the base of an abrupt leftward deflection. On the induction logs, ES2 is picked at the base of an abrupt rightward deflection. However, in some induction logs, there is an unusual leftward deflection due to salt-water saturation. This is also picked as the base of ES2. In cores, ES2 is characterized by a sharp lithologic change from mudstone or siltstone to thick structureless sandstone (Facies 5). Marker 5 (M5) is defined as the top of the fill of the ES2 incision (or channel), or its correlative surface. In channelized wells, M5 is defined as a very sharp rightward deflection on the gamma-ray and density porosity logs (Appendix B). In unchannelized wells, it is defined as a small rightward deflection on the gamma-ray logs and a small leftward kick on the induction logs. Marker 6 (M6), Marker 7 (M7), Marker 8 (M8) and Marker 9 (M9) are defined as rightward deflections (higher API values) on the gamma-ray logs and leftward kicks on the induction logs (Appendix B). Their log signatures are most prominent in the northwestern part of the study area, and become weaker gradually away from that area. Erosional Surface 3 (ES3) is defined as the base of an abrupt rightward deflection on the gamma-ray logs and the base of an abrupt leftward deflection on the induction logs. The top of the Montney Formation (TM) is defined as the base of a very sharp rightward deflection on induction logs and the base of an abrupt rightward deflection on gamma-ray logs. It is noteworthy that although the gamma-ray signatures of ES3 and TM are similar, their induction log signatures are very different. ES3 is defined as the base of a leftward deflection, but TM is defined as the base of a rightward deflection (Appendix B).

All of the cross sections were made using both the induction (right) and gamma-ray (left) logs. Induction logs proved best for detailed correlation, but gamma-ray logs were useful in confirming the more difficult induction picks. Although density porosity logs have not been used in cross sections, they played a supplemental role in defining the base and top of the successions of thick structureless sandstones.

The base of the Montney Formation (BM) has been chosen as a datum for most of the cross sections for the following reasons: (i) Towards the east, the sub-Jurassic and a number of intra-Triassic unconformities truncate progressively older strata of the Montney Formation so that upper markers are absent in the eastern part of the study area. (ii) Whereas most of the markers established in the western part of the study area become gradually weaker and difficult to recognize toward to the east, BM is very prominent and easily recognizable throughout the entire study area wherever the Montney Formation is present.

M4 has been used as a datum in some detailed cross sections that examine channel morphology. In doing so, it is argued that M4 represented as flat a sea floor as could reasonably be reconstructed at that time.

Seven large well log cross sections have been included in the thesis (Fig. 4-1). They were selected from a network of more than 60 working cross sections. Three of the sections (A-A', B-B' and C-C') have been constructed to show the stratigraphic relationship between the eastern part of the study area characterized by clinoform successions, and the central and western part showing base of
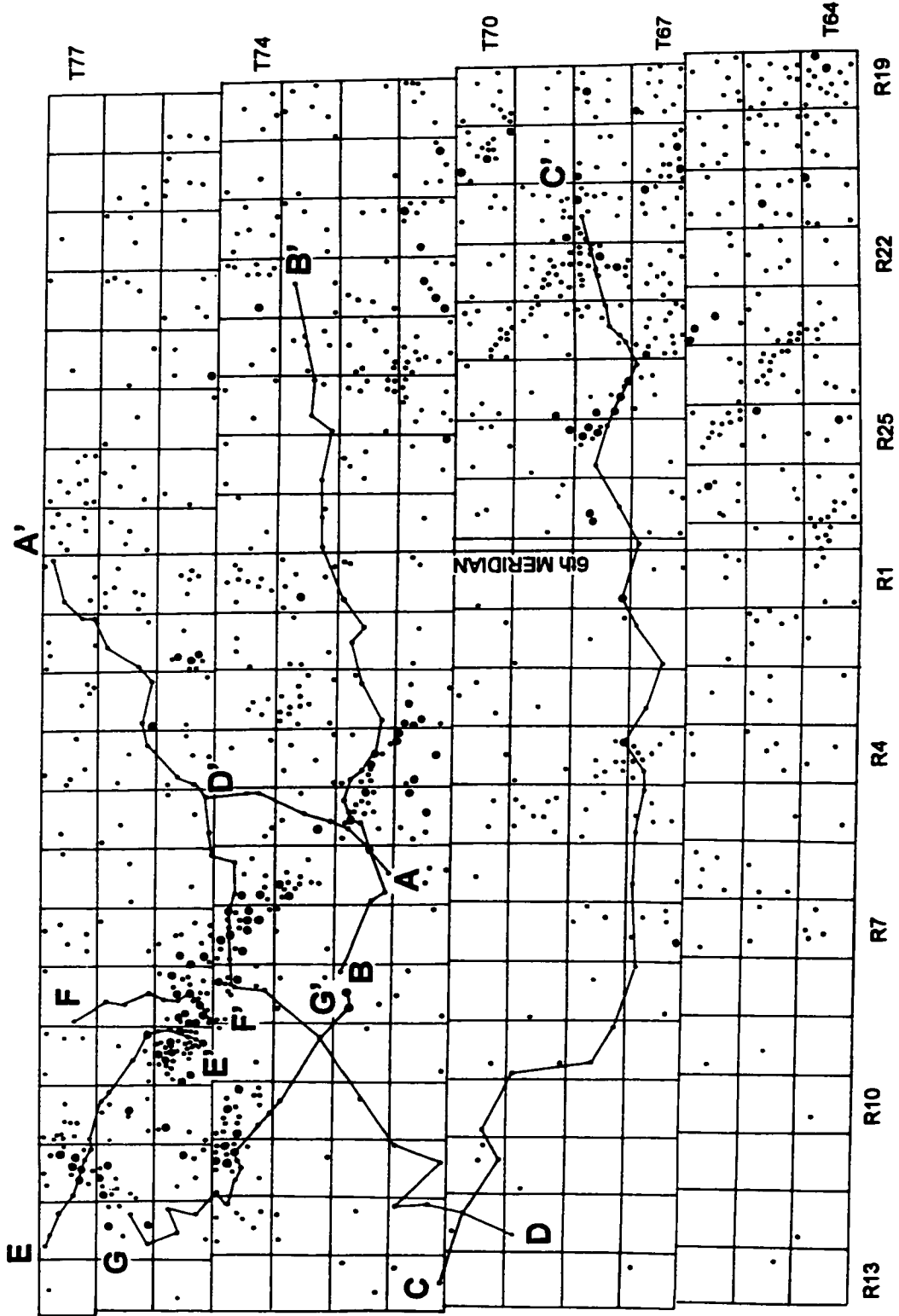
clinoform or basin floor successions. The remaining four cross sections (D-D' to G-G') show the vertical and lateral relationships within the deeper part of the basin. These cross sections were chosen because they best represent the vertical and lateral changes in geology within the study area. Three shorter cross sections ( H-H', I-I' and J-J') have been constructed to show details of the channel morphology. Finally, one cross section (K-K') has been constructed between the subsurface study area and outcrop, to show the stratigraphic relationship between the subsurface and outcrop.

## 4.2 Well Log Cross Sections

### 4.2.1 Cross Section A-A'

Cross section A-A' (Fig. 4-2) illustrates the stratigraphic relationship between the underlying clinoformal succession (Unit A) and overlying successions to the southwest. M1 and M2 are very prominent between 4-3-72-6W6 and 6-4-73-5W6. They become weaker to the northeast, but their general log characteristics are preserved until 2-11-76-4W6. M3 and M4 are prominent between 4-3-72-6W6 and 6-4-73-5W6, but they become difficult to recognize northeastward and are interpreted to onlap the clinoform near 6-22-73-5W6 and 10-12-74-5W6 respectively. M5 and M6 are easily correlated in the southwestern wells, but become difficult to correlate as their log signals become weaker to the northeast. M7 and overlying markers are very difficult or impossible to correlate in this section because their log signals are too weak or completely lost.

# NOTE TO USERS

Page(s) not included in the original manuscript
are unavailable from the author or university.  The
manuscript was microfilmed as received.

70

This reproduction is the best copy available.

Unit A (between BM and M1) consists of a series of southwesterly-dipping clinoforms and their equivalent successions. The clinoforms thin dramatically downslope (southwestward). In the northeastern wells (between 2-36-77-1W6 and 4-8-76-3W6) the thickness of Unit A is relatively constant, ranging from 155 m to 164 m. However, from 4-8-76-3W6 southwestward, Unit A becomes gradually thinner and is only 49 m thick in 4-3-72-6W6. In northeastern wells, the base of the dolomitized coquina beds is an erosional surface (ES1) as shown by truncation of a regional log marker between 8-13-77-2W6 and 4-29-77-1W6. ES1 appears to pass into a conformable surface to the southwest. The lower part of Unit A (BM to ES1) is characterized by aggradation with slight progradation, whereas the upper part (ES1 to M1) of Unit A shows prominent progradation to the southwest. The restored angle of the clinoforms using present compacted thickness is not as impressive as cross section A-A' implies - it is only about 0.2 to 0.3 degrees.

Unit B and the lower part of Subunit C1 gradually onlap against the former clinoform slope. Subunit B1 onlaps against the former clinoform slope (M1) between 2-11-76-4W6 and 4-8-76-3W6. More prominent onlapping appears to occur against the M2 surface. Between 6-22-73-5W6 and 10-13-74-5W6, Subunits B2 , B3 and the lower part of Subunit C1 onlap against M2. It appears that the whole of Unit B and lower part of Subunit C1 are absent north of 4-8-76-3W6.

A prominent feature of Subunit C1 is a deeply incised channel (ES2) in 16-29-72-5W6 as evidenced by erosion of regional log markers. The serrated induction log profiles in 10-13-72-6W6 and 6-4-73-5W6 have been truncated and

replaced with blocky responses in 16-29-72-5W6. Cores in nearby wells indicate that whereas the serrated interval consists of alternating thin-bedded sandstones and siltstones with abundant mud partings (Facies 4), the blocky interval (16-29-72-5W6) consists of thick structureless sandstones 29 m thick (Facies 5). In a nearby well, 7-31-72-5W6, the channel is even more deeply incised into the underlying sediments and the channel-fill succession reaches 41 m in thickness. Subunit C2 has a relatively constant thickness, but it is difficult to know the trends of Unit D and higher units in this section because their associated markers are too weak to recognize. Between 4-3-72-6W6 and 4-8-76-3W6, the Montney Formation is overlain by the Doig Formation, but from 11-1-76-3W6 northeastward, it is overlain unconformably by the Jurassic Fernie Formation. Northeastward, the sub-Jurassic unconformity cuts progressively deeper into the Montney Formation.

## 4.2.2 Cross Section B-B'

Cross section B-B' (Fig. 4-3) illustrates stratigraphic relationships between the eastern part of the study area and the central part. M1 is easily recognised across this entire area. M2 and M3 are very prominent in the western part of the section but become weaker to the east. M4 has been recognized in most wells in this section. M5 and upper markers become weaker and unrecognizable eastward.

As in cross section A-A', Unit A consists of westerly-dipping clinoforms. However, the thickness and slope gradient in this section are less than those of section A-A'. In eastern wells (10-7-73-25W5 to 13-16-73-24W5), the thickness is

# NOTE TO USERS

Page(s) not included in the original manuscript are unavailable from the author or university. The manuscript was microfilmed as received.

73

This reproduction is the best copy available.

UMI

relatively constant (121 m to 129 m), but westward from 10-7-73-26W5 it becomes gradually thinner and is only 40 m thick in 7-36-72-8W6. The restored angle of the clinoforms is about 0.1 degree.

Unlike section A-A', the prominent onlapping of Units B and C against the former clinoform has not been recognized in section B-B'. The thickness of Subunit B1 has a maximum value of 17 m in 14-14-72-4W6 and 10-23-72-3W6, and it decreases eastward and westward. Subunits B2 and B3 become gradually thinner eastward from 37 m in 6-18-72-6W6 to less than 5 m in 10-23-72-3W6. Subunit C1 thins gradually to the west. A deeply incised channel in Subunit C1 is present in 9-28-72-5W6 as shown by the truncation of regional log markers. The fill is up to 39 m thick, and cores show that it consists of thick structureless sandstones with very thin mudstones layers. The thickness of Subunit C2 is relatively constant between 10-21-72-5W6 and 11-32-72-1W6, but it decreases rapidly from 10-21-72-5W6 westward. The remaining upper units thicken rapidly from 10-21-72-5W6 westward. Between 7-36-72-8W6 and 11-32-72-1W6, the Montney Formation is overlain by the Doig Formation, but from 10-7-73-26W6 eastward, it is overlain unconformably by the Jurassic Fernie Formation. Eastward, the sub-Jurassic unconformity cuts progressively deeper into the Montney Formation.

## 4.2.3 Cross Section C-C'

Cross section C-C' (Fig. 4-4) illustrates the stratigraphic relationship between the eastern and western parts of the study area, over a distance of about 200 km.

# NOTE TO USERS

Page(s) not included in the original manuscript are unavailable from the author or university. The manuscript was microfilmed as received.

75

This reproduction is the best copy available.

UMI

M1 and M2 are very prominent between 8-36-67-8W6 and 11-29-67-3W6. Their log signatures become weaker both to the east and west, but their characteristic log signatures are preserved and enable the log markers to be recognized. Between 6-36-67-27W5 and 7-3-67-27W5, correlation of M1 is difficult, but other markers above and below M1 suggest that the stratigraphic position of M1 is very close to the top of the dolomitized coquina beds in the eastern part of the sections. M3 and M4 are easily recognizable west of 11-29-67-3W6. These markers appear to converge between 6-18-67-2W6 and 6-35-67-2W6. Correlation of M5 is difficult because of its subtle log signature and long distance of this section from the channel. Correlation of M6 is also difficult because of its subtle log signature and long distance from the northern areas where M6 can be more easily recognized.

As in sections A-A' and B-B', Unit A consists of westerly-dipping clinoforms. However, in this section, Unit A is much thinner. In eastern wells (from 6-36-67-27W5 eastward), the thickness of Unit A is relatively constant, ranging from 94 m to 102 m. However, from 6-36-67-27W5 it thins westward and varies in thickness from 24 m (11-31-69-9W6) to 42 m (12-27-70-12W6). The restored angle of the clinoforms is about 0.1 degree.

The base of the dolomitized coquina beds is characterized by a regional erosional surface (ES1) as evidenced by truncation of log markers between 10-36-67-24W5 and 13-22-68-22W5. ES1 appears to become a conformable surface to the west. The dolomitized coquina beds are characterized by blocky log responses, and are very well developed between 7-3-68-24-W5 and 13-22-68-22W5.

Thicknesses range from 8 m to 13 m. The coquinas thin rapidly to the west and cannot be traced beyond 3-9-68-24W5. Unit B is well developed in this section as compared with section A-A' and B-B'. Between 7-31-67-5W6 and 6-2-68-4W6, it has a maximum thickness of 60 m and thins gradually away from these wells. The thickness trends of Subunits B1, B2 and B3 suggest their progradation to the west.

Subunit C1 has a relatively constant thickness of about 40 - 50 m between 6-18-67-2W6 and 14-20-68-25W5. Its thickness decreases gradually to the west to less than 5 m in the westernmost well. Core in 6-2-68-4W6 shows that the base of Subunit C1 has a sharp lithologic transition from dark mudstone (Facies 1) to thin-bedded turbidite sandstone (Facies 4), and may indicate an erosional contact. The channel incision (ES2) of sections A-A' and B-B' is absent in this section. Between 10-1-68-9W6 and 11-32-67-6W6, Subunit C2 is relatively thick (more than 60 m). Its thickness decreases to the east and west, but more rapid thinning occurs to the west.

Thickness trends of Unit D, Subunit E1 and Subunit E2 are similar to that of Subunit B2, in that thinning occurs in both directions from a well showing the maximum thickness. However, the depocenter gradually moved to the west. It is noteworthy that the combined thickness of Unit C, D and E decreases dramatically from 6-20-68-9W6 westward. Unit F is very thin or absent to the east of 10-1-68-9W6. It becomes thicker rapidly from 11-3-70-11W6 westward and reaches 35 m in 11-4-71-13W6. It appears that the rapid thinning of Unit F to the east is due to a combination of depositional thinning and an erosional event (ES3). Unit G is very

thin or absent to the east of 11-3-70-11W6. It becomes dramatically thicker to the west and reaches 80 m in 11-4-71-13W6. From 6-36-67-27W5 westward, the Montney Formation is overlain by the Doig Formation, but from 14-20-68-25W5 eastward, it is overlain unconformably by the Jurassic Fernie Formation. Eastward, the sub-Jurassic unconformity cuts progressively more deeply into the Montney Formation.

### 4.2.4 Cross Section D-D'

Cross section D-D' (Fig. 4-5) illustrates stratigraphic relationship between the north-central part of the study area and the southwest. This section does not show all of the clinoform successions but covers only the distal part of the clinoforms and their deeper equivalent successions. Although lateral thickness changes of each depositional unit are appreciable, most of log markers can be fairly well correlated. Unit A decreases gradually in thickness to the southeast, with slight variations. As in section A-A', Subunits B2, B3 and the lower part of Subunit C1 onlap against Subunit B1. Subunit C1 contains a deeply incised channel (ES2) as evidenced by erosion of regional log markers. The channel cuts about 20 m into the underlying sediment. Unlike sections A-A' and B-B', thick structureless sandstones (Facies 5) occur not only within the channel but also outside the channel, up to 10 km from the channel axis. The sandstones gradually become thinner and finer away from the channel axis (e.g. in wells 7-30-74-7, 7-27-74-7 and 10-3-74-8). Subunit C2, and Units D, E and F have almost same thickness trends as shown in section C-C'. The

# NOTE TO USERS

Page(s) not included in the original manuscript are unavailable from the author or university. The manuscript was microfilmed as received.

79

This reproduction is the best copy available.

thickness trends show a gradual southwestward shift in position of the depocenters. Unit G becomes thicker rapidly to the southwest.

## 4.2.5 Cross Section E-E'

Cross section E-E' (Fig. 4-6) illustrates the stratigraphic relationship between the Valhalla field (T75 R9W6M) and the Glacier field (T77 R12W6M). Although lateral thickness variations of each unit occur, all the log markers can be easily correlated. Unit A and Subunit B1 have relatively uniform thicknesses except that Unit A in the northwestern 3 wells (6-32-77-12, 11-28-77-11 and 10-23-77-12) is slightly thicker than elsewhere. A prominent feature of Subunit B2 is development of the interval characterized by low values in gamma-ray logs and high values in induction logs in Glacier field (11-10-77-11, 6-11-77-11 and 7-1-77-11). The log signals of the interval gradually weaken laterally. Between 1-16-76-9 and 14-6-77-10, the thickness of Subunit B3 and Unit C increases rapidly from 30 m to 63 m. Unit C1 contains a deeply incised channel (ES2) as shown by the truncation of regional log markers. Thick structureless sandstones (Facies 5) occur even outside the deepest part of the channel as shown by blocky log responses in 8-25-75-9W6 and 6-36-75-9W6. The sandstone thins laterally and passes into mudstone away from the channel axis. Unit D also contains turbidite deposits (Facies 4 and 2) interbedded with mudstones, characterized by serrated log signals. The turbidites pass laterally into mudstones, as indicated by lateral weakening of log signals, but significant erosional surfaces have not been

Figure 4-6. Cross section E-E', composed of gamma-ray and induction well logs.

Oriented NW-SE. Note a deeply incised channel in 6-11-75-9W6. Black bar

indicates cored interval.

# NOTE TO USERS

Page(s) not included in the original manuscript are unavailable from the author or university. The manuscript was microfilmed as received.

81

This reproduction is the best copy available.

UMI

recognized. The thicknesses of Unit D and Subunit E1 decrease slightly to the northeast. Subunit E2 has a relatively uniform thickness. Unit F has a maximum thickness in the northwestern wells of about 70 m. It thins gradually to the southeast as a result of erosion (ES3), as shown by the truncation of regional log markers. Unit G has a relatively uniform thickness ranging from 20 m to 30 m.

## 4.2.6 Cross Section F-F'

Cross section F-F' (Fig. 4-7) illustrates the stratigraphic relationship from the Valhalla field (T74 R8W6) northward. All log markers are very easily correlated. In the northern wells, Subunit B2 is characterized by the interval of low values on gamma-ray logs and high values on induction logs. The log signals of the interval gradually weaken laterally. Subunit C1 shows a deeply incised channel (ES2) centered in 6-6-75-8W6. The channel cut about 20 m down into the underlying sediment at its axis and becomes shallower away from the axis. Thick structureless sandstone (Facies 5) occurs away from the channel axis (up to 14 m thick in well 6-8-75-8, 7-16-75-8 and 15-21-75-8), but the sandstone succession becomes thinner away from the channel. Subunit B3, and Units C and D become thicker gradually to the north, and Units E and F are slightly thicker in southern wells. The thickness of Unit G is relatively constant and ranges from 12 m to 15 m.

## 4.2.7 Cross Section G-G'

Cross section G-G' (Fig. 4-8) illustrates the stratigraphic relationship

# NOTE TO USERS

Page(s) not included in the original manuscript are unavailable from the author or university. The manuscript was microfilmed as received.

83-84

This reproduction is the best copy available.

UMI

between the Glacier field (T76 R12W6M) and the Knopcik field (T74 R10W6M). Most of the log markers are very easily correlated. Unit A and Subunit B1 become slightly thinner to the northwest. Unit B2 in 14-14-76-12 is characterized by an interval of low API gamma-ray values. The log signals of the interval gradually weaken southwestward. The most prominent feature of this section is the extremely reduced thickness of the interval between M2 and M6 in 5-25-74-12. In this well, Subunits B2 and B3 were not deposited or were removed by erosion. From this well both to the southeast and northwest, the interval between M2 and M6 becomes gradually thicker. Wells 5-25-74-12, 9-20-74-11, 2-22-74-11 and 7-23-74-11 show a channel incision and the interval is characterized by the low API values on the gamma-ray logs. Unit D becomes thicker to the southeast. Unit E has a maximum thickness of 90 m in 5-25-74-12 (the same well that showed a minimum thickness for the M2-M6 interval) with thickness decreasing both northwestward and southeastward. Unit F becomes thinner to the southeast by erosional truncation (ES3). Unit G thins to the southeast and it is absent southeast of 2-11-73-9.

## 4.2.8 Cross Sections H-H', I-I' and J-J'

Cross sections H-H', I-I' and J-J' (Fig. 4-10) illustrate the detailed morphology of the channel incision with respect to adjacent beds. In these sections, M4 was used as the datum to prevent possible distortion caused by differential subsidence before channel incision took place. Inferred upstream (southeast) section H-H' shows a narrow, deeply incised channel. The channel incision in 9-28-72-5W6 is
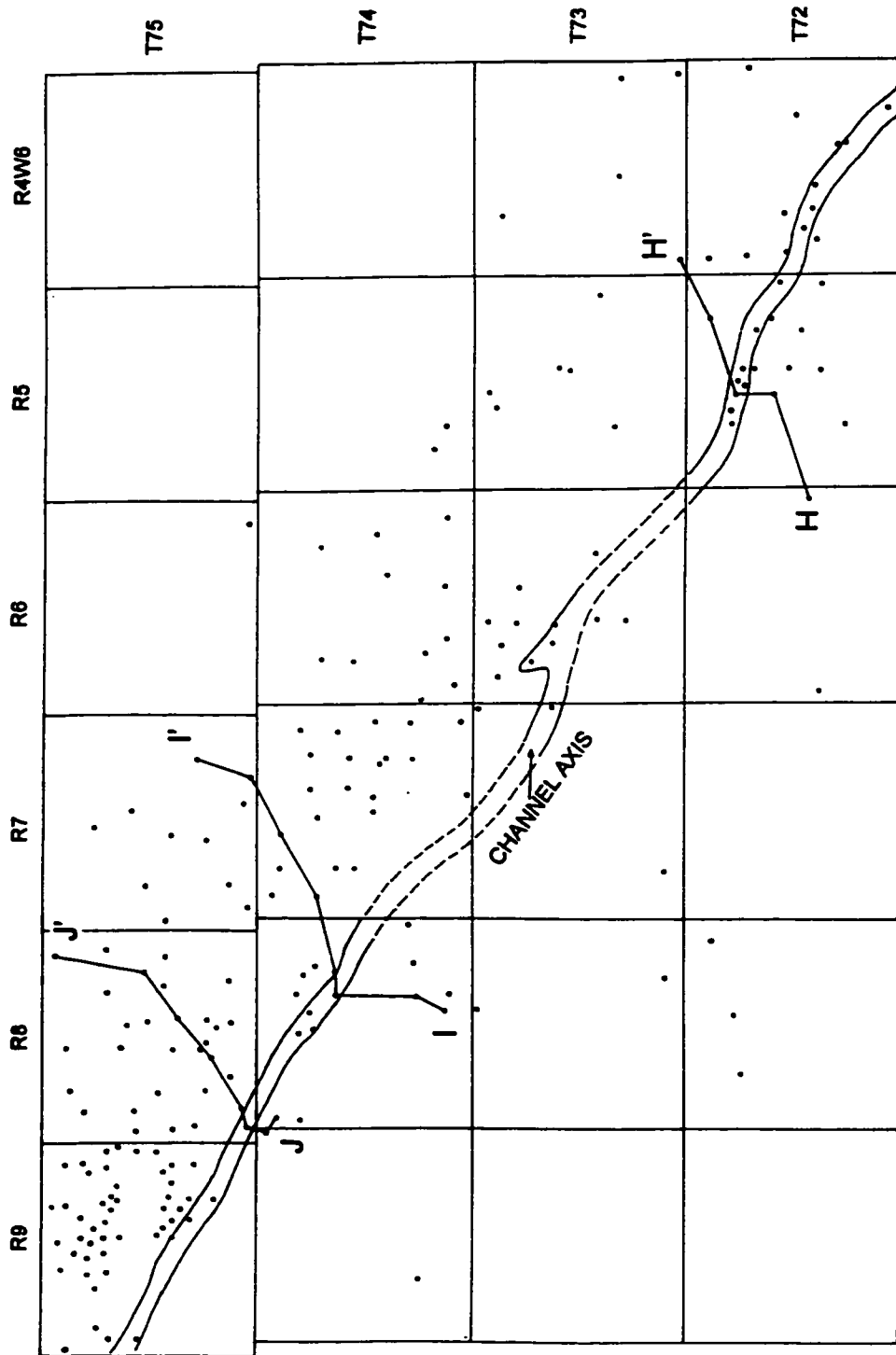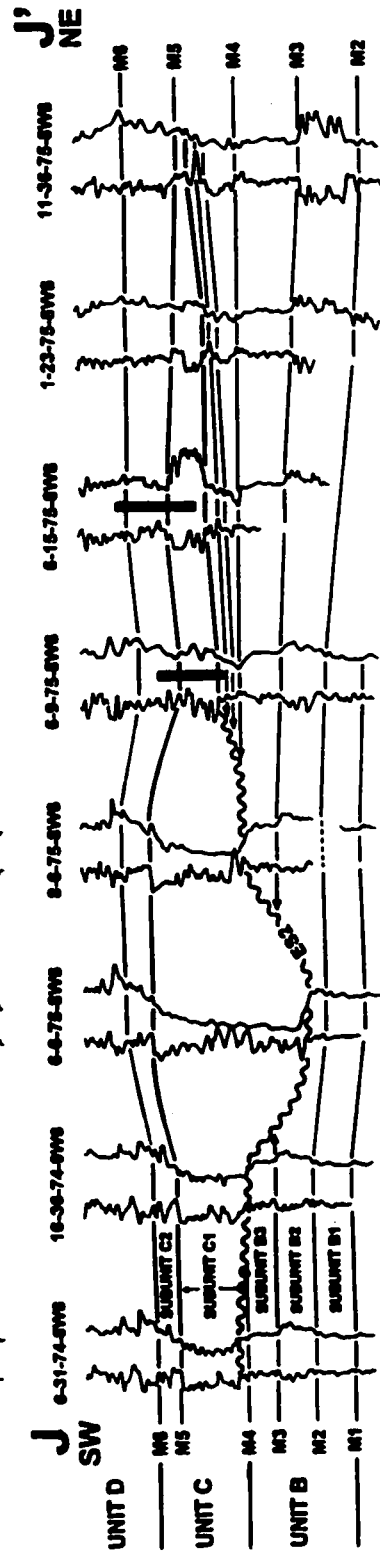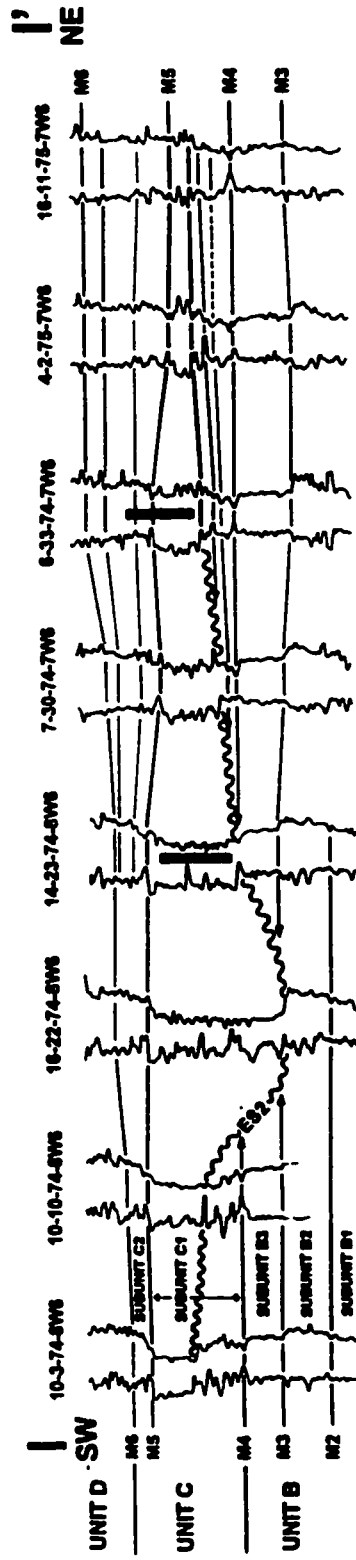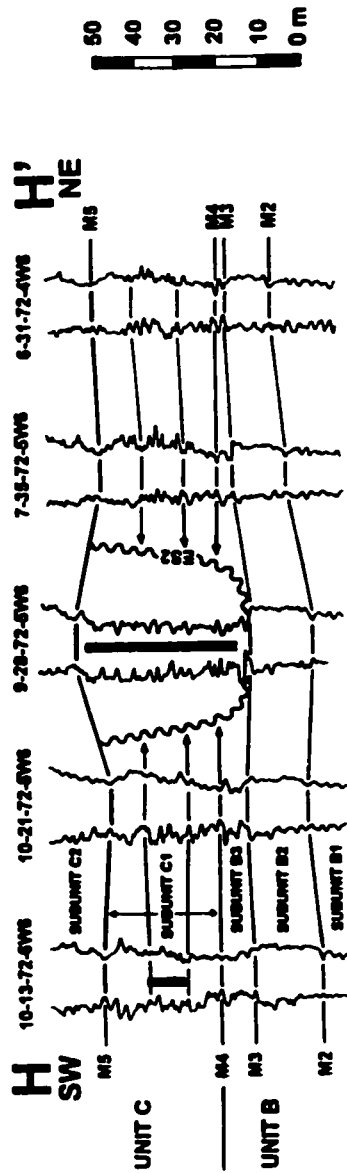
evidenced by the erosion of regional log markers and their replacement by a leftward-deflected blocky response in the induction log. In density-porosity logs, the interval is characterized by very prominent blocky responses. In 9-28-72-5W6, the entire 36 m of core consists of thick structureless sandstones with very thin mud layers (Facies 5). However, in core 10-13-72-6W6 outside the channel, the rocks consist of thin bedded sandstones alternating with abundant mudstones (Facies 4). Well logs and cores indicate that in the upchannel position, the channel is relatively narrow (about 1 km) and that thick sandstones occur only within the channel.

Downstream sections I-I' and J-J' show different channel morphologies from the upchannel section H-H'. In 16-22-74-8W6 in section I-I', the channel cut down into the lower part of Subunit C1, Subunit B3 and the uppermost part of B2, replacing the original rocks with thick sandstones. The channel becomes gradually shallower toward the margins and is broader than the channel in H-H'. Also, in I-I' and J-J', the thick structureless sandstones occur not only within the channel (as in H-H') but also outside the channel. From 6-33-74-7W6 to the northeast, the base of the thick structureless sandstone succession appears to be more conformable and less erosional on the underlying sediment, suggesting that the area is outside the channel. The sandstones thin laterally and grade into mudstones away from the channel axis. Farther downchannel, section J-J' shows almost identical charactetistics to section I-I'.

The change from a deeply incised channel in the southeast to a shallower, wider channel to the northwest is part of the reason for inferring sediment transport

from southeast to northwest, and hence the upstream position of section H-H'.

## 4.2.9 Cross Section K-K'

Cross section K-K' (Fig. 4-12) illustrates the stratigraphic relationship between the subsurface and outcrop. Three wells (6-21-76-12W6, 6-5-76-12W6 and 6-20-75-13W6) lie within the main study area. Well c-27-E/93-P-6 lies within the deformed belt, and the outcrop sections have been constructed from Gibson's (1972) description. Although the recognition of some of the log markers becomes difficult to the southwest, the existence of some prominent markers such as M1, M3, M4, ES3 and TM makes reasonable correlations possible. The most prominent markers are ES3 and TM. Both are characterized by a very sharp change of gamma-ray signature from low to high API values. It is unclear whether ES3 in this section is an erosional surface or not, but the very sharp deflection in the gamma-ray logs possibly favors an erosional surface. At the base of the Doig Formation, the rapid oscillations of the gamma-ray log (this stratigraphic interval has been commonly called "the phosphatic zone") are well developed between 6-21-76-12W6 and a-10-A/93-P-10, thus defining the TM surface in these wells. However TM in c-27-E/93-P-6 is more difficult to pick because of an apparent change in the gamma-ray response in that well. It appears that in the deepest part of the basin, the phosphatic zone characterized by high gamma-ray values was not well developed. In c-27-E/93-P-6, some intervals having high gamma-ray values occur, but their stratigraphic positions are lower than that of the gamma-ray zone at the
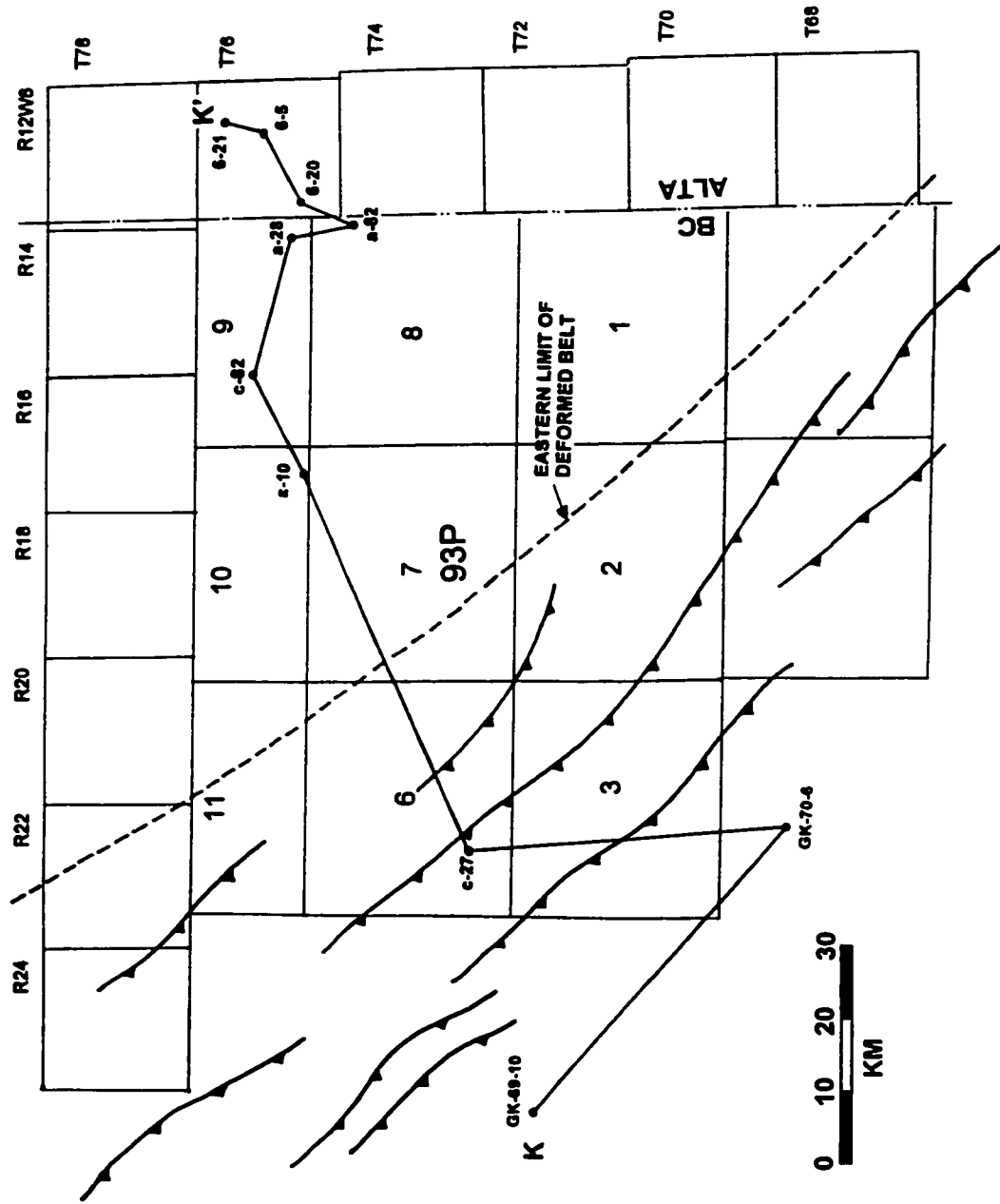
# NOTE TO USERS

Page(s) not included in the original manuscript are unavailable from the author or university. The manuscript was microfilmed as received.

91

This reproduction is the best copy available.

base of the Doig Formation. Gibson and Edwards (1990b) correlated TM in a-10-A/93-P-10 to the base of interval X. However, considering the gradual thickening of Unit G southwestward in the section, their correlation is unlikely. Miscorrelations of TM are shown in the literature, caused mostly by the confusion of TM with ES3. For example, the top of the Montney Formation in several wells (13-11-77-16W6, 11-11-80-17W6 and 6-9-85-19W6) in Figure 16.12 of Edwards et al. (1994) is not the real top of the Montney Formation (TM) but ES3 surface. Mispicking of TM is also shown in their isopach map, Figure16.24 (Figure 2-3 in this thesis), where the extremely thin values (less than 50 m to 150 m) of the Montney Formation in northeastern British Columbia east of Williston Lake is the result of confusion of TM with ES3 surface. In that area, the real thickness of the Montney Formation ranges from 195 to 340 m. It should be noted that the ES3 horizon is not the top of the Montney. In the Montney type section well (Fig. 2-2A), the top of the Montney lies about 120 feet (36 m) above the ES3 horizon.

The thicknesses of Units A and B are relatively constant with a slight thinning of Subunit B3 to the southwest. Units C and D become gradually thinner to the southwest. Units E and F thin rapidly to the southwest. Unit G has a very different thickness trend from those of the underlying units, and thickens very rapidly to the southwest. In a-10-A/93-P-10 and c-24-E/93-P-6, its thickness exceeds 150 m.

In the outcrop sections (GK-70-6 and GK-69-10), the most distinctive and easily recognizable lithologic boundary occurs at the base of the Whistler Member. At several localities in outcrop, the basal part of the Whistler Member commonly

contains a phosphatic pebble conglomerate with pebbles up to 2 inches (5 cm) in diameter. In GK-69-10, the basal two feet (60 cm) of the Whistler Member contains angular and well rounded phosphatic clasts and grains up to 1 inch (2.5 cm) in diameter. GK-70-6 also contains phosphatic clasts and grains up to ½ inch (1.25 cm) diameter in the basal part of the Whistler Member. This conspicuous lithologic boundary occurs 81 m above the base of the Phroso-Vega Siltstone Members in GK-70-6 and 120 m above the base in GK-69-10. In several nearby outcrops, the boundary occurs 81-129 m above the base of the Phroso-Vega Siltstone Member. The boundary occurs abruptly at the top of a coarsening succession in both GK-70-6 and GK69-10. The basal phosphatic pebble interval of the Whistler Member in outcrop has traditionally been correlated with the basal phosphatic shale interval (high gamma-ray zone) of the Doig Formation. However, the cross section suggests that the basal phosphatic pebble interval of the Whistler Member in outcrop is better correlated with ES3 in subsurface, where ES3 is characterized by a very sharp gamma-ray peak at the top of a slight coarsening-upward succession.

More detailed correlations below ES3 between the subsurface and outcrop are much more difficult. Above ES3, interval X (the basal part of the Llama Member) is characterized by dense and well indurated (commonly cliff-forming) rocks in outcrop. It appears to be correlated with interval X as characterized by a blocky gamma-ray response in c-27-E/93-P-6. Exact correlation of the base of the Doig Formation with outcrop sections is very difficult. Even between outcrops, the lithologic changes of some intervals near the inferred boundary are variable.

The Whistler Member contains ammonoids indicating a lower and middle Anisian age. The overlying Llama Member contains ammonoids indicating a late Anisian to late Ladinian age. In the subsurface, little is known of the faunas. The only known ammnoids are from one locality (7-7-80-12W6), just above the base of the Doig Formation. They have been identified by Stelck (in Hunt and Ratcliff, 1959) as *Nathorsitites* and *Parapopanoceras* indicating a Ladinian age. Later Tozer (1967) reexamined these specimens and suggested that they indicate an early Anisian age. He stated that "Professor Stelck permitted the writer to examine these specimens, which are fragmentary and not well preserved. The best specimen is the outer part of a whorl showing a ceratitic suture. What remains of this specimen suggests identification with *Grambergia ovinus* (McLearn) or *Grambergia nahwisi* (McLearn)." Tozer's suggestion is not compatible with the correlations in this study. It is possible that the specimens are not well enough preserved for exact identification.

## CHAPTER 5:   GEOMETRIES OF STRATIGRAPHIC UNITS

### 5.1  Introduction

The cross sections in Chapter 4 demonstrated the continuity of many regional log markers and erosional surfaces. Now that these markers have been correlated, stratigraphic units defined by the markers can be mapped. This chapter focuses on the geometries of stratigraphic units defined by the isopach maps.

Because of progressive deep truncation by post-Montney unconformities, and difficulties in tracing markers eastward, only the isopach map for Unit A covers the entire study area. The remaining isopach maps cover the area west of R2W6M. Instead, part of British Columbia from the Alberta/British Columbia border to the edge of deformed belts has been mapped. The British Columbia area contributes significantly to the understanding of regional trends in unit geometries. In several isopach maps, some areas (particularly in the northwest around T81 R23W6M) have not been contoured because of difficulties in recognizing the markers. However isopach maps for several units combined enable recognition of overall patterns of sediment accumulation.

### 5.2  Unit A

The isopach map of Unit A is shown in Figure 5-1. The most prominent features of Unit A are 1) southwesterly-dipping clinoforms and 2) the "offset" of

R23W6         R20'

5

40

30  20

10

10

20

30
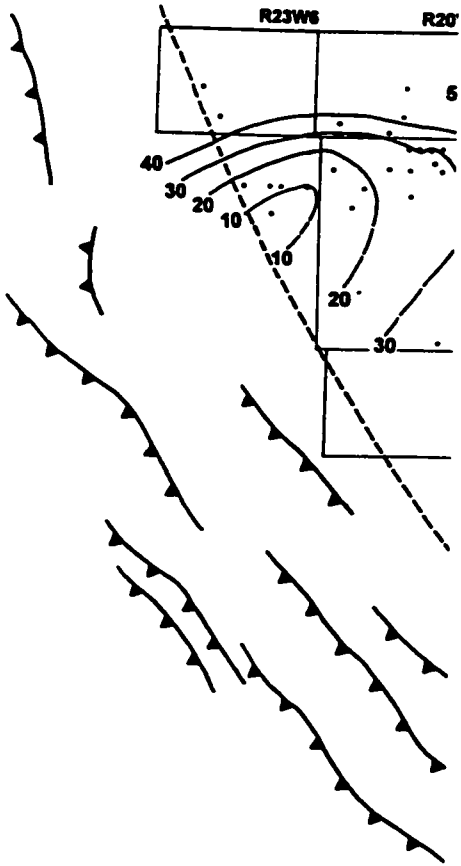
EASTERN LIMIT OF
DEFORMED BELT

isopachs in Glacier field (around T77 R12W6). Overall, Unit A thins to the southwest with a dominant northwest to southeast isopach trend. The thickest accumulation of sediment is in T77 R1W6M where Unit A is about 160 m. Wedge or lobate shapes are defined by the 130-160 m isopachs, but for isopachs lower than 120 m, the trends are straight and parallel, striking northwest to southeast. Assuming that BM is horizontal, the angle of the clinoform calculated from the isopach map is about 0.2 degrees around T76 and 0.08 degrees around T70 (in the calculation, the 50-100 m isopachs were used and the calculations refer to compacted thicknesses).

One prominent feature of the map is the northeastward "offset" of the northwest-southeast trending isopachs from the the British Columbia/Alberta border to the area of T78 R10W6. The offset of the 40 m and 50 m isopachs is about 50 km. An offset with almost the same orientation also occurs in Unit B, but its location is about 1-2 km southeast of that in Unit A.

Although the overall trend of Unit A shows thinning toward the deformed belt (to the southwest), some irregularities occur in the deeper part of the basin where isopachs show Unit A to be 10 to 20 m thinner or thicker than surrounding areas. The thin area (informally named the"75-11 High") around T75 R11W6 shows thinner sediment accumulation than surrounding areas in Units A, B and C. The lowest isopach values occur in the northwest (T81 R23W6M) where the minimum thickness of Unit A is only 7 m.

## Unit A: Possible Structural Influences

The overall southwestward thinning trend and the distribution of dolomitized coquina beds in the eastern part of the map (east of the dotted line) suggest that the main source of Unit A was to the northeast. However, the isopach map for Unit A also suggests that sediment accumulation was influenced by Paleozoic structures. Comparison of the isopach map (Fig. 5-1) with the Paleozoic fault map (Fig. 7-8) suggests that very thick sediment accumulation in the northeastern part of the area may have been influenced by the reactivation of Paleozoic faults. The Rycroft, Teepee and Dunvegan Faults (Fig. 7-8) trend northwest to southeast and are all downthrown on the northeastern side. These faults seem to have partially influenced sediment accumulation, as suggested by the difference of thickness between T77 R1W6M and T64 R22W5M. In both areas, the uppermost part of Unit A is capped by dolomitized coquina, indicating similar water depths at the final stage of Unit A in both areas. However, Unit A in T77 R1W6M is about 70 m thicker than in T64 R22W6M. The thickness difference seems to be the result of differential subsidence of fault blocks. The lobate isopachs between 140 m and 160 m, and the protruding tongues of dolomitized coquina beds, all trending northeast to southwest, suggest that faults trending northeast to southwest also influenced sediment accumulation. The southwestward "offset" of isopachs from T78 R10W6 to T77 R13W6 also suggests the influence of faults on sediment accumulation. No fault has previously been reported in that area. The "offset" is parallel to the northeast to southwest-trending Paleozoic faults and it persists into

Unit B. The lowest isopach values (7 m) in T81 R23W6M suggest structural influence on sediment accumulation, because this area lies on the Hudson Hope Low where Carboniferous and Permian sediments are thickest. The 7 m isopach occurs over the Paleozoic graben axis, and indicates the change from maximum subsidence (Paleozoic) to minimum subsidence (Mesozoic).

## 5.3 Unit B

The isopach map of Unit B is shown in Figure 5-2. The most prominent features of Unit B include (1) the development of the depocenters in the southeastern and northwestern part of the map area, onlapping against the former clinoform, (2) the "offset" of isopachs in the Glacier Field area, and (3) thin sediment accumulation in the area around T75 R11W6. The thickest sediment accumulations occur in two areas, around T81 R14W6 (up to 98 m) and T65 R5W6M (up to 65 m). The T65 R5W6 thick trends NNE-SSW. Note particularly that in the T71-77 R2-7, Unit B thins dramatically against the clinoform defined in Unit A. Unit B is again relatively thin (slightly less than 20 m) in the area of the "75 -11 High" defined in Unit A. The "offset" of isopachs in the Glacier Field area is also present, but its location is 1-2 km southeast of that in Unit A.

The isopach map of Subunit B1 is shown in Figure 5-3, and is similar to the map of Unit B (Fig. 5-2). As in Unit B, the thickest sediment accumulation developed in the southeastern part of the study area. The isopach thick is up to 38 m, and is centered in T67 R4W6M. It trends north to south. Subunit B1 is very thin

UNIT B

SUBUNIT B1

EASTERN LIMIT OF
DEFORMED BELT

SUBUNIT B2

EASTERN LIMIT OF
DEFORMED BELT

103
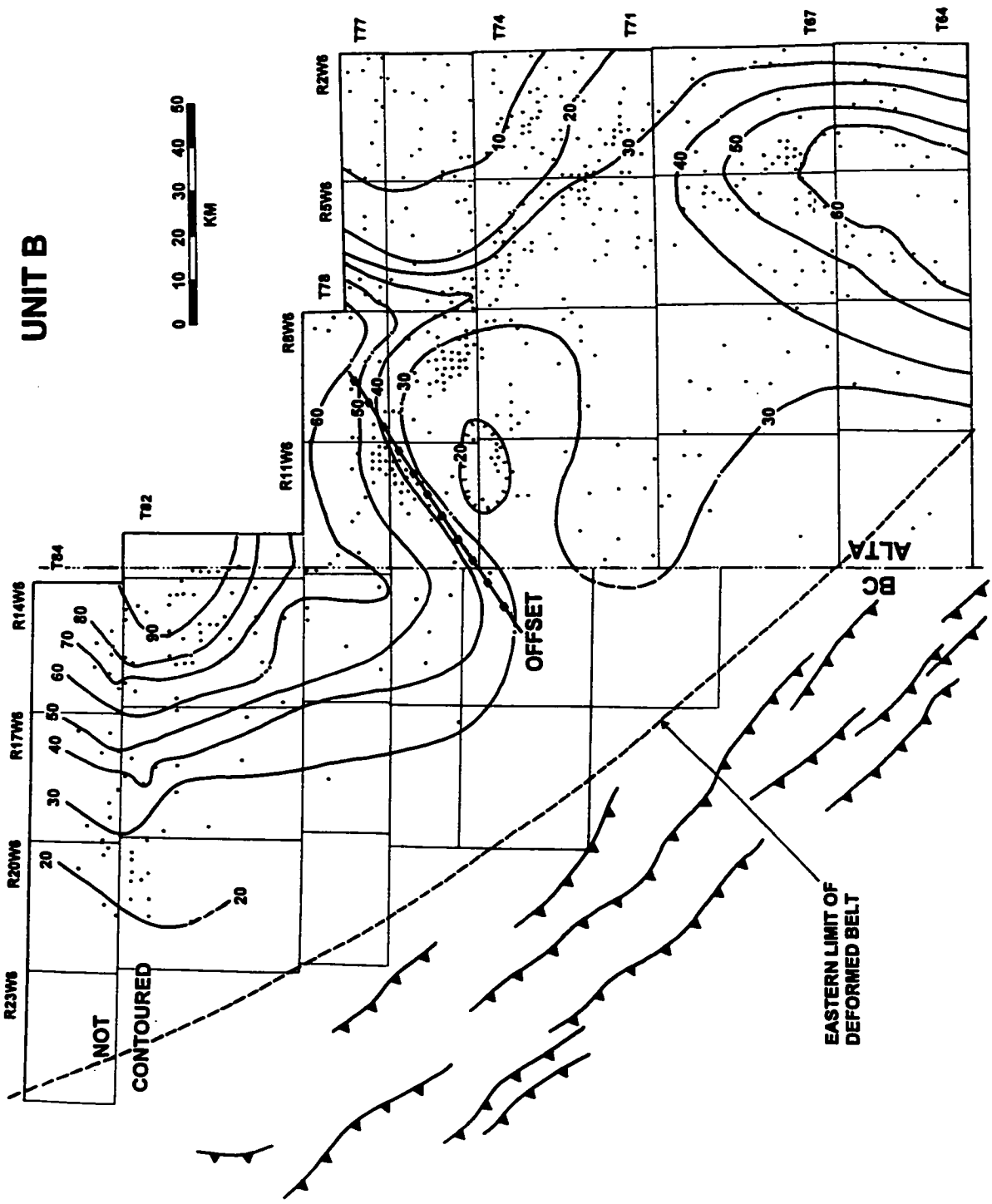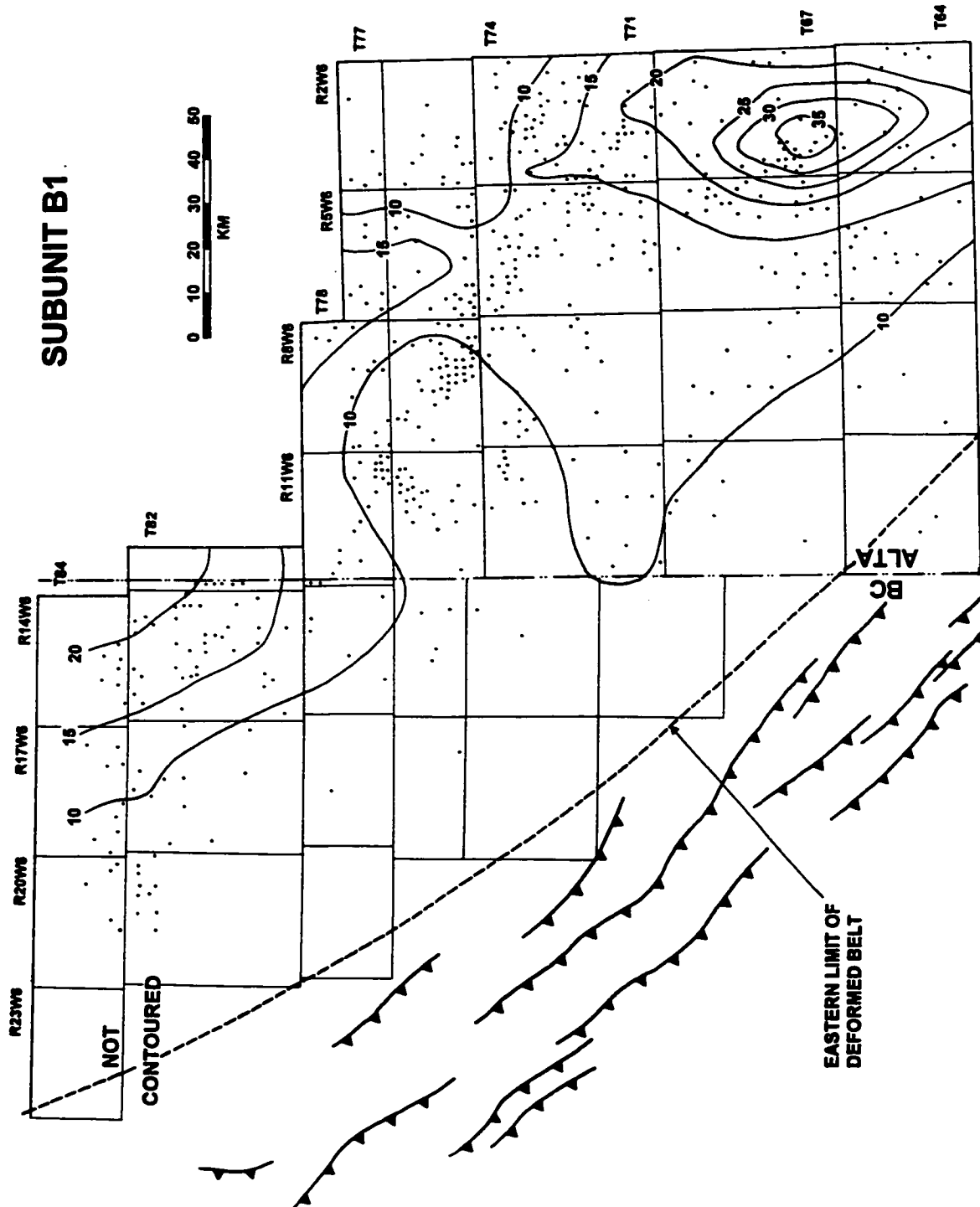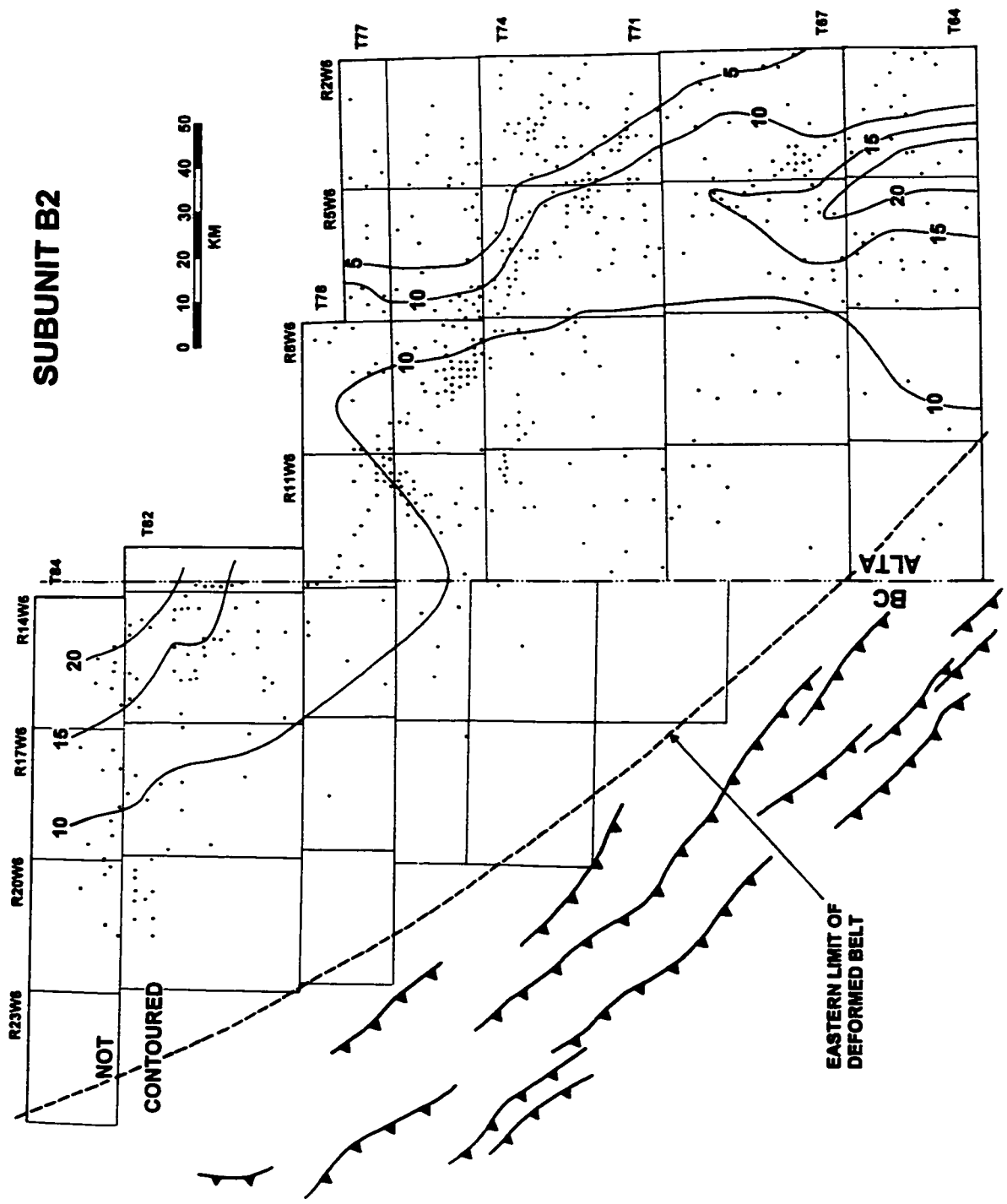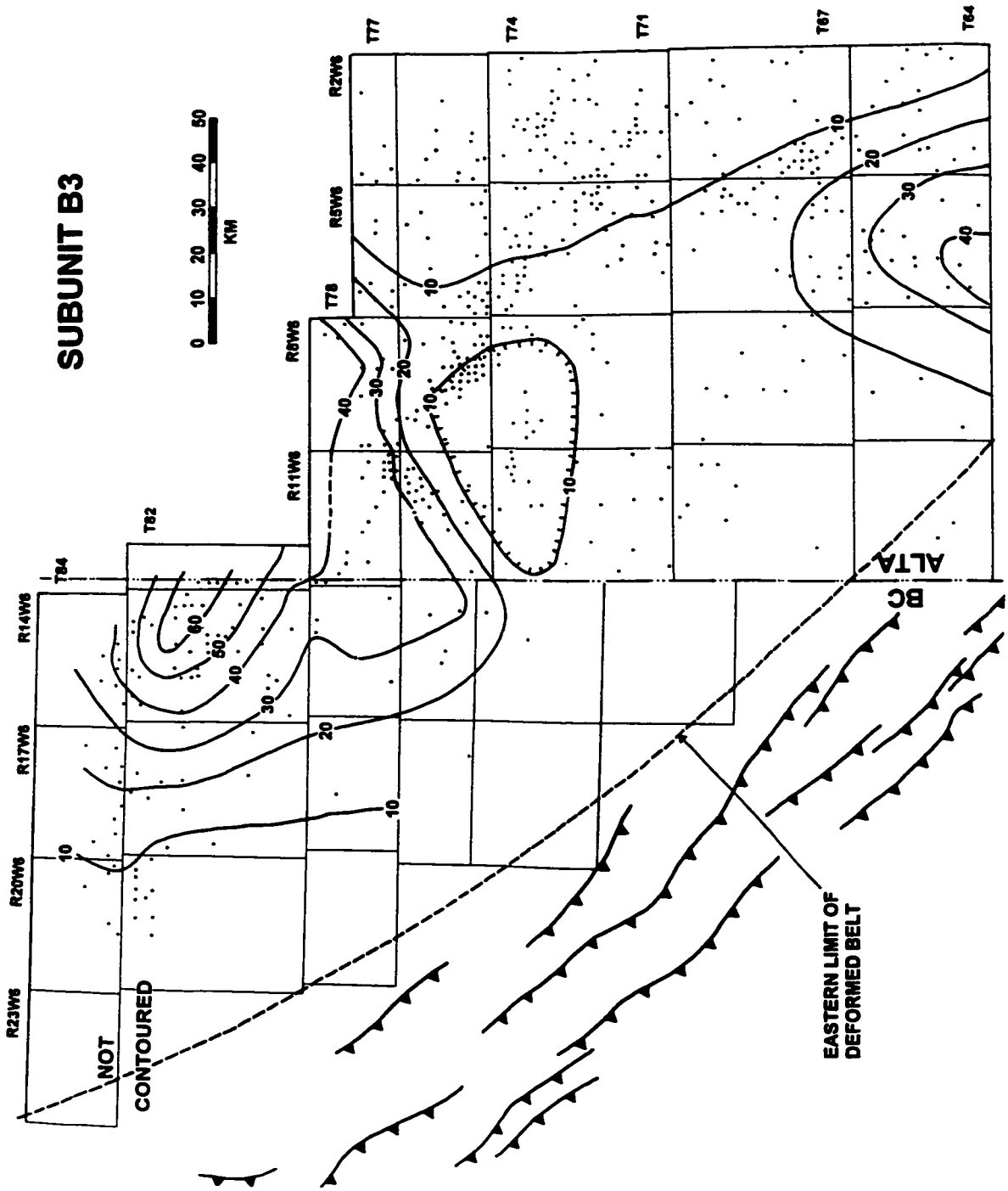


SUBUNIT B3

where Unit A is thickest.

The isopach map of Subunit B2 is shown in Figure 5-4, where the isopachs are very similar to those of Unit B and Subunit B1. The thickest sediment accumulation is up to 23 m in the area of T64 R4W6M. Isopach trends are also roughly north to south. Comparison of Figure 5-4 and Figure 5-3 shows that the depocenter shifted slightly southward. Subunit B2 is consistently very thin, north of about T70.

The isopach map of Subunit B3 is shown in Figure 5-5. The general pattern is similar to that of Subunits B1 and B2, but the B3 depocenter has shifted westward compared with the B2 depocenter. However, a B3 depocenter has developed in the T81 R14W6M area; it is lobate or wedge-like and trends northwest to southeast. The thick is up to 65 m and lies on the axis of the Paleozoic Fort St. John Graben.

## Unit B: Interpretation

Basin reorganization took place between Unit A and Unit B. Northwest-southeast trending clinoform deposition in Unit A, with the main sediment source to the northeast, was abandoned. Unit B onlapped against the former clinoform slope and is very thin or absent on the upper part of the slope. The Subunit B1 depocenter lies on the top of the lower part of the clinoform. New depocenters trending north-south (Subunits B1 and B2) and northeast-southwest (Subunit B3) occur in the southeast, and may indicate a gradual change of basin configuration. The Unit B depocenter (trending northeast to southwest) in the southeast suggests

that in the southern part of the study area, the main source was to the southeast.

The wedge-like shape of the thick sediment accumulation in Subunit B3 around T81 R14W6M and its development over the axis of the Paleozoic Fort St. John Graben indicate reactivation of Paleozoic faults. The persistence of thin sedimentation on the "75-11 High", and the strong northeast-southwest isopach trends in Glacier Field also suggest structural control on sediment accumulation.

## 5.4 Unit C

The isopach map of Unit C is shown in Figure 5-6. The most prominent features of Unit C are 1) the very thick sediment accumulation in the southeast, and 2) the development of two depocenters in the northwest. Unit C is slightly thicker than 90 m in the southeast. It thins gradually to the northwest. The isopachs trend consistently northeast-southwest. Note that the isopach trends in Unit C, particularly in the area T64-77 R2-13, are almost perpendicular to the trends in Unit A. The northeast -southwest trend changes in the northwestern part of the area, where the dominant trend is northwest to southeast. Two areas of thicker accumulation developed around T77 R11W6 and T82 R17W6, with maximum thicknesses of about 45 m. The "75-11 High" area defined in Units A and B is again present, with relatively thin deposits (< 20 m) on top.

The isopach map of Subunit C1 is shown in Figure 5-7, with trends similar to those in Unit C. The thickest sediment accumulation developed in the east, with thinning to the west and northwest. It is noteworthy that the northwest-pointing

UNIT C

SUBUNIT C1

# SUBUNIT C2



EASTERN LIMIT OF
DEFORMED BELT
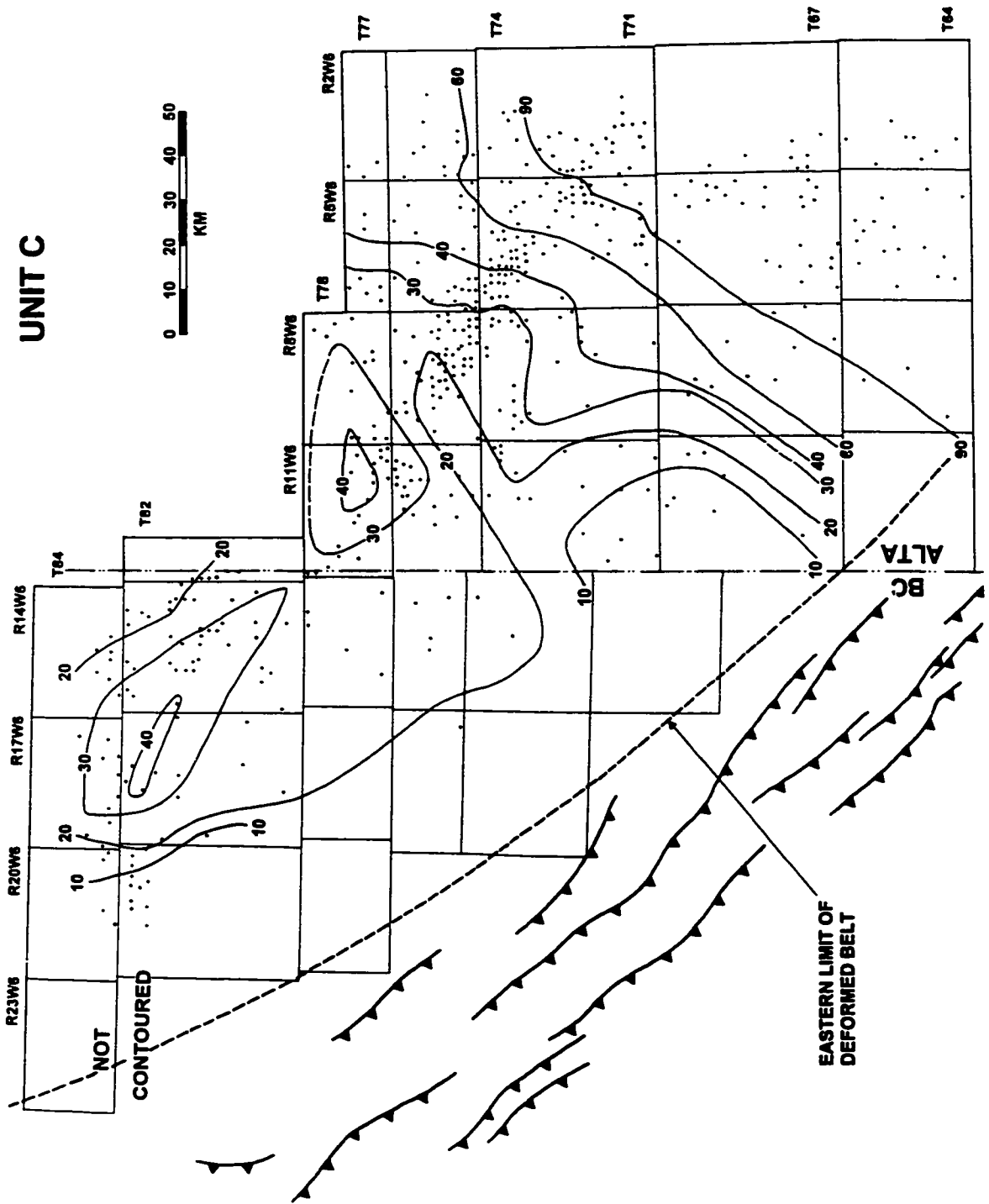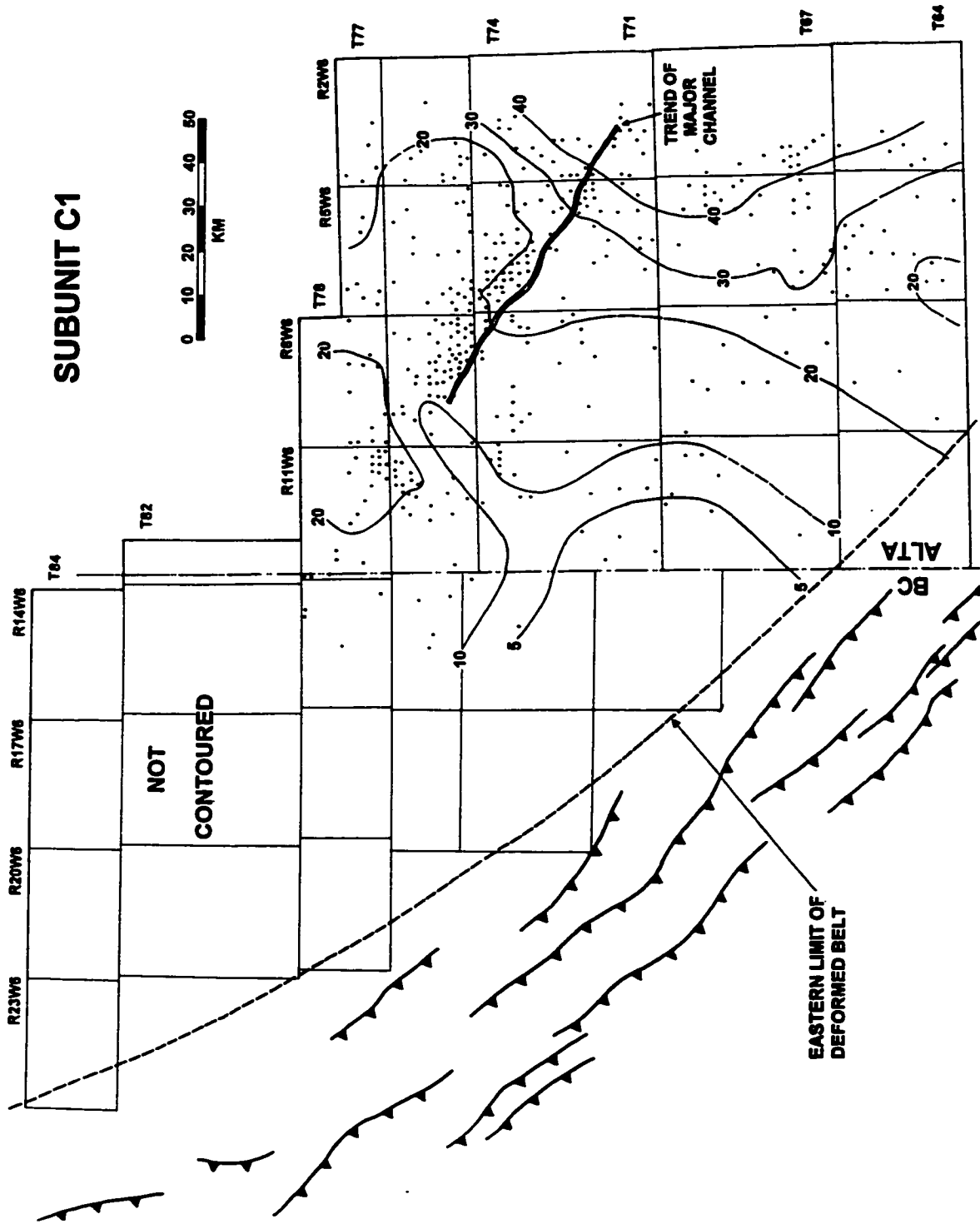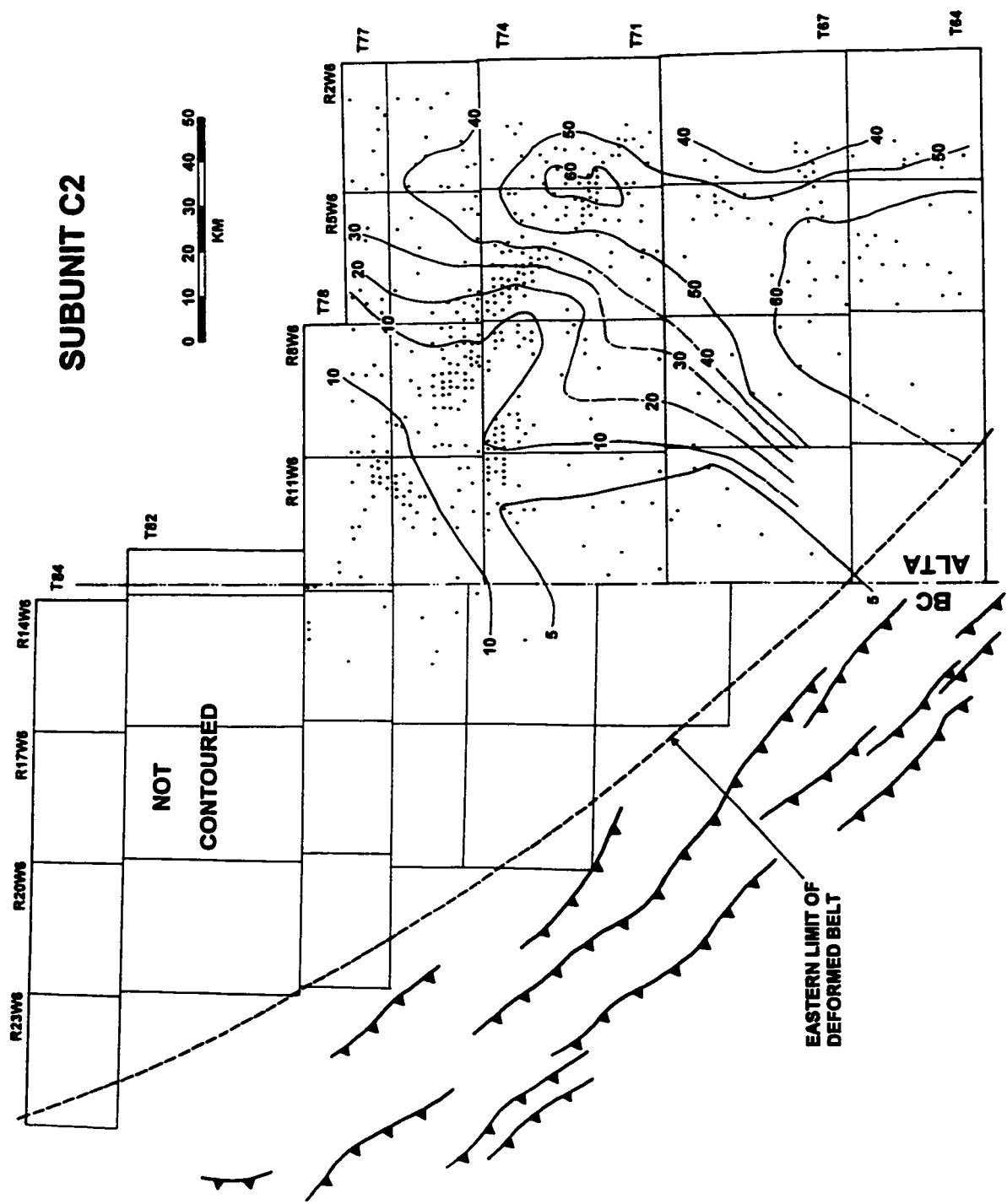
tongue defined by the 20 m isopach around T73 R7W6 is closely related to the location of the Montney channel, as defined in Figure 4-9. Note that the previously inferred dispersal direction for the channel, southeast to northwest, is supported by the overall direction of sediment thinning defined by the isopachs in Figure 5-7.

The isopach map of Subunit C2 is shown in Figure 5-8. The most prominent feature of the map is the development of a thick (maximum of about 70 m) tongue of sediment that trends NNE-SSW in the southeastern part of the area. In general, Subunit C2 thins northwestward away from this tongue.

The overall northwestward thinning (Figures 5-6, 5-7 and 5-8) suggests that the main sediment source was in the south and southeast. The 40 m isopach (Figure 5-6) may suggest either areas of increased subsidence, or another source in the north or northeast.

## 5.5 Unit D

The isopach map of Unit D is shown in Figure 5-9. A thick accumulation of sediment is defined by the 50 m and 60 m isopachs in the area of T77 R7W6M; it is wedge-shaped and trends northwest-southeast. Another thick accumulation occurs in the T83 R17W6M area, where the thick again trends northwest-southeast. Unit D becomes thinner southwestward, to less than 10 m in the deformed belt. Over most of the area, the isopachs trend northwest-southeast, but in the southeast, they have a northeast-southwest orientation, similar to those in Unit C.

Comparison of Units D and C (Figures 5-9, 5-6) indicates that fundamental

UNIT D

EASTERN LIMIT OF
DEFORMED BELT
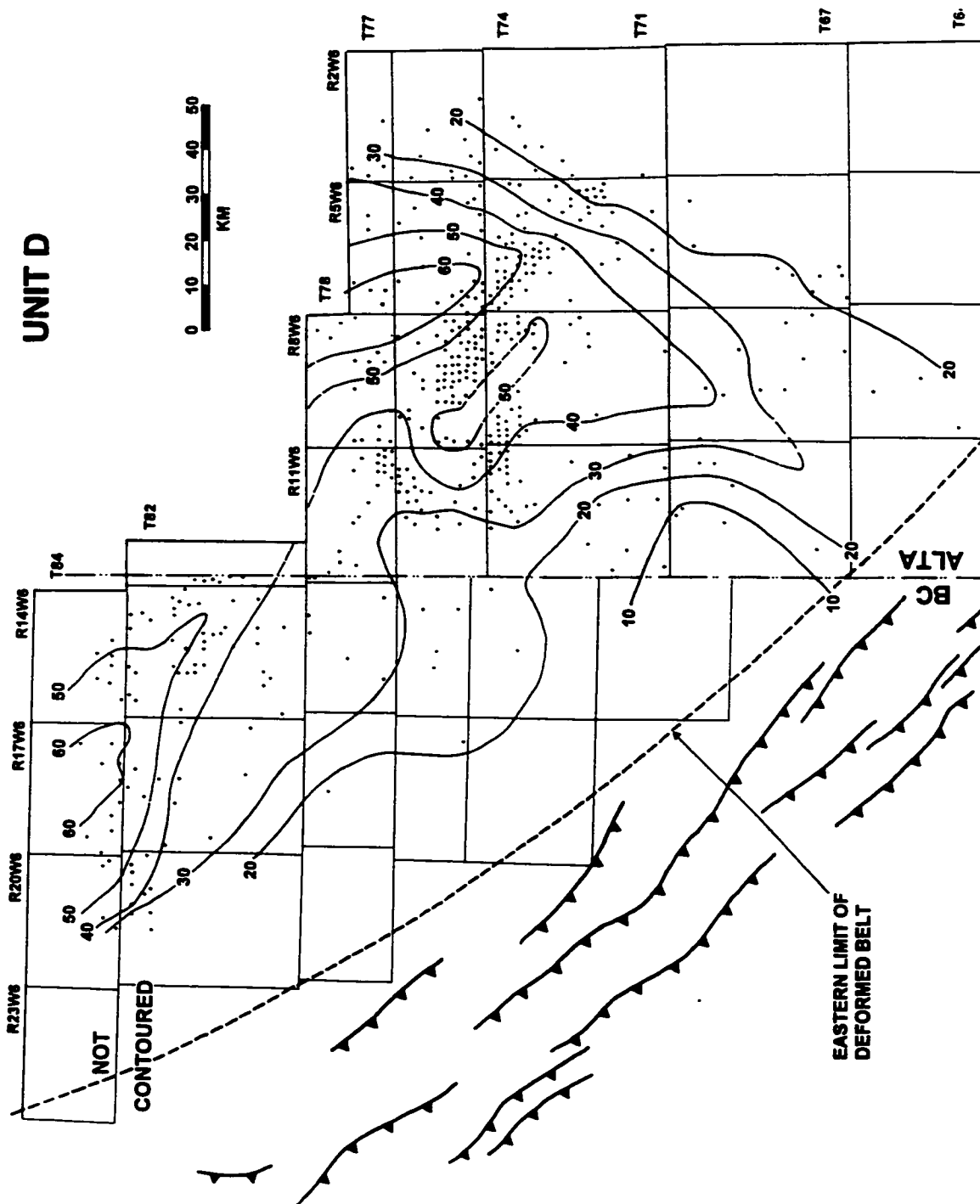
changes in the sediment accumulation pattern occurred between Units C and D. The thick Unit C depocenter in the southeast is not present in Unit D but a new depocenter has developed in the area around T77 R7W6M. Unit D is thick in the T83 R17W6M area, and its occurrence over the axis of the Paleozoic Fort St. John Graben suggests the reactivation of Paleozoic faults.

## 5.6 Unit E

The isopach map of Unit E is shown in Figure 5-10. The most prominent feature is a thick (up to 86 m) accumulation of sediment centered in T74 R12W6M. The thick is elongate and trends north to south. In the northwest, isopachs trend northwest-southeast and Unit E becomes thinner to the southwest.

Comparison of Unit E (Fig. 5-10) and Unit D (Fig. 5-9) indicates a southwestward shift of the depocenter from T77 R7W6 to T74 R12W6. The isopach maps of Subunits E1 and E2 are shown in Figure 5-11 and 5-12. Subunits E1 and E2 have very similar isopach trends to Unit E.

## 5.7 Unit F

The isopach map of Unit F is shown in Figure 5-13. A thick (up to 58 m) accumulation of sediment occurs in the T76 R12W6 area. Comparison of Unit F (Fig. 5-13) with Unit E (Fig. 5-10) indicates a northward shift of the depocenter from T74 R12W6 to T76 R12W6.

UNIT E

EASTERN LIMIT OF
DEFORMED BELT

SUBUNIT E1

SUBUNIT E2

UNIT F
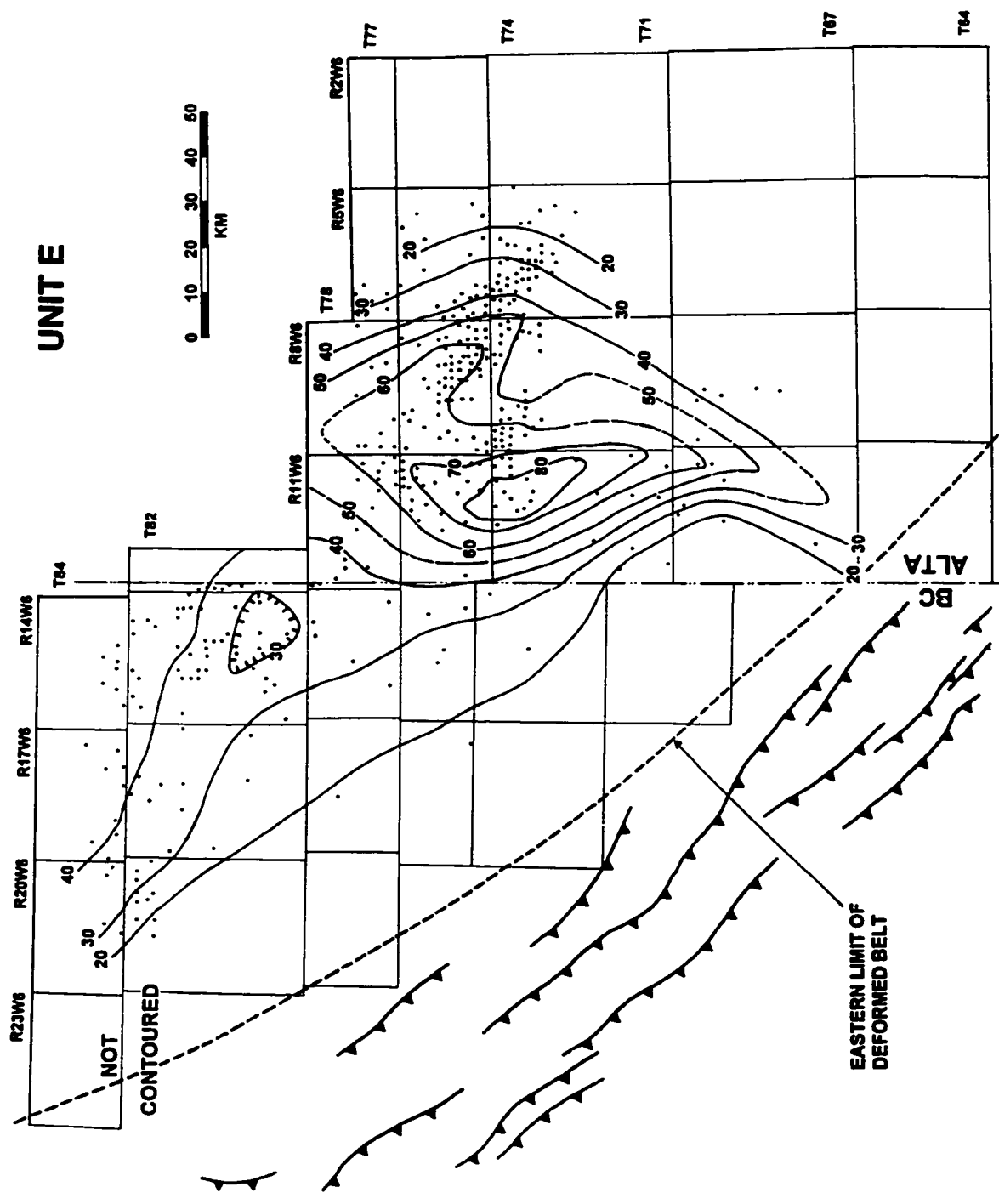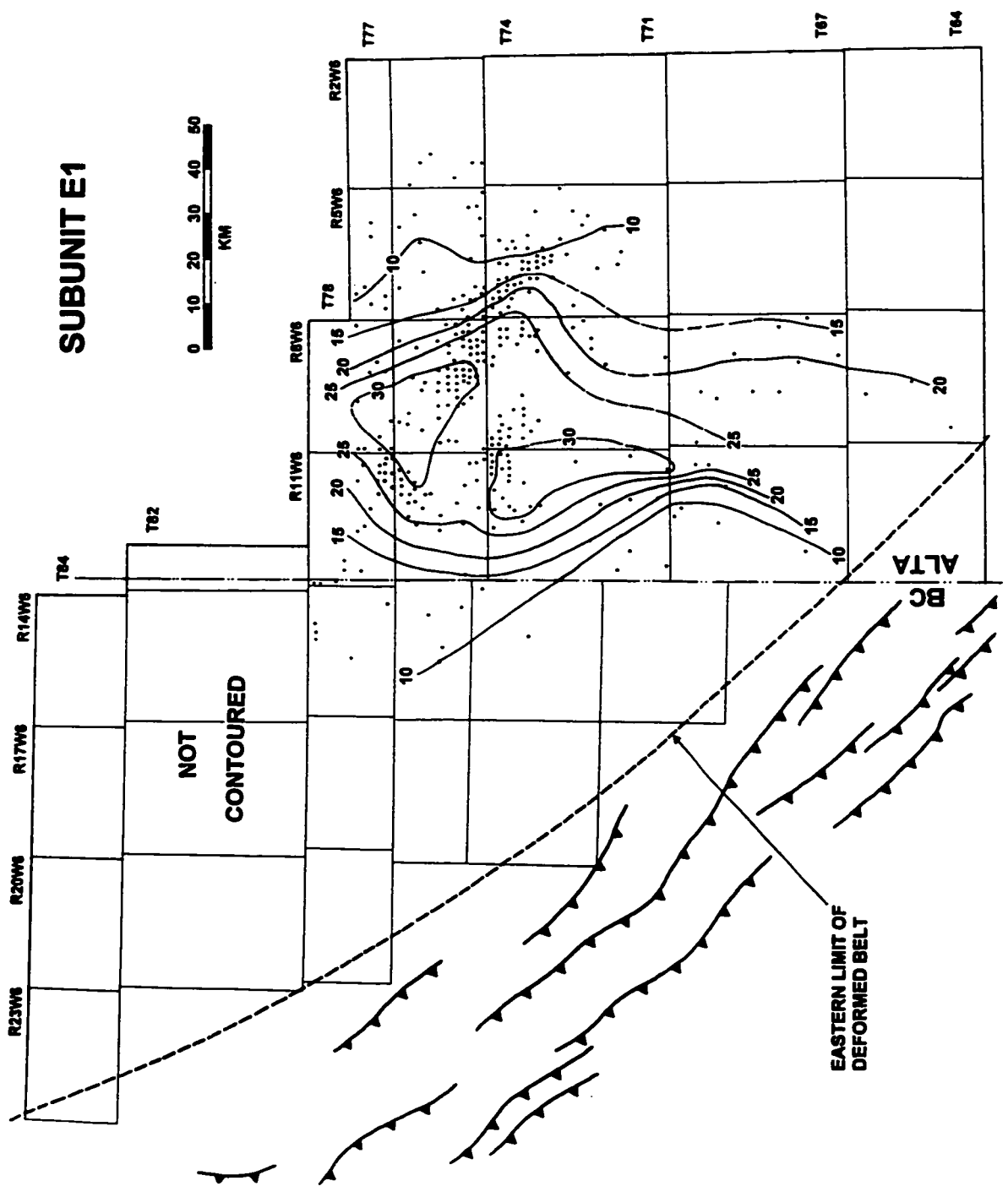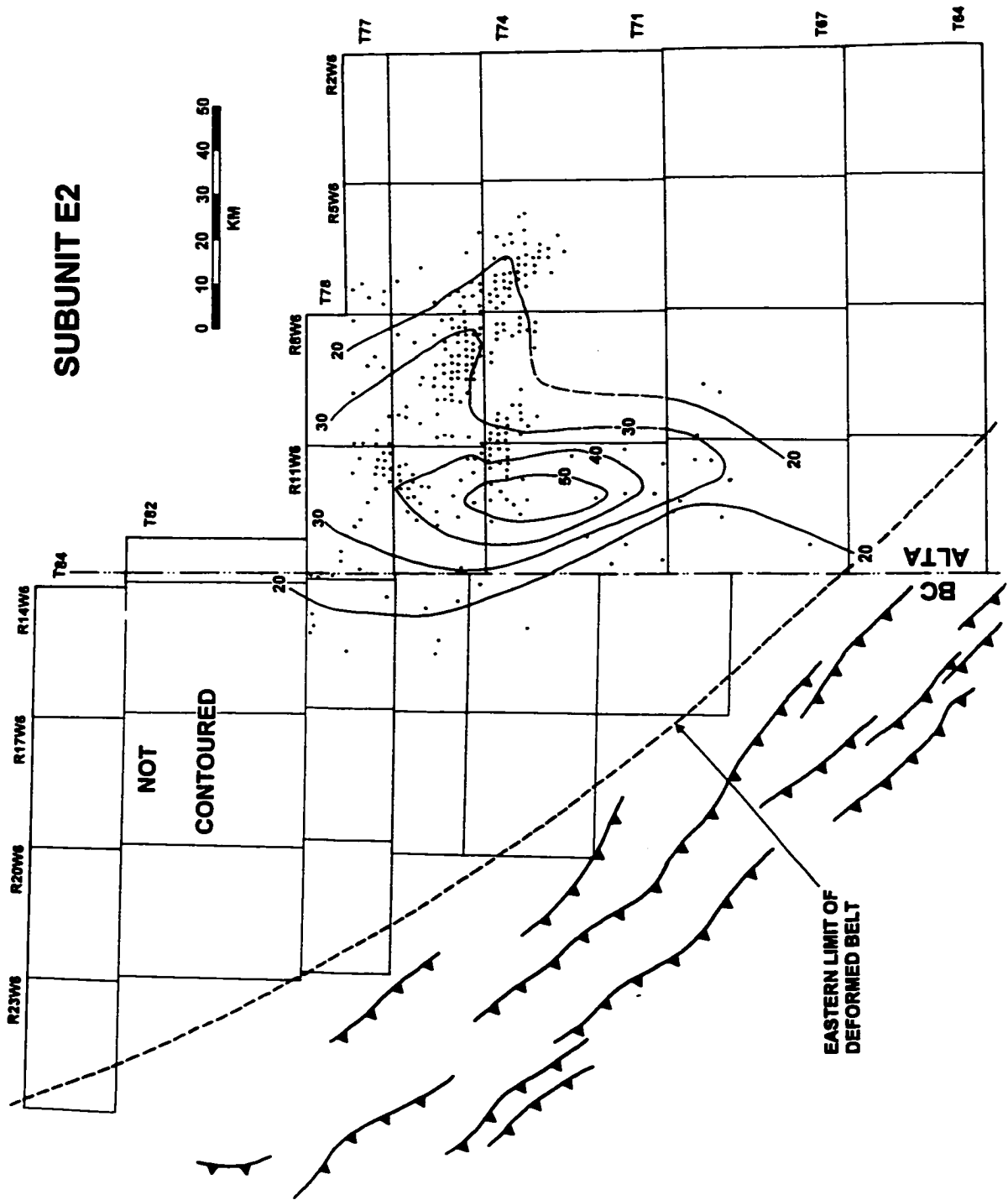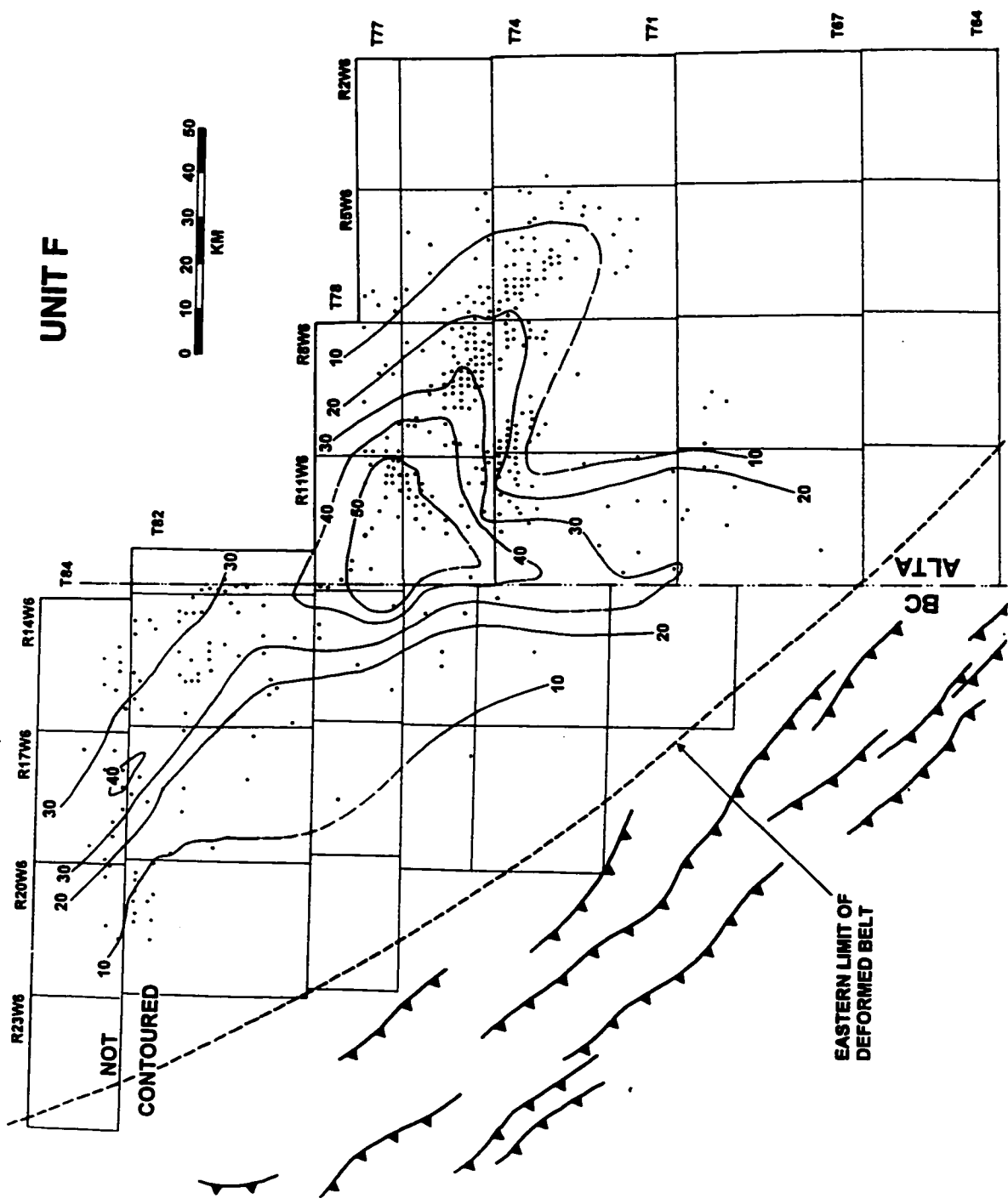
## 5.8 Unit G

The isopach map of Unit G is shown in Figure 5-14. It differs from all previous units in that the sedimentary wedge thickens southwestward, towards the deformed belt. In the deformed belt, Unit G is commonly thicker than 150 m, and approaches 200 m in places. To the northeast, Unit G thins to less than 40 m, and to the southeast, it thins to less than 10 m. The dominant trend of the contour lines is northwest-southeast in British Columbia, with a change to northeast -southwest or north-south in Alberta.

The inversion of thickness trends (Units A to F, compared with Unit G) suggests a fundamental change of tectonic regimes between Unit F and Unit G.

## 5.9 Combined Thickness of Units A and B

The isopach map of the combined thickness of Units A and B is shown in Figure 5-15. The map shows the thickness distributions just before main turbidite deposition. In general, Units A plus B become thinner to the southwest, except the southeastern part of the map. The most important feature of the map, also prominent in the individual map of Units A (Fig. 5-1) and B (Fig. 5-2), is the northeastward "offset" of the northwest-southeast trending isopachs from the British Columbia/Alberta border to the area of T78 R9W6. The offset of the 90 m isopach is about 55 km. Another prominent feature of the map is the "75-11 High", defined by the 50 m isopach.

UNIT G

EASTERN LIMIT OF
DEFORMED BELT

UNITS A and B

EASTERN LIMIT OF
DEFORMED BELT
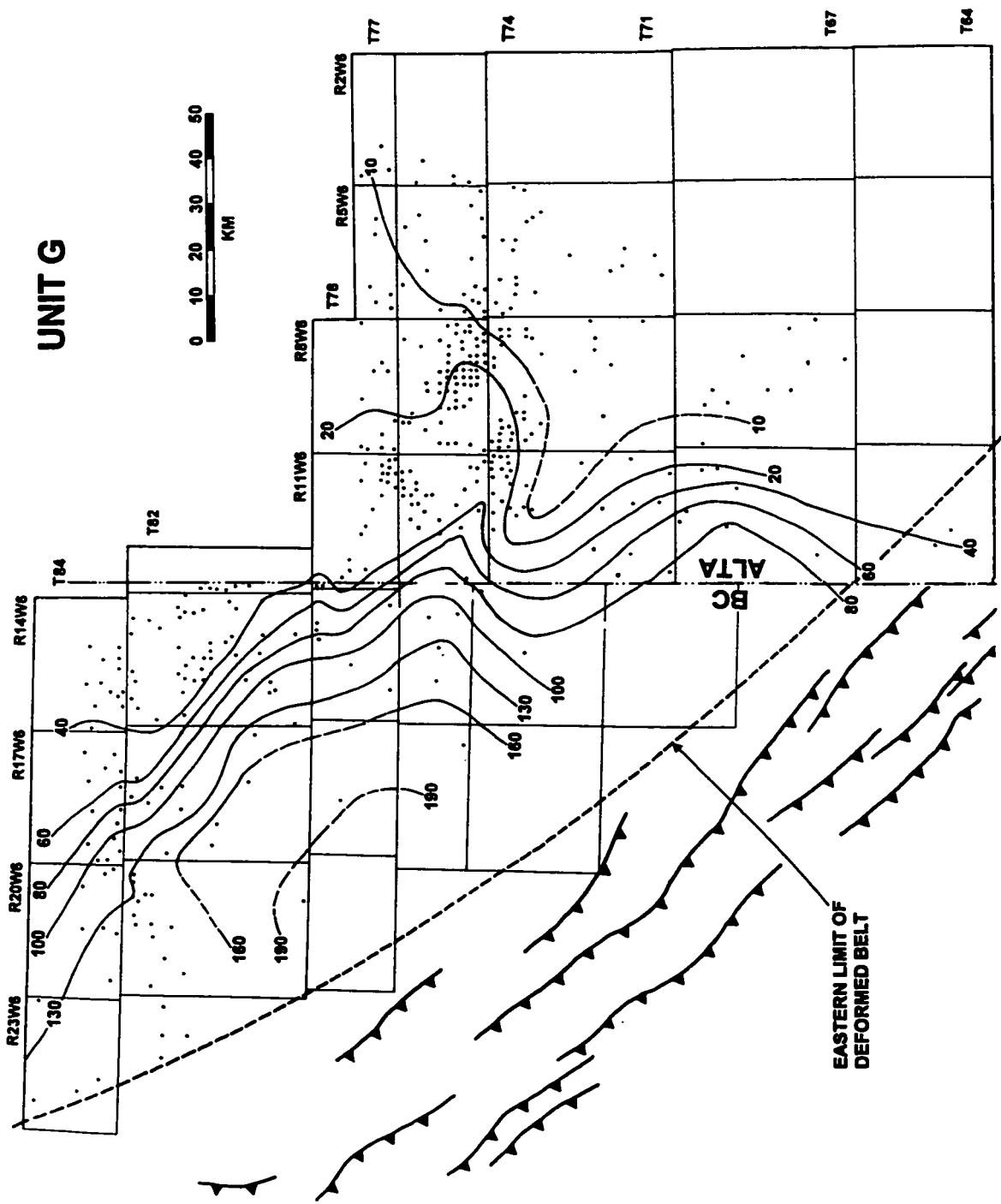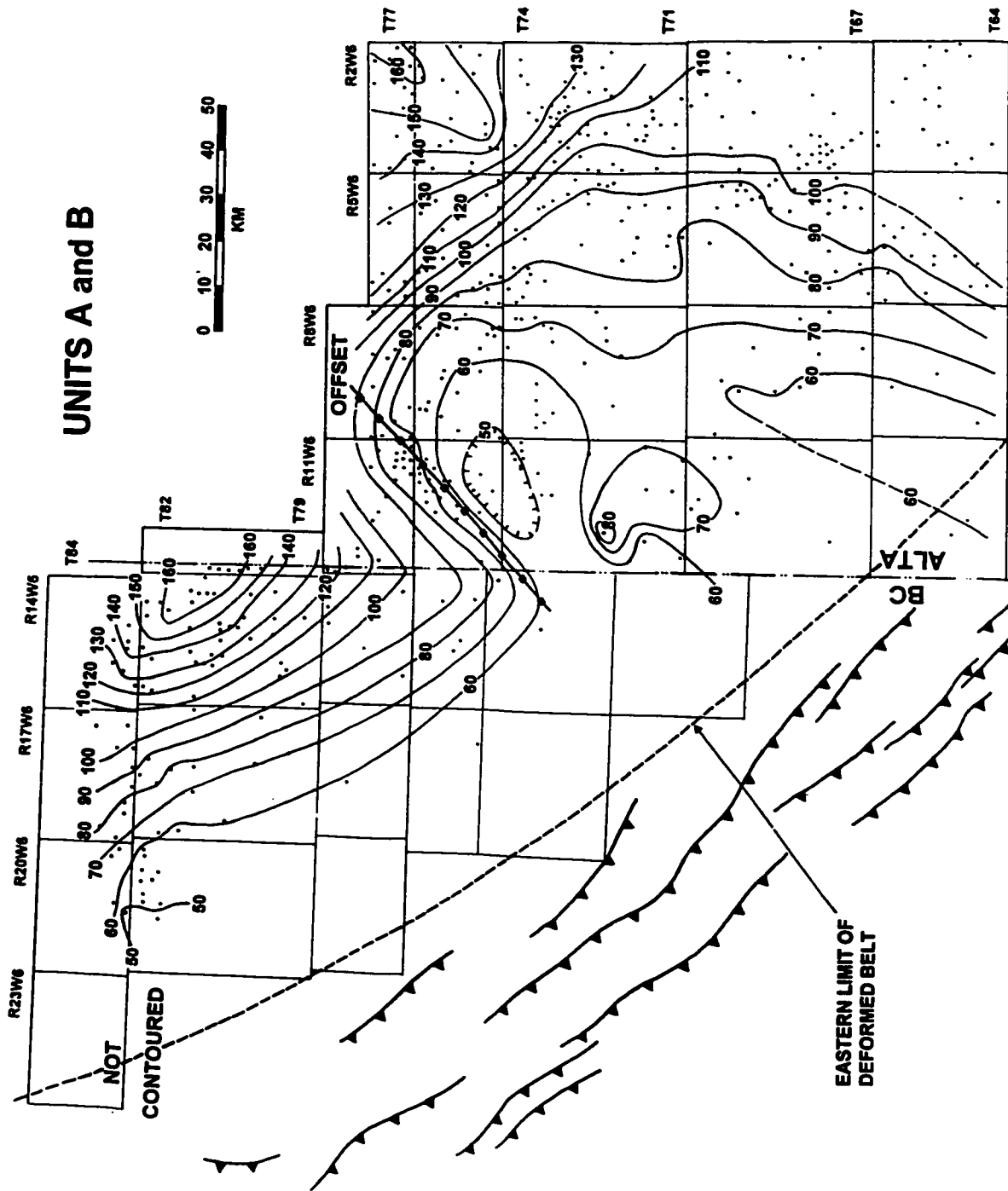
## 5.10 Combined thickness of Units A to F

The isopach map of the combined thickness of Units A to F is shown in Figure 5-16. This map shows particularly the isopach trends in the northwestern corner of the study area; this part of the area cannot be mapped for the individual Units B through F. However, the presence of the very prominent log marker ES3 in the northwest enables mapping of the combined thickness of Unit A to F.

For most of the area, the isopachs trend northwest to southeast and indicate a gradual thinning to the southwest. This trend appears to change in the northwest (T83 R23) although few data points are available. The overall trends of 130 m, 150 m, and 170 m isopachs are more or less linear suggesting a strong structural influence on sediment accumulation, with greater subsidence to the northeast. In the area around T81 R23, the combined thickness of Units A to F is less than 70 m, again suggesting a strong structural influence on sediment accumulation. This thin area lies on the top of the Hudson Hope Low, where the Carboniferous and Permian sediments are thickest. The thin Triassic succession suggests a structural inversion from the Permian. The thickest sediment accumulation, defined by the 270 m and 290 m isopachs lies over the Paleozoic Fort St. John Graben, again suggesting the reactivation of Paleozoic faults.

## 5.11 Total Thickness of the Montney Formation

The isopach map of the entire Montney Formation is shown in Figure 5-17. The thickness ranges from 190 m to 338 m. In the south, the Montney Formation

UNITS A to F

EASTERN LIMIT OF
DEFORMED BELT

120

MONTNEY FORMATION

EASTERN LIMIT OF
DEFORMED BELT
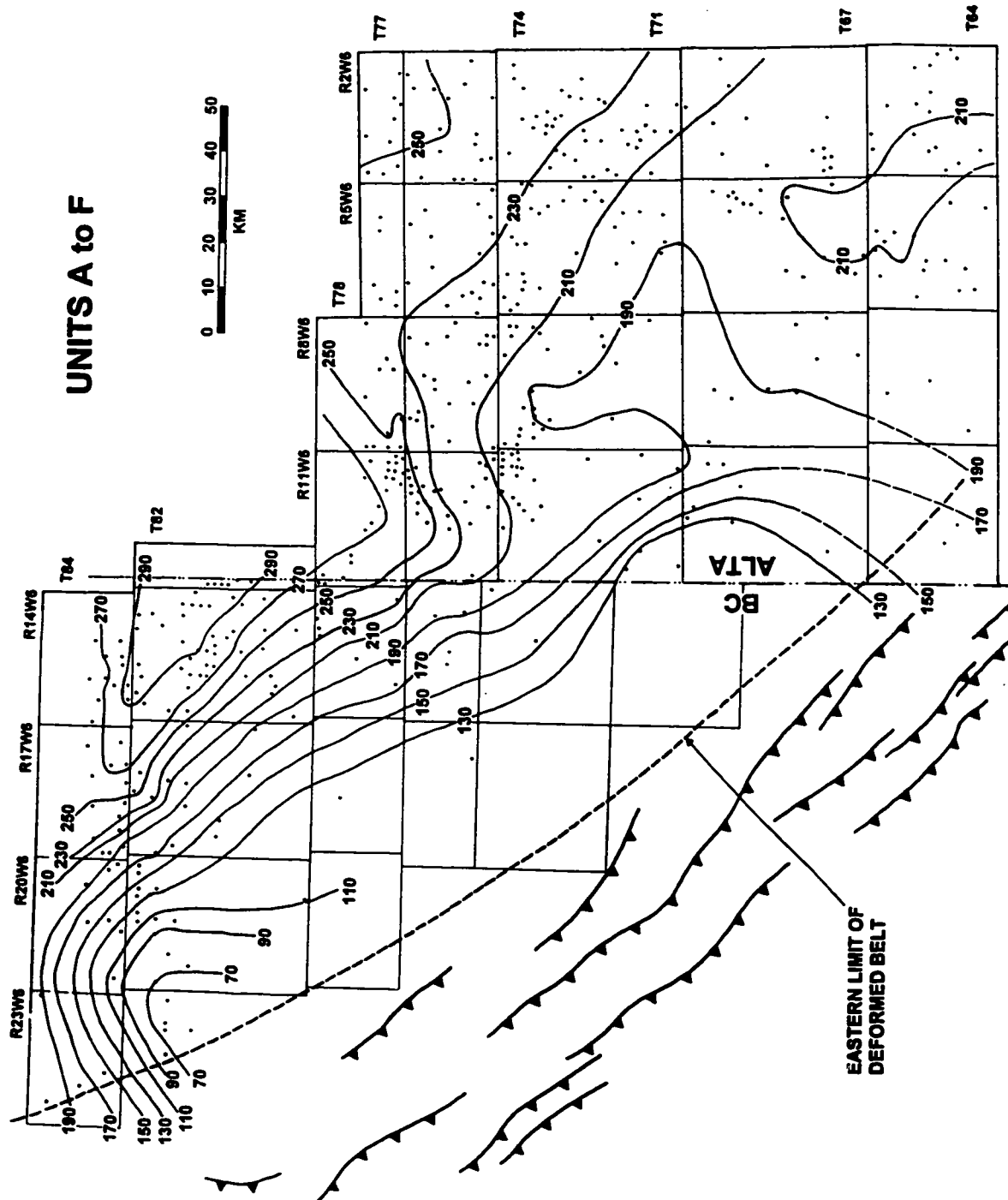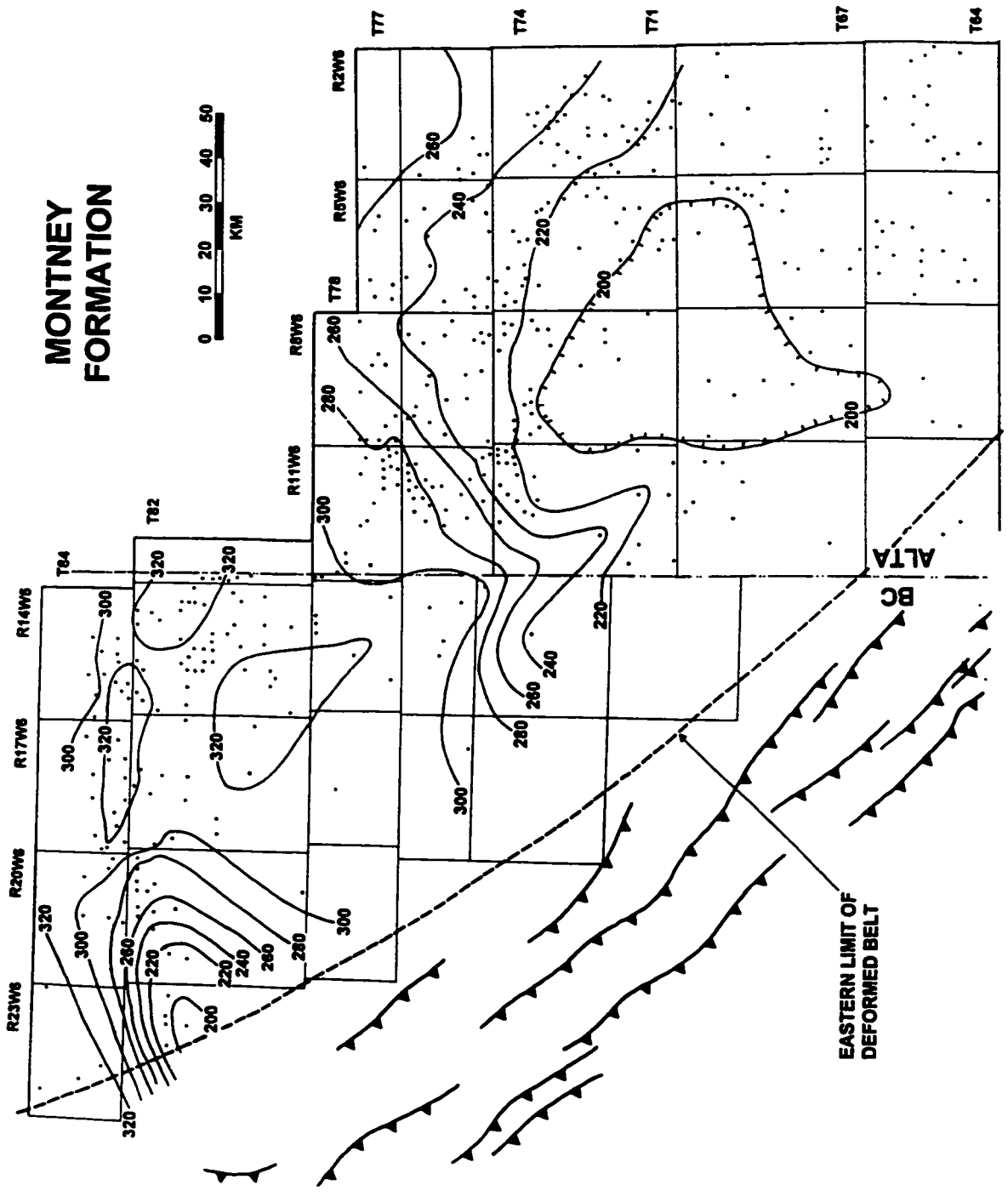
is relatively thin, ranging from 190 m to 220 m. It thickens to the northwest and northeast, and it is thicker than 300 m over most of British Columbia. A thin area occurs in the northwest (T81 R23), with a minimum of 190 m.

## 5.12 Summary

A summary of basin evolution is given in Figure 5-18. Unit A consists of southwesterly thinning clinoforms with a maximum thickness of about 160 m around T77 R1W6M. The restored dip of the clinoforms is about 0.08-0.2 degrees. The isopach trends and the distribution of dolomitized coquina beds in the uppermost part of Unit A suggest that the source was in the northeast. The isopach trends of Unit B are very different from those of Unit A, suggesting major basin reorganization. Northwest-southeast trending clinoform deposition was abandoned. Unit B onlaps against the former clinoform slope, and it is very thin or absent on the upper part of the slope, especially where Unit A is thickest. Two thick sediment accumulations developed, one in the T81 R14W6 area and the other in the T65 R5W6 area. The southeastern depocenter shifted southwestward from Subunit B1 through Subunit B3. The thickest sediment accumulation in Unit C developed in the southeastern part of the study area. Unit C thins northwestward, suggesting that at least south of T75, the main sediment source for Unit C was to the southeast. The overall northwestward thinning of Unit C also supports the previously inferred dispersal direction for the channel, southeast to northwest. In Unit D, two depocenters developed; one is centered around T77 R7W6M and the other around

| Unit A | clinoform dipping SW and striking NW-SE |
|--------|------------------------------------------|
| | **basin reorganization** |
| Unit B | onlapping against the slope; depocenter in the southeast |
| Unit C | channel incision trending SE-NW; northwestward thinning trend |
| Unit D | a new depocenter (around T77 R7); abandonment of the Unit C depocenter |
| Unit E | southwestward shift of the depocenter from Unit D |
| Unit F | northward shift of the depocenter from Unit E |
| | **basin reorganization** |
| Unit G | thickest sediments in the SW, and regional thinning to the NE |

T83 R17W6M. Comparison of Unit D and Unit C indicates the abandonment of thick sediment accumulation in the southeastern part of the map. The most prominent feature of Unit E is the development of the depocenter centered around T74 R12W6M. Comparison of Unit E to Unit D indicates a southwestward shift of the depocenter and disappearance of the depocenter around T83 R17W6M. Unit F is characterized by the development of the depocenter centered T76 R12W6M. Comparison of Unit F to Unit E indicates a northward shift of the depocenter. All of the units below Unit G thin gradually toward the deformed belt, but Unit G thickens gradually to the southwest.

Several of the isopach maps suggest structural controls on the sedimentation of the Montney Formation. Abrupt changes of source area, the occurrences of new depocenters at different location, and a thin area over the Paleozoic graben suggest structural controls on sediment accumulations. The inversion of the thickness trend between Unit F and Unit G suggests a fundamental change of tectonic regime.

# CHAPTER 6: FACIES AND FACIES ASSOCIATIONS OF UNITS

## 6.1 Unit A

In the eastern part of the study area, Unit A consists of at least 5-6 coarsening upward cycles or successions. The exact number of the cycles is not clear because of progressively deeper northeastward truncation of the Montney Formation by the sub-Jurassic unconformity. Near the subcrop edge, the preserved Unit A becomes thicker southwestward, but the sediment grain size becomes finer and the coarsening upward trend becomes less prominent.

In the easternmost part of the study area, the coarsening upward trend is 10-50 m thick. It is very prominent in well logs, especially gamma-ray and SP logs. Logs commonly exhibit a smooth funnel-shape with an abrupt top. However, there are no cores that completely penetrate a full coarsening upward succession. Thus, combination of some cores is necessary to illustrate a complete coarsening upward succession.

In each coarsening upward succession, the facies association commonly begins with Facies 3 (bioturbated silty mudstones to muddy siltstones). In Figure 6-1A, slightly bioturbated silty mudstones (sleeves 9 to 13) abruptly overly relatively clean, weakly flat-laminated sandstones (Facies 8)(sleeves 1 to 8). The mud-dominated lower part (silty mudstones) becomes coarser and gradually changes into muddy siltstones upwards. The bioturbated silty mudstones to muddy siltstone
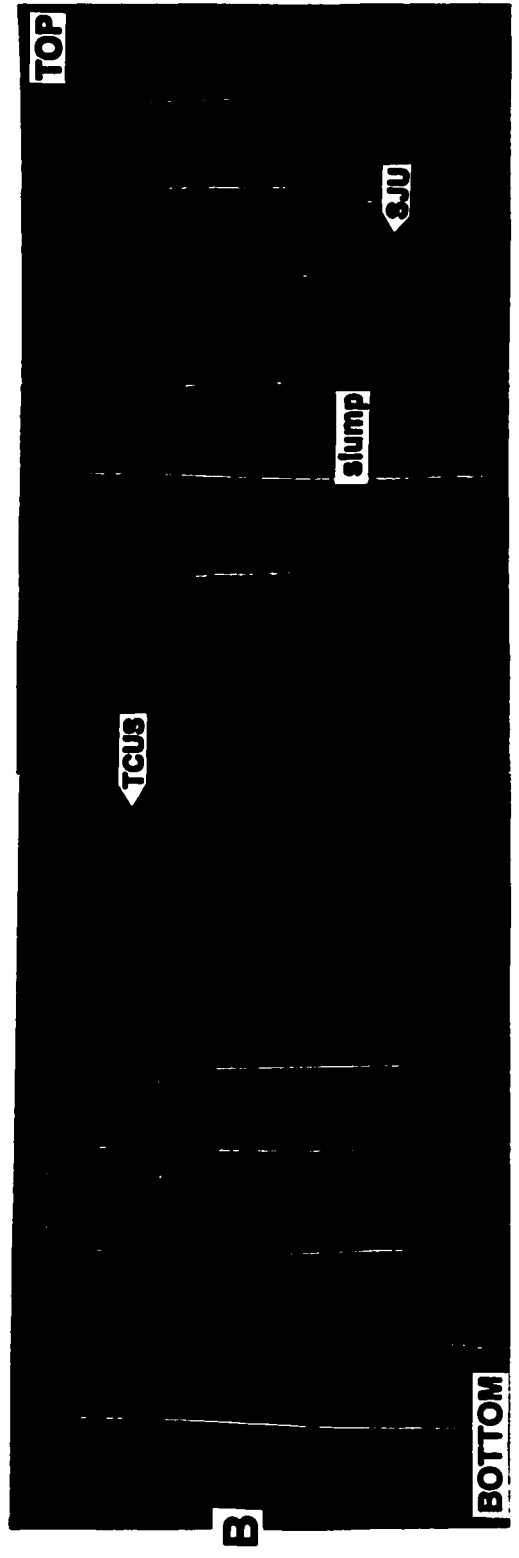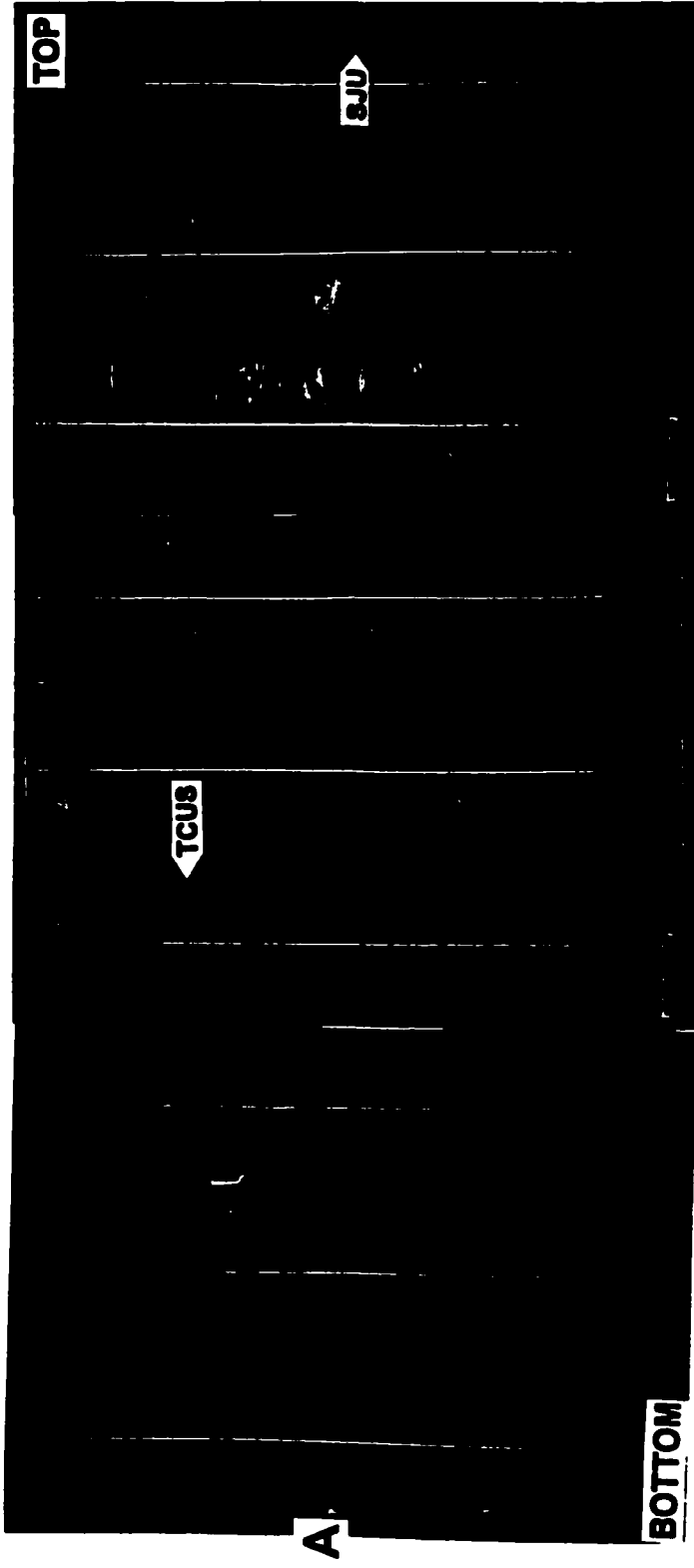
(sleeves 14 to 16) are gradually replaced by mud-laminated or -interbedded sandstones and siltstones (Facies 6). An example of gradual upward change from Facies 3 to Facies 6 is shown Figure 6-2. There, muddy siltstone (sleeves 1 to 6, and 18 to 19) gradually change upward into mud laminated sandstones (sleeves 7 to 10, and 20 to 21) as the interlaminated and interbedded mud becomes thinner and less frequent. Mud-laminated or mud-interbedded sandstones and siltstones (Facies 6) are gradually replaced upward by relatively clean, flat-laminated to structureless sandstones (Facies 8)(sleeves 11 to 17, and 22 to 24). The core shows two coarsening upward sequences.

Successions in which Facies 8 comprises the uppermost portion are most common, but in some successions near the subcrop edge, Facies 8 is commonly interbedded with or overlain by dolomitic coquina beds (Facies 9). In Figure 6-3, the core consists of weakly laminated sandstones, and dolomitic coquina beds. The lower 4m (sleeves 2 to 9) of the core consists of relatively clean sandstones, but above, the core consists of dolomitic sandstones with various proportions of shell fragments and dolomitic coquina beds up to 2.5 m thick. Most sandstones are commonly weakly flat-laminated or structureless, but some sandstones show slightly inclined laminations (sleeve 26) or wave ripples in their upper parts. Most of the dolomitic coquina beds contain small shell fragments (>5 mm), but some intervals show complete internal molds of shells (see Figure 3-9C). Figure 6-4 shows a gradual upward facies change from Facies 8 to Facies 9. There, flat-laminated to structureless sandstones (Facies 8)(sleeves 9 to 15) pass upward into

TOP

TCUS

BOTTOM
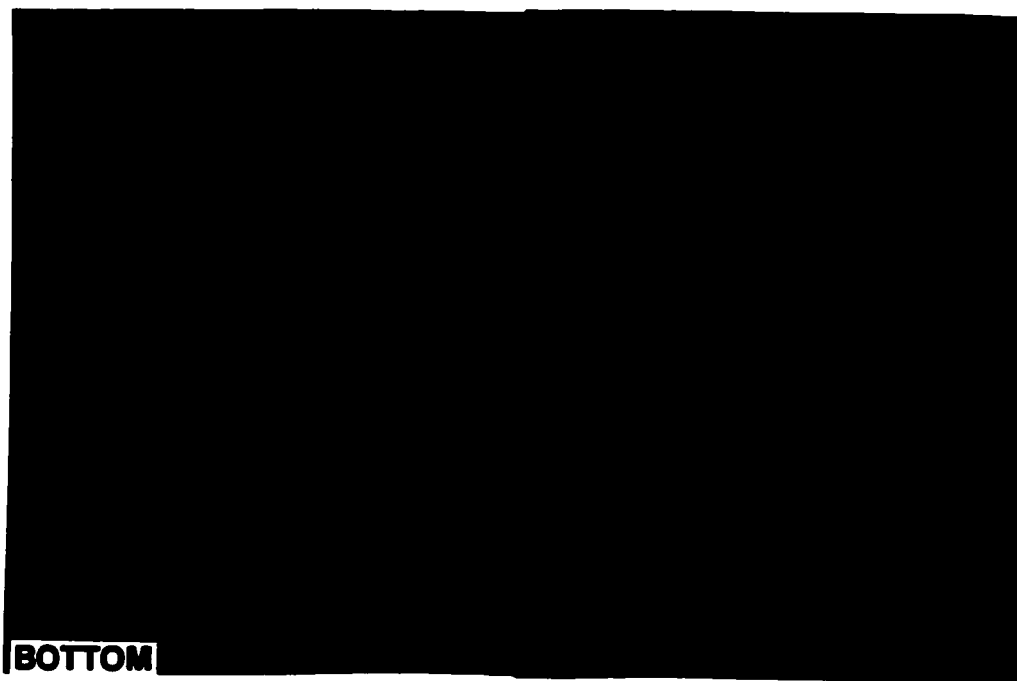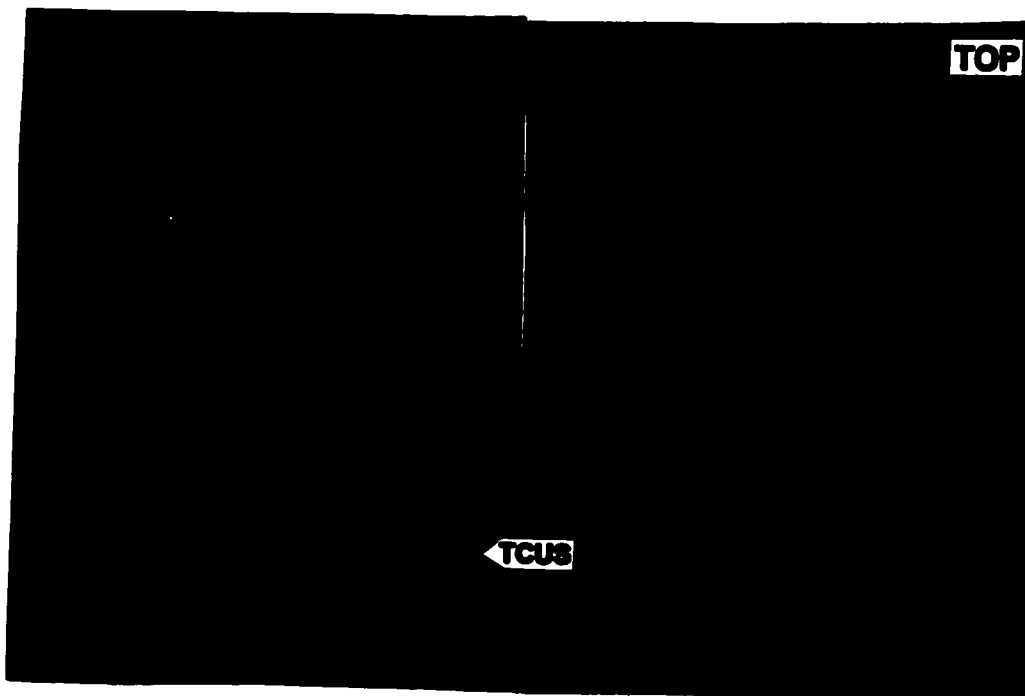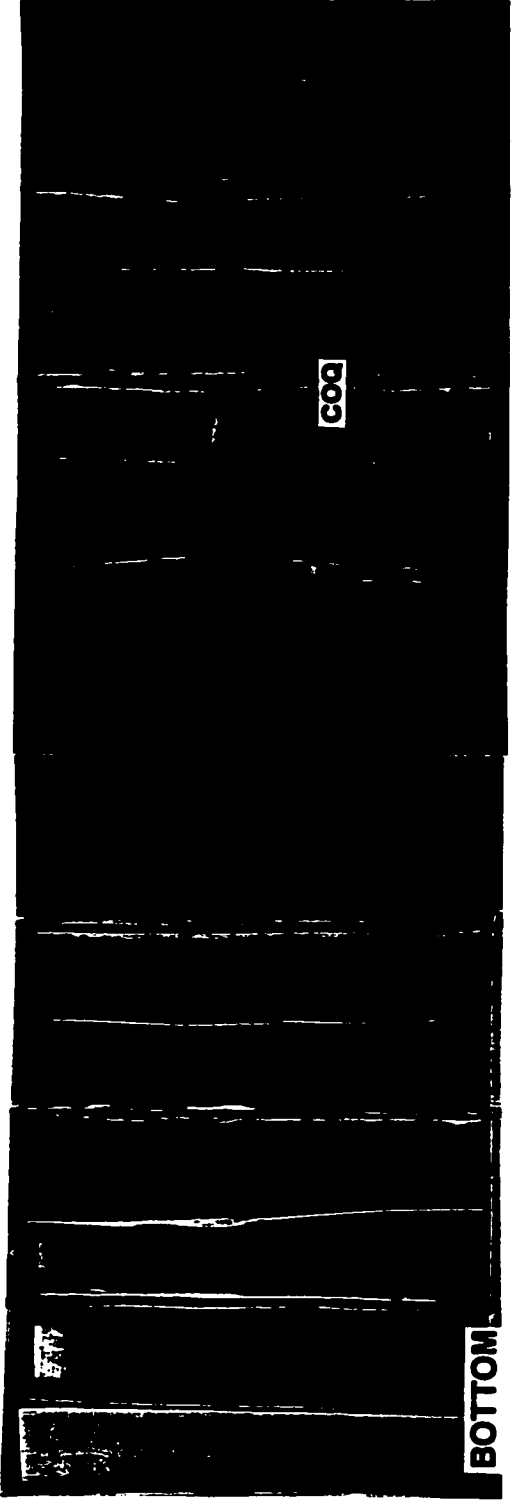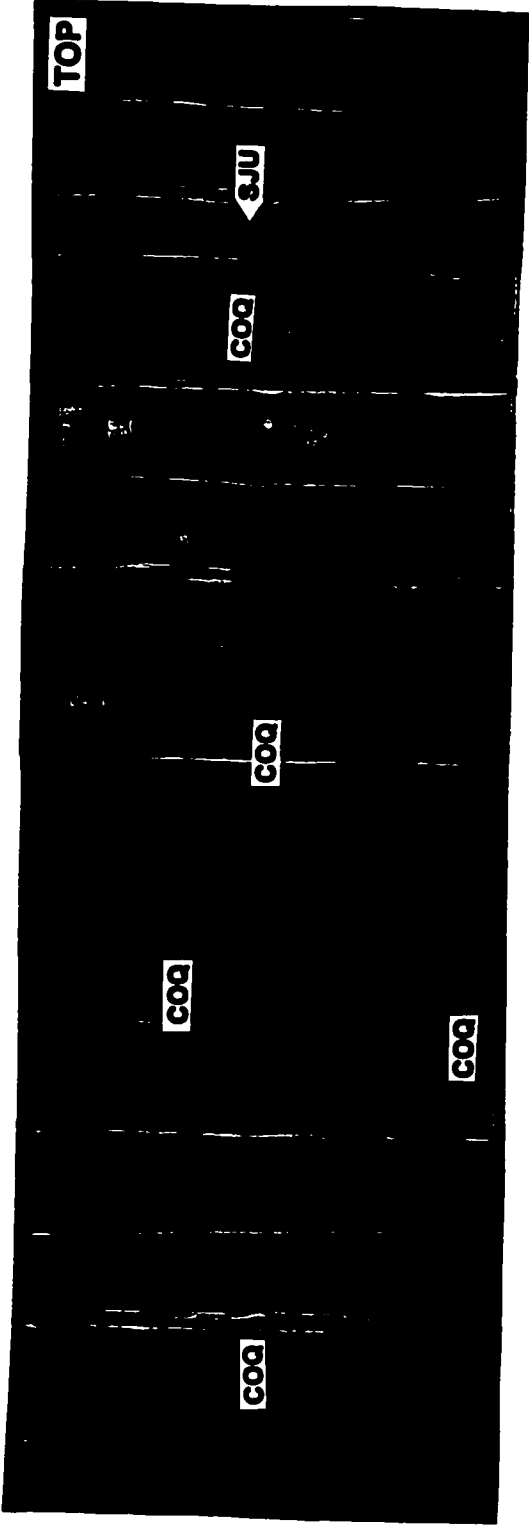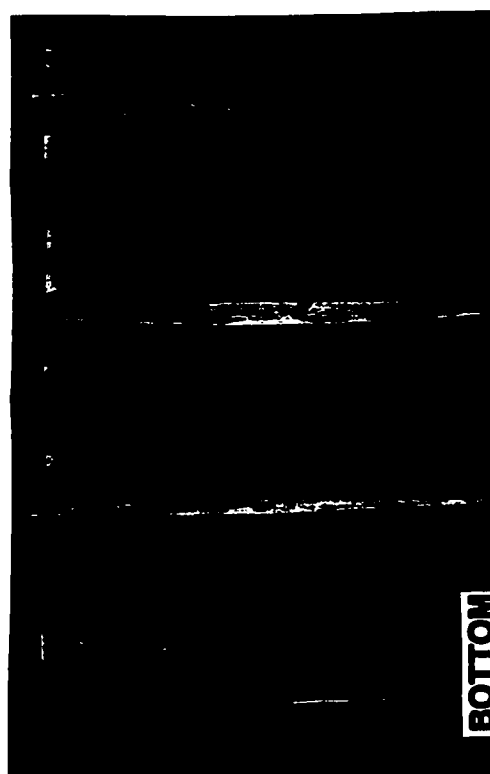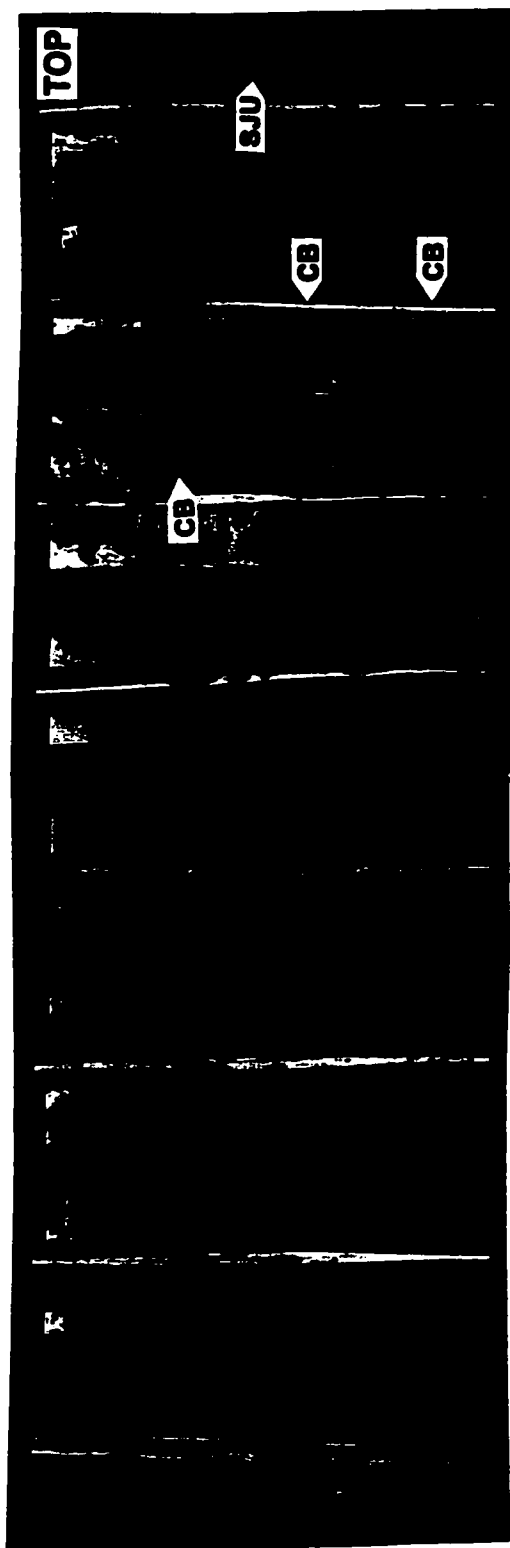
dolomitic coquina beds as the proportion of sandstones decreases and the proportion of dolomitic coquina beds increases upwards. Note that the dolomitic coquina beds are commonly cross-bedded (sleeves 24 and 25) or contain slightly inclined stratification (sleeve 21 and 22). These structures preserved in this core suggest that the commonly massive appearance of the dolomitic coquina beds are partially the result of intense dolomitization, destroying any original sedimentary structures. Thick successions of dolomitic coquina beds commonly occur in the uppermost portion of coarsening-upward successions, and are sharply overlain by mudstones or siltstones in the basal part of subsequent coarsening successions. The idealized, complete facies association is illustrated in Figure 6-5. The complete facies association may not always occur, and incomplete coarsening upward successions in which some parts of the lower and/or upper divisions are missing, are much more common. Examples of top-absent associations are shown in Figures 6-1 and 6-2. There, Facies 8 comprises the upper portion of coarsening upward successions, and Facies 9 does not occur. The example of bottom-absent association is shown in Figure 6-6B. There, the coarsening upward succession begins with Facies 6, and Facies 3 does not occur.

The coarser sediments (Facies 9, 8, 6 and 3) in the eastern part of the study area become finer southwestward and grade into mudstones (Facies 1) in the deeper part of the basin.

The most extensive and thickest dolomitic coquina beds occur in the uppermost part of Unit A (Figure 6-7). This coquina succession does not occur as

FACIES

3

9

8
9

8

6b

6a

3

10-50

0 m
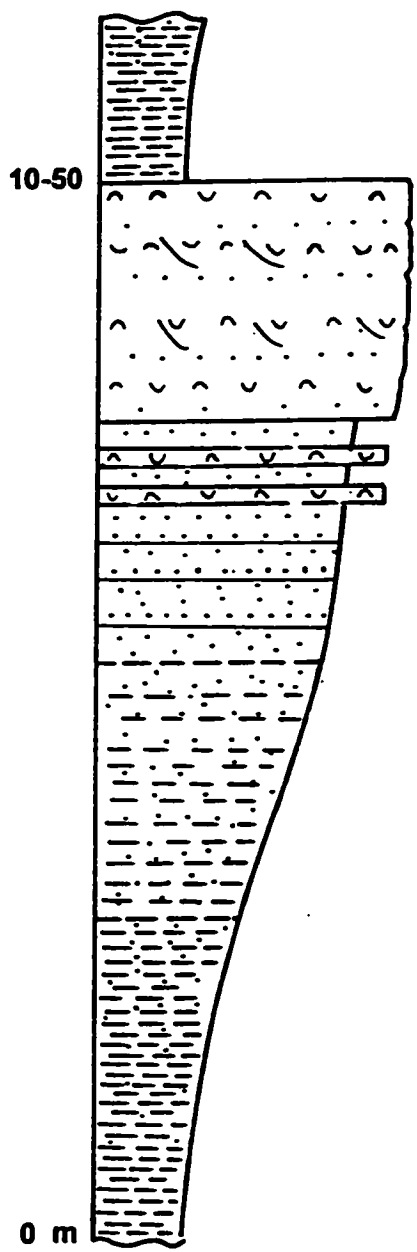
sh    sit    vf    f    m
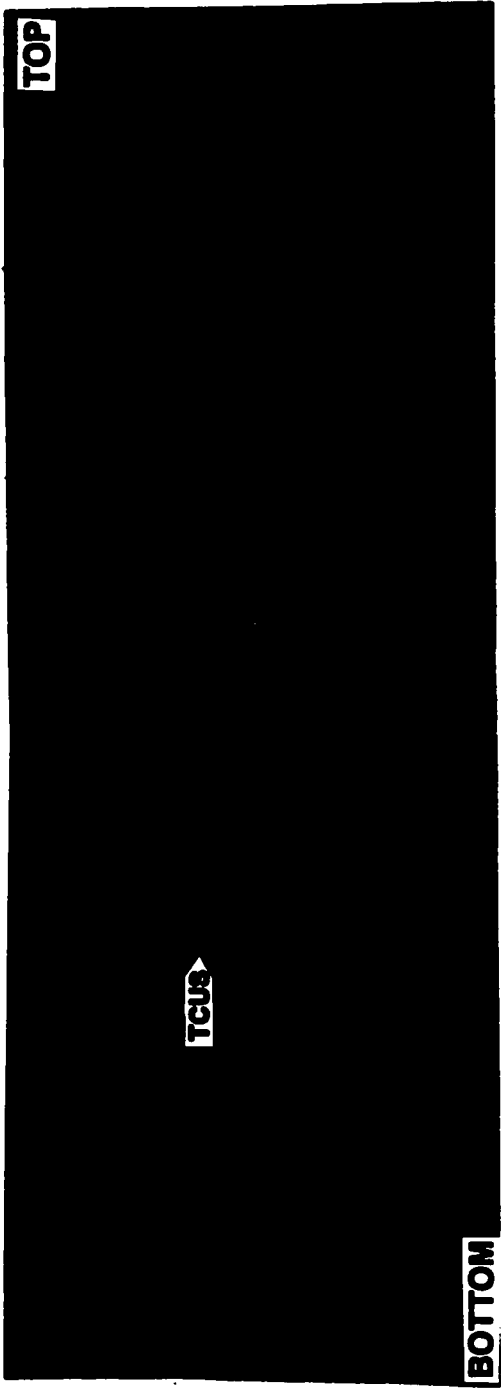
A
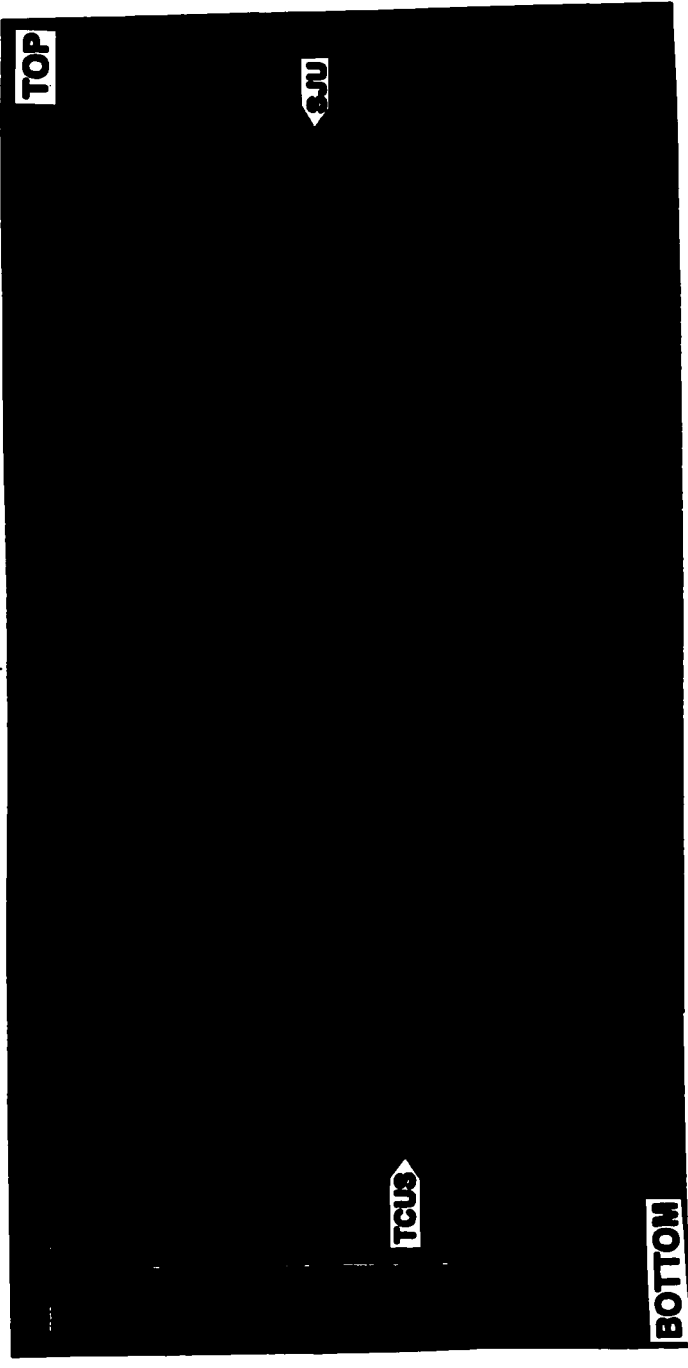
B
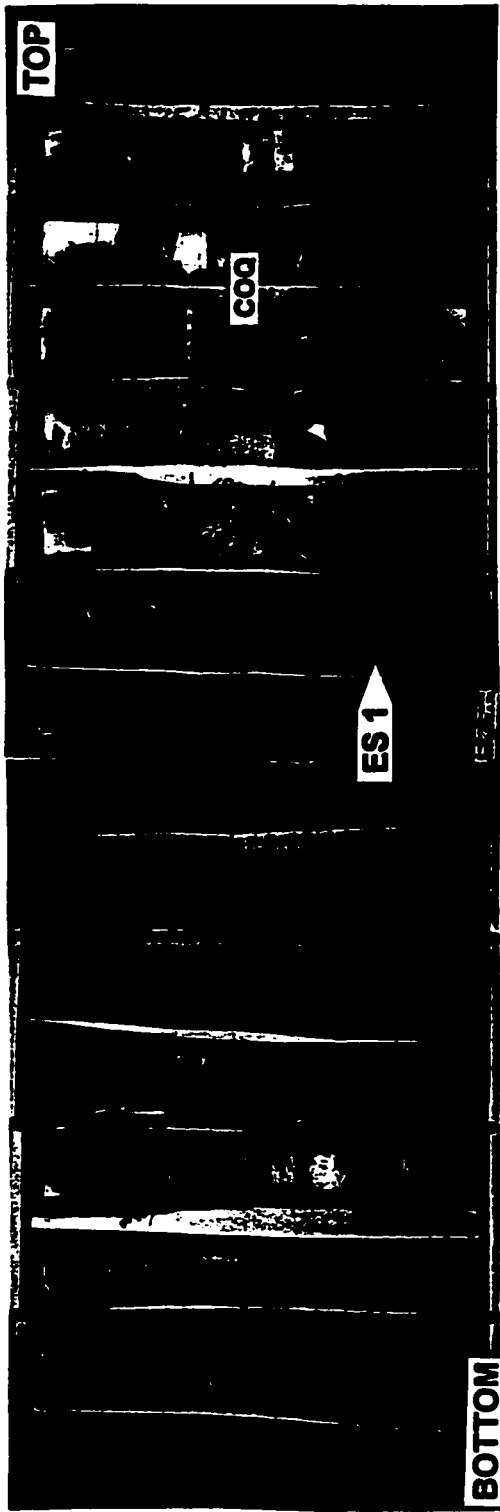
A
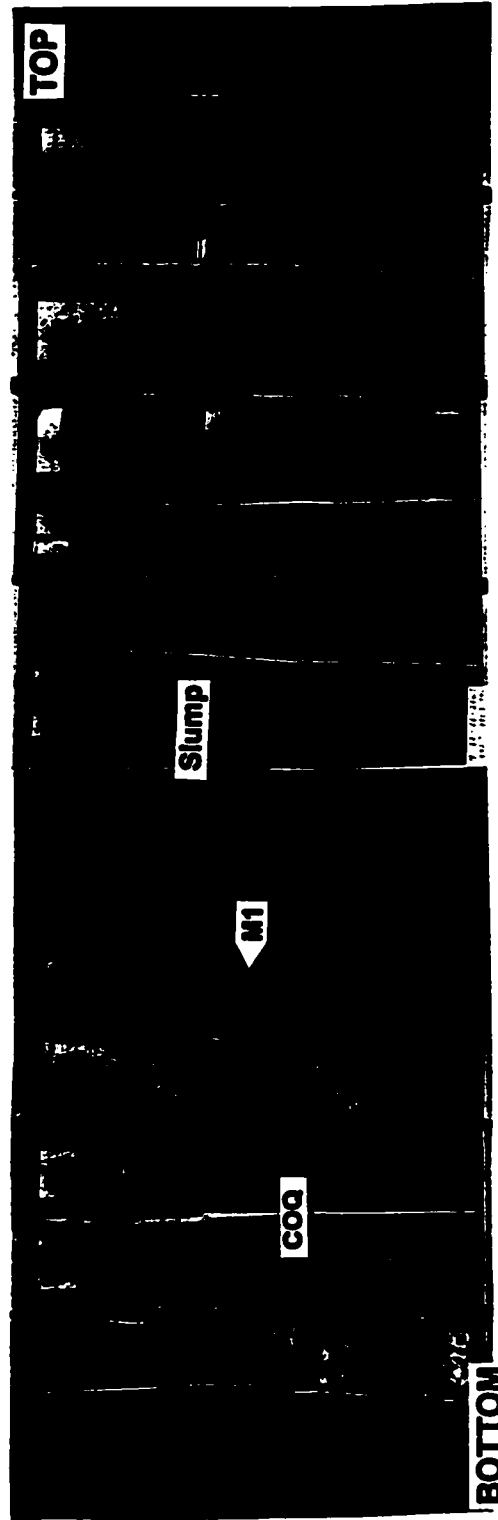
B

the upper portion of coarsening upward succession; instead, the coquina beds *abruptly* overly Facies 3 on Erosional Surface 1 (ES1 in Fig. 6-7A, see also Appendix A-2) and are sharply overlain by silty mudstones (Facies 3)(M1 in Fig. 6-7B; see also Appendix A-3). More detailed descriptions of these coquina beds will be given in Chapter 7.

## 6.2 Unit B

In the eastern part of the study area, several cores penetrate Unit B, but only a few of them penetrate the lower boundary of Unit B. The lower contact of Unit B is represented by a sharp boundary with dark mudstones overlying dolomitic coquina beds of Unit A (see Figures 6-7B and 3-9D; see also Appendixes A-2 and A-3). In core 15-7-68-24W5 (Fig. 6-8), the lower 5-6 m (sleeves 1 to 8) consists of silty mudstones to muddy siltstones (Facies 3) with mud-laminated or interbedded sandstones and siltstones (Facies 6) in some intervals. The lower succession grades upward into sandstones and siltstones with HCS beds (Facies 7).

An important characteristic of Unit B in the eastern part of the study area is the extensive development of slumped and deformed sediment (sleeve 7 to 10 in Fig. 6-7B; see also Appendix A-3). About 50 % of the cores through Unit B show large slumps thicker than 3 m. The location of wells containing large slumped deposits is closely related to the western margin of the dolomitic coquina beds in the uppermost part of Unit A.

In the western part of the study area, Unit B consists mostly of dark

TOP

slump

BOTTOM
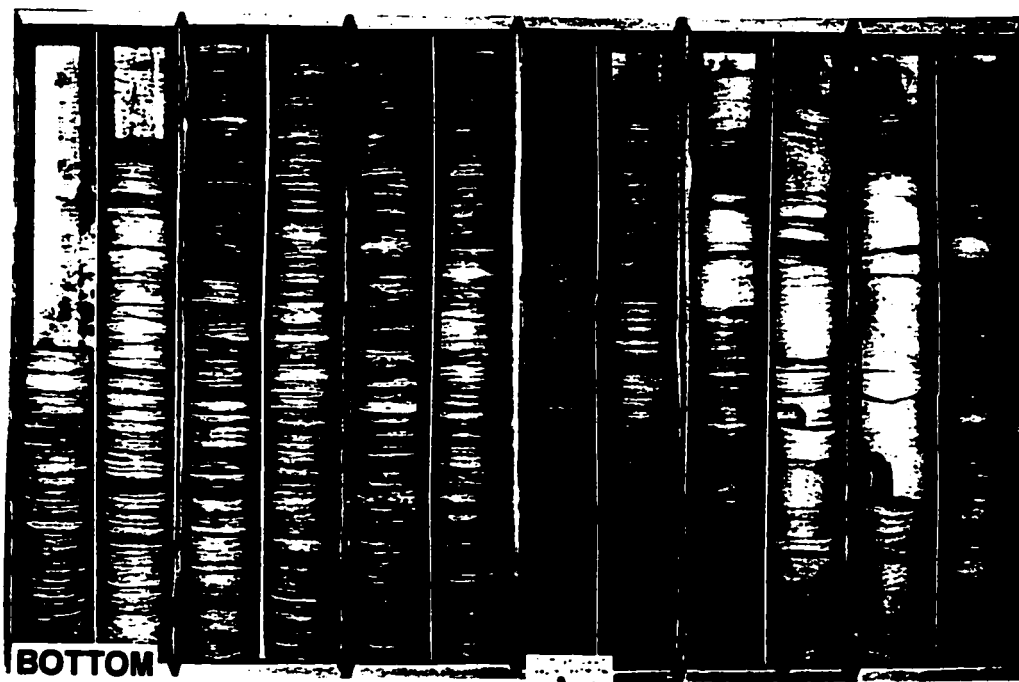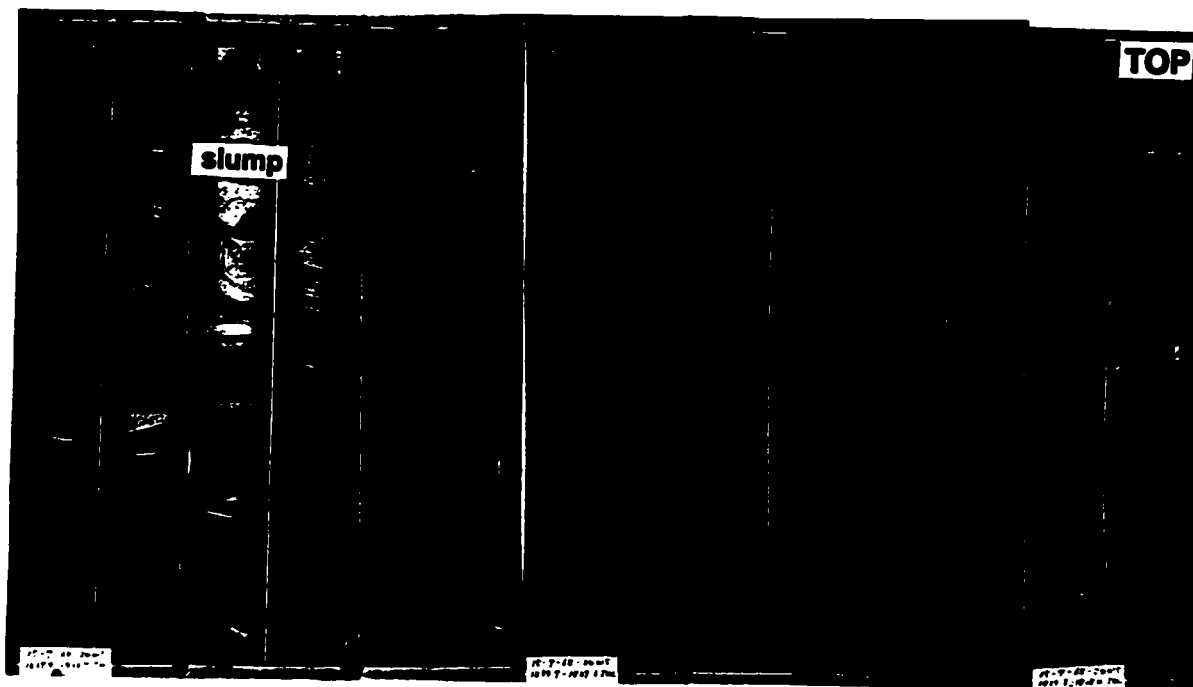
mudstones (Facies 1). In core 7-5-67-7W6, the recovered 18 m succession consists entirely of Facies 1. Silty laminations are very rare, and there are no vertical facies changes in the entire succession. In several other cores (7-23-74-11W6, 14-19-74-10W6, 6-25-74-11W6, and 2-27-74-11W6), Unit B consists entirely of Facies 1. However, in the northwestern part of the study area (Glacier Field, around T76-77 R11-12W6), Subunit B2 contains coarser sediments consisting of fine-grained sandstones and coarse siltstones.

Core 6-15-77-11W6 (Fig. 6-9, see also Appendix A-38) shows a typical facies of coarse sediments developed in Subunit B2. In the core, the lowest 1m is Subunit B1, and consists of dark mudstones (Facies 1). However, Subunit B2 (M2-M3) contains sharply based thin-bedded sandstones and siltstones (Facies 4), and thick, structureless sandstones. Most of sandstones and siltstones are structureless, but some beds are weakly flat-laminated. The upper parts of some beds show grading into mudstones. Some of thick sandstone beds contain small (<1 cm) mud clasts in their basal parts. Interbedded mudstone intervals range from 20 cm to 1.7 m in thickness. The upper 7m (Subunit B3) of the core consists of dark mudstones (Facies 1).

The coarse sediments interpreted as turbidites in Subunit B2 pass laterally into mudstones as shown by gradual weakening of the log signals in both gamma-ray and induction logs in well log cross section E-E' (Fig. 4-6). Note that in Figure 4-6, the blocky responses in Subunit B2 in 11-10-77-11W6 and 6-11-77-11W6 are gradually weaker to the northwest and southeast. The isopachs of this sandy and
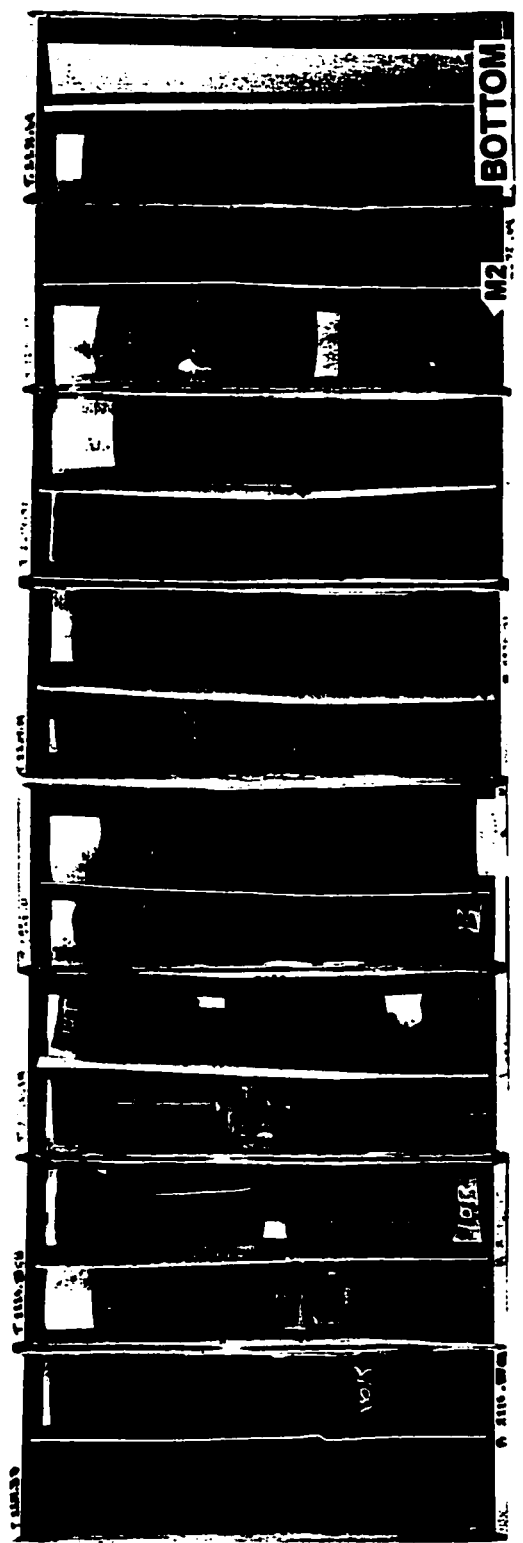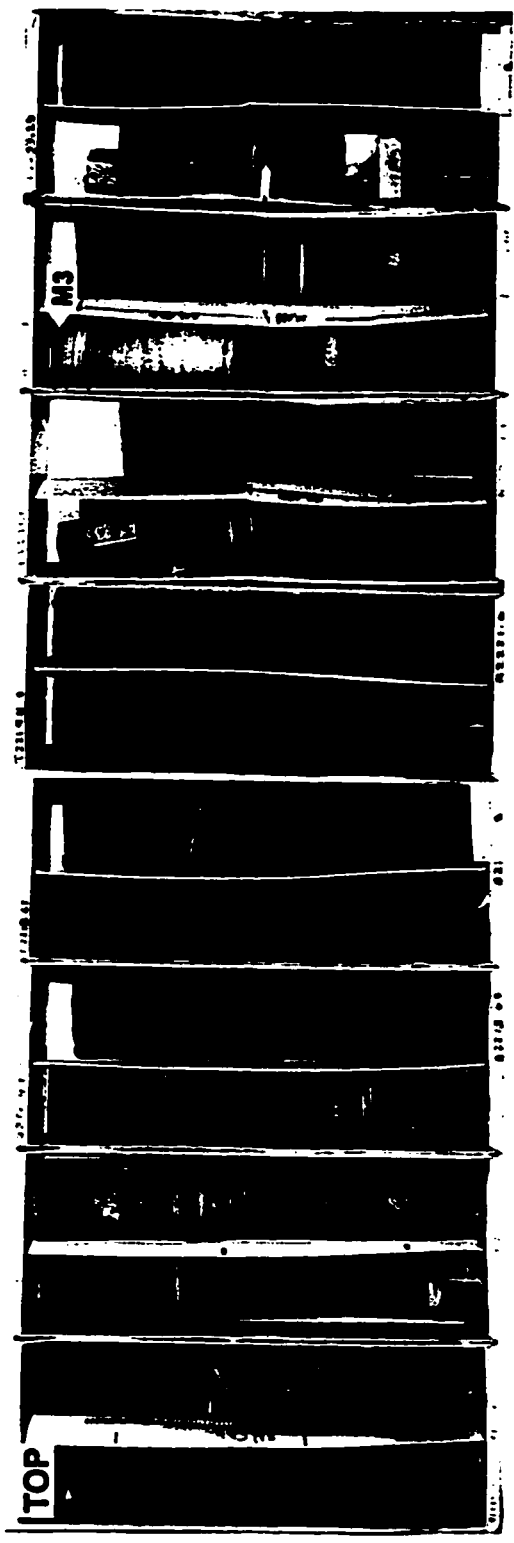
silty turbidites are shown in Figure 6-10. The sandy and silty turbidites body is elongate, trending northeast to southwest. Its maximum thickness is about 10 m.

About 30 km east of the Glacier Field, Subunit B2 appears to contain sandy and/or silty turbidite deposits. In cross section F-F' (Fig. 4-7), Subunit B2 from 7-33-75-8W6 to 11-18-77-8W6, is characterized by the higher values in induction logs and lower values in gamma-ray logs than those of Subunit B1 and B3. Although this interval has not been cored in this area, its similar log signature and same stratigraphic position as the turbidite deposits in the Glacier Field suggest similar lithologies. However, the less prominent log signals in the density-porosity logs suggest that the turbidite deposits in this area are much more thinly bedded, and/or contain much more interbedded mudstones than those in the Glacier Field. The coarse deposits pass laterally into mudstones as suggested by the gradual weakening of the log signal. The isopachs of thess probable sandy and silty turbidites are shown in Figure 6-10. The turbidite body is elongate and trends northwest to southeast, almost perpendicular to the turbidite deposits in the Glacier Field.

Over most areas in the deeper part of basin, Subunit B3 (interval between M3 and M4) consists mostly of dark mudstones (Facies 1) and contains only small amount of alternating siltstones and mudstones (Facies 2). However, around the Manir Field (T71 R4W6 and surrounding areas) Subunit B3 contains sharply based thin-bedded sandstones and siltstones (Facies 4) interpreted as turbidites (see Appendixes A-4 to A-7). The thickness of the turbidite deposits ranges about 1-2
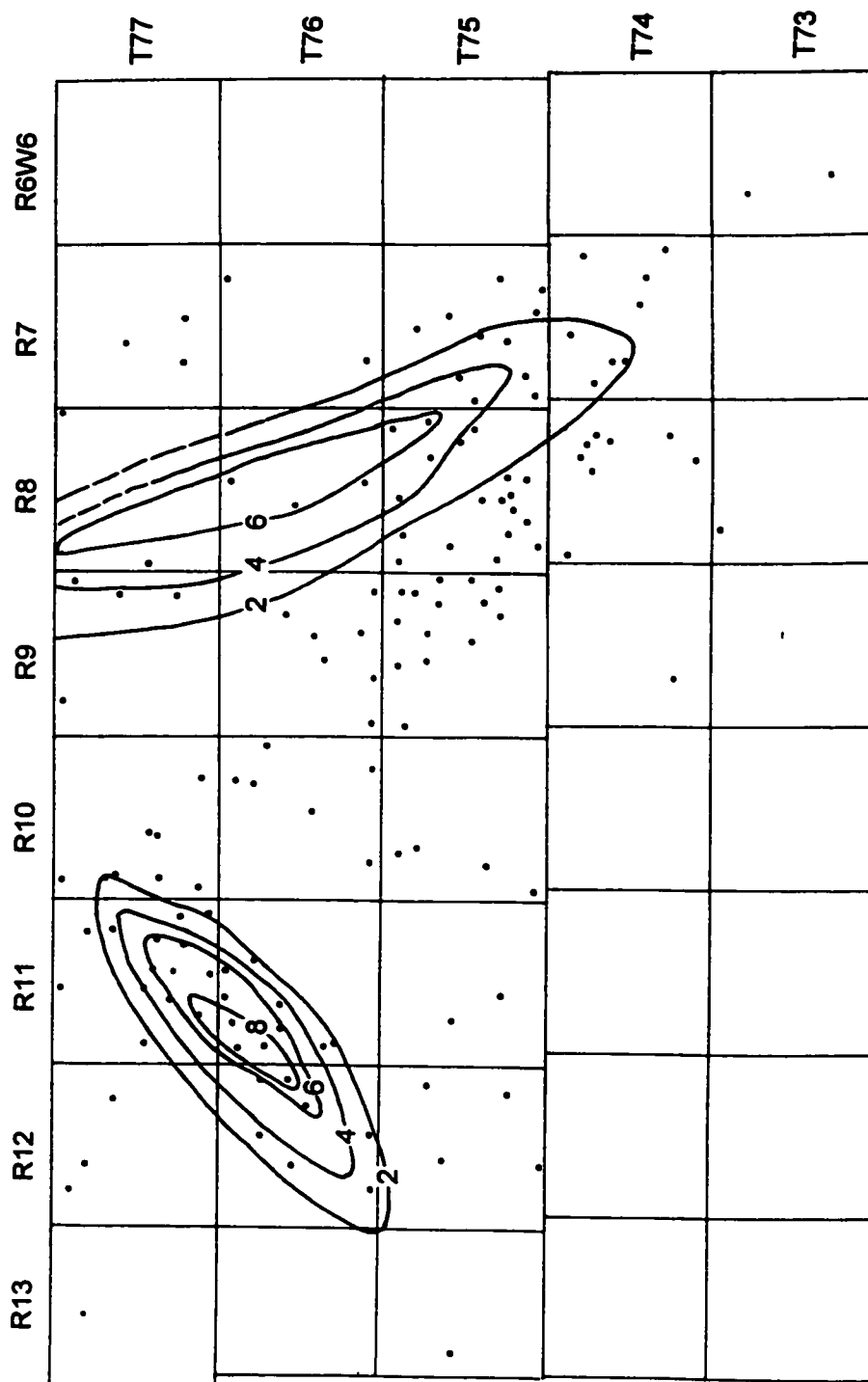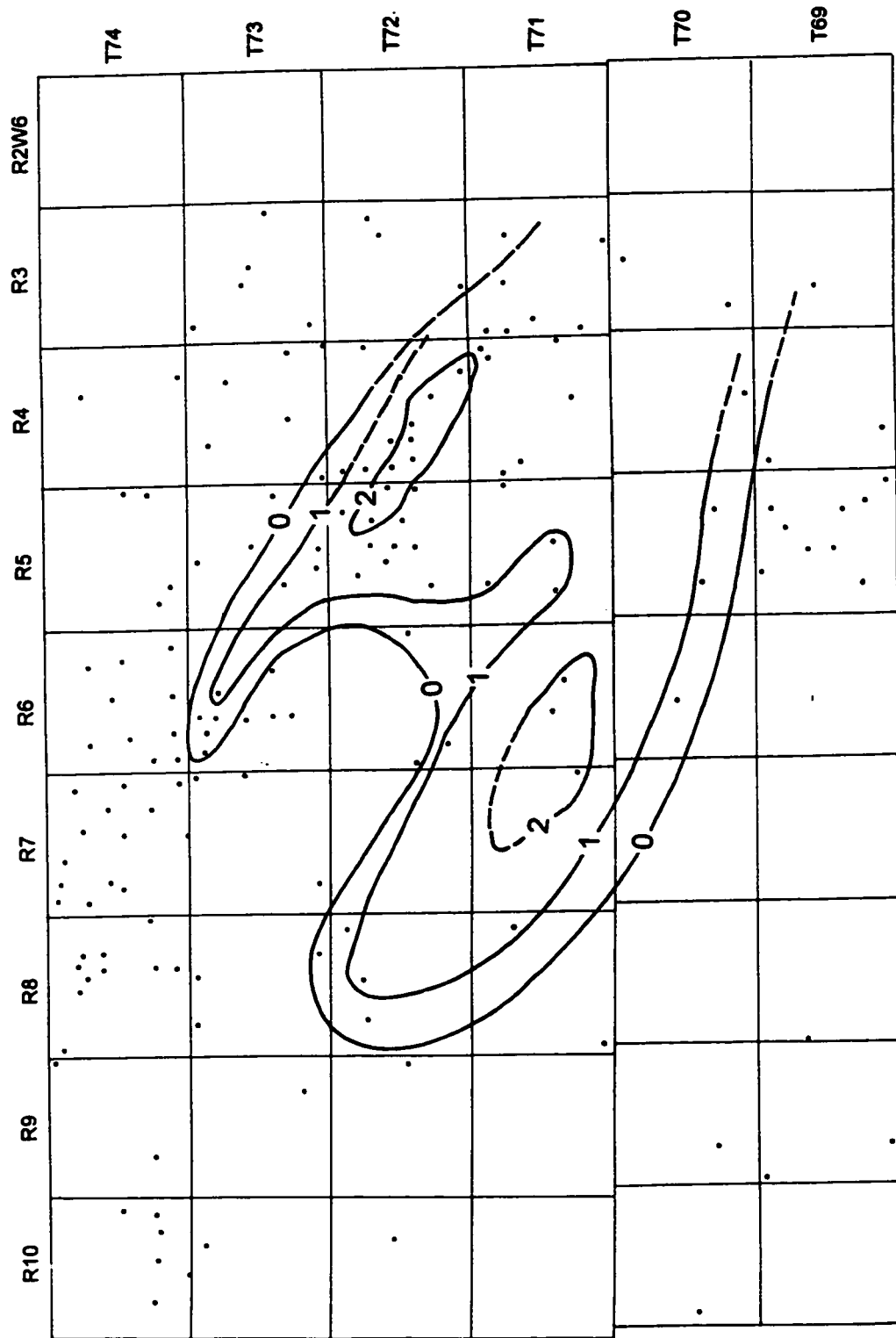
m, and rarely exceeds 3 m. The thickness trend of the turbidites (mainly Facies 4) within Subunit B3 is shown in Figure 6-11. The body is elongate and trends northwest to southeast, bifurcating to the northwest.

## 6.3 Unit C

### 6.3.1 In the East

Unit C in the eastern part of the study area consists mostly of sandstones and siltstones associated with HCS beds (Facies 7). Thus, Unit C is very similar to the upper part of Unit B. Core 4-1-69-25W5 (Fig. 6-12) represents a typical facies association of Unit C in the eastern study area. The core consists mostly of Facies 7 and some intervals are slumped. Vertical facies changes are not prominent although in the upper part of the core, individual sand/silt beds are slightly thicker and interbedded mud layers are less common than those in the lower part.

### 6.3.2 In the West

Unit C in the western study area (west of 6th Meridian) commonly contains turbidite facies. Core 6-30-71-3W6 (Fig. 6-13, Appendix A-4) shows a typical facies association of the lower part of Unit C. Unit C (above M4) consists mostly of sharply-based thin-bedded sandstones and siltstones (Facies 4), with some mudstones(Facies 1) and silt/mud alternation (Facies 3) intervals. Some of dark mudstone intervals are up to 0.8 m thick (eg., sleeves 50 and 51, 26.15-26.95 m in

# NOTE TO USERS

Page(s) not included in the original manuscript are unavailable from the author or university. The manuscript was microfilmed as received.

143-144

This reproduction is the best copy available.

UMI

Appendix A-4). Sandstones and coarse siltstones are commonly structureless or very weakly laminated in their lower parts, but they grade upward into dark mudstones in their upper parts.

In 5-20-74-6W6 (Fig. 6-14, Appendix A-12) about 40 km northwest of 6-30-71-3W6, Unit C (above M4) is much finer and thinner. The lower 6 m of Unit C (above M4) consists mostly of mudstones (Facies 1)(sleeves 4 to 12, 2.2-8.2 m in Appendix A-12), and interbedded siltstones are rare and very thin. This finer interval grades upward into alternating siltstones and mudstones (Facies 2), and sharply based thin-bedded sandstones (Facies 4)(sleeve 12 to 17, 8.2-12.4 m in Appendix A-12). The middle part is capped by 2.8 m of structureless sandstones (sleeve 18 to 22, BSS to M5). Northwestward fining is indicated by core 6-25-75-8W6 (Fig. 6-15, see also Appendix A-23) about 20 km northwest of 5-20-74-6W6. In the core, Unit C below the structureless sandstone succession consists mostly of dark mudstones. Interbedded siltstones and sandstones are thin (<10 cm) and much less common than in 5-20-74-6W6.

Westward fining and thinning of Unit C is indicated in well log cross section C-C' (Fig. 4-4). In 6-2-68-4W6, the lower 20 m succession in Unit C consists mostly of Facies 4 with some intervals consisting of Facies 1. The log signals suggest that the coarse sediments in 6-2-68-4W6 are gradually finer to the west, and in 6-20-68-9W6, the correlative interval seems to consist of mudstones. In 6-20-68-9W6, the coarse interval occurs in a higher stratigraphic position than 6-2-68-4W6, indicating westward progradation of sandy and silty turbidite deposits.
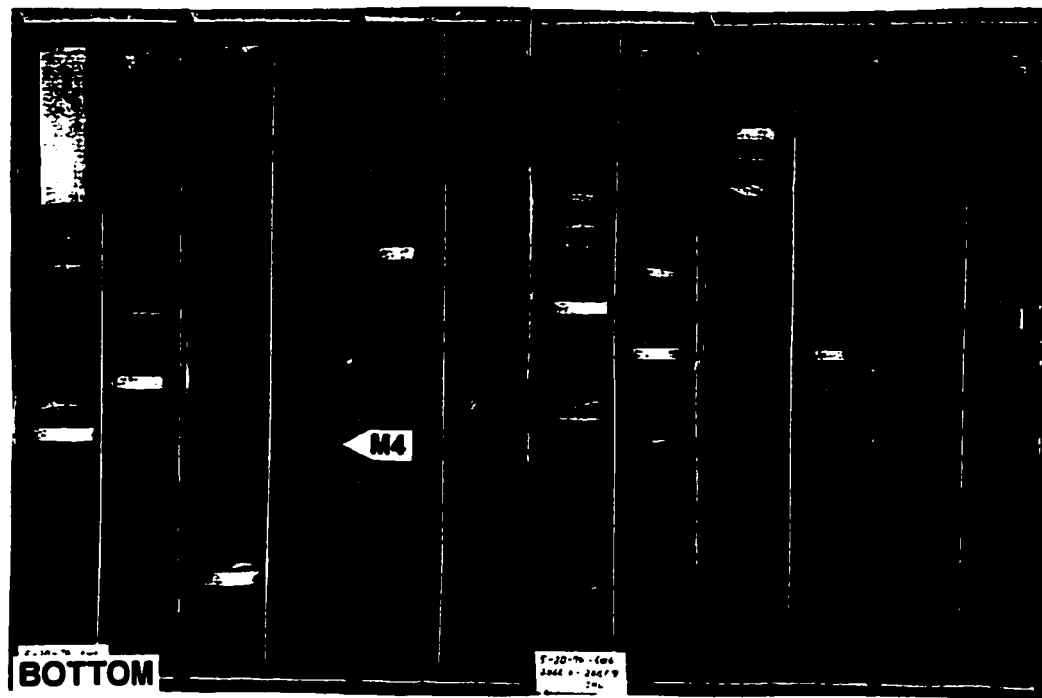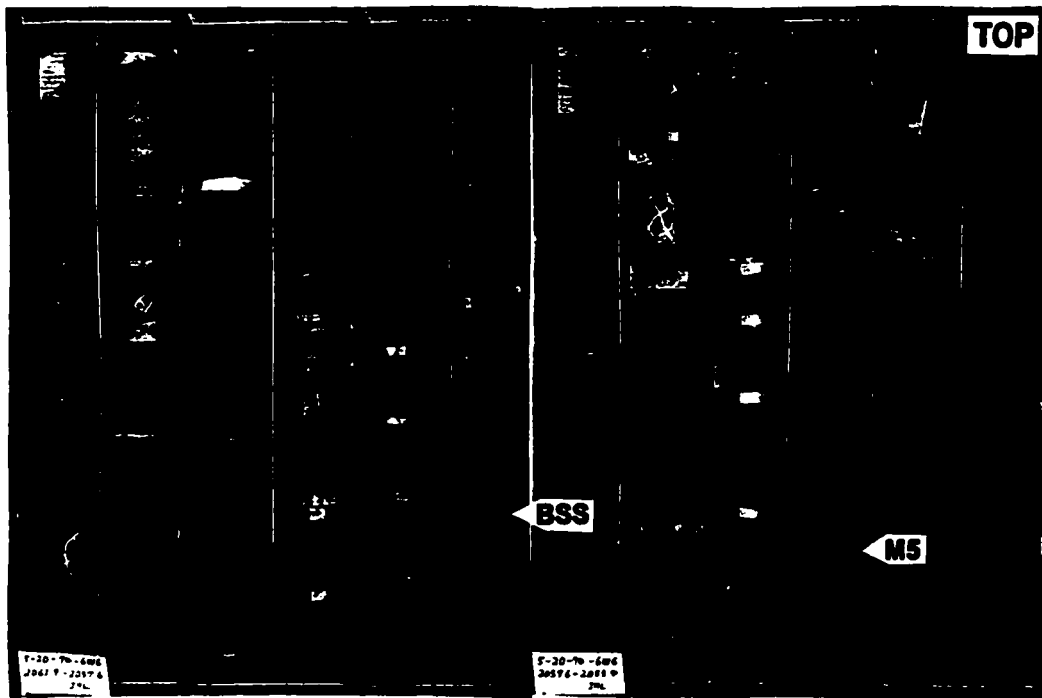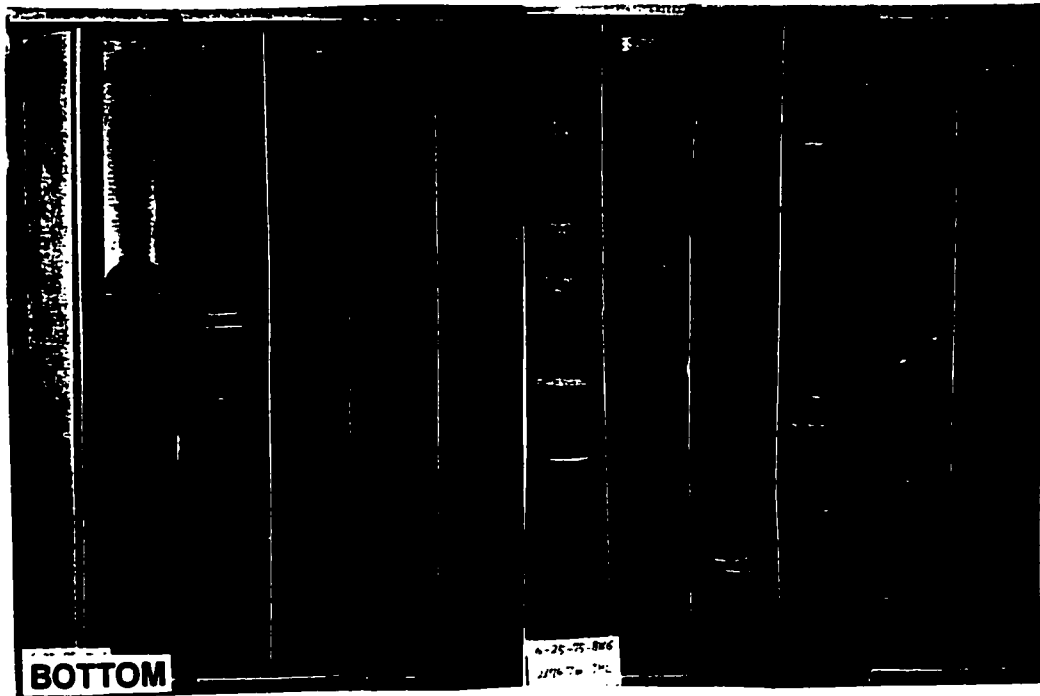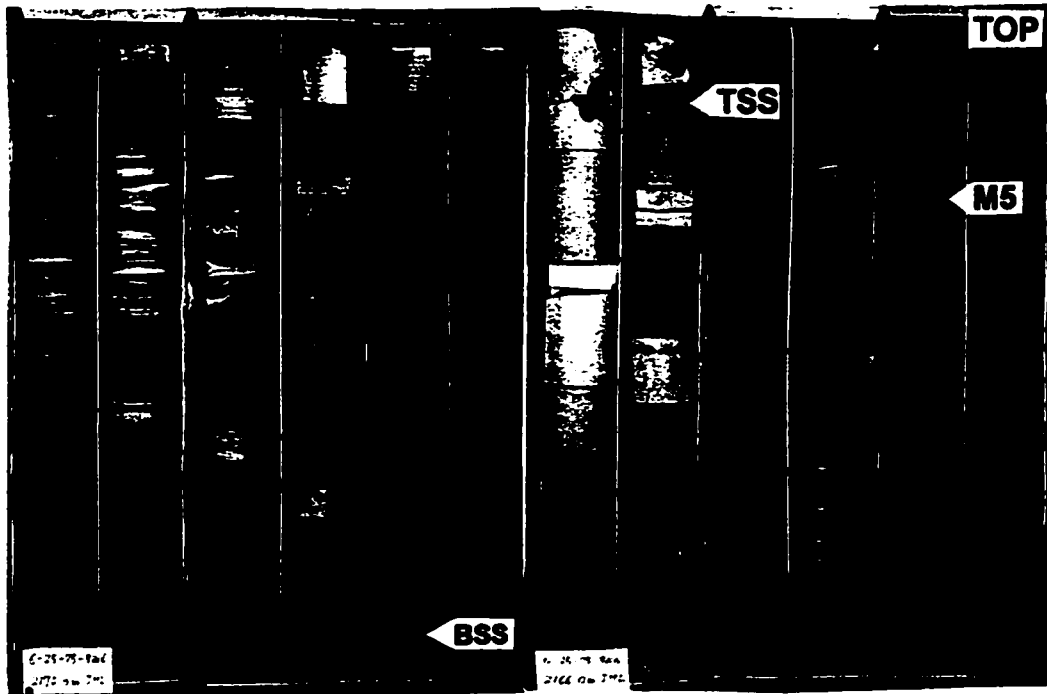
Sheet-like turbidite (sandy to silty) deposition in Unit C covers a large area. Wells near the southwestern edge of the study area, 8-11-65-13W6 and 16-31-64-12W6 have not been cored, but well log signatures suggest that an interval at least 10-15 m thick, occurring about 70 m above the base of the Montney Formation, contains sandy and/or silty turbidites. The sheet-like turbidites seem to extend into the outcrop. According to Gibson (1972), in the Meosin Mountain (about 40 km southwest of the southwestern edge of the study area), a 20 m (64 ft) succession, 52 m above the base of the Triassic consists of siltstones to very fine-grained sandstones. The beds are medium to thick bedded, up to 1.2 m (4 ft). This coarse sediment interval is correlated in this thesis with the sandy to silty turbidite interval of Unit C.

### 6.3.3 Channel Facies

A prominent feature of Unit C is a deeply-incised channel (Figs. 6-17, 6-21). The recognition of the channel in well logs, and the morphology of the channel profile have been discussed in Chapter 4.

Core 16-35-71-4W6 (Figs. 6-16, 6-17; Appendix A-5) shows a typical channel-fill facies in the updip channel area. The lowest 1 m of the channel-fill sediments (sleeves 21 and 22, 16.6-17.6 m in Appendix A-5) above ES2 (Fig. 6-16) contains abundant mud clasts commonly larger than core diameter. The mud-clast unit passes upward into a succession of thick, structureless sandstones (Facies 5)(sleeves 23 to 54, 15.6-32.8 m in Appendix A-5). The sandstone beds are

# NOTE TO USERS

Page(s) not included in the original manuscript are unavailable from the author or university. The manuscript was microfilmed as received.

149

This reproduction is the best copy available.

UMI

commonly thicker than 2 m. Interbedded mudstones are rare, and range from 5 to 30 cm in thickness. A 40 cm interval above the structureless sandstone succession contains abundant mud clasts (sleeve 55, 32.8-33.2 m in Appendix A-5). This is overlain by a succession of mudstones and siltstones (sleeves 56 to 64). Comparison of 16-35-71-4W6 (Fig. 6-16, Appendix A-5) and 6-30-71-3W6 (Figs. 6-13, Appendix A-4) shows that in core 6-30-71-3W6 (outside channel), the dominant facies consists of sharply based thin-bedded sandstones and siltstones. The thick structureless sandstone succession (Fig. 6-16) is not observed.

Farther downdip in 6-11-75-9W6 (Fig. 6-17, Appendix A-24), the 18 m long core consists entirely of thick structureless sandstones with only very thin mud layers. Well log profiles in this well suggest that the total thickness of structureless sandstone succession is 35 m. In well 6-25-75 -8W6 (Fig. 6-15, 6-17; Appendix A-23) about 10 km away from the channel axis, the succession consists only of 2.8 m of structureless sandstones.

Three core cross sections have been constructed to show channel geometries and facies (Figs. 6-17 to 6-20). Cross section X-X' (Fig. 6-18) shows a typical channel geometry and facies in the upchannel area. In all three wells, the lower parts of the cores consist of dark mudstones. The mudstone succession is abruptly overlain by the thin-bedded sandstone interval (Subunit B3). The thin-bedded sandstones interval is overlain by a muddy interval above M4. In wells outside the channel (6-30-71-3W6 and 15-10-72-4W6), Unit C consists mostly of thin-bedded sandstones and siltstones with some mudstone intervals. However,
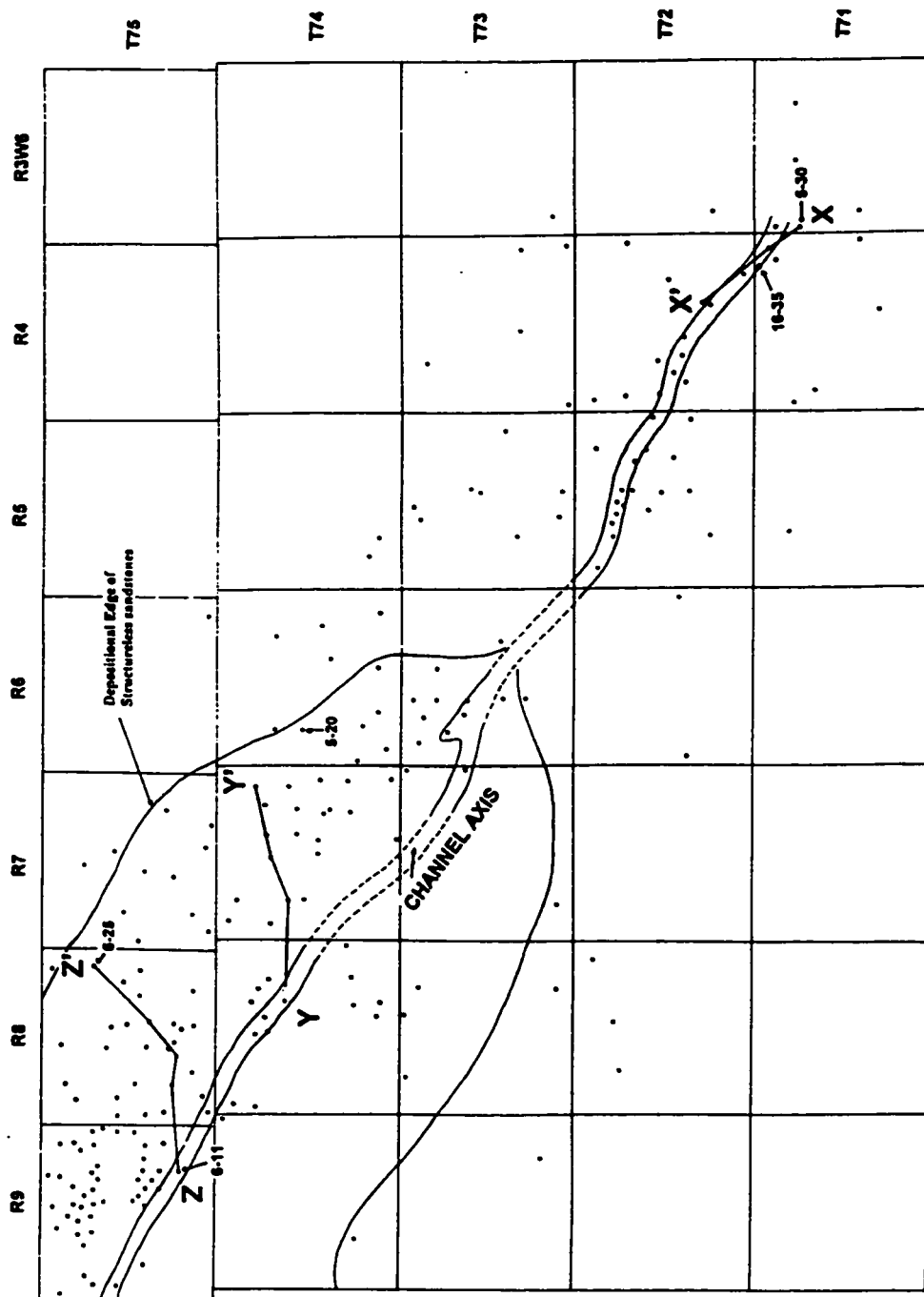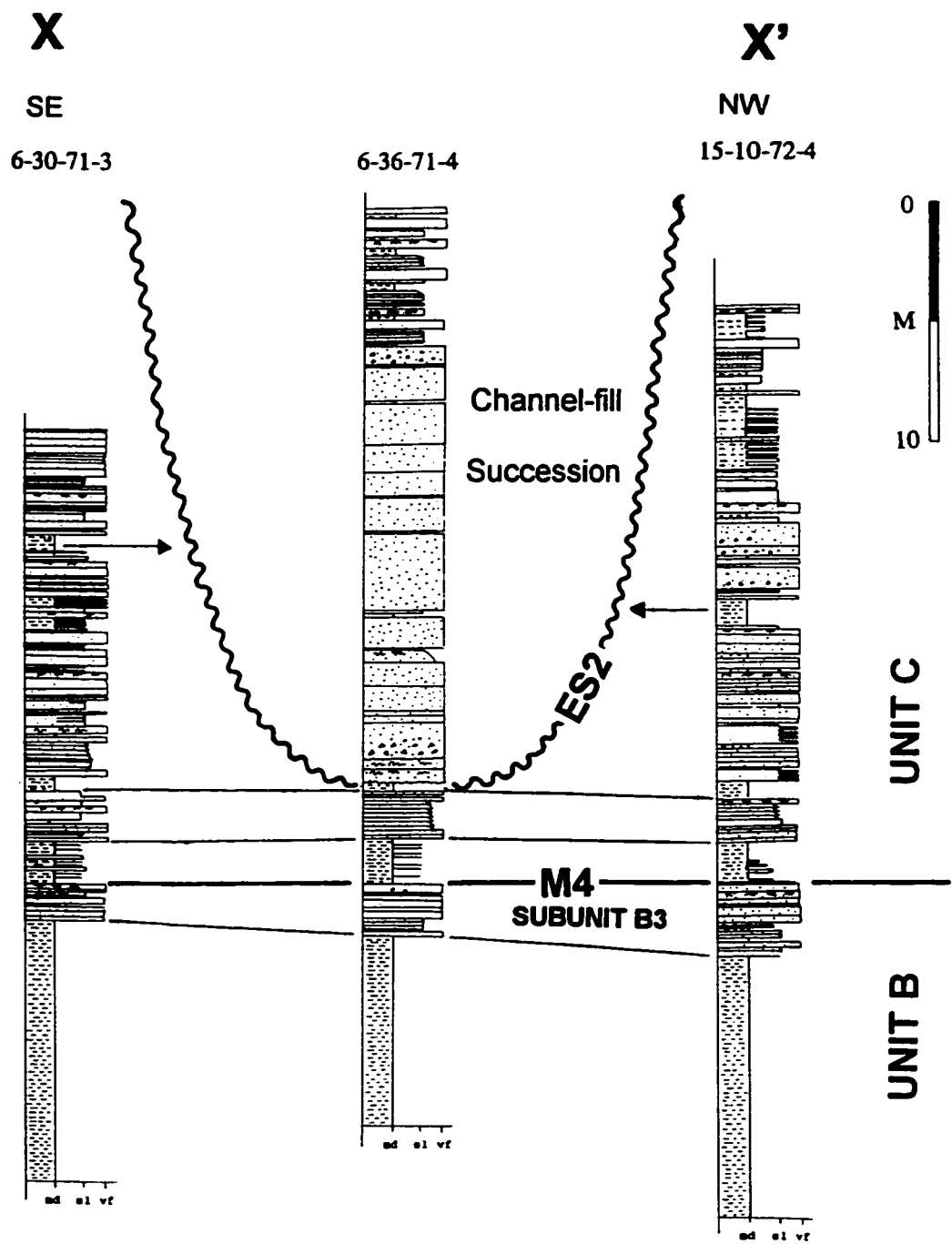
in 6-36-71-4W6, the channel cuts deeply into Unit C, and the channel is filled with thick structureless sandstones. The basal part of the channel-fill succession contains abundant mud clasts. The upper part of the channel was not filled with structureless sandstones but with finer sediments, similar to those outside the channel. However, in the upchannel area, channel incision depth commonly ranges from 30 to 40 m (see Fig. 7-2), and well log correlations suggest that the finer sediments above the structureless sandstone succession in 6-36-71-4W6 are also channel-fill deposits rather than extensive sheet-like deposits.

Cross section Y-Y' (Fig. 6-19) shows the typical morphology of the channel and facies succession in the downchannel area. In 14-23-74-8W6, the 16 m core consists mostly of thick structureless sandstones. The well log suggests that the thickness of the sandstone succession in this well is about 22 m. The well is slightly away from the deepest part of the channel. In a nearby channel axis well, 16-28-74-8W6, the log signature suggests that the thickness of structureless sandstone succession is 42 m. The remaining three cores (Fig. 6-19) are from areas outside the channel. Unlike the updip section X-X', the thick structureless sandstones spread away from the channel axis, with thicknesses up to 10 m (but the thicknesses drop to zero at the dege). The bases of the sandstones are very sharp, but well log correlations suggest that there is no significant erosion at the base of the sandstones. Farther downchannel, section Z-Z' (Fig. 6-20) shows almost identical characteristics to those of section Y-Y'.

An isopach map of this channel-related sandstone (mainly structureless

Z' NE

6-25-75-8

6-15-75-8

6-9-75-8

6-8-75-8

Z SW

6-11-75-9

M5

ES2

M

0

10
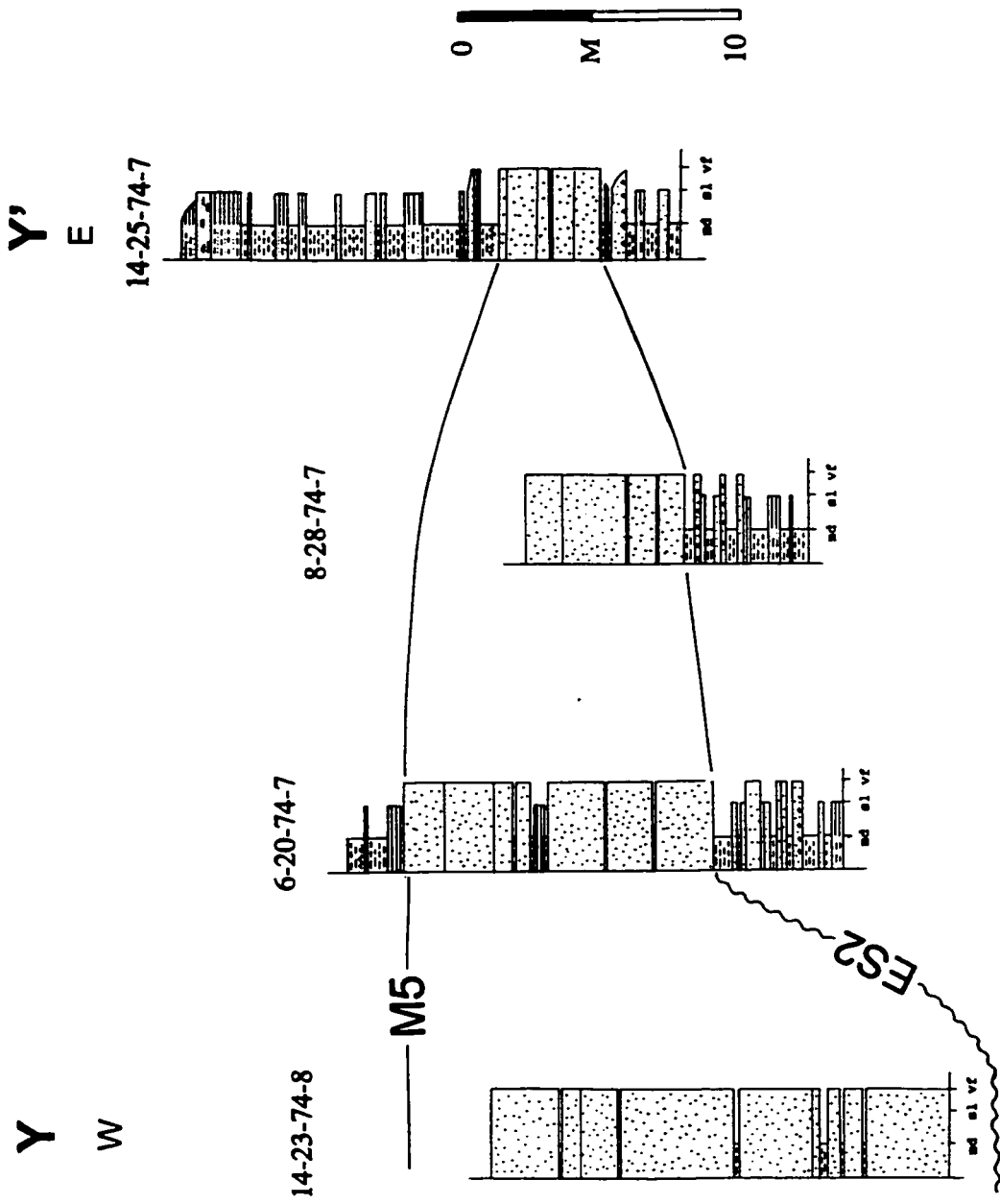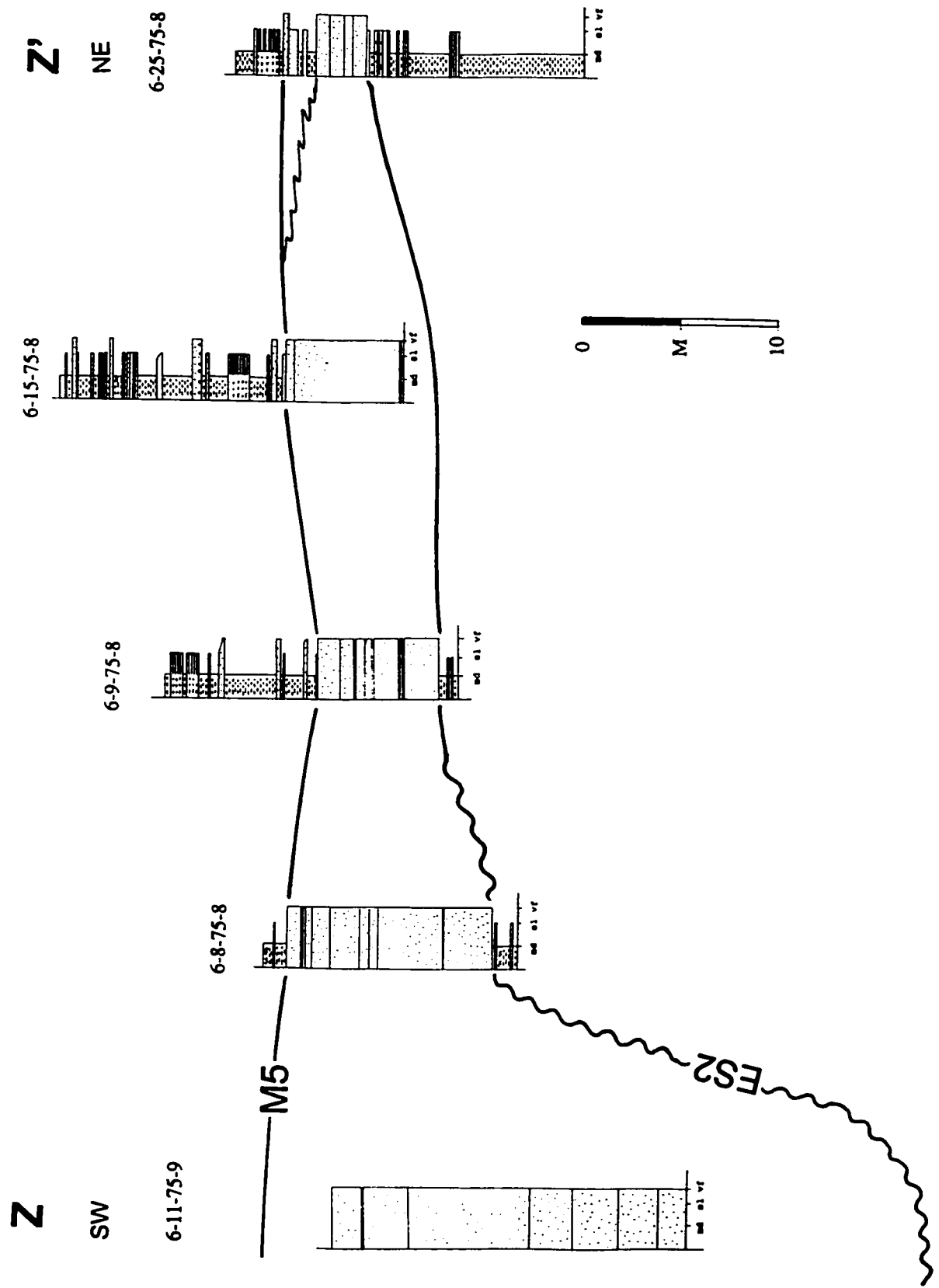
sandstones) succession is shown in Figure 6-21. A prominent feature of the map is a relatively straight, deeply incised channel that trends southeast to northwest (T71 R3W6 to T75 R9W6). The main channel axis is approximately identified by a sandstone succession thicker than 20 m (in detail, recognition of a channelized well is based on the presence of downcutting at the base of structureless sandstone succession in cross sections; all wells containing structureless sandstones thicker than 15 m are channelized, but some wells containing structureless sandstone thinner than 10 m are also channelized, see Chapter 4 for the discussion of the recognition of the channel). Although the maximum isopach value in the map is 20 m, in several wells, the sandstone succession is thicker than 30 m, and in some wells thicker than 40 m (see Fig. 6-22). The main channel (yellow in Fig. 6-21) does not extend northwest of T75 R9W6. The isopach map suggests that the main channel turns abruptly southwestward in T75 R10W6. In T75 R10W6, no well penetrated the channel axis area, but several wells between T75 11W6 and T74 R12W6 contain sandstone successions thicker than 10 m. In those wells, the channel has cut down into the underlying sediments, and Subunits B2 and B3 are commonly missing (see wells 5-25-74-12W6 to 7-23-74-11W6 in cross section G-G' (Fig. 4-8); see also Appendix A-34). This northeast-southwest trending channel is interpreted as the downstream extension of the southeast-northwest trending main channel. Although the sandstone succession is thinner than in the main channel, the erosional base of the northeast-southwest trending channel has almost the same stratigraphic position as that of the southeast-northwest trending main

Depositional Edge of
Structureless Sandstones
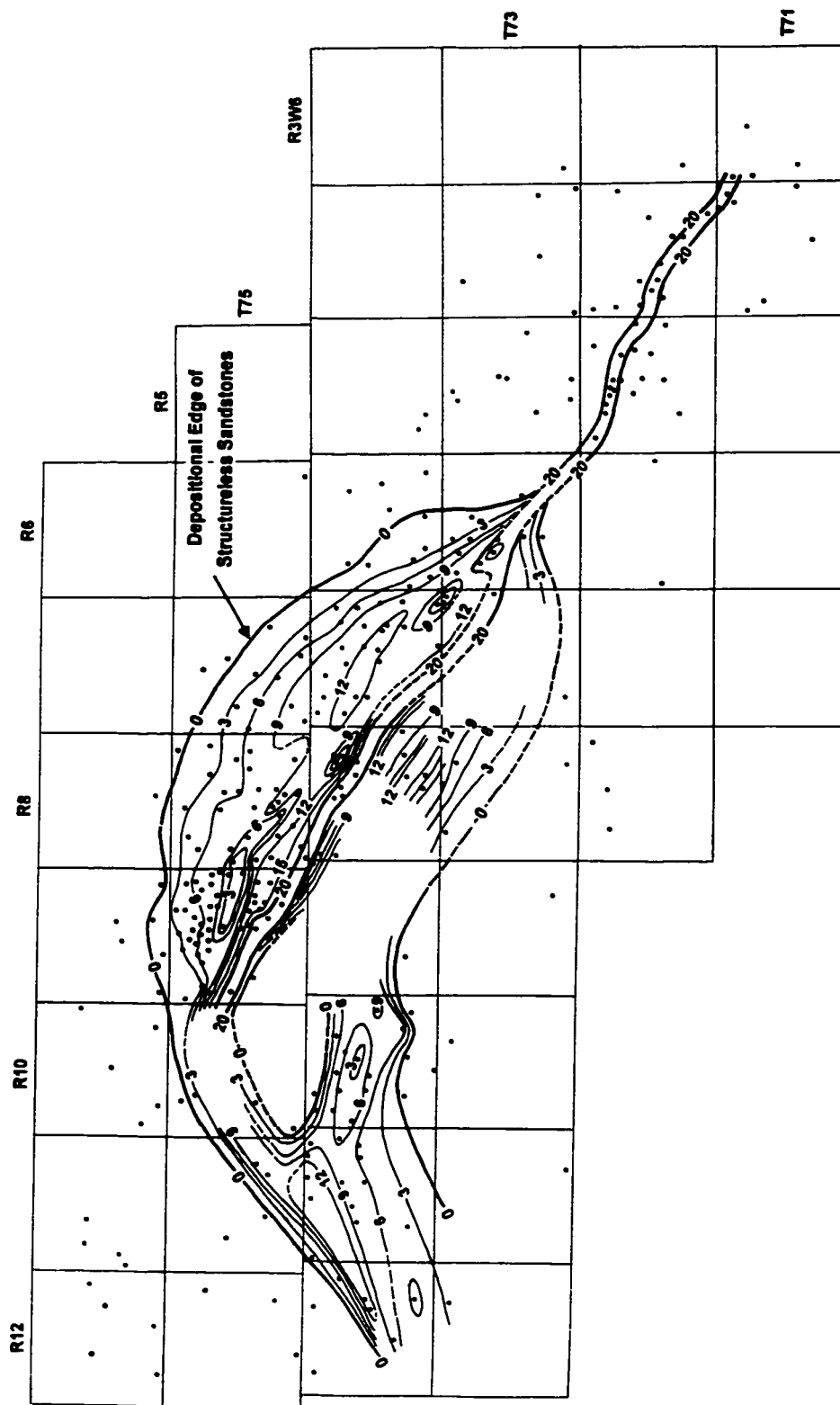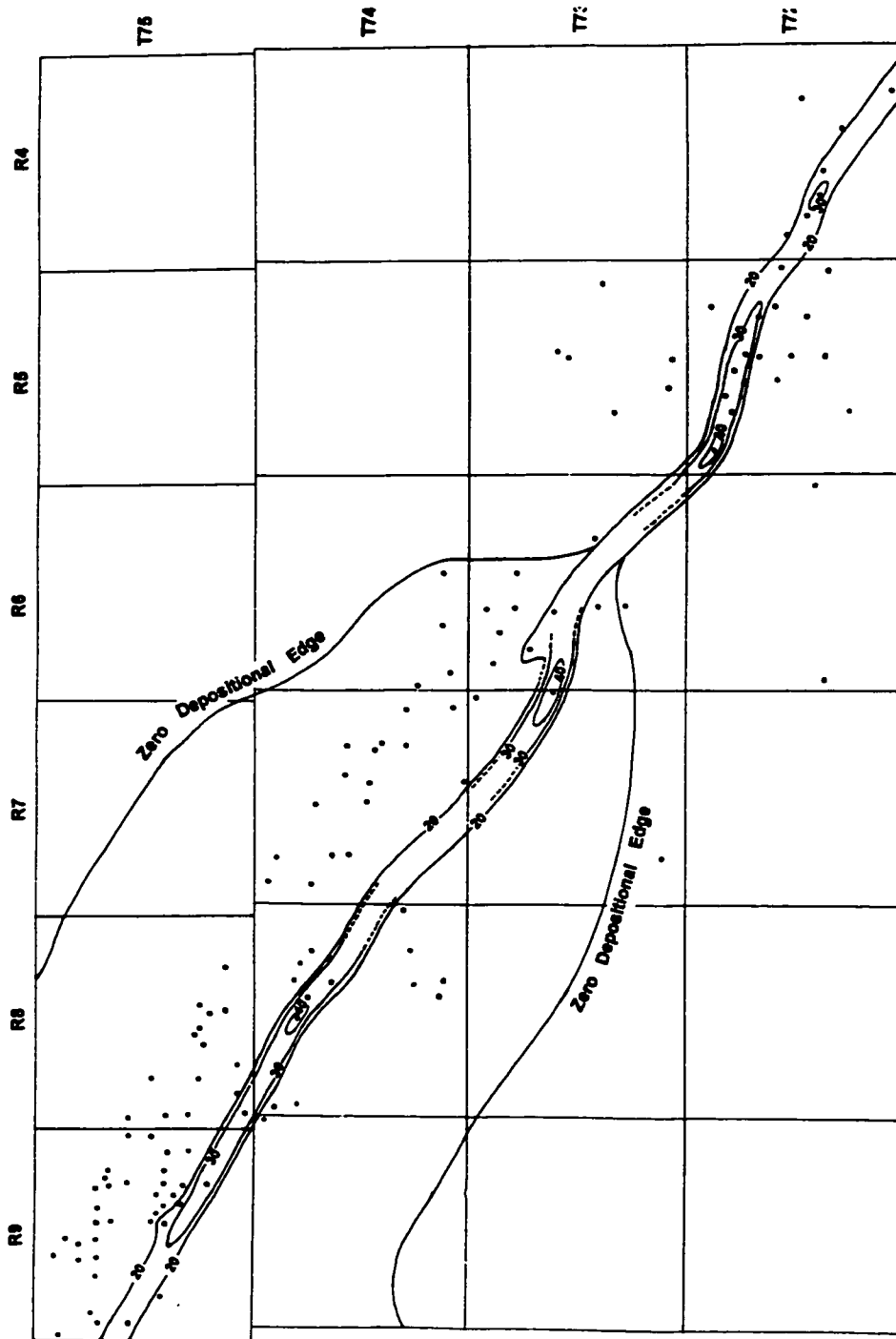
channel.

Another deeply incised channel occurs in T74 R10W6 (Fig. 6-21). In that area, although the sandstone succession is much thinner ( 6 to 10 m) than in the southeast-northwest trending main channel, the erosional base of the channel has almost the same stratigraphic position as that of the main channel, and the underlying sediments of Subunits B2 and B3 are commonly missing (see Appendixes A-32 and A-33). The isopachs in the area suggest that the channel bifurcates to the west. The channel appears to be connected to the southeast-northwest trending main channel because the channel in T74 R 10W6 incised the underlying sediments as deeply as the main channel. A notable feature of the channel in T74 R10W6 is that the sandstone succession is much thinner than in the main channel. Correlations suggest that the sandstone succession of the channel in T74 R10W6 is correlated with only the lower part of the sandstone succession of the main channel.

Another prominent feature of Figure 6-21 is the downchannel change of sand body geometry. In the upchannel area (between T71 R3W6 and T72 R5W6), the thick structureless sandstones are completely confined within a narrow channel. However, farther downslope they spread out of the channel for a distance of up to 10 km, gradually thinning away from the channel axis to the zero isopach. A few variations of isopachs are indicated by locally thinner deposition outside the main channel. The elongate thinner areas are parallel or subparallel to the main channel axis. More detailed discussions on the deposition of the structureless sandstones

will be given in Chapter 7.

## 6. 4 Unit D

Only a few cores are available in Unit D, and they are very widely spaced. Most of the original, shallower eastern facies of Unit D have been removed by the sub-Jurassic unconformity. Core 13-5-68-1W6 (Fig. 6-23) near the subcrop edge contains relatively clean sandstones. The thickness of the individual sandstones is variable, but some beds are thicker than 50 cm. Thin sandstone beds are commonly well laminated, but thick beds are weakly-laminated or structureless. Flat laminations are most common, but laminations in some beds are slightly undulating. Some thick sandstones contain abundant coquina shell fragments and small mud clasts (sleeves 17 to 19). The uppermost 2.5 m is severely slumped (sleeves 23 to 26). In 4-28-68-26W5 and 1-29-68-26W5, the cores (15.5-16.9 m thick) consist entirely of sandstones. There, sandstones beds are commonly thicker than 1 m, and are very weakly laminated or structureless.

Farther to the northwest, core 6-1-76-9W6 (Fig. 6-24, Appendix A-30) consists of sharply-based thin-bedded sandstones and siltstones (Facies 4), and interbedded dark mudstones (Facies 1). Most of the sandstone and siltstones beds are thinner than 30 cm, but some beds are thicker than 50 cm. The bases of sandstones and siltstones are always very sharp. The grading into mud in the upper part of the sandstones and siltstones is most common, but a sharp upper boundary is also common. The sandstones and siltstones are interpreted as
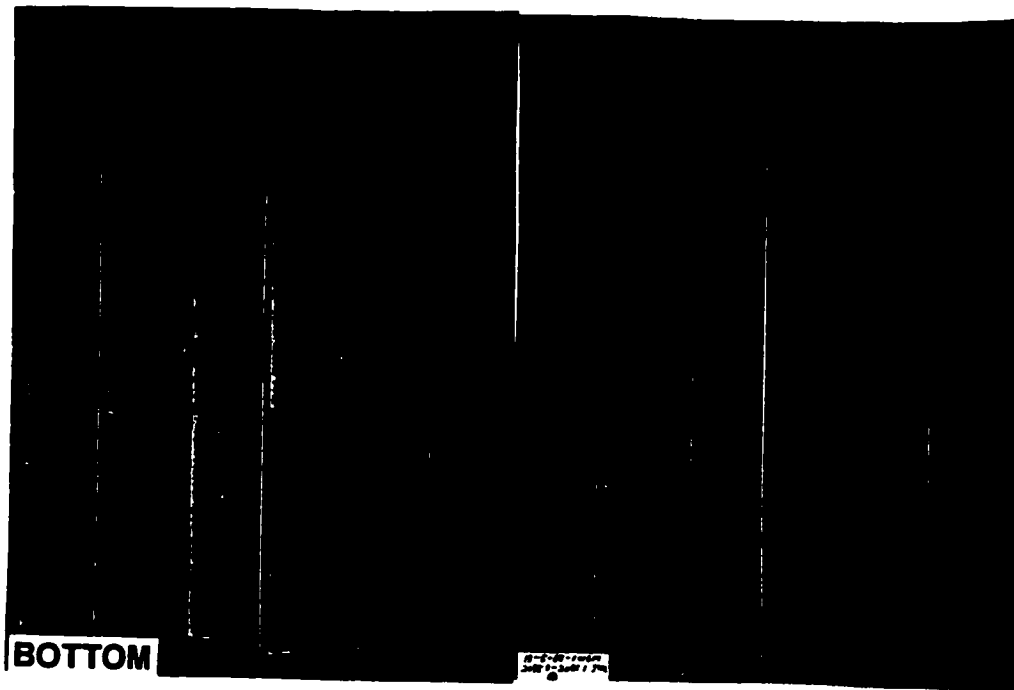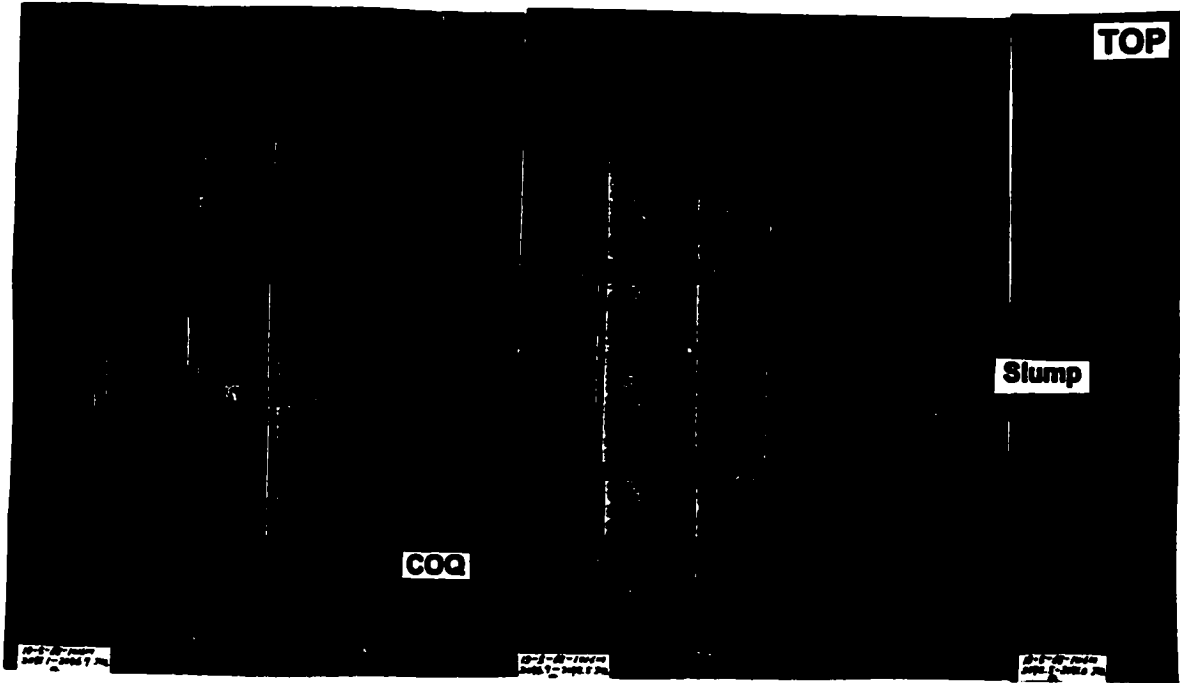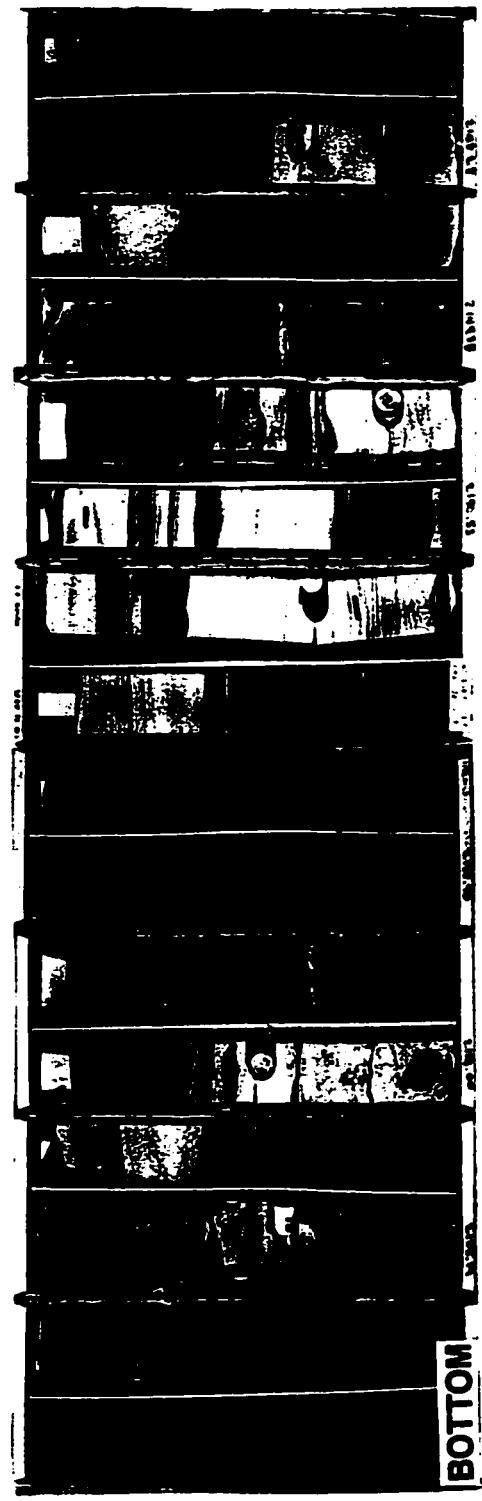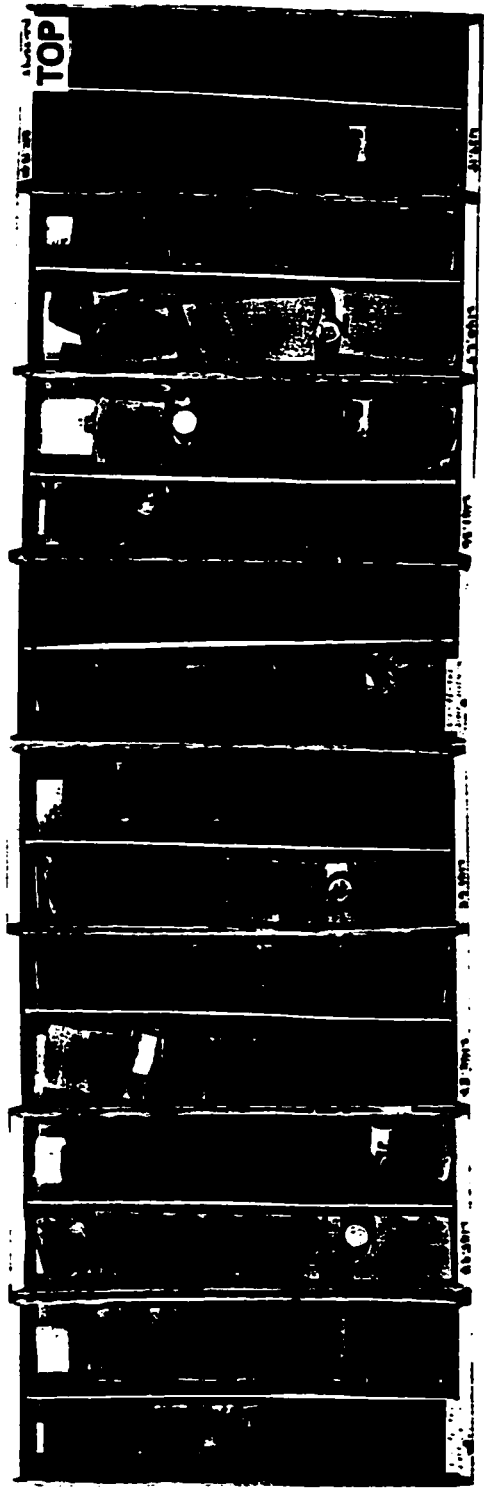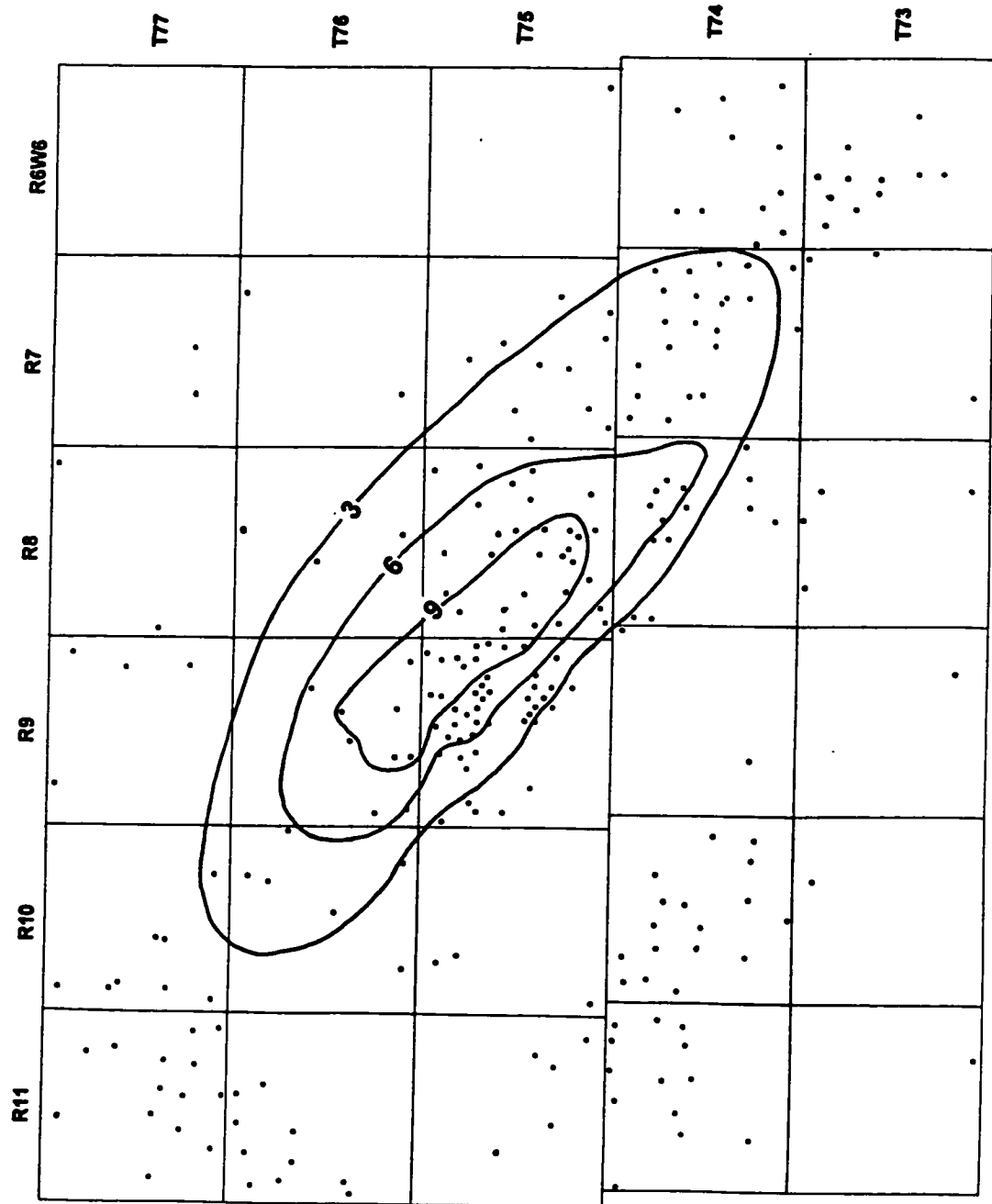
turbidites. The thicknesses of the interbedded mudstones varies from a few cm to 1 m, and the volume percentage of the mudstones is 60-70 %. Core 6-1-76-9W6 is the only one in that area. However, well log correlations suggest that these sandy or silty turbidites (mainly Facies 4) occur over an area of several townships (Fig. 6-25). The coarse sediment body trends northwest to southeast, and its maximum thickness is about 13 m. Well log correlations suggest that there is no channel incision deeper than 5 m. Most of the coarse beds recognized by prominent peaks in the well logs are thinner than 1.5 m and rarely exceed 2 m. Most peaks can be relatively easily correlated laterally. However, blocky responses up to 4 m thick in a few wells may indicate small channel incisions.

## 6.5 Units E, F and G

Units E, F and G are thick in the western part of the study area, and they become rapidly thinner to the east due both to reduced deposition and also to erosion at the sub-Jurassic unconformity. Few cores are available in Units E, F and G, and no core has been examined in this study. This discussion is based on the characteristics of well log signatures and correlations.

Comparison of well log signatures of Unit E with those of Unit D suggests that Unit E also contains coarse (sandy or silty) turbidite deposits. Recognition of such turbidites is based on very prominent peaks in well logs which have identical log characteristics to those of sandy or silty turbidites in Unit D. The volume percentage of these coarse sediments seldom exceeds 10 %, and mud deposition

dominates Unit E. The coarse sediments in Unit E cover a much smaller area than those in Unit D, and the main depositional area of these sediments in Unit E is slightly to the southwest of the depocenter of Unit D.

Unit F is characterized by a coarsening upward succession in well logs where the upper part of Unit F is preserved (see well log cross sections E-E'( Fig. 4-6) and G-G'(Fig. 4-8)) . Over a large area, the upper part of Unit F has been eroded and it has been preserved only in the area close to the Alberta/British Columbia border. Where the upper part of Unit F is preserved, well logs suggest that it consists mostly of sandstones and coarse siltstones.

The well log signature of Unit G suggests that it consists of much finer sediments (probably mudstones) than unit F. The base of Unit G (ES 3) is very sharp and apparently erosional, with local concentrations of phosphatic clasts (Sherwin, 1998, personal communication). In some wells near the outcrop (see well log cross section K-K'), some intervals represented by prominent sandy signatures seems to contain sandy or silty turbidites. It is notable that Davies et al. (1987) recognized a sandstone unit in the uppermost part of the Montney in the Gordondale area, just north of the northwestern edge of the study area, and designated it the "Gordondale sandstone". They interpreted it as a shoreface sandstone deposit. However, this sandstone unit does not occur in the study area.

# CHAPTER 7: INTERPRETATION AND DEPOSITIONAL HISTORY

## 7.1 Montney Formation as Clinoform Deposition

The Montney Formation is characterized by a series of southwesterly or westerly-dipping clinoforms with a maximum dip of about $0.3°$ (Fig. 7-1). The most prominent clinoforms are developed in Unit A (BM to M1). In Figure 7-1A, correlations of the well log markers show that Unit A consists of a more steeply inclined proximal part and a more flat-lying distal part. The steeply inclined part has a dip of 0.2 to $0.3°$ whereas the distal part of Unit A is nearly flat. The clinoforms of Unit A are capped with dolomitized coquina beds. The lower part of Unit A (BM to ES1) is mostly characterized by aggradation, but the upper part (ES1 to M1) shows prominent progradation to the southwest. Unit A thins to the southwest and the clinoforms have approximately 100 m of compacted topographic expression from the toe to the top, with at least 30 km of progradation (Fig. 7-1A).

Unit A in Figure 7-1B shows clinoforms similar to those in Figure 7-1A, but Unit A is much thinner and the angle of the slope is gentler (about $0.1°$). The isopach map of Unit A (Fig. 5-1) shows the location of the slope at the final stage of Unit A. The slope is indicated by the area showing rapid thickness changes in the isopach map. The slope trends northwest to southeast and dips to the southwest. From Figures 7-1 and 5-1, it follows that: (1) sediment was transported into the area from the northeast; (2) the sediment added to the slope resulted in

# NOTE TO USERS

Page(s) not included in the original manuscript are unavailable from the author or university. The manuscript was microfilmed as received.

167

This reproduction is the best copy available.

UMI

southwestward progradation; (3) the most prominent progradation occurred during the deposition of the upper part of Unit A (coquina beds and their time equivalent interval); (4) the clinoforms have a compacted topographic expression from the toe to the top up to 100 m. The original relief was greater but has been reduced by compaction; (5) present dips of the inclined surfaces range up to about 0.3°, but the original (decompacted) dip was greater.

Units above Unit A also show the characteristics of clinoform deposition, but clinoforms are less prominent. In Figure 7-1B, Unit B (M1 to M4) is characterized by broad clinoforms, but basinward (westward) thinning of the clinoforms is less prominent than that in Unit A. The slope angle decreases stratigraphically upward and the distinction of the slope and basin floor becomes difficult. Isopach maps (Figs. 5-2 to 5-5) suggest that the depocenter prograded slightly to the southwest. It should be noted that in Figure 7-1A, Unit B onlaps the former slope and clinoform deposition did not occur. Comparison of Figure 7-1 and isopach maps (Figs. 5-2 to 5-5) suggests that during deposition of Unit B, clinoform deposition occurred only in the active depositional area (in the south of the study area). Other areas are characterized by onlap.

It appears that the units above B also show clinoform deposition with overall progradation westward or southwestward, but the morphological subdivision of the units into topset, foreset and bottomset is more difficult. It should be noted that overall sediment accumulation in the units was greatly influenced by structural activities, as suggested in Chapter 5. In particular, rapid thinning of Units C (M4 to

M6) and D (M6 to M7) in the distal parts of the section in Figure 7-1B seems to has been caused by structural influence (see Chapter 5).

## 7.2 Shallowing upward Succession and Coquina Deposition

### 7.2.1 Shallowing upward Succession

In the eastern part of the study area, Unit A consists of several coarsening upward successions (see Chapter 6.1). In each coarsening upward succession, the facies association commonly begins with bioturbated silty mudstones to muddy siltstones (Facies 3) which become coarser upward. The bioturbated silty mudstones to muddy siltstones are gradually replaced upward by mud-laminated or mud-interbedded sandstones/siltstones (Facies 6). Mud-laminated or mud-interbedded sandstones/siltstones are gradually replaced upward by relatively clean, flat-laminated to structureless sandstones (Facies 8). The top of the succession may contain dolomitic coquina beds (Facies 9). Most of the facies contacts are gradational and the idealized facies succession is illustrated in Figure 6-5 (see Chapter 6.1 for detailed description).

The facies association summarized in Figure 6-5 is interpreted as a prograding shallowing upward succession. However, the facies association is significantly different from those produced by storm- and wave-dominated prograding shorelines. One of the most significant characteristics of the facies succession in Figure 6-5 is the absence of wave-formed sedimentary structures. Throughout Unit A, wave-formed sedimentary structures such as wave rippled

sandstones, HCS beds and SCS beds are very rare, suggesting that wave processes had a very limited role in the formation of the successions. The absence of wave-formed sedimentary structures in Unit A will be contrasted with the abundant wave-formed sedimentary structures in Units B and C.

Davies et al. (1997) interpreted the "heterolithic sandstone-siltstone facies" (Facies 6 in this thesis) as tidal sandflat deposits, and suggested that "shallow facies" in the Montney Formation were commonly tidally-influenced. Their main evidence of tidal influence in the Montney Formation is the presence of "couplets" defined by finer siltstone interlaminated with very fine-grained sandstones (see Figs. 3-6 C and D). They interpreted the "couplets" to reflect tidal sedimentation, with each set recording a flood-stillwater-ebb-stillwater cycle. However, although the "couplet" facies are commonly developed in the tidal environment, it is not restricted to that environment. Thus, recognition of tidal sedimentation ideally requires some characteristic features of tidal deposits, such as herringbone cross stratification and bundled cross bedding. However, in the Montney Formation, these tidal sedimentary structures are absent. Also recognition of tidal deposits requires not only examination of individual sedimentary structures but also consideration of their setting within vertical and lateral facies succession. A common vertical succession of tidal deposits is a fining upward succession produced by the lateral accretion of tidal channels accompanied by tidal flat progradation, but these have not been recognized in Facies 6.

In summary, the main characteristics of the succession summarized in Figure

6-5 are : (1) a coarsening upward trend with coquina beds at the top; (2) the absence of wave-formed sedimentary structures; and (3) the absence of facies and facies associations typical of a tidal setting. From these criteria, the facies association (Fig. 6-5) is interpreted as a prograding shallowing upward succession, but not shallow enough for shoreface/inner shelf environments.

## 7.2.2 Coquina Deposition

In the study area, several successions of coquina beds occur in the upper portions of coarsening upward successions. However, the coquina bed succession in the uppermost part of Unit A (CSUA) does not occur as the upper portion of a gradual coarsening upward succession. The base of the CSUA is not gradational from underlying sediments but very sharp (Fig. 6-7A).

The CSUA is the most extensive and thickest of the coquina bed successions. Its preserved width commonly ranges from 20 to 30 km, and its maximum width reaches 60 km (Fig. 5-1). Its thickness varies from a depositional zero edge to 20 m, and commonly exceeds 8 m. Various origins for the CSUA have been proposed, including (1) tidal channel deposits (Bower, 1998); (2) transgressive shoreface deposits (Henderson and Zonneveld, 1998); and (3) forced regressive shoreface deposits (Davies et al., 1997; Sherwin, 1998).

The CSUA has the following characteristics:

(1) The base is characterized by sharp erosional truncation. In cores, the erosional surface (ES1) consists of a sharp boundary between dolomitic sandstones with

various proportions of coquina fragments and the underlying bioturbated mudstones and siltstones (Fig. 6-7A). Well log correlations suggest the erosional surface (ES1) is regional, more than 30 km wide (see Figs. 4-4 and 7-1). In cross sections, ES1 is manifested by the truncation of underlying well log markers. ES1 cuts progressively deeper landward (northeastward), and it passes westward into a conformable surface in the deeper part of the basin (Fig. 4-4).

(2) the coquina beds grade into sandstones, siltstones and mudstones basinward, and their equivalent succession thickens downslope. In several wells (4-8-76-3W6 to 10-13-74-5W6 in Fig. 7-1A), the succession equivalent to the coquina beds exceeds 60 m in thickness, and the overall sediment accumulation pattern suggests a southwestward progradation.

(3) The base of the coquina bed succession steps basinward (southwestward) over progressively deeper facies. In well 3-23-68-22W5, the coquina beds overlie Facies 6 (mud-laminated or interbedded sandstones and siltstones), but in well 6-30-67-23W5 about 20 km southwest of 3-23-68-22W5, the coquina beds overlie Facies 3 (silty mudstones to muddy siltstones), suggesting stepped accumulation of the coquina beds over progressively deeper facies.

(4) The coquina succession is internally heterolithic, with various thicknesses of fine-bioclastic sandstones, siltstones and mudstones, suggesting multi-event deposition. Thick coquina beds commonly contain mud clasts or mud pebbles in their basal parts.

(5) The coquina succession shows an overall coarsening and thickening trend

upward. The lower part of the succession commonly contains weakly laminated bioclastic sandstones with a few shell fragments, and interbedded siltstones and mudstones. The thickness of individual coquina beds ranges from 10 to 30 cm. Stratigraphically upwards, bed thickness increases and the proportion of interbedded mudstones/siltstones decreases. The uppermost part of the coquina succession contains much more abundant shell fragments than the lower part, and interbedded mudstones are very rare. The thickness of individual coquina beds commonly exceeds 70 cm. The coarsening upward trend of the coquina succession is very prominent in the distal (southwestern) part of the coquina accumulation, whereas in the proximal part, the trend is less prominent where the lower part of the coquina succession commonly consists of thick coquina beds with few interbedded siltstones and mudstones.

(6) Some of coquina beds, and interbedded sandstones and siltstones are bioturbated by *Lingulichnus* burrows.

(7) The top of the coquina succession is sharply overlain by mudstones. The basal part of the overlying mudstones commonly contains mud-clasts 1-2 cm long or a thin lag of coquina clasts.

Above all, the erosional truncation (ES1) at the base of the coquina succession is not local but regional. The preserved erosional truncation is at least 30 km in width. The regional extent of ES1 suggests that ES1 is not a local tidal channel incision surface. Furthermore, the coquina succession does not show the fining upward trend, characteristic of tidal channel deposits. Instead, overall

coarsening upward trends are common. Also, the extensive occurrence of the coquina succession in a belt 400 km long by 30 to 60 km wide (Davies and Sherwin, 1997) suggests that the interpretation of the coquina succession as a tidal channel deposit is problematic.

Henderson and Zonneveld (1998) interpreted the coquina succession as a transgressive shoreface deposit, based mostly on the composition of coquinas and distribution of conodonts. They suggested that much of the bioclastic detritus was pirated from the underlying lingulid dominated coquinal sandstones, and that the upper part of the coquina succession is bivalve dominated, which may imply more open marine conditions as the transgression became established. They also proposed that the coquina succession contains the only conodont specimens of *Furnishins* which is characteristics of proximal, often restricted marine settings. A transgressive shoreface interpretation for the coquina succession is supported by the presence of micropavements of glauconite at the base of the coquina succession (Davies and Sherwin, 1997).

However, a transgressive shoreface interpretation cannot account for some of the sedimentary characteristics described above. Firstly, seaward thickening of the coquina-equivalent succession and its progradational stacking patterns in cross sections are difficult to explain in terms of a transgressive interpretation. Secondly, the very extensive occurrence of the CSUA (up to 60 km in width) is difficult to reconcile with a transgressive shoreface interpretation. In the literature (i.e., Walker and Plint, 1992), transgressive shoreface deposits are long (tens of km)

and narrow (only a few km). Thirdly, a transgressive shoreface interpretation does not explain the overall coarsening and thickening upward trend of the coquina succession. The vertical trend of the coquina succession suggests gradual shallowing, rather than deepening. Furthermore, Davies and Sherwin (1997) described karst-like breccias and coarse-grained, very well rounded quartz grains and interpreted the latter as aeolian deflation lags at the top of the coquina succession. Thus, the top of the coquina succession would have been (at least locally) subaerially exposed.

The sedimentary characteristics described above suggest that the coquina succession was deposited during regional shallowing conditions. Preliminary palynological data indicate that the coquina succession was deposited near the Dienerian-Smithian contact (Davies et al., 1997). An age of late Dienerian for the coquina succession would coincide with a global fall in sea level at that time (Embry, 1997). The lateral and vertical relationships of the coquina succession are similar to those in sharp-based, forced regressive shoreface successions (Plint, 1991). Identification of the specific shoreface sedimentary structures in the coquina succession is difficult because of the pervasive dolomitization that has destroyed original sedimentary structures. The erosional surface (ES1) at the base of the coquina succession is interpreted as a regressive surface of erosion formed by wave scouring on the shelf during a period of fall of relative sea level.

## 7.3 Turbidite Deposition

### 7.3.1 Turbidite Facies

In Chapter 3, Facies 2 (alternation of siltstones and mudstones), Facies 4 (sharply based thin-bedded sandstones and siltstones) and Facies 5 (thick, structureless sandstones) have been interpreted as turbidites based on sedimentary structures such as sharp bases (Facies 2, 4 and 5), common occurrences of sole marks (Facies 2 and 4), normal grading (Facies 2 and 4), mud clasts in the lower part of the beds (Facies 2, 4 and 5), structureless nature without evidence of bioturbation (Facies 5), and absence of shallow water indicators (Facies 2, 4 and 5). However, complete Bouma sequences (1962) are rare.

The Bouma Sequence, commonly considered as a model for "classical turbidites", shows a consistent set of internal sedimentary structures. Although the Bouma sequence is considered to describe typical turbidite beds, the literature shows that there are many different turbidite facies and that some of them cannot be described in terms of the Bouma sequence (i.e. Walker and Mutti, 1973; Walker, 1978, 1992; Mutti and Ricci Lucchi, 1972; Stow and Shanmugam, 1980; Piper and Stow, 1991). The Bouma Sequence is relatively well suited to medium-grained sandy beds, but it suits neither relatively coarse-grained turbidites (i.e. Facies A and B in Walker and Mutti, 1973) nor relatively fine-grained turbidites (i.e. mud turbidites in Piper and Stow, 1991).

A prominent characteristic of the Montney turbidites is their relatively fine grain size, ranging from silt to lower very fine sand. It never exceeds upper very

fine sand, suggesting that coarser sediments were not available in the source area. The very rare occurrence of a complete Bouma sequence in the Montney turbidites, especially in Facies 2 (alternation of siltstones and mudstones), is partially attributed to fine grain size. In Facies 2, many beds contain only Bouma's divisions $T_d$ and $T_e$, or $T_c$ to $T_e$. Stow and Shanmugam (1980) have suggested nine divisions, numbered $T_0$ to $T_8$, for fine-grained (silt to clay size) turbidites. The structures in these nine divisions are equivalent to the topmost C and DE divisions of the Bouma sequences, and divisions equivalent to Bouma's A and B divisions are not present. Stow and Shanmugam (1980) have interpreted the sequences to be the result of deposition during passage of a muddy turbidity flow.

Another prominent feature of the Montney turbidites is a very weakly developed graded bedding. In many beds of Facies 4 and 5, grading occurs only in the uppermost few mm to few cm of the beds, and the remaining parts of the beds do not show discernible macroscopic grain size change. The degree of grading in a turbidite bed is partly controlled by the availability of a range of grain sizes, and very well sorted material in the source area will make graded bedding difficult to discern. An extreme example occurs in the Pleistocene-Neogene turbidites in the eastern Atlantic (Sarnthein and Diester-Haass, 1977), where sandy turbidites are devoid of graded bedding, are well sorted, and contain almost no fine fraction or mica. Sarnthein and Diester-Haass (1977) have suggested that the sands were blown from the Sahara desert onto the shelfbreak by offshore winds during low stands of sea level, and transported by turbidity currents into the deep sea. The

very limited grading of the Montney turbidites can also be explained in terms of well sorted sediments in the source area. According to Davies et al. (1997), about 77 % of the coarse siltstones and very fine sandstones of the Montney are very well sorted, and the rest are well sorted. In particular, seven of eight siltstone samples fall into the very well sorted category. Davies et al. (1997) have stated that this degree of sorting in silt grades is unusual, and suggested that aeolian transport was a major process in transporting sediment into the ocean.

Some of the Montney turbidites have sharp upper boundaries with overlying sediments. Some workers (e.g. Shanmugam et al., 1993; Stanley, 1987, 1988, 1993; Duan et al., 1993) have suggested that the sharp tops of turbidites indicate reworking by bottom currents (contour currents). However, the presence of sharp tops in turbidites can also be explained in other ways. Turbidity currents can erode previously deposited beds, and also can deposit non-graded, sharp-topped beds if the late stage of the turbidity current by-passes the depositional site. Stow et al. (1998) have suggested that sharp or erosive contacts within turbidite sequences, coupled with supplementary, distinctively different characteristics above and below, such as bioturbation, anomalous grain sizes and common reverse graded bedding, can indicate reworking by bottom currents. However, the absence of these supplementary structures in the Montney turbidite succession suggests that the sharp upper boundary in the Montney turbidites can be better explained as a result of truncation by subsequent turbidity currents, or bypass of the late stage of the turbidity current rather than reworking by bottom currents.

In Chapter 6.3.2, it has been shown that the Facies 4-dominant interval passes laterally through Facies 2-dominant interval into Facies 1-dominant interval to the northwest (downslope). This lateral change of facies suggests that significant proportions of the dark mudstones (Facies 1) in the Montney Formation were transported by turbidity currents (i.e. they are muddy turbidites), rather than being hemipelagic deposits.

## 7.3.2 Turbidite Systems

### 7.3.2.1 Unchannelized, Sheet-like Turbidite System

Although a channel-related turbidite system developed in the Montney Formation, unchannelized turbidite systems are much more common and constitute the bulk of turbidite sedimentation. A channel-related turbidite system occurs only in Unit C, whereas unchannelized turbidite systems developed in Units B, C, D, and possibly in E, F, and G (see Chapter 6).

Unchannelized turbidite systems consist mostly of Facies 4 (sharply based thin-bedded sandstones and siltstones), Facies 2 (alternation of siltstones and mudstones), Facies 1 (dark mudstones), and small amount of Facies 5 (thick structureless sandstones).

Of the unchannelized turbidite systems, the one in Unit C is the most extensive and thickest. This turbidite system covers a large part of the study area (from T 65 R25W5 beyond the western margin of the study area). Northwestward sediment transport is suggested by the isopach pattern of Unit C (Fig. 5-6). In the

southeastern part of the area, Unit C is thicker than 90 m, and it gradually thins to less than 30 m in the northwest. Northwestward sediment transport is also supported by lateral facies changes. Unit C, particularly Subunit C1 around T71-72 R3-4W6 consists mostly of Facies 4 (sharply based thin-bedded sandstones and siltstones), with small amounts of Facies 2 (alternation of siltstones and mudstones) and 1 (dark mudstones). These Facies 4 turbidites gradually change into Facies 2 and/or Facies 1 turbidites to the northwest. Individual bed thickness decreases and overall grain size becomes finer to the northwest. In T75 R9W6, Facies 1 constitutes more than 80 % of Unit C, and Facies 3 is very rare or absent. Beyond T75 R9W6 to the northwest, Unit C consists entirely of Facies 1, and Facies 3 and 2 do not occur.

Northwestward deepening of the sea is suggested by some occurrences of wave-formed sedimentary structures in the southeastern turbidite beds. In several cores around T71-72 R3-4W6, some turbidite beds contain wave ripples in their upper parts, suggesting deposition above storm wave base. However, wave-formed sedimentary structures do not occur beyond T72 R5W6 to the northwest. It is also notable that in the south-easternmost part of the area (T68-69 R24-25W5), Unit C consists of much shallower facies, including Facies 7 (sandstones and siltstones associated with HCS beds).

Generally, sediments of Subunit C1 are coarser and their bed thicknesses are greater than those of Subunit C2, but with some exceptions. In some areas, Subunit C1 shows an overall upward trend of grain size coarsening and increase

in bed thickness. The most prominent coarsening and thickening upward trend in Subunit C1 developed north of T71. In the southern area, Subunit C1 does not show an overall coarsening and thickening upward trend although smaller-scale coarsening and/or fining upward trends are locally developed. However, an overall northwestward or westward progradation of turbidite sedimentation is suggested by a shift in turbidite depocenters to higher stratigraphic positions northwestward or westward (see Chapter 6).

Unchannelized turbidite systems also occur in Subunit B2, but cover much smaller areas than those in Unit C (Fig. 6-10). Two turbidite systems are developed and have almost perpendicular trends. The system in Glacier Field consists of Facies 4, 2, 1 and 5. A prominent characteristic of this system is the common occurrence of thick-bedded turbidites. Sandstones thicker than 40 cm are common, and a few beds are about 1 m thick. However, channel incision has not been positively recognized. Another characteristic of this system is the elongate external shape with its NE-SW trend. In turbidite systems in Subunit B2, prominent vertical facies trends have not been recognized. Recognition of sediment transport directions for Subunit B2 turbidite systems is difficult, but may be tentatively inferred by comparison of the location of the systems with the isopach map of Unit A (Fig. 5-1). Subunit B2 turbidite systems are located at or near the slope break of southwesterly-dipping clinoforms of Unit A. This may suggest that the source of the Subunit B2 turbidite systems was to the northeast. The almost perpendicular occurrence of two systems in same stratigraphic position may suggest structural

controls on sediment accumulation.

An unchannelized turbidite system (no incision deeper than 5 m) also developed in Unit D (Fig. 6-25). It consists mostly of Facies 4 and 1, and does not show any prominent vertical facies changes. The similar location and external morphology of this system to the Subunit B2 systems may suggest similar sediment transport direction. Units E and G appear to contain turbidites, but there is no core control. The volume of probable turbidites is very small.

## 7.3.2.2 Channel-related Turbidite System

A channel-related turbidite system developed in Unit C, and its location and general morphology have been given in Chapter 6. The most prominent characteristics of the turbidite system are (1) a relatively straight main channel trending southeast to northwest, (2) deep channel incision up to 41 m, (3) an abrupt change of channel course to the southwest in the distal part of the channel, and (4) an elongate external form of associated sandstones, parallel to the main channel.

Channel-fill sediments consist mostly of thick structureless sandstone with only a very small amount of thin mudstones. The basal few meters of channel-fill sediments commonly contain large mud clasts. The channel-fill succession shows no discernible vertical facies changes. Upward thinning and fining trends, suggested to be typical of submarine channel-fill successions (Mutti and Ricci Lucchi, 1972), are almost absent in the channel-fill succession in the Montney Formation. Instead, the top of the channel-fill succession is commonly represented

by a very sharp facies change from thick structureless sandstone (Facies 5) to dark mudstone (Facies 1).

In Chapter 6, northwestward sediment transport was indicated because of (1) a northwestward thinning and fining trend for Unit C (Fig. 5-6) and (2) the northwestward spread of the associated sandbody geometry (Fig. 6-21). More evidence for northwestward flow direction is shown by the longitudinal channel profile (Fig. 7-2). In Figure 7-2, the sea floor surface before channel incision (SBI) lies 145 m above the base of the Montney Formation (BM) in T71 R3W6. SBI gently dips to the northwest, and lies 65 m above BM in T75 R9W6. The gradient of the slope is very gentle, about 0.06-0.07°. In the more distal part of the channel (T75 R9 to T74 R12), SBI is almost flat.

The depth of channel incision is represented by the distance between SBI and BOC (base of channel)(Fig. 7-2). The incision is more than 30 m deep in upchannel areas, and reaches 41 m in well 7-31-72-5W6. It decreases downstream and ranges from 10 to 15 m in the distal part of the section (T75 R9 to T74 R12). The channel-fill succession consists mostly of structureless sandstones and is 46 m thick in well 9-24-73-7W6. It thins gradually both upchannel and downchannel. In the distal part of the section, the channel-fill succession is about 15 m thick. In the middle and distal part of the section, the top of the structureless sandstone succession (TOSS) lies 7-14 m above SBI. However, in the upchannel area (T71 R3 to T72 R5), TOSS lies below SBI, indicating that in the upchannel area, only the lower part of the channel-fill consists of structureless sandstones (Facies 5). There,
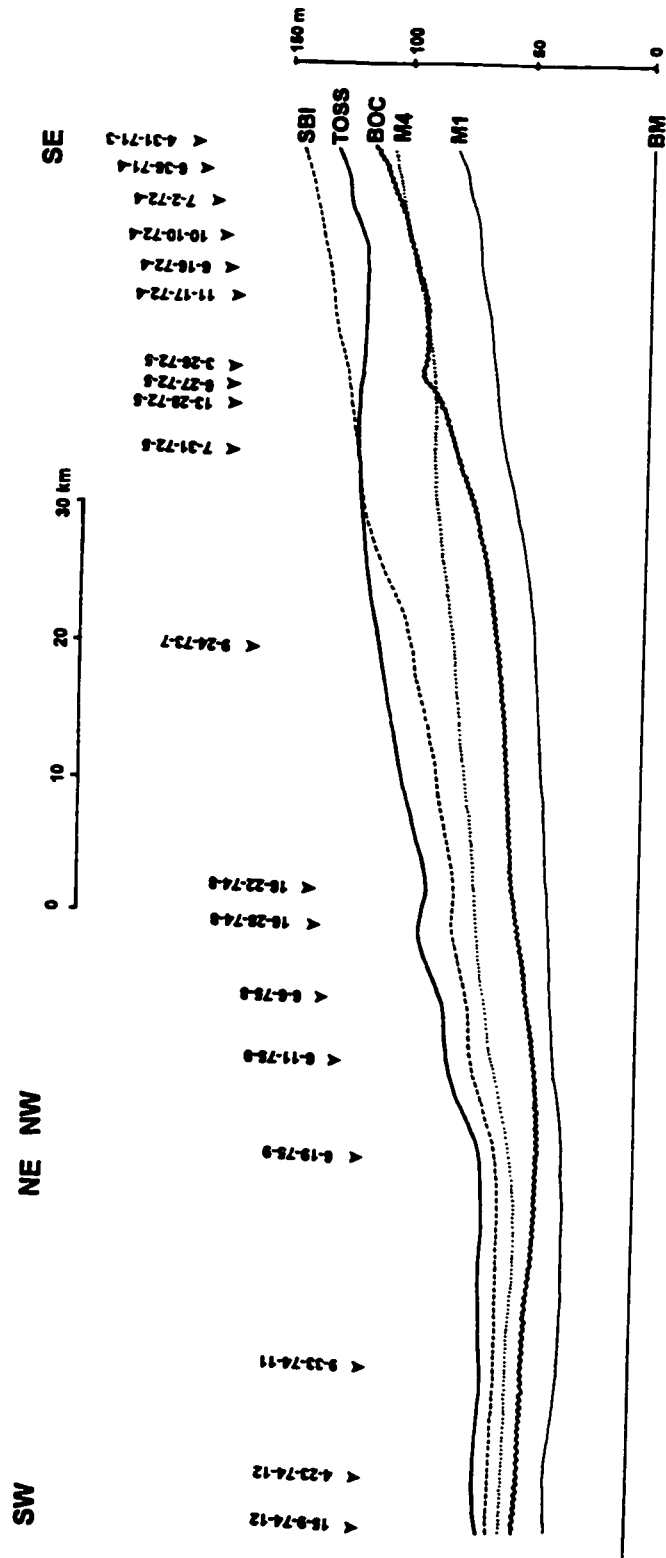
the upper part of the channel-fill consists mostly of Facies 4 (sharply based thin-bedded sandstones and siltstones) and Facies 2 (alternation of siltstones and mudstones). The relationship of SBI and TOSS illustrates the plan-view geometry of the associated sandstones (see Fig. 6-21). Comparison of Figure 7-2 and Figure 6-21 shows that in the upchannel area where SBI overlies TOSS, the structureless sandstone succession is completely confined within the channel. However, farther downslope where SBI underlies TOSS, structureless sandstones occur not only within the incised channel but also outside the channel, spreading for a distance of up to 10 km.

It should be mentioned that the isopach map (Fig. 6-21) may have a slightly biased data base, with most of the wells drilled on seismic indications of sand, with few wells drilled between the sands. Seismic data show that the main channel is bounded by mudstones, interpreted as levees. These levees are discontinuous and parallel to the main channel. However, they cannot be recognized on the isopach map (Fig. 6-21) because of lack of data near the margin of the main channel. A possible levee indicated by the isopach map consists of the low values for sand thickness (less than 6 m) near the northeastern margin of the main channel in T74 R8W6. The location of the anomaly is close to the main channel margin (a few hundred meters), and well logs in the area suggests sediments are much muddier than in the nearby channel-fill.

The presence of levees or interchannel areas containing a very reduced amount of sand near the main channel margin, as indicated by the seismic data,

suggests that the sandstones outside the main channel filled smaller channels fed by the main channel. Alternatively, they may represent sheet-like deposits from nonchannelized overbank flows. If the sandstones outside the main channel (Fig. 6-21) represent sediment infill of smaller channels fed by the main channel, the erosional base of each smaller channel might have a stratigraphically different position, and the sandbody should be characterized by narrow strips of sand. However, the correlations (Figs. 7-3 and 7-4) detailed in this study suggest that the bases of sandstone successions (BSS) outside the main channel always have the same stratigraphic position, and the sandbody is not broken into narrow strips of sand. It is laterally very extensive without any indication of nearby interchannel (muddier) facies. These aspects suggest that the sandstones outside the main channel may represent sheet-like deposits from unchannelized overbank flows, rather than sediment infill of smaller channels.

The correlations (Figs. 7-5 and 7-6) reveal strong fault-controls on the thickness of accumulated sandstones and on facies distribution. In cross section L-L' (Fig. 7-6A), well 6-11-75-6 represents a channel axis position where 35 m of the channel-fill succession consists entirely of thick structureless sandstones. However, the adjacent well 12-17-75-9 does not contain sandstones, and consists mostly of mudstones. Correlation between the two wells shows that log markers are offset about 20 m, suggesting that well 12-17-75-9 has been uplifted about 20 m relative to well 6-11-75-9. Another relatively uplifted block is shown by well 14-22-75-9. The thickness of the structureless sandstone succession in well 14-15-75-9

Depositional edge of structureless sandstones

channel axis

Depositional edge of structureless sandstones

channel · axis

T75

T74

T73

R6

R7

R8

R9

N

N'

O

O
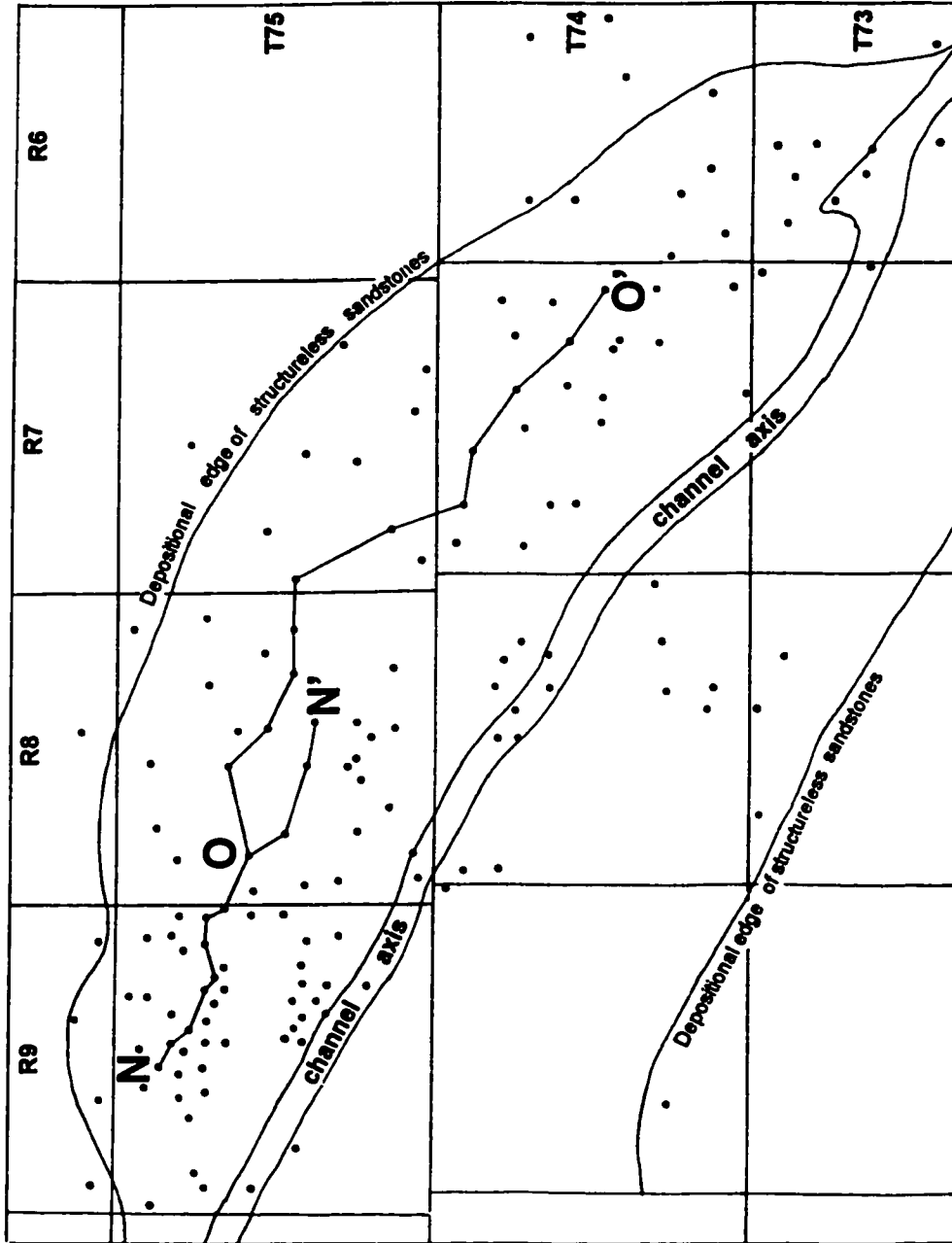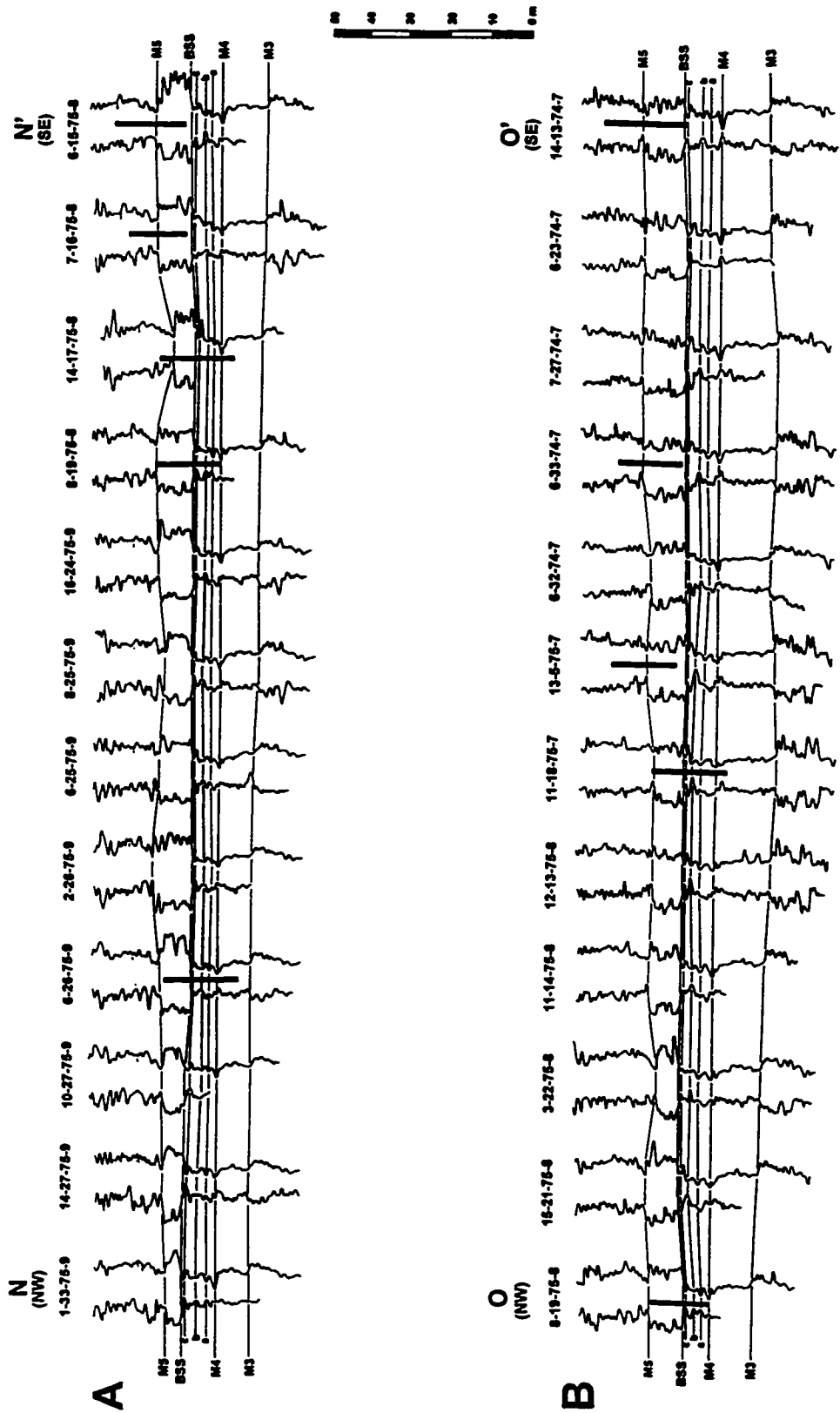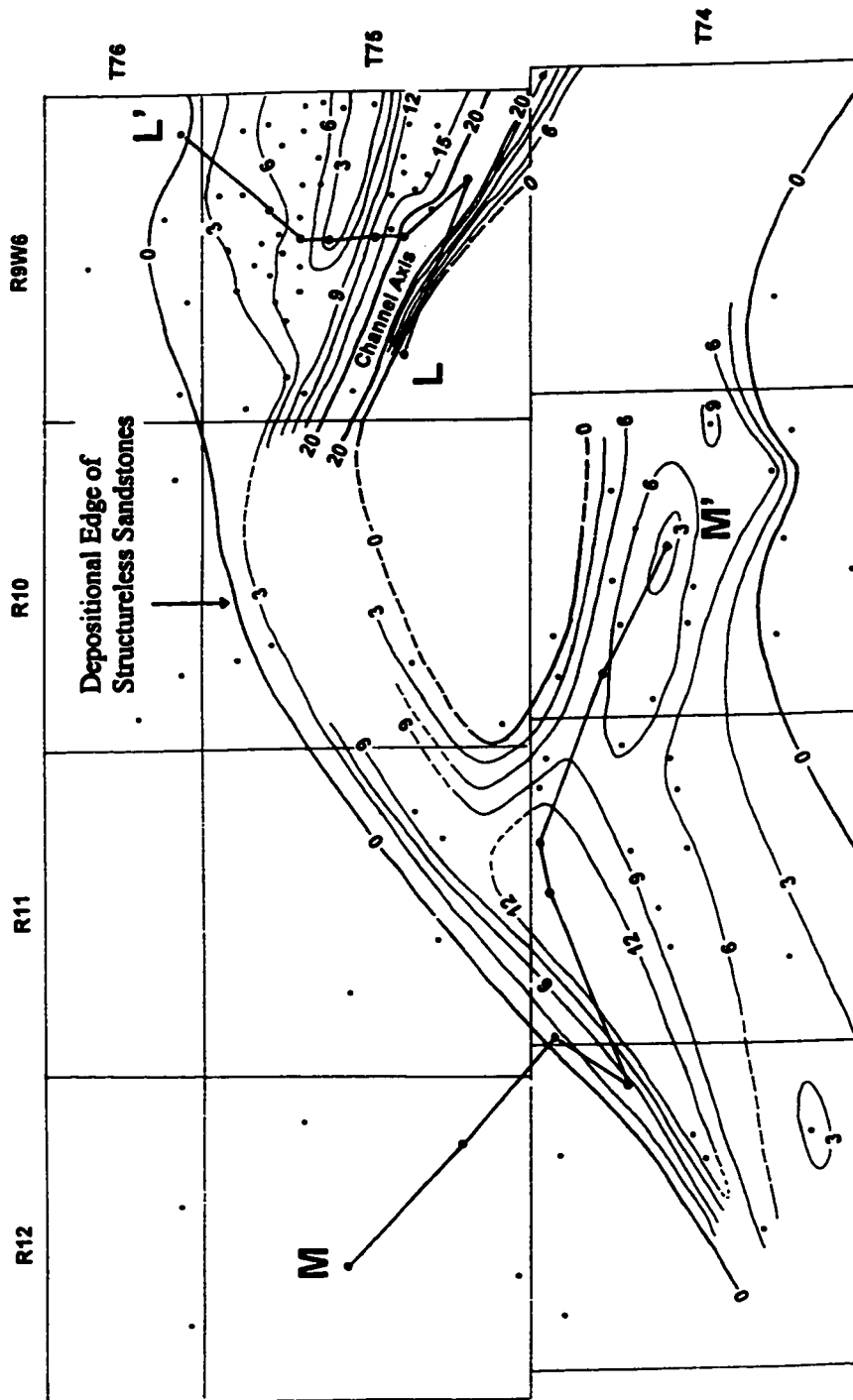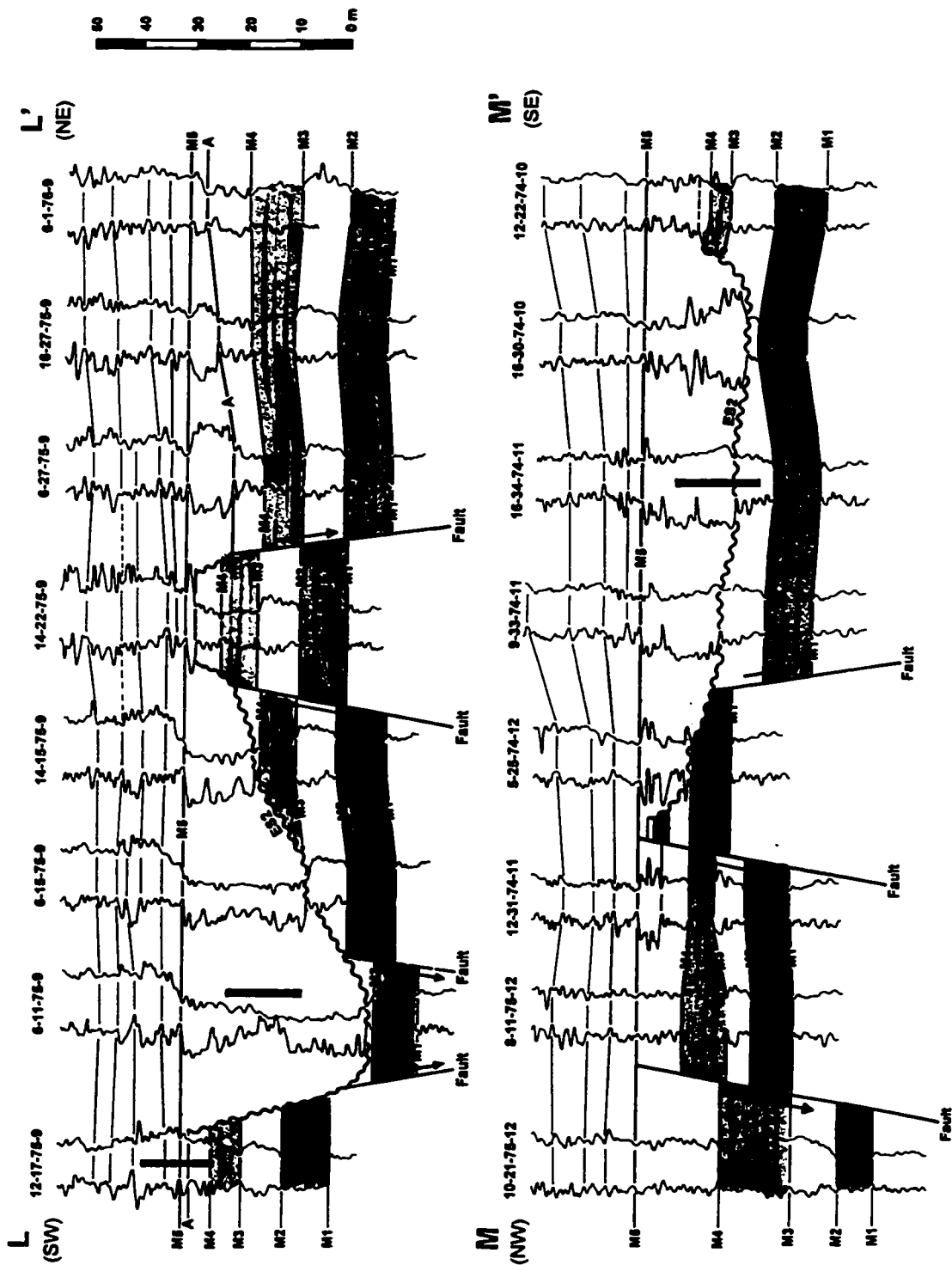
is 13 m, and 8 m in well 6-27-75-9. However, in well 14-22-75-9 in the uplifted block there is only 1-2 m of sandstone, suggesting about 10 m of uplift relative to the adjacent wells. The faults recognized in cross section L-L' (Fig. 7-6A) were active between A and M5 because both strata below A and above M5 have no significant thickness changes across the faults.

The abrupt change of the channel direction from SE-NW to NE-SW in T75 R10W6 (Fig. 6-21) also reflects synsedimentary faulting. Cross section M-M' (Fig. 7-6B) suggests relative movements of the blocks. The block containing well 5-25-74-12 was uplifted about 16 m relative to the southeastern block. The incised channel characterized by the structureless sandstone succession developed in the southeastern downthrown block, and the uplifted block defines the northwestern margin of the incised channel. The fault between 10-21-75-12 and 8-11-75-12 was active as early as Subunit B2 (the interval between M2 and M3) deposition in that significant thickness change of Subunit B2 occurs across the fault. Neither of the faults were active after M5.

All synsedimentary faults recognized in the study area are shown in Figure 7-7. The faults are parallel or subparallel to the axis of the incised channel. The faults have two dominant orientations, NW-SE and NE-SW. It is noteworthy that the location of the northwestern margin of the distal part (channel portion trending NE-SW) of the channel almost coincides with the southwestward extension of a Permian fault (Fault P) or a Devonian fault (Fault D) in Figure 7-8. The relative movements of the Faults P and D also coincide with those of the faults in cross

T76

T75

T74

T73

R6W6  R7  R8  R9  R10  R11  R12

Depositional Edge of
Structureless Sandstones

Channel Axis

Fault P

Fault P

Fault D

Dunvegan Ft.

Rycroft Ft.

Channel

Teepee Ft.

T77

T74

T70

T67
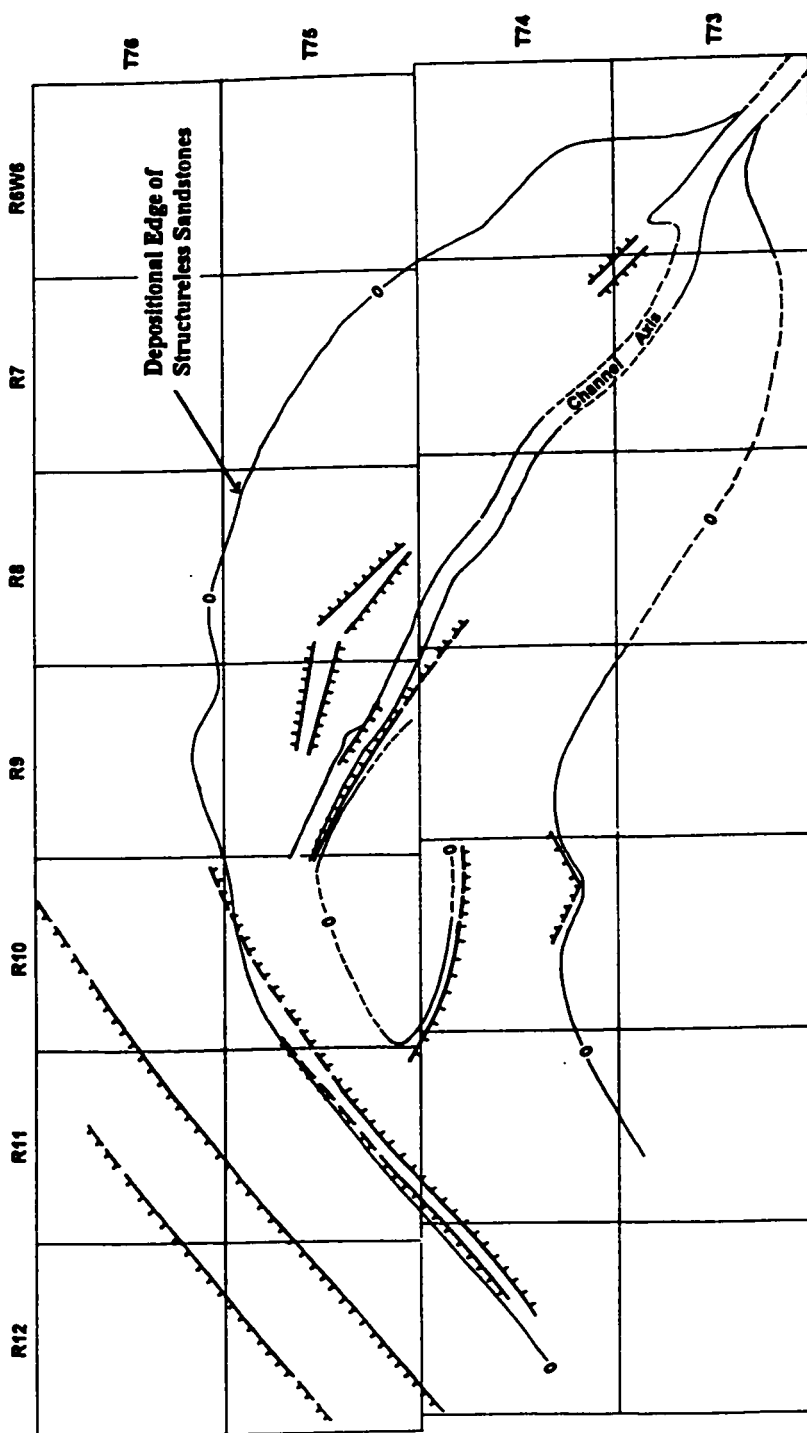
T64

BC

ALTA

6th MERIDIAN

R13    R10    R7    R4    R1    R23
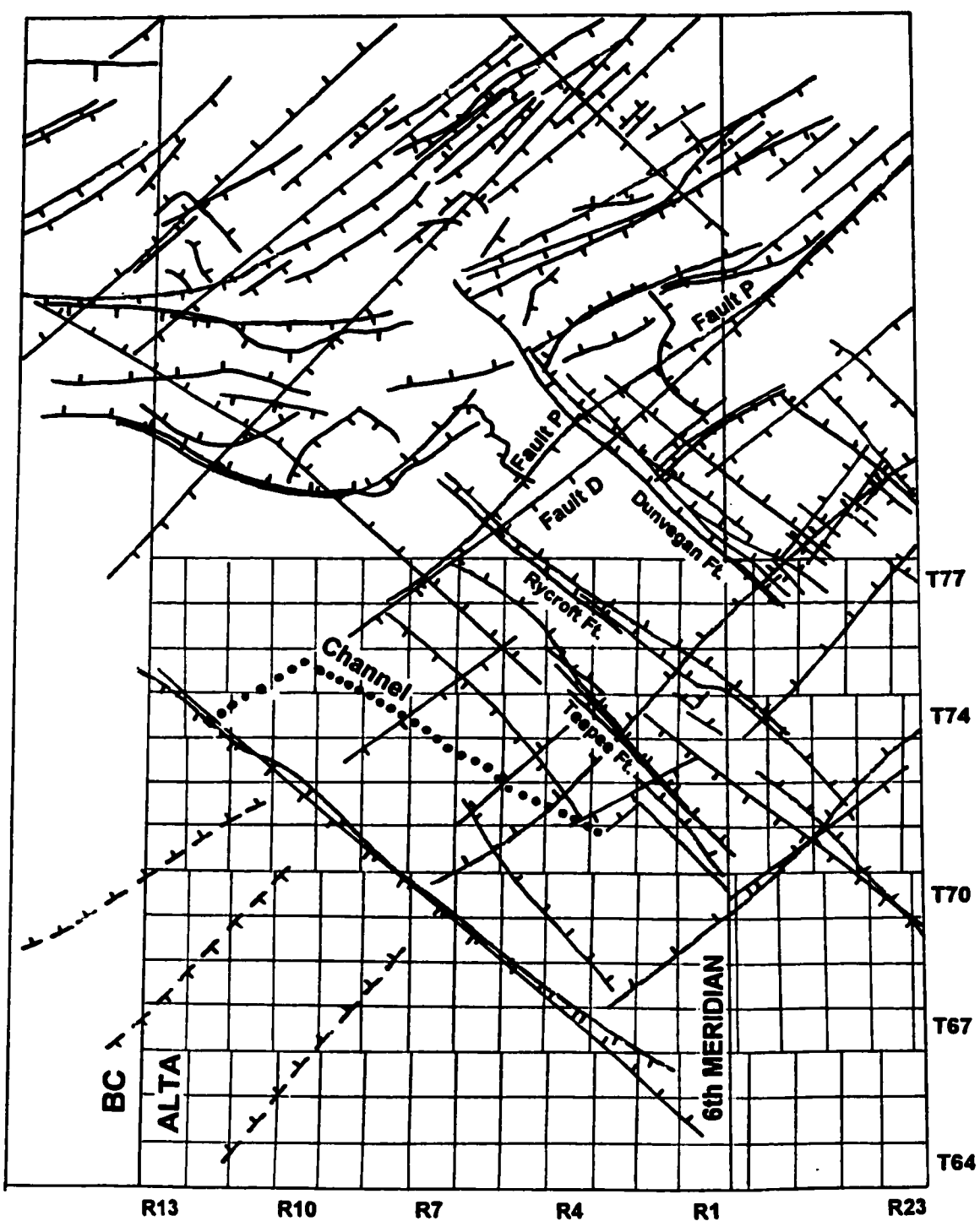
section M-M' (Figure 7-6B) in that the southwestern block is downthrown. However, the NW-SE faults and SE-NW main channel (Figure 7-7) slightly diverge (10-30°) from the NW-SE Paleozoic faults (Fig. 7-8).

In deeply incised areas, suggested by gamma-ray signatures (i.e., 6-11-75-9 and 6-15-75-9 in cross section L-L' in Figure 7-6A), the channel-fill succession (the interval between ES2 and M5) can be divided into two parts, a lower bell-shaped interval and an upper funnel-shaped interval. Note that the gamma-ray signatures do not indicate any vertical changes in lithology of sediments. In cores, the entire channel-fill succession consists of thick structureless sandstones with very thin mudstone partings without discernable vertical facies change, despite a systematic gamma ray change. The log signatures may be related to varying concentrations of radioactive elements in mineral grains such as phosphates. However, the systematic changes in the gamma-ray signatures in the deeply incised areas enable lateral correlations of the associated sandstone succession to be made. For example, compare the gamma-ray signature of the sandstone succession (the interval between ES2 and M5) in well 6-11-75-9 and 6-15-75-9 with that in well 14-15-75-9 (Fig. 7-6A). In well 14-15-75-9 (located on the margin of the incised channel), only the upper funnel-shaped interval exists and the lower bell-shaped interval does not exist. Also, in wells 6-27-75-9, 16-27-75-9 and 6-1-76-9 (located outside the incised channel), only the upper funnel-shaped interval occurs, and there is no indication of the lower bell-shaped interval. This relationship suggests that sediment infill of the incised channel began before sediment deposition outside

the channel.

With gradual sediment infill of the incised channel, topographic relief between the channel floor and channel margin gradually decreased. When sediment deposition on the channel margin took place, there was apparently no significant topographic relief between the channel axis and the channel margin. Thus sand-laden turbidity currents spread for a distance up to 10 km from the channel axis. During active sand deposition outside the main channel, the area defined by the zero depositional edge, particularly to the northeast of the main channel (Figure 6-21), was a wide, morphologically low area confined between adjacent topographic highs. A broad low in the area defined by the zero depositional edge is inferred from the very constant facies distribution over the whole depositional area.

Most of the structureless sandstone succession beyond the incised channel axis is comformable with the underlying sediments. However, some turbidity currents outside the area of the channel axis were powerful enough to do some erosion. For example, in core 8-24-75-9W6 (Appendix A-26), the structureless sandstone succession directly overlies M4, and at least 6 m of the underlying sediment was eroded. In core 11-22-75-8W6 (Appendix A-22), sandstones with large mudstone clasts sharply overlie muddy sediments, and correlations suggest that at least 2 m of the underlying sediment was eroded.

A very wide channel incision (6-7 km) occurs in T74 R10W6 (Fig.6-21). There, although the sandstone succession is much thinner (6-10 m) than in the

main channel, the erosional base of the channel has almost the same stratigraphic position as that of the main channel. Seismic data suggest that the location of the channel gradually moved to the north. Correlations between the deposits of the main channel axis and the deposits in the channel of T74 R10W6 suggest that the entire structureless sandstone succession in T74 R10W6 is equivalent only to the lower part of the main channel. It appears that during the deposition of the upper part of the sandstone succession in the main channel, the channel in T74 R10W6 no longer existed, and mud deposition took place in this area.

In most cores, the top of the structureless sandstone succession is represented by a very sharp lithologic boundary from structureless sandstones (Facies 5) to dark mudstones (Facies 1). This sharp lithologic upper boundary of the sandstones succession suggests an abrupt abandonment of the turbidite system.

## 7.3.3 Major Controls on Turbidite Deposition

### 7.3.3.1 Introduction

In general, the accumulation of turbidite deposits is controlled by three main factors; sea level variation, tectonic setting and activity, and type and rate of sediment supply (Stow et al., 1985; Pickering et al., 1989; Mutti and Normark, 1987). These factors are not independent of one another. For example, tectonic factors play an important role in determining sediment type and supply, basin floor morphology, and local fluctuation of relative sea level. Isolation of one of these

factors is very difficult, and commonly only the combined influence of the factors is discernable.

Recent literature has emphasized the influence of sea level fluctuations on the development of turbidite systems (Mutti, 1985; Posamentier and Vail,1988; Walker, 1992). It has been shown that turbidites tend to accumulate preferentially during sea level falls (e.g., Piper and Normark, 1983; Feeley et al., 1990; Nelson, 1990; Weimer, 1990), when coastal depositional systems prograde across the shelf and the depocenters move progressively toward the shelf/slope break. Higher rates of sediment accumulation at the shelf/slope break may cause slope failure, and also result in thicker sedimentary accumulations (Coleman et al., 1983, 1984). During high stands of sea level, sediment transport across the shelf into canyons tends to diminish because most sediment is trapped in nearshore environments. Fans tend to become inactive and the fan surface is commonly blanketed by hemipelagic sediment.

Tectonic movements influence turbidite sedimentation by affecting rates of uplift and denudation, slope gradient, type and rate of sediment supply, and the position of relative sea level (Stow et al., 1985; Mutti and Normark, 1987; Pickering et al., 1989). Tectonic activity may increase sediment supply by rapid uplift and denudation in the hinterland, and by steepening slope gradients. Local tectonic activity can influence channel erosion, filling, abandonment and rejuvenation. Sediment type and the rate of sediment supply affect fan morphology (Galloway, 1998; Reading and Richards, 1994).

### 7.3.3.2 Eustatic Sea Level Changes

Moslow and Davies (1997) and Davies et al. (1997) have suggested that the late Dienerian or early Smithian global sea level fall is related to the formation of the turbidite complex in the Valhalla-La Glace fields (the channel-related turbidite system in this thesis). However, detailed correlations in the study raise questions about the relationships between eustatic sea level changes and turbidite deposition.

Haq et al. (1987) have recognized four 2nd and 3rd order cycles of coastal onlap-offlap in the early Triassic. In these cycles, sea level falls occurred at the end of Dienerian (3rd order), in early Spathian (3rd order), late Spathian (3rd order) and earliest Anisian time (2nd order). Embry (1997) has recognized two 2nd order sequence boundaries and two 3rd order sequence boundaries. The ages and orders of these global sequence boundaries are near the Permian-Triassic boundary (2nd order), late Dienerian (3rd order), late Smithian (3rd order), and near the Spathian-Anisian boundary (2nd order)(see Fig. 7-9).

The biostratigraphic zonation of the Montney Formation does not have sufficient resolution to allow detailed correlations between global sea level changes (e.g. Embry, 1997) and the Montney successions. However, some recent biostratigraphic studies, including palynology-based biostratigraphic zonation (Davies et al., 1997) and conodont-based biostratigraphic zonation (Henderson and Zonneveld, 1998) allow approximate correlations between global sea level changes and the Montney successions. Comparison of the biostratigraphic data with the Montney successions suggests that the late Dienerian sequence boundary can be

| PERIOD/ EPOCH/ AGE | | | T-R CYCLE  R ——— T | MONTNEY UNITS | MAIN TURBIDITE DEPOSITION |
|---|---|---|---|---|---|
| TRIASSIC | MIDDLE | ANISIAN | | Unit G | |
| TRIASSIC | EARLY | SPATHIAN | 2nd | Unit F | |
| TRIASSIC | EARLY | SPATHIAN | | Subunit E2 | |
| TRIASSIC | EARLY | SMITHIAN | 3rd | Subunit E1 | |
| TRIASSIC | EARLY | SMITHIAN | | Unit D | ●● |
| TRIASSIC | EARLY | SMITHIAN | | Unit C | ●●●● |
| TRIASSIC | EARLY | SMITHIAN | | Subunit B3 | |
| TRIASSIC | EARLY | SMITHIAN | | Subunit B2 | ●● |
| TRIASSIC | EARLY | SMITHIAN | | Subunit B1 | |
| TRIASSIC | EARLY | DIENERIAN | 3rd | Unit A | |
| TRIASSIC | EARLY | GRIESBACHIAN | | Unit A | |
| PERMIAN | LATE | TATARIAN | 2nd | | |

correlated with the top of Unit A, and the Spathian-Anisian boundary with the top of Unit F in this thesis. Although recognition of the late Smithian sequence boundary in the Montney successions is more difficult, the sequence boundary appears to lie at or near the top of Subunit E1. Based on the above correlations, it appears that turbidite sedimentation in the Montney Formation does not correlate well with global low stands of sea level (see Fig. 7-9). In the Montney Formation, volumetrically significant turbidite sedimentation occurs in Subunit B2, and Units C and D. Moslow and Davies (1997) and Davies et al. (1997) have suggested that the turbidite complex in the Valhalla-La Glace field (the channel-related turbidite system in Unit C in this thesis) was emplaced during the late Dienerian or early Smithian global low stand of sea level. Correlations in this study suggest that the turbidite system in Unit C is much younger than the Dienerian-Smithian sequence boundary (top of Unit A). Furthermore, other volumetrically significant turbidite systems (developed in Subunit B2, and Units C and D) are not correlated with any of 2nd or 3rd order of global low stands of sea level.

### 7.3.3.3 Tectonics

The Peace River Arch and the Dawson Creek Graben Complex strongly influenced Triassic sediment accumulation. For example, the Triassic succession has its maximum thickness along the Dawson Creek Graben Complex.

Major tectonic activity in the Montney Formation is indicated by abrupt changes in isopach patterns between depositional units. Unit A is characterized by

southwesterly-dipping clinoforms. The isopach trends of Unit A (Fig. 5-1) suggest that the source was in the northeast. The isopach trends of Unit B (Fig. 5-2) are very different from those of Unit A. The southwesterly-dipping clinoforms were abandoned, and thick sediment accumulation trending NE-SW occurred in the southern part of the study area. The overall isopach patterns of Unit B suggest that the main source was in the southeast. The switching of the depocenters and the changes of isopach patterns between Unit A and Unit B strongly suggest a major reorganization of the basin between the two units.

In the southern part of the study area, the NE-SW trending isopach patterns that developed in Unit B persisted not only until the end of the Montney Formation but also into the Halfway-Doig Formations, and the Pardonet-Baldonnel Formations (Edwards et al., 1994). These strong NE-SW isopach trends in the southern part of the study area suggest that sediment accumulation was strongly controlled by reactivation of NE-SW trending, Paleozoic fault systems (Fig. 7-8). The reactivation of the Paleozoic fault systems probably resulted in northwestward deepening of the southern part of the basin. Local steep slopes can be inferred from the common slumping observed in Units B and C. The extensive development of turbidite deposits and the development of the channel-related turbidite system in Unit C may suggest that tectonic activity was most active during deposition of Unit C. The remarkably straight incised channel, the abrupt change of the channel direction, and the synsedimentary faulting in the turbidite system also reflect strong tectonic influence.

# CHAPTER 8: MONTNEY TURBIDITES IN A WORLD CONTEXT

## 8.1 Introduction

In the deeper part (southwestern) of the study area, the Montney Formation commonly contains turbidites at several stratigraphic intervals. Two different styles of turbidite system occur in the Montney Formation: (1) an unchannelized, sheet-like turbidite systems and (2) a channel-related turbidite system.

In the literature, turbidite deposition has commonly been interpreted in terms of submarine fan deposition. In the 1970's, several depositional models for submarine fans were proposed (Normark, 1970, 1978; Normark and Piper, 1972; Mutti, 1977, 1979; Mutti and Ricci Lucchi, 1972, 1975; Mutti and Ghibaudo, 1972; Walker, 1978; Walker and Mutti, 1973). Despite slight differences, all of these models are characterized by channel-feeding-lobe (C-F-L) architectures.

In the 1980's, more sophiscated instruments (including side-scan sonar, bathymetric swath-mapping systems, and multifold seismic-profiling systems) made the detailed mapping of large modern fans possible. Relatively well-studied, large modern fans include the Amazon (Damuth et al., 1983a, 1983b, 1988; Manley and Flood, 1988; Flood et al., 1991), Mississippi (Bouma et al., 1985, 1989; Weimer, 1989, 1990, 1991; Twichell et al., 1991), Indus (McHargue and Webb, 1986; Kolla and Coumes, 1987; McHargue, 1991), Rhone (Droz and Bellaiche, 1985; O'Connell et al., 1991), and Laurentian (Masson et al., 1985; Normark et al., 1983; Piper and

Normark, 1982; Piper et al., 1985). These studies have shown that the upper and middle parts of large modern fans are characterized by distributary channel systems with large levees (channel-levee systems). The overall features of the large modern fans are significantly different from those of the relatively small C-F-L fan systems.

The main purpose of this chapter is to examine similarities and dissimilarities between the turbidite systems in the literature and the turbidite systems in the Montney Formation, and to show some analogues to the turbidite systems in the Montney Formation.

## 8.2 Montney Turbidites in a World Context

The most prominent feature of the channel-related turbidite system (Fig. 6-21) in the Montney Formation is the remarkable straightness of the channel, despite the relatively fine grained nature of the system (lower very-fine sand). However, modern submarine channels are commonly sinuous, particularly on modern fans in which the dominant sediment is relatively fine (Damuth et al., 1983a, 1983b, 1988; Twichell et al., 1991; Droz and Bellaiche, 1985; Weimer and Link, 1991). On the Amazon fan, nearly all channels show considerable sinuosity with well-developed meanders. Channel cutoff and abandoned meander loops are also observed (Damuth et al., 1983a, 1983b, 1988). The Mississippi and Rhone fans also show highly sinuous channels (Twichell et al., 1991; Droz and Bellaiche, 1985), as do many other fans (Clark et al., 1992; Weimer and Link, 1991; Bouma et al., 1985).

In Chapter 7, it has been shown that the location of the channel in the Montney turbidite system was controlled by synsedimentary faults, at least in some reaches of the channel. Some modern submarine channels and canyons are also controlled by faults, and they commonly show prominent linear geometries (Yerkes et al., 1967; Graham and Bachman, 1983). Redondo submarine canyon and channel, southern California, trends west-southwest for about 15 km from its head near the shoreline, and is unusually straight. Yerkes et al. (1967) have shown that this canyon formed along a structural trough that was created by faulting in the middle Pleistocene. Newport canyon-channel, the northerly feeder to the La Jolla fan system, is also straight. Graham and Bachman (1983) have shown that the position of the Newport channel is controlled by the geometry of a buried basement structure. Loma sea valley, the southern feeder of the La Jolla fan system, is also remarkably straight, and is located along the faulted eastern face of Coronado Bank (Graham and Bachman, 1983). Graham and Bachman (1983) have shown that the position of the straight La Jolla fan valley is also controlled by the geometry of a buried, hard-rock structure.

The channel in the Montney turbidite system is not only straight but shows an abrupt change (about 60°) in the channel direction from SE-NW to NE-SW. In Chapter 7, it was shown that the abrupt change of the channel direction was caused by faulting. The channel reach trending NE-SW developed along the southeastern downthrown fault block and the uplifted block defines the northwestern margin of the channel. In the literature, examples of abrupt change of channel trend are

unusual. A possible example of abrupt change of channel trend controlled by structural influences is the La Jolla fan valley and channel. The upper reach of the La Jolla fan valley is linear and trends ESE-WNW. About 11 km from its head, the fan valley turns abruptly to the southwest and continues in a relatively straight course, thus having an overall curvilinear trend. The origin of the abrupt turn is not clear, but some data give a hint of structural control for the abrupt turn. Mudie et al. (1970) have mapped the sea floor of La Jolla fan using side-scan sonar, and have detected prominent lineaments on the fan surface. The lineaments are discontinuous and show prominent NE-SW trends parallel to the fan valley. Mudie et al. (1970) have proposed that the lineaments are the surface traces of active (or recently active) faults. Additional evidence of a structural control on the sharp turn of the fan valley is given by seismic data. Some seismic profiles show that at least some parts of the NE-SW trending fan valley appear to be located along faults (see seismic profiles G, N, O and Q in Shepard et al., 1969).

Other examples showing abrupt channel turns occur in submarine channels crossing fracture zones. A good example is the Cascadia channel in the northeastern Pacific ocean. Before entering the Blanco fracture zone, Cascadia channel trends southward for about 200 km. It makes an abrupt right-angle turn to the southwest where it enters the Blanco fracture zone. For the next 150 km it winds westward, confined between the submarine ridges and mountains of the fracture zone (Embley, 1985; Griggs and Kulm, 1973). A similar abrupt channel turn occurs in the Maury channel, Pacific ocean where it enters Gibbs fracture

zone (Cherkis et al., 1973).

Another prominent feature of the channel in the Montney Formation is its deep incision into underlying sediment. The channel incised underlying sediment to a maximum depth of about 40 m, and the channel itself has been filled mostly with thick structureless sandstones with large mud clasts in the basal part of the succession. An ancient example of an incised channel occurs in the Cambrian St. Roch Formation, Quebec Appalachians (Hubert et al., 1970; Rocheleau and Lajoie, 1974), where a channel incised up to 88 m into mudstones and thinly-bedded turbidites. The channel itself has been filled with conglomerate and massive sandstones. Another possible ancient example of an incised channel is the upper Miocene Doheny Channel at Dana Point, southern California (Bartow, 1966; Normark and Piper, 1969; Piper and Normark, 1971). The channel cut (about 20 m deep) into siltstone and silty shale with interbedded fine sandstones interpreted as turbidites. The lower part of the channel-fill consists of massive sandstones and some of sandstones contain pebbles up to 25 cm diameter, with huge slabs of Monterey chert up to several meters long. The upper part of channel-fill consists of sandy and silty turbidites. The upper Cretaceous Wheeler Gorge Conglomerate in Southern California is also an example of an incised channel (Walker, 1985). The conglomerate abruptly overlies a 240 m thick mudstone sequence. Although the base of the conglomerate is planar, the abrupt appearance of coarse clastics and the thinning- and fining-upward sequence suggest channel filling. In the Indus fan, the outer shelf and slope is characterized by erosional canyon floor and walls

(McHargue and Webb, 1986). The canyon is very wide (30 km) and deep (1500 m). Gullies (2-3 km in width and 250 m in depth) also occur along the slope.

A modern example of an incised channel occurs in the La Jolla Fan, offshore southern California. Here, the channel deeply incised the modern fan surface up to 90 m (Normark and Piper, 1969). The sediments of the channel consists dominantly of sand with some mud, whereas on the fan surface outside the channel, sediments are dominated by mud. Most sediments currently by-pass the fan area and are deposited in the San Diego Trough (Graham and Bachman, 1983). Another modern example of an incised channel occurs in the upper Monterey Fan, offshore central California, where the fan-valley deeply incises the fan surface to a depth of about 400 m. The channel relief decreases downfan, but even in the lower fan, it commonly approaches to 100 m. Seismic reflection profiles indicate that the channel incised into horizontally bedded sediments on the fan surface (Normark,1970; Normark et al., 1984).

The sandbody geometry of the channel-related turbidite system in the Montney Formation (Fig. 6-21) is similar to that of C-F-L system, especially Mutti's type II system (1985), in that the sandbody geometry defined by the depositional edge of the sandstones consists of an elongate "lobe". In detail, however, the channel-related turbidite system in the Montney Formation is significantly different other C-F-L systems. Lobes in C-F-L systems were originally defined as non-channelized bodies displaying thickening upward successions. In contrast, the deposits of the lobe-like sandstone body in the Montney Formation consist mainly

of thick structureless sandstones which do not show thickening and coarsening upward trends. It has been suggested in Chapter 7 that, based on facies distribution, the sandbody reflects deposits on a broad topographic low rather than lobe deposits.

It has been shown in Chapter 7 that sand accumulation and facies distribution in the system (Fig. 6-21) have been strongly controlled by tectonic activity. Some ancient turbidite systems show structural controls on the facies distribution, thickness and overall geometry of turbidite deposits (Wilson et al., 1992; Sinclair, 1994). In the Aberystwyth Grits turbidite system in Wales (Wilson et al., 1992), syndepositional movement on faults was the major control on facies development and system geometry. Wilson et al. (1992) have shown that thick sandstone accumulation was largely restricted to topographic lows created by syndepositional faulting. Mud-dominant sediments were deposited on the uplifted blocks. They suggested that bathymetric lows created by syndepositional faulting focused sand-carrying turbidity currents, resulting in thick accumulation of sandstones within downthrown blocks. In the Annot Sandstone (lower Oligocene) of southeastern France (Sinclair, 1994), sandy turbidite deposits were confined to a bathymetric low a few to several kilometers wide between adjacent growth anticlines. There, lateral confinement by slopes resulted in a wedge-shaped sandstone body in cross section.

A characteristic of the Montney turbidite systems is the common absence of channel development. Except for the channel-related turbidite system in Unit C

(Fig. 6-21), the Montney lacks channels. Modern submarine fans are characterized by channels and channel-levee systems; they also have large feeder channels on the upper part of the fan surface. In submarine fans, sheet-like turbidites occur in the lower part of the system, but they are related to upfan channels. However, in the Montney Formation, the sheet-like turbidite systems do not appear to be related to channels farther upslope. This absence of channels suggests depositional environments that are unlike modern submarine fans.

Sheet-like turbidite deposits occur in several depositional environments, including the base-of-slope, the distal part of the fan surface, the basin plain and even in interchannel areas. Distinction between non-fan sheet-like turbidite deposits and sheet-like turbidites of distal lobes and/or the lower fan is not possible if the upcurrent depositional environments are not available for examination. In the literature, however, sheet-like turbidite deposits commonly have been interpreted as outer fan lobes without any evidence of the existence of channels in upcurrent areas (i.e. Mutti et al., 1978; Ricci Lucchi and Valmori, 1980). Rare examples of non-fan turbidite systems in the literature result in part from the difficulty or recognizing non-fan turbidite system in limited outcrops.

In the literature, nonchannelized turbidite system are relatively common in the Devonian and Carboniferous sequences in the Appalachian Basin (Walker, 1971; Walker and Sutton, 1967; Moore and Clarke, 1970; Woodrow and Isley, 1983; Lundegard et al., 1985). In the Susquehanna Valley area of Pennsylvaina, the Upper Devonian sequence contains a classic turbidite succession grading up

into slope shales, shelf deposits and coastal fringe deposits(Walker, 1971). In the turbidite succession, proximal turbidites and deep channels are absent. Several Devonian exposures in New York and Pennsylvania are characterized by thin-bedded turbidites, and they do not have any evidence of deep channels (Woodrow and Isley, 1983). The upper Devonian sequence in Virginia, West Virginia and Tennessee also contains unchannelized turbidite successions (Lundegard et al., 1985). In the turbidite succession, siltstone and sandstone beds are thin (<30 cm). Beds are even and persistent.

Elsewhere, nonchannelized turbidite systems are very rare in the literature. Very extensive sheet-like turbidites occur in the Cretaceous Gault Formation of the East Alps (Hesse, 1974). There, the sheet-like turbidite are laterally continuous over 100 km and there is no indication of the presence of channel. The Tebilet Palaezoic Inlier of southern Morocco consists of a thick (2 km) succession from basin-plain turbidites to shallow marine deposits (Graham, 1982). There, the turbidites consist of fine to very fine sand and most beds are thinner than 30 cm. Amalgamation of turbidites is very rare and beds are laterally persistent across the width of the exposures. The thick, shallowing upward succession from basin plain through slope to shallow marine completely lacks channel facies. The Fernie-Kootenay (Jurassic) transition, southern Alberta contains silty and sandy turbidites (Hamblin and Walker, 1979). There, the turbidite beds are thin (<50 cm, average 4-7 cm) and very evenly bedded. The turbidite succession lacks channels and is overlain by thick hummocky cross stratified shallow marine storm beds.

Turbidites are generally regarded as deep water deposits (Stanley and Kelling, 1978; Nelson and Nilson, 1984; Bouma et al., 1985; Pickering et al., 1989; Weimer and Link, 1991). However, a relatively shallow water depth during emplacement of the Montney turbidites is suggested by the occurrences of some wave ripples in the turbidite successions (see Chapter 7.3.2). Although rare, the literature clearly indicates the existence of shallow-water turbidites (Kumar and Slatt, 1884; Lundegard et al., 1985; Graham, 1982; Hamblin and Walker, 1979; Rosenthal and Walker, 1986). Kumar and Slatt (1984) have estimated that turbidite deposits in the Pennsylvanian Tonkawa Sandstone in Oklahoma were deposited in a water depth of 305-407 m at maximum and 120-190 m at minimum. For the upper Devonian turbidite sequences in the central and southern Appalachian Basin, water depth has been estimated about 140-210 m (Lundegard et al., 1985). In the Jebilet Palaezoic inlier of southern Morocco (Graham, 1982), the upper part of the turbidite succession passes upward into a shoreface sandstone succession through a 100-200 m interval, suggesting relatively shallow-water turbidites. In the Fernie-Kootenay transition, southern Alberta (Hamblin and Walker, 1979), the turbidite succession is abruptly overlain by HCS beds. Although the sharp base of HCS beds may reflect a slight lowering of sea level, the overall vertical relationship indicates relatively shallow depth during turbidite emplacement.

## CHAPTER 9: THIS THESIS VERSUS PREVIOUS WORKS

### 9.1 Stratigraphy and Source

The top of the Montney Formation (TM) is defined by phosphatic shales (commonly called "phosphatic zone") of the basal part of the Doig Formation (Armitage, 1962). In well logs, the boundary is defined by an abrupt increase in gamma-ray values, commonly greater than 150 API and as high as 500 AP. In the deeper part of the basin (in the southwest), however, some intervals characterized by high gamma-ray values also occur in the upper part of the Montney Formation, resulting in the common mis-identification of the top of the Montney Formation. The top of the Montney Formation defined by some authors (i.e. Gibson and Edwards, 1990; Edwards et al., 1994; Davies et al., 1997) is not consistent. Mispicking of TM in the literature is mostly caused by the confusion of the true TM and the ES3 horizon. In the Montney isopach map of Edwards et al. (1994), the extremely small values (less than 50 m to 150 m) occur around northeastern British Columbia. However, this study shows that the small values are the result of confusion of TM and ES3 surface (see Fig. 2-2). In that area, the real thickness of the Montney ranges from 195 m to 340 m (see Fig. 5-16). It is noteworthy that, although the gamma-ray signatures of TM and ES3 are similar, their induction log signatures are very different. In induction logs, ES3 is represented by a leftward deflection, whereas TM is represented by a rightward deflection.

All published works on correlation between the outcrop belt and subsurface (e.g. Gibson, 1974, 1975; Gibson and Barclay, 1989; Gibson and Edwards, 1990; Edwards et al., 1994; Davies et al., 1997) have suggested that the phosphatic pebble interval at the base of the Whistler Member in the outcrop belt should be correlated with the phosphatic shale (characterized by high gamma-ray values in well logs) of the basal part of the Doig Formation. However, this study shows that the phosphatic pebble interval at the base of the Whistler Member might possibly be correlated with a phosphatic shale interval (in the basal part of Unit G in this study) within the Montney Formation, not with the basal phosphatic interval of the Doig Formation (see Chapter 4.2.9 for detailed discussion).

All existing studies (i.e. Barss et al., 1964; Gibson, 1989, 1990; Gibson and Barclay, 1989; Gibson and Edwards, 1990; Gibson and Poulton, 1994; Edwards et al., 1994; Davies et al., 1997) have suggested that sediments of the Montney Formation were derived from the northeast or east. However, this study shows that although much of the Montney sediment was derived from a northeastern or eastern source, the main source of at least Units B and C was from the southeast. Beyond the study area to the north, the northeastern or eastern source appears to have persisted through the whole Montney succession.

## 9.2 Turbidite Deposition

Moslow and Davies (1996, 1997) have recently discussed turbidite deposition in the Montney Formation. Several aspects of their work differ from the

results presented in this study. The main differences are briefly discussed below.

(1) Moslow and Davies (1996, 1997) have suggested that the turbidite complex in the Valhalla and La Glace fields (the channel-related turbidite system in Unit C in this thesis), was fed by channels trending northeast to southwest, with the source of the turbidity currents in the northeast (see Figure 2-13). However, results presented in this study strongly indicate that in the channel-related turbidite system (Figs. 6-21 and 6-22), the main part of the deeply-incised channel trends southeast to northwest. The flow of the turbidity currents was from the southeast. The incised channel in this system cut as much as 40 m into the underlying sediments and the maximum thickness of the sandstone succession in the channel axis reaches 47 m. Moslow and Davies (1996, 1997) did not recognize this deeply incised channel.

The southeastern source of the turbidity currents is supported by (1) the orientation of the incised channel (southeast-northwest); (2) the overall sandbody geometry of the channel fill; (3) the complete confinement of structureless sandstones to the narrow upchannel position (in the southeast) and the spreading of the sandstones out of the channel at the downchannel (northwestern) end (Fig. 6-21); (4) the longitudinal channel profile with a northwesterly-dipping channel base (Fig. 7-2); and (5) overall northwestward thinning and fining of Unit C (see Chapter 6.3.2).

It should be noted that the value of 2° for the slope on which turbidity currents were generated (Moslow and Davies, 1997) is a miscalculation. The

gradient of the southwesterly-dipping depositional slope defined by their map is about 0.2°, not 2°.

(2) Moslow and Davies (1997) have noted that the channel-fill successions in the Valhalla-La Glace fields (the channel-related turbidite systems in this thesis) show a pronounced upward decrease in sandstone bed thickness and an increase in frequency of mudstone beds. They also noted that the lobe successions in the Glacier field (unchannelized, sheet-like turbidite system in Subunit B2 around T76 R11W6 in this thesis) show an upward increase in sandstone bed thickness. However, examination of about 70 cores from these turbidite systems reveals that the thickening- and thinning- upward trends described by Moslow and Davies (1997) are almost absent. No discernible upward increase or decrease in sandstone bed thickness or in frequency of mudstone beds was detected in this study.

Moslow and Davies (1997) have also described channel margin, levee and overbank facies in the Valhalla-La Glace fields (for example, the wells 14-22-75-9, 8-24-75-9 and 6-9-75-8 in Figure 9-1A). These deposits are muddier and thinner sand beds than channel fill. However, this study shows that the deposits interpreted as channel margin, levee and overbank facies by Moslow and Davies lie on topographic highs caused by synsedimentary faulting (see Chapter 7.3.2.2). Thus, the control of the muddier and thin sand facies may be structural rather than sedimentological (see Chapter 7.3.3). Furthermore, those deposits trend northwest

to southeast, perpendicular to their proposed channel trend.

(3) Moslow and Davies (1997) suggested that the Valhalla-La Glace turbidite system (channel-related turbidite system in Unit C in this thesis) is similar to Walker's (1992) depositional model of channel-levee complexes (Fig. 9-1). However, the overall aspect of the turbidite system is not well described by the channel-levee model.

First, extensive levee and overbank deposits do not occur in the turbidite systems as described earlier in this thesis. Their "levee and overbank- like" deposits reflect only sediment accumulation on relatively uplifted blocks. Secondly, their schematic diagram (Fig. 9-1B) indicates the presence of at least 3 channel-levee systems which are laterally-coalescing or cross-cut and which have isolated sandbodies. If their suggestion is correct, the base of each channel-levee system must have a different stratigraphic position and the system should be characterized by narrow isolated sandbodies. Their figures (Figs. 9-1A and 9-1B) depict small channels with variable stratigraphic positions and erosional bases, and that sandbodies are isolated within narrow channels. However, in the correlations detailed in this thesis, the bases of the sandstone successions always have the same stratigraphic position (not erosional bases), and the sandbody is not broken into narrow strips of sand but is laterally very extensive (see Fig. 7-4 for laterally extensive sandbody geometry). It should be noted that the wells, including 14-22-75-9, 8-24-75-9 and 6-9-75-8 (Fig. 9-1), lie on topographic highs caused by

synsedimentary faulting (see Fig. 7-6). Thirdly, Moslow and Davies' (1997) interpretation of the turbidite system is largely based on (1) failure to recognize the southeast-to-northwest channel, and (2) the suggestion of a northeast-to-southwest channel trend and associated facies distributions. These aspects of their work indicate that interpretation of northeast-to -southwest channel-levee complexes is inappropriate. In addition, Walker's (1992) model is largely based on large modern fans (e.g. Amazon, Mississippi, Rhone). These are much larger than the Montney turbidite system; for example, in the Mississippi, each channel-levee complex is commonly a few to several hundred meters thick, whereas the Montney turbidite system is thinner than 15 m except in the deeply incised channel.

(4) Moslow and Davies (1997) have suggested that the turbidite system in the Valhalla-La Glace fields developed at the toe of slope with contemporaneous deposition of coquina beds in the uppermost part of Unit A during a fall or lowstand of global sea level. Thus, they imply a genetic relationship between the turbidite deposits and the coquina beds (see Fig. 2-14). However, this study shows that all of the turbidite deposits in the Montney Formation are stratigraphically higher than the coquina beds, indicating that there is no genetic relationship between the turbidites and the coquinas. Furthermore, the development of turbidite systems in the Montney Formation may not have been related to global sea level fluctuations, but rather to local tectonic activity(see Chapter 7.3.3).

(5) Moslow and Davies (1997) suggested that the turbidite systems in the Valhalla-La Glace fields and Glacier field have same stratigraphic position. However, this study shows that the Glacier turbidite system (the unchannelized, sheet-like turbidite system in Subunit B2 around T76 R11W6 in this thesis) is older than the Valhalla-La Glace turbidite system (the channel-related turbidite system in Unit C in this thesis). Furthermore, the channel-related turbidite system has a southeastern source whereas the Glacier turbidite system has a northeastern source (see Chapters 6.2 and 6.3).

## CHAPTER 10: CONCLUSIONS

(1)  The Montney Formation in the Peace River Arch area forms a sedimentary wedge up to 350 m thick on the craton margin, and is characterized by southwesterly- or westerly-dipping clinoforms with a maximum dip of about 0.3°.

(2) The Montney Formation has been divided into seven depositional units, Units A to G, based on the most prominent well log markers and comparison of sedimentary facies between cores.  Some of these units have been divided into subunits.

(3)  Correlations between the outcrop belt and surface suggest that the phosphatic pebble interval at the base of the Whistler Member in the outcrop belt may possibly be correlated with the phosphatic interval in the basal part of Unit G within the Montney Formation, not with the basal phosphatic shale interval of the Doig Formation.

(4)  Three major erosional surfaces, ES1, ES2 and ES3, have been recognized in the Montney Formation.  ES1 and ES3 are regional erosional surfaces, and ES2 is a deep channel incision.

(5) Deposition of the Montney Formation was strongly influenced by tectonic activity. Two major episodes of basin reorganization have been recognized in the Montney: one occurred between Unit A and Unit B, the other between Unit F and Unit G.

(6) The overall source of sediment in the Montney Formation was from the northeast. However, the source was variable both in time and space. During deposition of Units B and C, the main source in the study area was from the southeast.

(7) In the deeper part of the basin (southwest), the Montney Formation commonly contains turbidite deposits. Two styles of turbidite systems have been recognized, unchannelized, sheet-like turbidite systems and a channel-related turbidite system. Unchannelized, sheet-like turbidite systems are much more common, occurring in Units B, C and D, and possibly E and G. They constitute the bulk of the turbidite deposits. The channel-related turbidite system occurs only in Unit C.

(8) The turbidite systems in Unit C and Subunit B3 had southeastern sources, whereas the turbidite systems in Subunit B2 and Unit D had northeastern or northern sources.

(9) The incised channel of Unit C cut down as much as 40 m into the underlying sediment. The channel is relatively straight and trends southeast to northwest for over 70 km. In the distal part, it turns sharply to the southwest following the margin of a downthrown fault block. Upslope, the width of the channel is about 1 km, but farther downslope (northwestward), it widens to 3-5 km.

(10) The fill of the Unit C channel consists mostly of thick structureless sandstones. Upslope, the sandstones are completely confined within the incised channel. Downslope, they spread out of the incised channel for a distance of about 10 km. The turbidite system had a southeastern source.

(11) Synsedimentary faulting strongly controlled the sandstone thickness and facies distribution in the channel-related turbidite system. Thick sand accumulation occurred in downthrown fault blocks whereas thinner and/or muddier sediments were deposited in relatively uplifted blocks.

(12) The deep channel incision, the remarkably linear channel (with its sharp turn in the distal part), the sand accumulation trend, and the abrupt abandonment of the channel-related turbidite system suggest that tectonic activity was a major control on the development of the turbidite system.

(13) The turbidite systems in the Montney Formation developed in relatively

shallow water, probably no deeper than a few hundred meters.

(14) The development of turbidite systems in the Montney Formation may not have been related to global sea level fluctuations, but instead to local tectonic activity.

# REFERENCES

Aitken, J.D., 1993, Chapter 4, Stratigraphy. *in* Stott, D.F. and Aitken, J.D., (eds.), Sedimentary cover of the craton in Canada. Geological Survey of Canada, p. 79-482.

Armitage, J.H., 1962, Triassic oil and gas occurrences in northeastern British Columbia, Canada. Journal of Alberta Society of Petroleum Geologists, v. 10, p. 35-56.

Bally, A.W., Gordy, P.L. and Stewart, G.A., 1966, Structures, seismic data, and orogenic evolution of southern Canadian Rockies. Canadian Society of Petroleum Geologists Bulletin, v.14, p. 337-381.

Barclay, J.E., Krause, F.F., Campbell, R.I. and Utting, J., 1990, Dynamic casting and growth faulting: Dawson Creek Graben Complex, Carboniferous-Permian Peace River Embayment, Western Canada. Bulletin of Canadian Petroleum Geology, v. 38A, p. 115-145.

Barss, D.L, Best, E.W. and Meyers, N., 1964, Triassic, Chapter 9. *in* McCrossan, R.G. and Glaister, R.P. (eds.), Geological history of Western Canada. Alberta Society of Petroleum Geologists, p. 113-136.

Bartow, J.A., 1966, Deep submarine channel in upper Miocene, Orange county, California. Journal of Sedimentary Petrology, v. 36, p. 700-705.

Beaumont, C., 1981, Foreland basins. Geophysical Journal of the Royal Astronomical Society, v. 65, p. 291-329.

Bhattacharya, J. and Walker, R.G., 1991, River- and wave-dominated depositional systems of the Upper Cretaceous Dunvegan Formation, northwestern Alberta. Bulletin of Canadian Petroleum Geology, v. 39, p. 165-191.

Bird, T.D., Barclay, J.E., Campbell, R.I. and Lee, P.J., 1994, Triassic gas resources of the Western Canada Sedimentary Basin, interior plains. Part I: Geological play analysis and resource assessment. Geological Survey of Canada, Bulletin 483.

Blatt, H., Middleton, G.V. and Murray, R.C., 1980, Origin of sedimentary rocks (2nd edition). Second Edition, Prentice-Hall, Inc., Englewood Cliffs, New Jersey. 782p.

Bouma, A.H., 1962, Sedimentology of some flysch deposits: a graphic approach to facies interpretation. Amsterdam, Elsevier, 168 p.

Bouma, A.H., Coleman, J.M., Stelting, C.E. and Kohl, B., 1989, Influence of relative sea level changes on the construction of the Mississippi fan. Geo-Marine Letters, v. 9, p. 161-170.

Bouma, A.H., Coleman, J.M. and DSDP Leg 96 Shipboard Scientists, 1985a, Mississippi Fan: Leg 96 Program and principal results. in Bouma, A.H., Normark, W.R. and Barnes, N.E. (eds.), Submarine fan and related turbidite systems. New York, Springer-Verlag, p. 247-252.

Bouma, A.H., Normark, W.R. and Barnes, N.E. (eds.), 1985b, Submarine fans and related turbidite systems. New York, Springer-Verlag, 351 p.

Bower, P., 1998, Kaybob South Triassic Coquina Pool. Canadian Society of

Petroleum Geologists/Canadian Society of Exploration Geophysicists/Canadian Well Logging Society, Joint Convention, Calgary, Plenary Oral Posters Core Workshop, p. 266.

Burchfiel, B.C. and Davis, G.A., 1975, Nature and controls of Cordilleran Orogenesis, western United States-extensions of an earlier synthesis. American Journal of Sciences, v. 275A, p. 363-396.

Burwash, R.A. and Krupicka, J., 1969, Cratonic reactivation in the Precambrian basement of western Canada. I. Deformation and chemistry. Canadian Journal of Earth Sciences, v. 6, p. 1381-1396.

Burwash, R.A. and Krupicka, J., 1970, Cratonic reactivation in the Precambrian basement of western Canada. II. Metasomatism and isostasy. Canadian Journal of Earth Sciences, v. 7, p. 1275-1294.

Cant, D.J., 1986, Hydrocarbon trapping in the Halfway Formation (Triassic), Wembley Field, Alberta. Bulletin of Canadian Petroleum Geology, v. 34, p. 329-338.

Cant, D.J., 1988, Regional structure and development of the Peace River Arch, Alberta: a Paleozoic failed-rift system? Bulletin of Canadian Petroleum Geology, v. 36, p. 284-295.

Cherkis, N.Z., Fleming, H.S. and Feden, R.H., 1973, Morphology of structure of Maury Channel, northeast Atlantic Ocean. Geological Survey of America Bulletin, v.84, p. 1601-1606.

Clark, J.D., Kenyon, N.H. and Pickering, K.T., 1992, Quantitative analysis of the

geometry of submarine channels: Implications for the classification of submarine fans. Geology, v. 20, p. 633-636.

Coleman, J.M., Prior, D.B. and Lindsay, J.F., 1983, Deltaic influences on shelf edge instability process. *in* Stanley, D.J. and Moore, G.T. (eds), The shelfbreak: critical interface on continental margins. Society of Economic Paleontologists and Mineralogists, Special Publication 33, p. 121-137.

Damuth, J.E., Flood, R.D., Kowsmann, R.O., Belderson, R.H. and Gorini, M.A., 1988, Anatomy and growth pattern of Amazon deep-sea fan as revealed by long-range side-scan sonar (GLORIA) and high-resolution seismic studies. American Association of petroleum Geologists Bulletin, v. 72, p. 885-911.

Damuth, J.E., Kolla, V., Flood, R.D., Kowsmann, R.O., Monteiro, M.C., Gorini, M.A., Palma, J.J.C., and Belderson, R.H., 1983a, Distributary channel meandering and bifurcation patterns on the Amazon deep-sea fan as revealed by long-range side-scan sonar (GLORIA). Geology, v. 11, p. 94-98.

Damuth, J.E., Kowsmann, R.O., Flood, R.D., Belderson, R.H. and Gorini, M.A., 1983b, Age relationship of distributary channels on Amazon deep-sea fan: implications for fan growth pattern. Geology, v.11, p. 470-473.

Davies, G.R., 1997, The Triassic of the Western Canada sedimentary Basin: tectonic and stratigraphic framework, paleogeography, paleoclimate and biota. Bulletin of Canadian Petroleum Geology, v. 45, no. 4, p. 434-460.

Davies, G. R., Moslow, T.F. and Sherwin, M.D., 1997, The Lower Triassic Montney Formation, west-central Alberta. Bulletin of Canadian Petroleum Geology,

v. 45, no. 4, p. 472-505.

Davies, G.R. and Sherwin, M.D., 1997, Productive dolomitized coquina facies of the Lower Triassic Montney Formation, Western Canada Sedimentary Basin. Canadian Society of Petroleum Geologists/Society for Sedimentary Geology (SEPM), Joint Convention, Calgary, Core Workshop Notes, p. 257-276.

Dilek, Y., 1994, The mode and nature of continental rifting along the northwestern periphery of Gondwanaland during the break-up of Pangea. *in* Embry, A.F. and Beauchamp (eds.), Pangea: Global Environments and Resources. Canadian Society of Petroleum Geologists, Memoir 17, p. 113-121.

Donaldson, W.S., Plint, A.G. and Longstaffe, F.J., 1998, Basement tectonic control on distribution of the shallow marine Bad Heart Formation: Peace River Arch area, northwest Alberta. Bulletin of Canadian Petroleum Geology, v. 46, p. 576-598.

Droz, L. and Bellaiche, G., 1985, Rhone deep-sea fan: morphostructure and growth pattern. American Association of Petroleum Geologists Bulletin, v. 69, p. 460-479.

Duan, T., Gao, Z., Zeng, Y. and Stow, D., 1993, A fossil carbonate contourite drift on the Lower Ordovician palaeocontinental margin of the middle Yangtze, Jiuxi, northern Hunan, China. Sedimentary Geology, v. 82, p. 271-277.

Duke, W.D., 1985, Hummocky cross-stratification. Tropical hurricanes, and intense winter storms. Sedimentology, v. 32, p. 167-194.

Dzulynski, S. and Walton, E.K., 1965, Sedimentary features of flysch and

greywackes. Amsterdam: Elsevier, 274p.

Edwards, D,E., Barclay, J.E., Gibson, D.W., Kvill, G.E. and Halton, E., 1994, Triassic strata of the Western Canada Sedimentary Basin. *in* Mossop, G.D. and Shetsen (comps.), Geological Atlas of the Western Canada Sedimentary Basin. Canadian Society of Petroleum Geologists and Alberta Research Council, p. 257-275.

Embry, A.F., 1988, Triassic sea-level changes: evidence from the Canadian Arctic Archipelago. *in* Wilgus, C.K., Hasting, B.S., Posamentier, H., Ross, C.A., Van Wagoner, J.C. and Kendall, C.G.St.C. (eds.), Sea-level Changes: an Integrated Approach. Society of Economic Paleontologists and Mineralogists, Special Publication no. 42, p. 249-259.

Embry, A.F., 1997, Global sequence boundaries of the Triassic and their identification in the Western Canada Sedimentary Basin. Bulletin of Canadian Petroleum Geology, v. 45, p. 415-433.

Embley, R.W., 1985, A locally formed deep ocean canyon system along the Blanco Transform, northeast Pacific. Geo-Marine Letters, v. 5, p. 99-104.

Feeley, M.H., Moore, T.C., Loutit, T.S. and Bryant, W.R., 1990, Sequence stratigraphy of Mississippi fan related to oxygen isotope sea level index. American Association of Petroleum Geologists, Bulletin, v. 74. P. 407-424.

Flood, R.D., Manley, P.L., Kowsmann, R.O., Appi, C.J. and Pirmez, C., 1991, Seismic facies and late Quaternary growth of Amazon submarine fan. *in* Weimer, P. and Link, M.H. (eds.), Seismic facies and sedimentary processes

of submarine fans and turbidite systems. New York, Springer-Verlag, p. 415-433.

Galloway, W.E., 1998, Siliciclastic slope and base-of-slope depositional systems: component facies, stratigraphic architecture, and classification. American Association of Petroleum Geologists Bulletin, v. 82, p. 569-595.

Gibson, D.W., 1968a, Triassic stratigraphy between the Athabasca and Smoky rivers of Alberta. Geological Survey of Canada, Paper 67-65.

Gibson, D.W., 1968b, Triassic stratigraphy between Athabasca and Brazeau rivers of Alberta. Geological Survey of Canada, Paper 68-11.

Gibson, D.W., 1969, Triassic stratigraphy of the Bow River-Crowsnest Pass region, Rocky Mountains of Alberta and British Columbia. Geological Survey of Canada, Paper 68-29.

Gibson, D.W., 1971a, Triassic stratigraphy of the Sikanni Chief River-Pine Pass region, Rocky Mountain Foothills, northeastern British Columbia. Geological Survey of Canada, Paper 70-31.

Gibson, D.W., 1971b, Triassic petrology of Athabasca-Smoky River region, Alberta. Geological Survey of Canada, Bulletin 194.

Gibson, D.W., 1972, Triassic stratigraphy of the Pine Pass-Smoky River area, Rocky Mountain Foothills and Front Ranges of British Columbia and Alberta. Geological Survey of Canada, Paper 71-30, 108 p.

Gibson, D.W., 1974, Triassic rocks of the southern Canadian Rocky Mountains. Geological Survey of Canada, Bulletin 230.

Gibson, D.W., 1975, Triassic rocks of the Rocky Mountain Foothills and Front Ranges of northeastern British and westcentral Alberta. Geological Survey of Canada, Bulletin 247.

Gibson, D.W., 1992, Stratigraphy, sedimentology, coal geology and depositional environments of the Lower Cretaceous Gething Formation, northeastern British Columbia and west-central Alberta. Geological Survey of Canada, Bulletin 431, 127 p.

Gibson, D.W. and Barclay, J.E., 1989, Middle Absaroka Sequence: The Triassic Stable Craton. in Ricketts, B.D. (eds.), The Western Canada Sedimentary Basin. Canadian Society of Petroleum Geologists, Special Publication no. 30, p. 219-232.

Gibson, D.W. and Edwards, D.E., 1990a, Triassic stratigraphy and sedimentary environments of the Williston Lake area and adjacent subsurface Plains, northeastern British Columbia. Field Trip Guidebook no. 6, Canadian Society of Petroleum Geologists, Basin Perspectives Conference, May 27-30, 1990, Calgary, Alberta.

Gibson, D.W. an Edwards, D.E., 1990b, An overview of Triassic stratigraphy and depositional environments in the Rocky Mountain Foothills and western Interior Plains, Peace River Arch area. in O'Connell, S.C. and Bell, J.S. (eds.), Geology of the Peace River Arch. Bulletin of Canadian Petroleum Geology, v. 38A, p. 146-158.

Gibson, D.W. and Poulton, 1994, Field guide to the Triassic and Jurassic

stratigraphy and depositional environments of the Rocky Mountain Foothills and Front Ranges in the Banff, Jasper and Cadomin areas of Alberta. Geological Survey of Canada, Open File 2780, 85 p.

Graham, J.R., 1982, Transition from basin-plain to shelf deposits in the Carboniferous flysch of southern Morocco. Sedimentary Geology, v. 33, p. 173-194.

Graham, S.A. and Bachman, S.B., 1983, Structural controls on submarine-fan geometry and internal architecture: upper La Jolla fan system, offshore southern California. American Association of Petroleum Geologists Bulletin, v. 67, p. 83-96.

Griggs, G.B. and Kulm, L.D., 1973, Origin and development of Cascadia deep-sea channel. Journal of Geophysical Research, v. 78, p. 6325-6339.

Hallam, A., 1994, The earliest Triassic as an anoxic event, and its relationship to the end-Paleozoic mass extinction. in Embry, A.F., Beauchamp, B. and Glass, D.J. (eds.), Pangea: Global Environments and Resources. Canadian Society of Petroleum Geologists, Memoir 17, p. 797-804.

Hamblin, A.P. and Walker, R.G., 1979, Storm-dominated shallow marine deposits: the Fernie-Kootenay (Jurassic) transition, southern Rocky Mountains. Canadian Journal of Earth Sciences, v. 16, p. 1673-1690.

Harms, J.C., Southard, J.B., Spearing, D.R. and Walker, R.G., 1975, Depositional environments as interpreted from primary sedimentary structures. Society of Economic Paleontogists and Mineralogists, Short Course 9, 161p.

Hart, B.S. and Plint, A.G., 1990, Upper Cretaceous warping and fault movement on the southern flank of the Peace River Arch, Alberta. Bulletin of Canadian Petroleum Geology, v. 38A, p. 190-195.

Haq, B.V., Hardenbol, J., Vail, P.R., Colin, J.P., Ioannides, N., Stover, L.E., Jan Du Chene, R., Wright, R.C., Sarq, J.F. and Morgan, B.E., 1987, Mesozoic-Cenozoic Cycle Chart, Version 3.1B. American Association of Petroleum Geologists.

Henderson, C.M., Richards, B.C. and Barclay, J.E., 1994, Permian strata of the Western Canada Sedimentary Basin. *in* Mossop, G. and Shetsen, I. (comps.), Geological Atlas of the Western Canada Sedimentary Basin. Canadian Society of Petroleum Geologists and Alberta Research Council, p. 251-258.

Henderson, C.M. and Zonneveld, J.P., 1998, Sequence biostratigraphic framework for the Montney Formation and tectonic origin of the mid-Montney sequence boundary, Peace River Basin, northwestern Alberta. Canadian Society of Petroleum Geologists/Canadian Society of Exploration Geophysicists/ Canadian Well Logging Society, Joint Convention, Calgary, Plenary Oral Posters Core Workshop, p. 267-268.

Hesse, R., 1974, Long-distance continuity of turbidites: Possible evidence for an Early Cretaceous trench-abyssal plain in the East Alps. Geological society of America Bulletin, v. 85, p. 859-870.

Hubert, C., Lajoie, J. and Leonard, M.A., 1970, Deep sea sediments in the lower

Paleozoic Quebec Supergroup. *in* Lajoie, J. (eds.), Flysch sedimentology in North America. Geological Association of Canada, Special Paper 7, p. 103-125.

Hunt, A.D. and Ratcliffe, J.D., 1959, Triassic stratigraphy, Peace River area, Alberta and British Columbia, Canada. American Association of Petroleum Geologists, Bulletin, v. 43, p. 563-589.

Kindle, E.D., 1944, Geological reconnaissance along Fort Nelson, Liard and Beaver rivers, northeastern British Columbia and southeastern Yukon: Canada. Geological Survey of Canada, Paper 44-16.

Kolla, V. and Coumes, F., 1984, Morpho-acoustic and sedimentologic characteristics of the Indus Fan. Geo-Marine Letters, v. 3, p. 133-139.

Kolla, V. and Coumes, F., 1987, Morphology, internal structure, seismic stratigraphy, and sedimentation of Indus Fan. American Association of Petroleum Geologists Bulletin, v. 71, 650-677.

Kumar, N. and Slatt, 1984, Submarine fan and slope facies of Tonkawa (Missourian- Virgilian) Sandstone in deep Anadarko Basin. American Association of Petroleum Geologists Bulletin, v. 68, p. 1839-1856.

Leckie, D., 1986, Rates, controls and sand-body geometries of transgressive-regressive cycles: Cretaceous Moosebar and Gates formations, British Columbia. American Association of Petroleum Geologists, Bulletin, v. 70, p. 516-535.

Lowe, D.R., 1988, Suspended-load fallout rate as an independent variable in the

analysis of current structures. Sedimentology, v. 35, p. 765-776.

Lundegard, P.D., Samuels, N.D. and Pryor, W.A., 1985, Upper Devonian turbidite sequence, central and southern Appalachian basin: Contrast with submarine fan deposits. *in* Woodrow, D.L. and Sevon, W.D. (eds.), The Catskill Delta. Geological Society of America, Special Paper 201, p. 107-121.

Manley, P.L. and Flood, R.D., 1988, Cyclic sediment deposition within Amazon deep-sea fan. American Association of Petroleum Geologists Bulletin, v. 72, p. 912-925.

Masson, D.G., Gardner, J.V., Parson, L.M. and Field, M.E., 1985, Morphology of Upper Laurentian Fan using GLORIA long-range side-scan sonar. American Association of Petroleum Geologists Bulletin, v. 69, p. 950-959.

McHargue, T.R., 1991, Seismic facies, processes and evolution of Miocene inner fan channel, Indus Submarine Fan. *in* Weimer, P. and Link, M.H. (eds.), Seismic facies and sedimentary processes of submarine fans and turbidite systems. New York, Springer-Verlag, p. 403-413.

McHargue, T.R. and Webb, J.E., 1986, Internal geometry, seismic facies, and petroleum potential of canyons and inner fan channels of the Indus Submarine Fan. American Association of Petroleum Geologists Bulletin, v. 70, p. 161-180.

McLearn, F.H., 1921, Mesozoic of upper Peace River, British Columbia. Geological Survey of Canada, Summary Report 1920, Part B, p. 1-6.

McLearn, F.H., 1930, Preliminary study of the fauna of the upper Triassic Schooler

Creek Formation, western Peace River, British Columbia. Transactions of the Royal Society of Canada, v. 24, series 3, section 4, p. 13-19.

McLearn, F.H., 1940, Notes on the geography and geology of the Peace River foothills. Transactions of the Royal Society of Canada, v. 34, series, 3, section 4, p. 63-74.

McLearn, F.H., 1941, Triassic stratigraphy of Brown Hill, Peace River Foothills, B.C. Transactions of the Royal Society of Canada, v. 35, series 3, section 4, p. 93-103.

McLearn, F.H., 1945, The lower Triassic of Liard River. Geological Survey of Canada, Paper 45-28.

McLearn, F.H., 1946, Upper Triassic faunas in Halfway, Sikanni Chief and Prophet basins, northeastern British Columbia. Geological Survey of Canada, Paper 46-25.

McLearn, F.H., 1947, Upper Triassic faunas of Pardonet Hill, Peace River foothills, British Columbia. Geological Survey of Canada, Paper 47-14.

McLearn, F.H. and Kindle, E.D., 1950, Geology of northeastern British Columbia. Geological Survey of Canada, Memoir 259, 236 p.

McMechan, M.E., 1990, Upper Proterozoic to Middle Cambrian history of the Peace River Arch: evidence from the Rocky Mountains. Bulletin of Canadian Petroleum Geology, v. 38A, p. 36-44.

Miall, A.D., 1976, The Triassic Sediments of Sturgeon Lake South and surrounding areas. *in* Lerand, M. (eds.), The Sedimentology of Selected Clastic Oil and

Gas Reservoir in Alberta. Canadian Society of Petroleum Geology, p. 25-43.

Monger, J.W.H. and Price, R.A., 1979, Geodynamic evolution of the Canadian Cordillera-Progress and Problems. Canadian Journal of Earth Sciences, v. 16, p. 770-791.

Moore, B.R. and Clarke, M.K., 1970, The significance of a turbidite sequence in the Borden Formation (Mississippian) of eastern Kentucky and southern Ohio. Geological Association of Canada, Special Paper, no. 7. P. 211-218.

Moslow, T.F. and Davies, G.R., 1996, Turbidite reservior facies of the Montney Formation, Vahalla and La Glace fields. in Osadetz (eds.), Canadian Society of Petroleum Geologists, Core Conference, p. 13-1 to 13-9.

Moslow, T.F. and Davies, G.R., 1997, Turbidite reservoir facies in the lower Triassic Montney Formation. Bulletin of Canadian Petroleum Geology, v. 45, no. 4, p. 507-536.

Mudie, J.D., Normark, W.R. and Cray, E.J. Jr., 1970, Direct mapping of the sea floor using side-scanning sonar and transponder navigation. Geological Society of America Bulletin, v. 81, p. 1547-1554.

Mutti, E., 1977, Distinctive thin-bedded turbidite facies and related depositional environments in the Eocene Hecho Group (south-central Pyrennes, Spain). Sedimentology, v. 24, p. 107-131.

Mutti, E., 1979, Turbidite et cones sous-marins profonds. in Homewood, P. (eds.), Sedimentation detritique (fluviatile, littorale et marine). Short course notes, Institut de Gelogie de l'Universite de Fribourg, Switzerland, p.353-419.

Mutti, E., 1985, Turbidite systems and their relations to depositional sequences. *in* Zuffa, G.G. (eds.), Provenance of arenites. Dordrecht, D. Reidel Publishing Company, p. 65-93.

Mutti, E. and Ghibaudo, G., 1972, Un esempio di torbiditi di conoide sottomarina esterna: le arenarie di San Salvatore (Formazione di Bobbio, Micene) nell'Appennino di Piacenza. Memorie dell'accademia delle Scienze di Torino, Classe di Scienze Fisiche, Matematiche e Naturali, Serie 4, n. 16, 40 p.

Mutti, E, Nilsen, T.R. and Ricci Lucchi, F., 1978, Outer fan depositional lobes of the Laga Formation (upper Miocene and lower Pliocene), east-central Italy. *in* Stanley, D.J. and Kelling, G. (eds.), Sedimentation in submarine canyons, trenches and fans. Dowden, Hutchinson & Ross, Inc., p. 210-223.

Mutti, E. and Normark, W.R., 1987, Comparing examples of modern and ancient turbidite systems: problems and concepts. *in* Leggett, J.R. and Zuffa, G.G. (eds.), Marine clastic sedimentology: concepts and case studies. London, Graham and Trotman, p. 1-38.

Mutti, E. and Ricci Lucchi, F., 1972, Le torbiditi dell'Appennino settentrionale: introduzione all'analisi di facies. Memorie della Societa Geologica Italiana, v. 11, p. 161-199. *English translation by* Nilson, T.H., 1978, International Geology Review, v. 20, p. 125-166.

Mutti, E. and Ricci Lucchi, F., 1975, Turbidite facies and facies association. *in* Mutti, E., Ricci Lucchi, F., Sagri, M., Zabzucchi, G., Ghibaudo, G. and Iaccarino, S. (eds.), Examples of turbidite facies and facies associations from selected

formations of the Northern Apennines. International association of

Sedimentologists, Guidebook to Field Trip A-11, 9th international Congress

of Sedimentology, p. 21-36.

Nelson, C.H., 1990, Estimated post-Messinian sediment supply and sedimentation

rated on the Ebro continental margin, Spain. Marine Geology, v. 95, p. 394-

418.

Nelson, C.H. and Nilsen, T.H., 1984, Modern and ancient deep-sea fan

sedimentation. Society of Economic Paleontologists and Mineralogists, Short

Course 14, 404 p.

Normark, W.R., 1970a, Growth patterns of deep-sea fans. American Association of

Petroleum Geologists Bulletin, v. 54, p. 2170-2195.

Normark, W.R., 1970b, Channel piracy on Monterey Deep-Sea Fan. Deep-Sea

Research, v. 17, p. 837-846.

Normark, W.R., 1978, Fan valleys, channels, and depositional lobes on modern

submarine fans: characters for recognition of sandy turbidite environments.

American Association of Petroleum Geologists Bulletin, v. 62, p. 912-931.

Normark, W.R., Gutmacher, C.E., Chase, T.E. and Wilde, P., 1984, Monterey Fan:

growth pattern control by basin morphology and changing sea levels. Geo-

Marine Letters, v. 3, p. 93-99.

Normark, W.R. and Piper, D.J.W., 1969, Deep-sea fan valleys, past and present.

Geological Society of America Bulletin, v. 80, p. 1859-1866.

Normark, W.R. and Piper, D.J.W., 1972, Sediments and growth patterns of Navy

deep-sea fan, San Clemente Basin, California borderland. Journal of Geology, v.80, p. 198-223.

Normark, W.R., Piper, D.J.W. and Stow, D.A.V., 1983, Quaternary development of channels, levees and lobes on middle Laurentian Fan. American Association of Petroleum Geologists Bulletin, v. 67, p. 1400-1409.

O'Connell, S., Normark, W.R., Ryan, W.B.F. and Kenyon, N.H., 1991, An entrenched thalweg channel on the Rhone fan: interpretation from a SeaBeam and SeaMARC I survey. *in* Osborne, R.H. (eds.), From shoreline to abyss: contributions in marine geology in honour of Francis parker Shepard. Society of Economic Paleontologists and Mineralogists, Special Publication 46, p. 259-270.

O'Connell, S.C., 1994, Geological History of the Peace River Arch. *in* Shetson, I. (comps.), Geological Atlas of the Western Canada Sedimentary Basin. Canadian Society of Petroleum Geologists and Alberta Research Council, p. 431-437.

O'Connell, S.C., Dix, G.R. and Barclay, J.E., 1990, The origin, history, and regional development of the Peace River Arch, Western Canada. Bulletin of Canadian Petroleum Geology, v. 38A, p. 4-24.

Pelletier, B.R., 1960, Triassic stratigraphy, Rocky Mountain Foothills, northeastern British Columbia 94J and I. Geological Survey of Canada, Paper 60-2.

Pelletier, B.R., 1961, Triassic stratigraphy of the Rocky Mountains and Foothills, northeastern British Columbia. Geological Survey of Canada, Paper 61-8.

Pelletier, B.R., 1963, Triassic stratigraphy of the Rocky Mountains and Foothills, Peace River District, British Columbia. Geological Survey of Canada, Paper 62-26.

Pelletier, B.R., 1964, Triassic stratigraphy of the Rocky Mountain Foothills between Peace and Muskwa rivers, northeastern British Columbia. Geological Survey of Canada, Paper 63-33.

Pelletier, B.R., 1965, Paleocurrents in the Triassic of northeastern British Columbia. in Middleton, G.V. (eds), Primary Sedimentary Structures and their Hydrodynamic Interpretation. Society of Economic paleontologists and Mineralogists, Special Publication no. 12, p. 233-245.

Pickering, K.T., Hiscott, R.N. and Hein, F.J., 1989, Deep marine environments: clastic sedimentation and tectonics. London, Unwin Hyman, 416 p.

Piper, D.J.W. and Normark, W.R., 1971, Re-examination of a Miocene deep-sea fan and fan valley, southern California. Geological Society of America Bulletin, v. 82, p. 1823-1830.

Piper, D.J.W. and Normark, W.R., 1982, Acoustic interpretation of Quaternary sedimentation and erosion on the channelled upper Laurentian Fan, Atlantic marine of Canada. Canadian Journal of Earth Sciences, v. 19, 1974-1984.

Piper, D.J.W. and Normark, W.R., 1983, Turbidite depositional patterns and flow characteristics, Navy submarine fan, California borderland. Sedimentology, v.30, p. 681-694.

Piper, D.J.W., Shor, A.N., Farre, J.A., O'Connell, S. and Jacobi, R., 1985, Sediment

slides and turbidity currents on the Laurentian Fan: sidescan sonar investigations near the epicentre of the 1929 Grand Banks earthquake. Geology, v. 13, p. 538-541.

Piper, D.J.P. and Stow, D.A.V., Fine-grained turbidites, *in* Cycles and events in stratigraphy. Berlin, Springer Verlag, p. 360- 376.

Plint, A.G., 1991, High-frequency relative sea level oscillations in Upper Cretaceous shelf clastics of the Alberta foreland basin: possible evidence for a glacio-eustatic control?, *in* MacDonald, D.I.M., (eds.), Sedimentation, tectonics and eustasy: International Association of Sedimentologists, Special Publication 12, p. 409-428.

Posamentier, H.W. and Vail, P.R., 1988, Eustatic controls on clastic deposition: II - Sequence and system tract models. *in* Wilgus, C.K., Hastings, B.S., Kendall, C.G.St.C., Posamentier, H.W., Ross, C.A. and Van Wagoner, J.C. (eds.), Sea-level changes: an integrated approach. Society of Economic Paleontologists and Mineralogists, Special Publication 42, p. 125-154.

Poulton, T.P., Tittemore, J. and Dolby, G., 1990, Jurassic stratigraphy, northwestern Alberta and northeastern British Columbia. Bulletin of Canadian Petroleum Geology, v. 38A, p. 159-175.

Price, R.A. and Mountjoy, E.W., 1970, Geological structure of the Canadian Rocky Mountain between Bow and Athabasca Rivers - a progress report. *in* Wheeler, J.O. (eds.), Structure of southern Canadian Cordillera. Geological Association of Canada, Special Paper no. 6, p. 7-25.

Price, R.A., 1981, The cordilleran foreland thrust and fold belt in the southern Canadian Rocky Mountains. *in* McLay, K.R. and Price, N.J., Thrust and Nappe tectonics. The Geological Society of London, Special Publication no. 9, p. 427-448.

Reading, H.R. and Richards, M., 1994, Turbidite systems in deep-water basin margins classified by grain size and feeder system. American Association of Petroleum Geologists Bulletin, v. 78, p. 792-822.

Reinson, G.E., Lee, P.J., Warters, W., Osadetz, K.G., Bell. L.L., Price, P.R., Trollope, F., Campbell, R.I. and Barclay, J.E., 1993, Devonian gas resources of the Western Canada Sedimentary Basin. Geological Survey of Canada, Bulletin 452, 157 p.

Ricci Lucchi, F. and Valmori, E., 1980, Basin-wide turbidites in a Miocene, over-supplied deep-sea plain: a geometrical analysis. Sedimentology, v. 27, p. 241-270.

Richards, B.C., 1989, Upper Kaskaskia Sequence: uppermost Devonian and Lower Carboniferous. *in* Ricketts, B.D. (eds.), Western Canada Sedimentary Basin - a Case History. Canadian Society of Petroleum Geologists, Special Publication no. 30, p. 164-201.

Richards, B.C., Barclay, J.E., Bryan, D., Hartling, A., Henderson, C.M. and Hinds, R.C., 1994, Carboniferous strata of the Western Canada Sedimentary Basin. *in*Mossop, G.D. and Shetson, I. (comps.), Geological Atlas of the Western Canada Sedimentary Basin. Canadian Society of Petroleum Geologist and

Alberta Research Council, p. 221-250.

Rocheleau, M. and Lajoie, 1974, Sedimentary structures in resedimented conglomerate of the Cambrian flysch, L'Islet, Quebec Appalachians. Journal of Sedimentology Petrology, v. 44, p. 826-836.

Ross, G.M., 1990, Deep crust and basement structure of the Peace River Arch region: constraints on mechanisms of formation. Bulletin of Canadian Petroleum Geology, v. 38A, p. 25-35.

Samthein, M and Diester-Haass, L., 1977, Eolian-sand turbidites. Journal of Sedimentary Petrology, v. 47, p. 868-890.

Shanmugam, G, Moiola, R.J. and Damuth, J.E., 1985, Eustatic control of submarine fan development. in Bouma, A.H., Normark, W.R. and Barnes, N.E. (eds.), Submarine fans and related turbidite systems. New York, Springer-Verlag, p. 23-28.

Shanmugam, G., Spalding, T.D. and Rofheart, D.H., 1993, Processes sedimentology and reservoir quality of deep-marine bottom-current reworked sands (sandy contourites): an example from the Gulf of Mexico. American Association of Petroleum Geologists Bulletin, v. 77, p. 1241-1259.

Shannon, P.M. and Naylor, D., 1989, Petroleum Basin Studies. London, Dordrecht and Boston, Gragam and Trotman, 206 p.

Shepard, F.P., Dill, R.F. and Von Rad, U., 1969, Physiography and sedimentary processes of La Jolla submarine fan and fan-valley, California. American Association of Petroleum Geologists Bulletin, v. 53, p. 390-420.

Sherwin, M.D., 1998, Sandstone-coquina lowstand shoreline trends in the Triassic

Montney, Doig and Halfway Formations; NE British Columbia, NW Alberta.

Canadian Society of Petroleum Geologists/Canadian Society of Exploration

Geophysicists/Canadian Well Logging Society, Joint Convention, Calgary,

Plenary Oral Posters Core Workshop, p. 471.

Sinclair, H.D., 1994, The influence of lateral basinal slopes on turbidite

sedimentation in the Annot Sandstones of SE France. Journal of

Sedimentary Research, v. A64, p. 42-54.

Stanley, D.J., 1987, Turbidite to current-reworked sand continuum in Upper

Cretaceous rocks, U.S. Virginia Islands. Marine Geology, v. 78, p. 143-151.

Stanley, D.J., 1993, Model for turbidite-to-contourite continuum and multiple

processes transport in deep marine settings: examples in the rock record.

Sedimentary Geology, v. 82, p. 241-256.

Stanley, D.J. and Kelling, G. (eds.), 1978, Sedimentation in submarine canyons,

trenches and fans. Dowden, Hutchinson & Ross, Inc., 395 p.

Stephenson, R.A, Zelt, C.A., Ellis, R.M., Hajnal, Z, Morel-al'Huissier, P., Mereu,

R.F., Northey, D.J., West, G.F. and Kanasewich, E.R., 1989, Crust and

upper mantle structure the origin of the Peace River Arch. Bulletin of

Canadian Petroleum Geology, 37, p. 224-235.

Stewart, J.N., 1972, Initial deposits of the cordilleran geosyncline: Evidence for a

late Precambrian (850 m.y.) continental separation. Geological Society of

America Bulletin, v. 83, p. 1345-1360.

Stott, D.F. and Aitken, J.D. (eds.), 1993, Sedimentary cover of the craton in Canada. Geology of Canada, no.5, Geological Survey of Canada, 826p.

Stow, D.A.V., Faugeres, J.C., Viana, A. and Gonthier, E., 1998, Fossil contourites: a critical review. Sedimentary Geology, v. 115, p. 3-31.

Stow, D.A.V., Howell, D.G. and Nelson, C.H., 1985, Sedimentary, tectonic, and sea-level controls. *in* Bouma, A.H., Normark, W.R. and Barnes, N.E. (eds.), Submarine fans and related turbidite systems. New York, Springer-Verlag, p. 15-22.

Stow, D.A.V. and Shanmugam, G., 1980, Sequence of structures in fine-grained turbidites: comparison of recent deep-sea and ancient flysch sediments. Sedimentary Geology, v. 25, p. 23-42.

Tozer, E.T., 1961, The sequence of marine Triassic faunas in western Canada. Geological Survey of Canada, Paper 61-6.

Tozer, E.T., 1963, Lower Triassic ammonoids from Tuchodi Lakes and Halfway River areas, northeastern British Columbia. Geological Survey of Canada, Bulletin 96, part 1, p. 1-28.

Tozer, E.T., 1967, A standard for Triassic time. Geological Survey of Canada, Bulletin 156.

Tozer, E.T., 1982, Marine Triassic faunas of North America: Their significance for assessing plate and terrane movements. Geologische Rundschau, v. 71, p. 1077-1104.

Tozer, E.T., 1984, The Trias and its ammonoids: the evolution of a time scale.

Geological Survey of Canada, Miscellaneous Report 35.

Twichell, D.C., Kenyon, N.H., Parson, L.M. and McGregor, B.A., 1991, Depositional patterns of the Mississippi fan surface: evidence from GLORIA II and high-resolution seismic profiles. *in* Weimer, P. and Link, M.H. (eds.), Seismic facies and sedimentary processes of submarine fans and turbidite systems. New York, Springer-Verlag, p. 349-363.

Walker, R.G., 1965, The origin and significance of the internal sedimentary structures of turbidites. Yorkshire Geol. Soc., Proc. 35, p. 1-32.

Walker, R.G., 1971, Nondeltaic depositional environments in the Catskill clastic wedge (Devonian) of central Pennsylvania. Geological Society of America Bulletin, v. 82, p. 1305-1326.

Walker, R.G., 1978, Deep-water sandstone facies and ancient submarine fans: models for exploration for stratigraphic traps. American Association of Petroleum Geologists Bulletin, v. 62, p. 932-966.

Walker, R.G., 1985, Mudstones and thin-bedded turbidites associated with the Upper Cretaceous Wheeler Gorge conglomerates, California: a possible channel-levee complex. Journal of Sedimentary Petrology, v. 55, p. 279-290.

Walker, R.G., 1992, Turbidite and submarine fans. *in* Walker, R.G. and James, N.E. (eds.), Facies models: response to sea level changes. Geological Association of Canada, p. 239-263.

Walker, R.G. and Mutti, E., 1973, Turbidite facies and facies associations. *in* Middleton, G.V. and Bouma, A.H. (eds.), Turbidites and deep water

sedimentation. Society of Economic Paleontologists and Mineralogists, Pacific Section, Short Course, p. 119-157.

Walker, R.G. and Plint, A.G., 1992, Wave- and storm-dominated marine systems. *in* Walker, R.G. and James, N.P. (eds.), Facies models: response to sea level changes. Geological Association of Canada, p. 219-238.

Walker, R.G. and Sutton, R.G., 1967, Quantitative analysis of turbidites in the upper Devonian Sonyea Group, New York. Journal of Sedimentary Petrology, v. 37, p. 1012-1022.

Weimer, P., 1989, Sequence stratigraphy of the Mississippi fan (Plio-Pleistocene), Gulf of Mexico. Geo-Marine Letters, v. 9, p. 185-272.

Weimer, P., 1990, Sequence stratigraphy, facies geometries, and depositional history of the Mississippi fan, Gulf of Mexico. American Association of Petroleum Geologists, Bulletin, v. 74, p. 425-453.

Weimer, P., 1991, Seismic facies, characteristics, and variations in channel evolution, Mississippi fan (Plio-Pleistocene), Gulf of Mexico. *in* Weimer, P. and Link, M.H. (eds.), Seismic facies and sedimentary processes of submarine fans and turbidite systems. New York, Springer-Verlag, p. 323-347.

Weimer, P. and Link, M.H. (eds.), 1991, Seismic facies and sedimentary processes of submarine fans and turbidite systems. New York, Springer-Verlag, 447 p.

Wilson, D., Davies, J.R., Waters, R.A. and Zalasiewicz, J.A., 1992, A fault-controlled depositional model for the Aberystwyth Grit turbidite system.

Geological Magazine, v. 129, p. 595-607.

Woodrow, D.L. and Isley, A.M., 1983, Facies, topography, and sedimentary processes in the Catskill Sea (Devonian), New York and Pennsylvania. Geological Society of America Bulletin, v. 94, p. 459-470.

Wright, G.N., McMechan, M.E., and Potter, D.E.G., 1994, Structure and architecture of the Western Canada Sedimentary Basin. *in* Shetson, I. (comps.), Geological Atlas of the Western Canada Sedimentary Basin. Canadian Society of Petroleum Geologists and Alberta Research Council, p. 25-40.

Yerkes, R.F., Gorsline, D.S. and Rusnak, G.A., 1967, Origin of Redondo submarine canyon, southern California. US Geological Survey Research Prof. Paper 575-C, p. 97-105.

# APPENDIX A

# LEGEND

## LITHOLOGY

mudstone/shale

silty mudstone

siltstone

very fine sandstone

mud-laminated sandstone

coquina

Subfacies 1C

## SEDIMENTARY STRUCTURES

:::::: sand lamina

/// cross bedding

rip-up mud clasts

slump

ripple cross-lamination

undulating lamina

$\mathcal{U}$ soft sediment deformation

water-escaping structure

## BEDDING CONTACTS

——— sharp

scoured

## ICHONOFOSSILS

Planolites

0 Skolithos

M1 = Marker 1
M2 = Marker 2
M3 = Marker 3
M4 = Marker 4
M5 = Marker 5

TSS = top of structureless sandstones
BSS = base of structureless sandstones
ES1 = Erosional Surface 1
ES2 = Erosional Surface 2

Legend to core logs in Appendix A

# Appendix A-1
## 3-23-68-22W5 (5105-5149 feet)
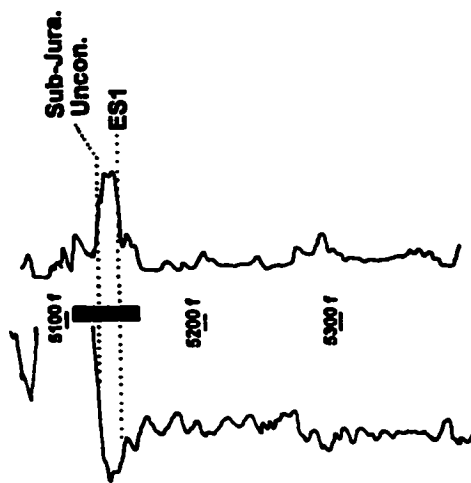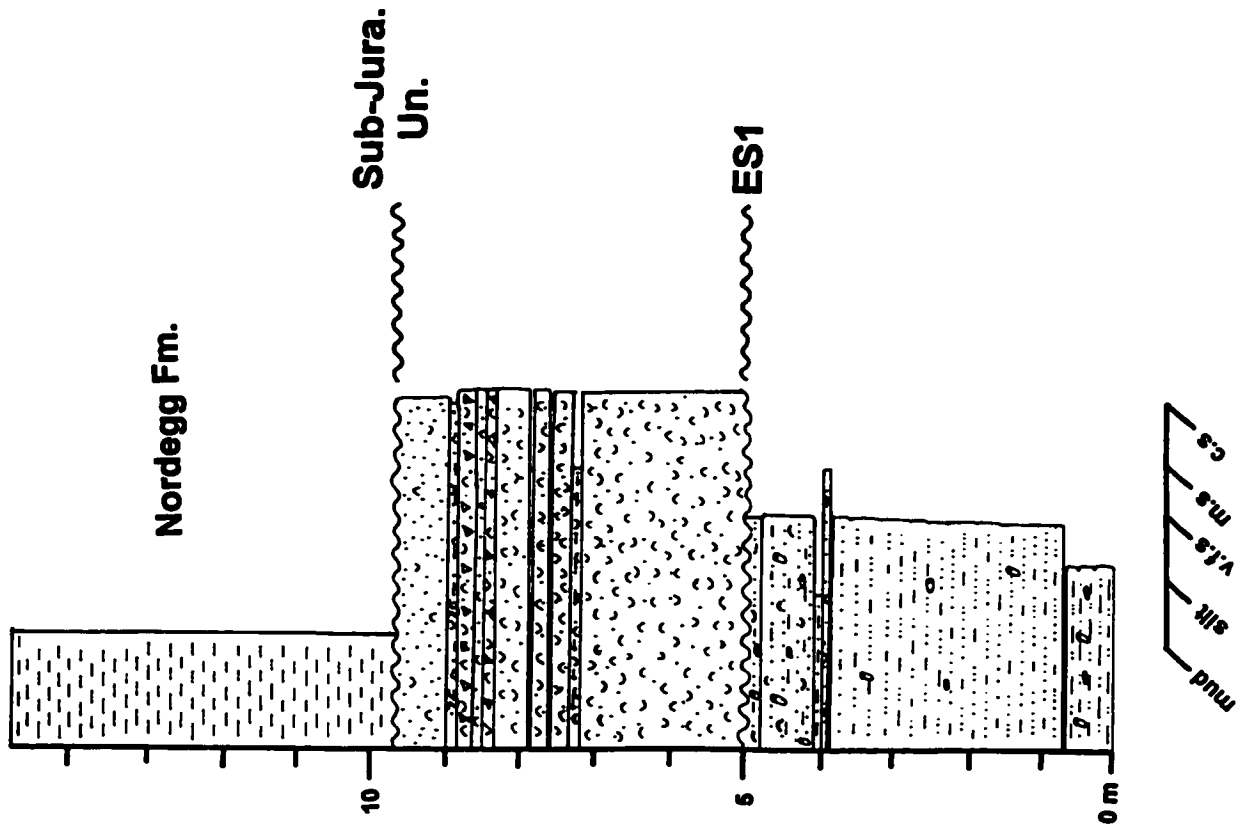
# Appendix A-2
## 6-30-67-23W5 (1840.0-1858.0 m)



Sub-Jura. Uncon.

1850

1875

M1

ES1

15

10

5

0 m

mud  silt  v.f.s  m.s  c.s

M1

ES1
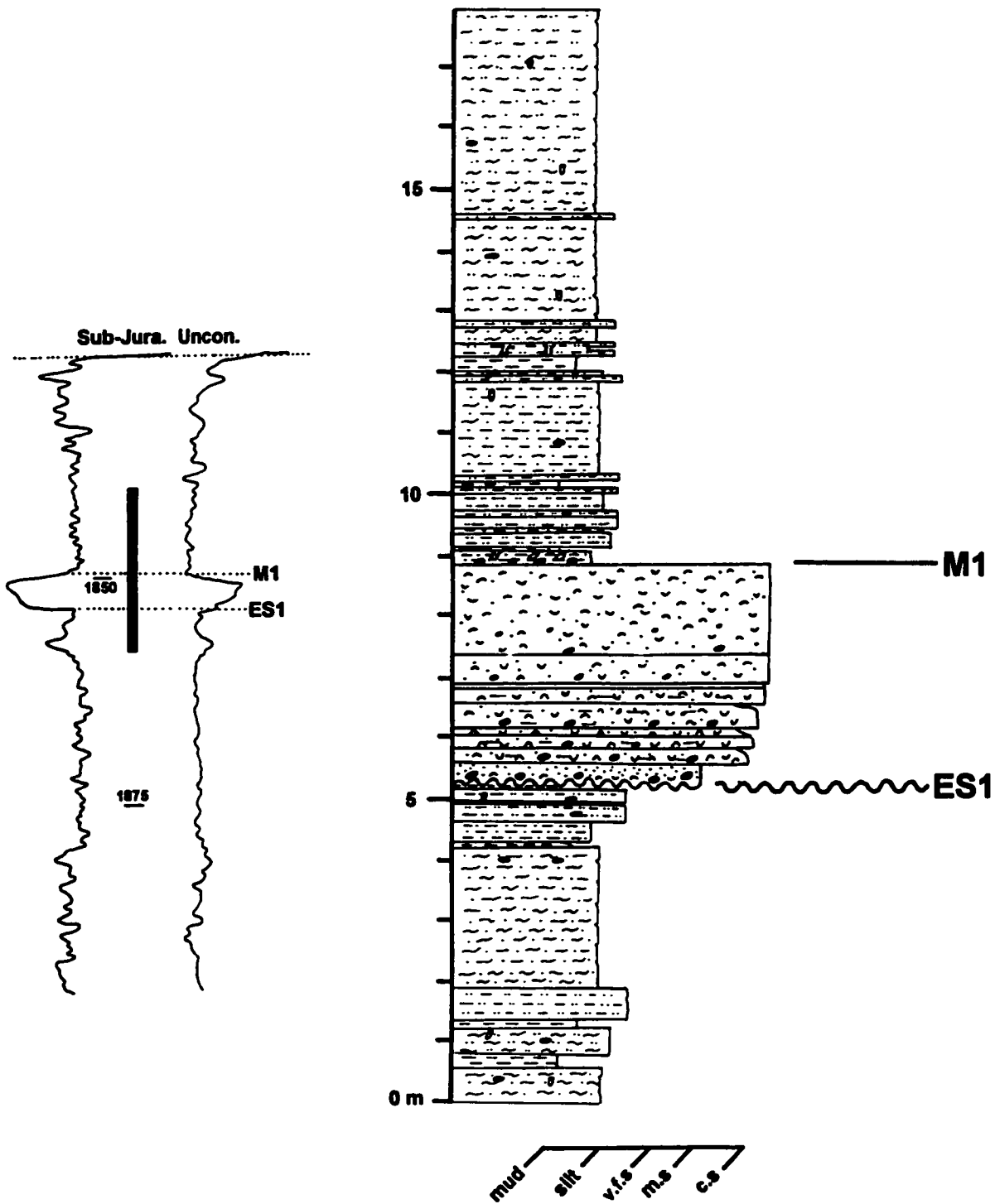
# Appendix A-3
## 7-3-68-24W5 (1814.0-1831.5 m)
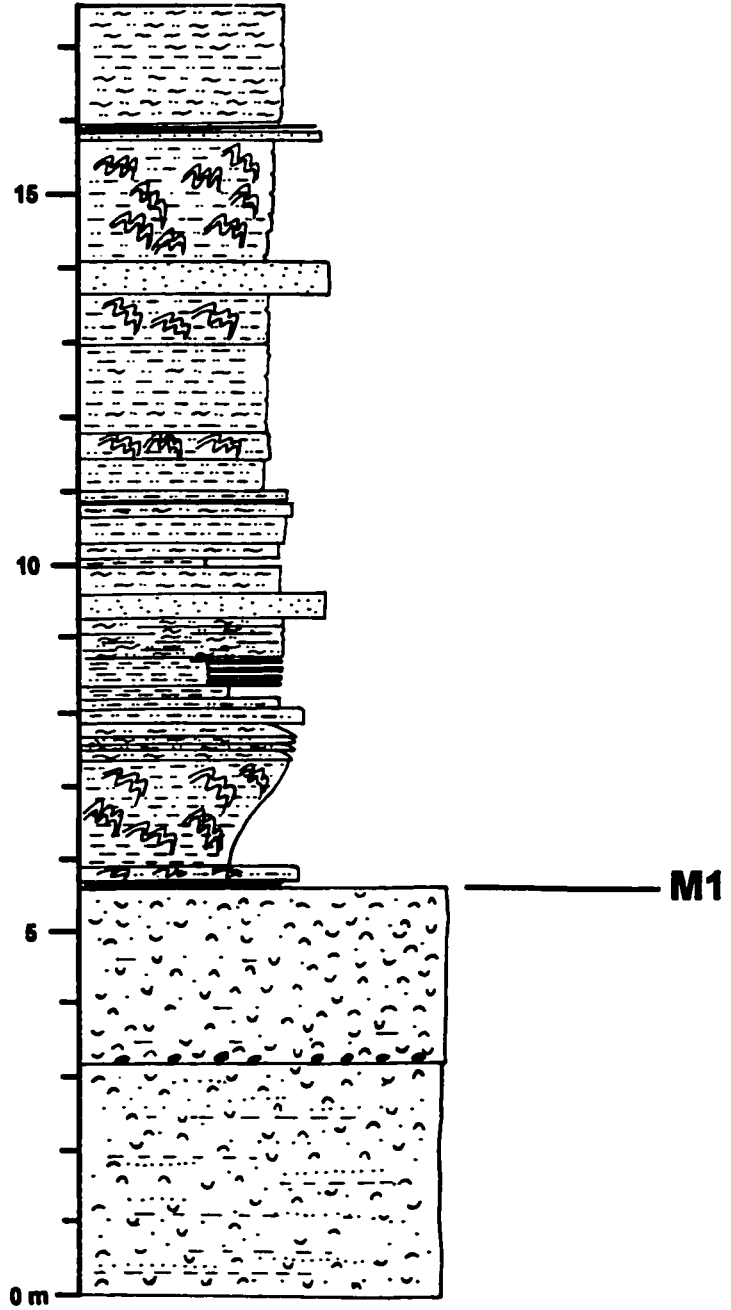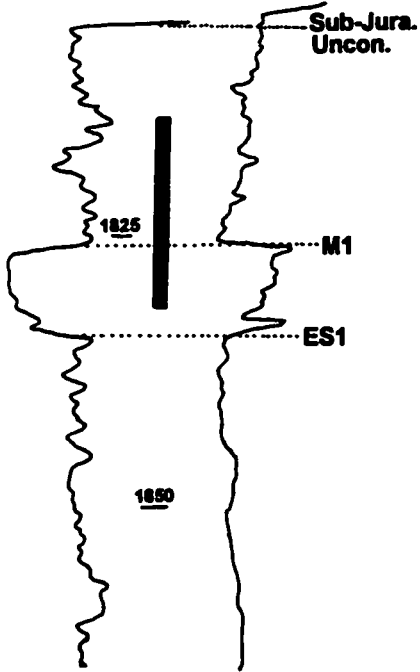
# NOTE TO USERS

Page(s) not included in the original manuscript are unavailable from the author or university. The manuscript was microfilmed as received.

254-259(APPENDIX A)

This reproduction is the best copy available.

UMI

# Appendix A-10
## 5-29-73-6W6 (2081.4-2099.6 m)



TSS=M5

2075

ES2

2100

M3

M2

15

10

5

ES2

0 m

mud    silt    v.f.s
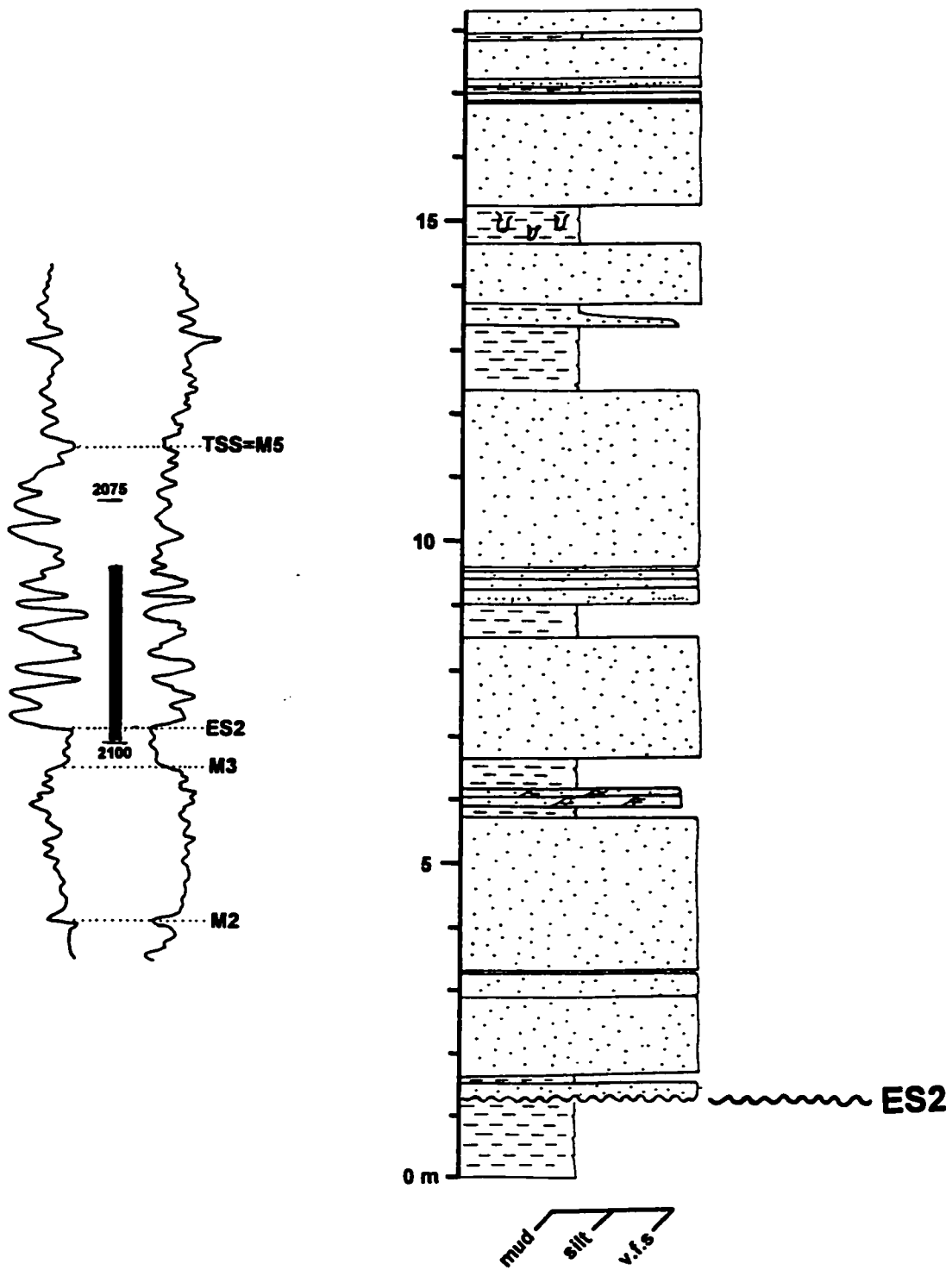
# Appendix A-11
## 6-8-74-6W6 (2049.0-2066.2 m)
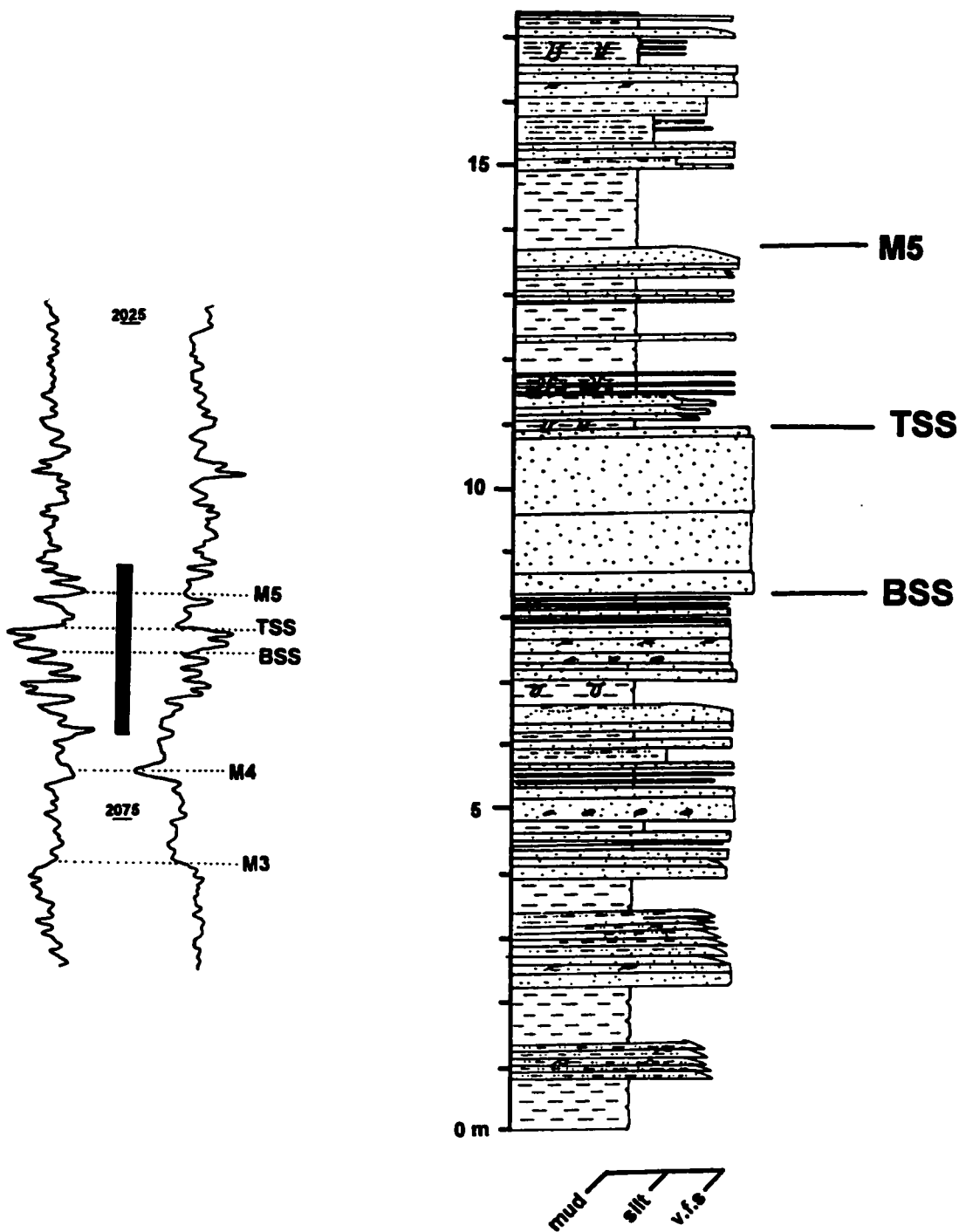
# Appendix A-12
## 5-20-74-6W6 (2051.5-2069.8 m)



TSS

BSS

M4

2050

TSS=M5

BSS

M4

2075

M3

15

10

5

0 m

mud   silt   v.f.s
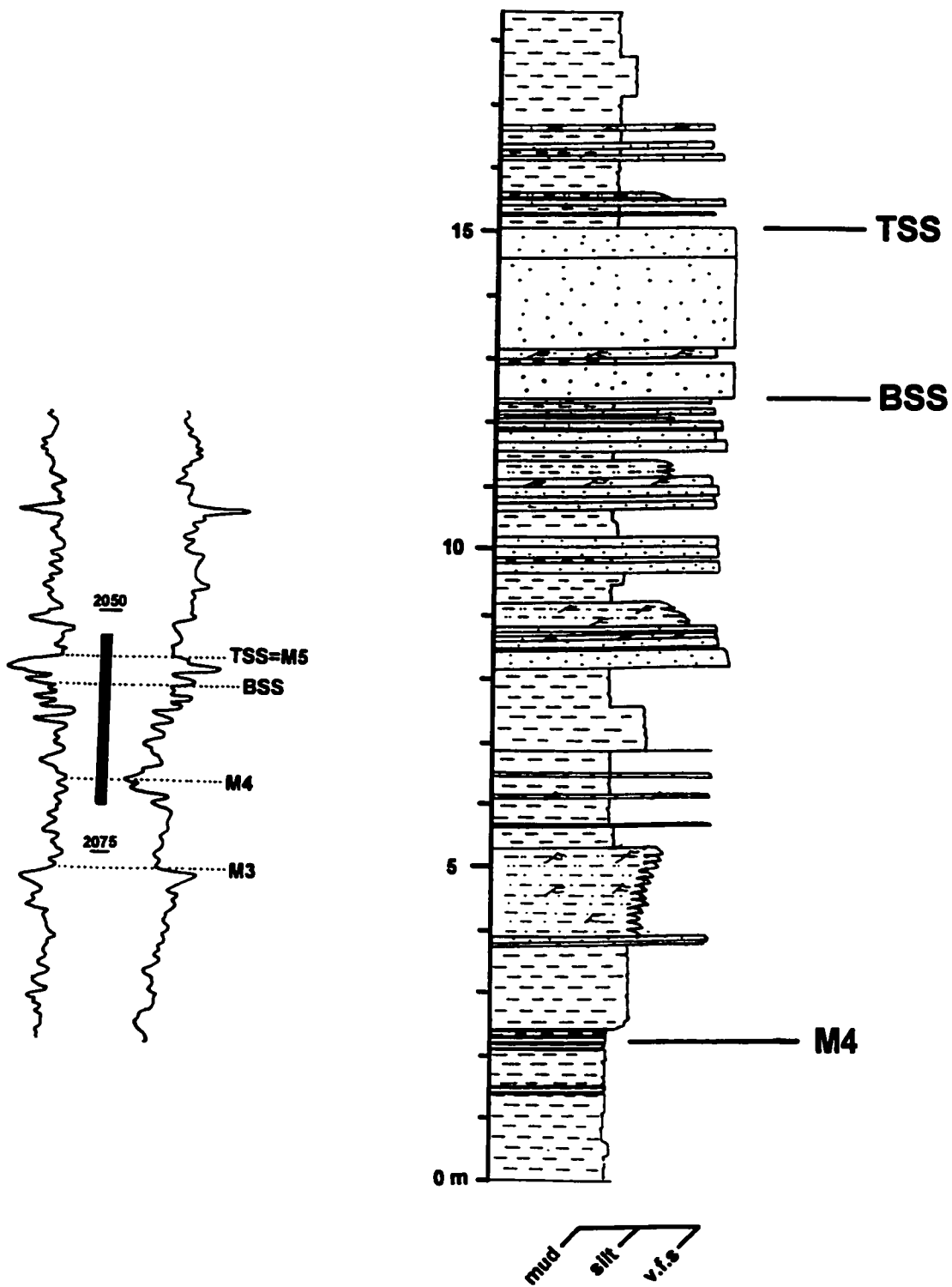
# Appendix A-13
## 14-13-74-7W6 (2055.5-2077.0 m)
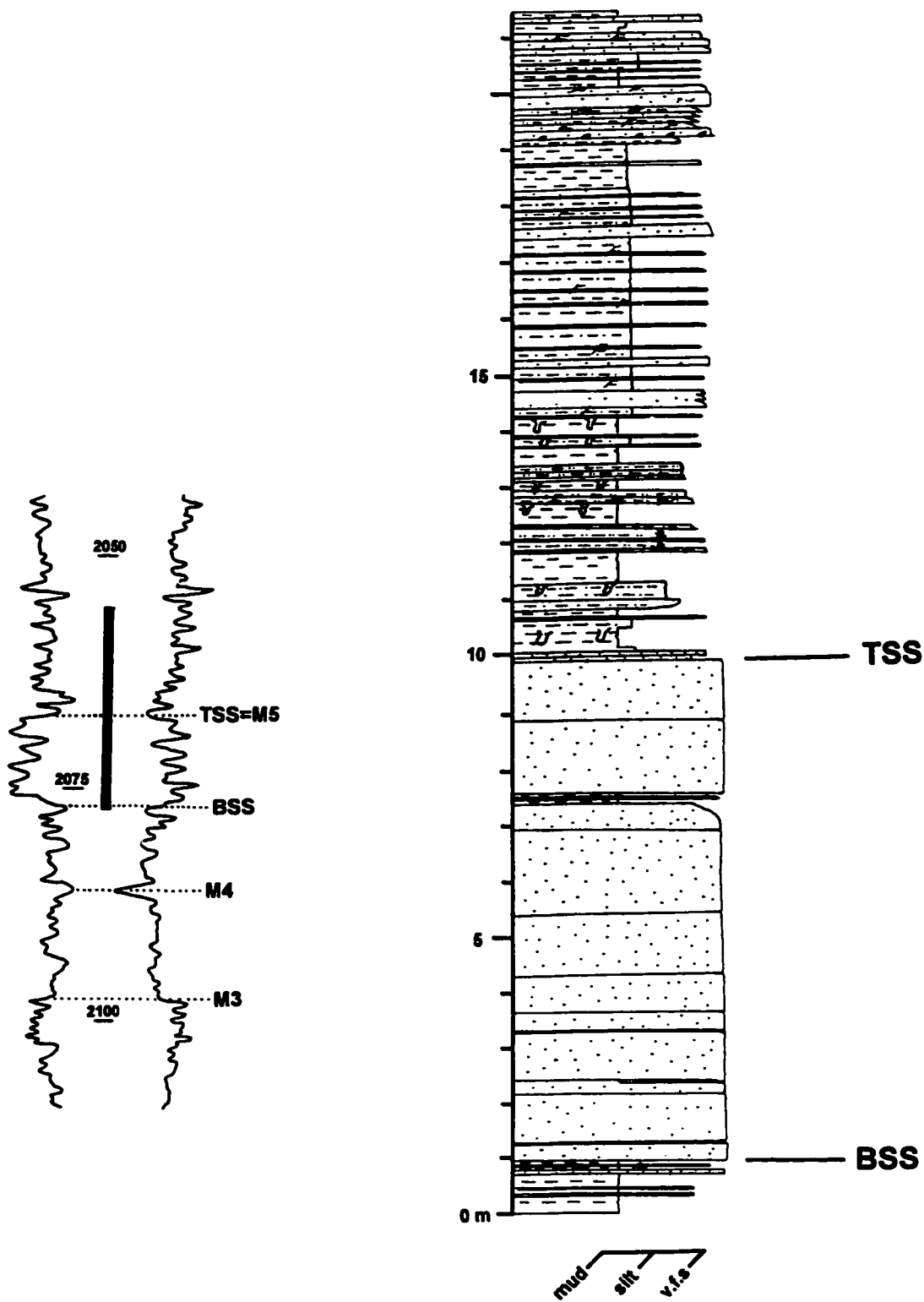
# Appendix A-14
## 6-20-74-7W6 (2130.5-2148.0 m)



TSS

15

2125

TSS=M5

ES2

2150

M4

5

ES2

M3

2175

0 m

mud    silt    v.f.s
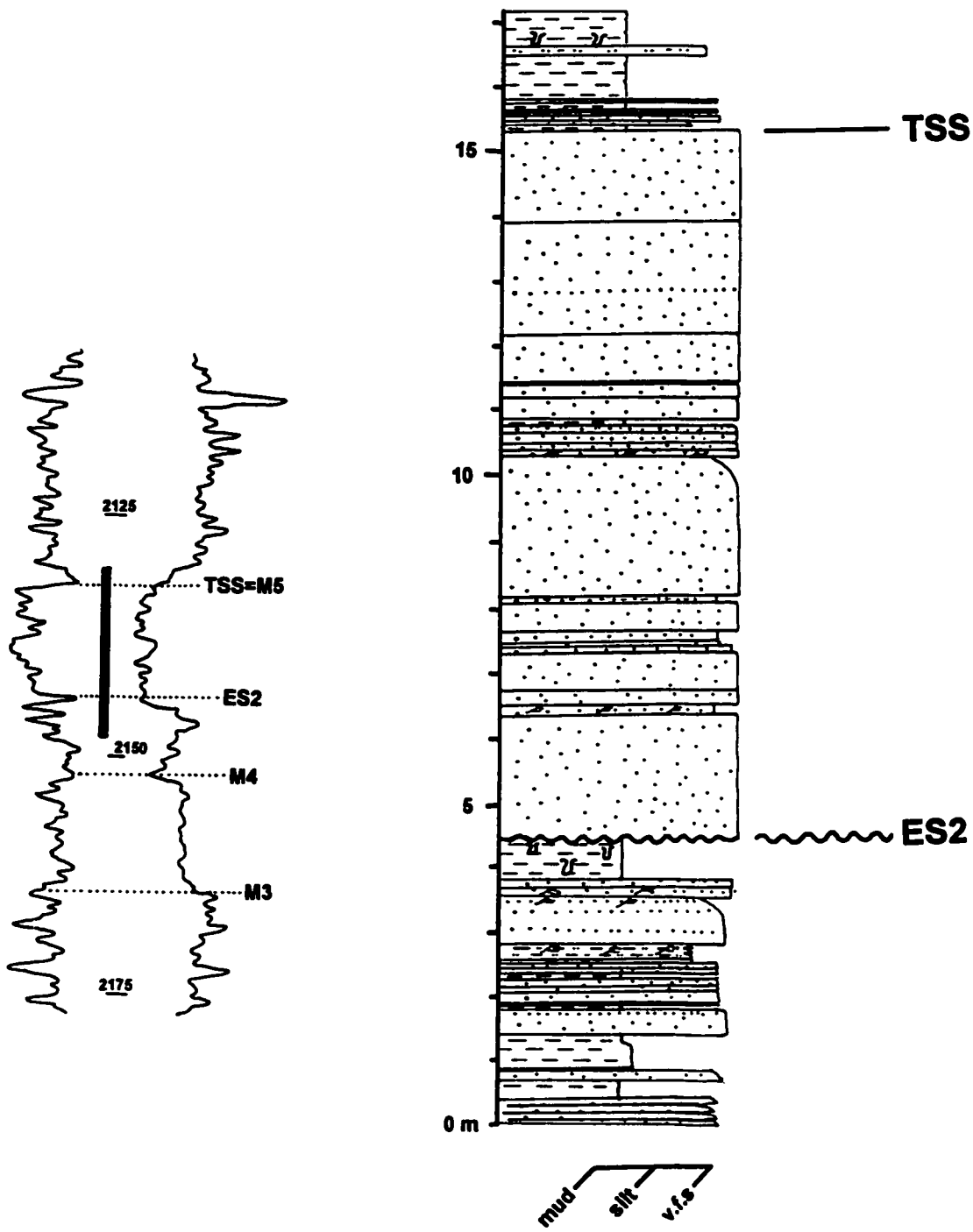
# Appendix A-15
## 14-25-74-7W6 (2084.0-2102.2 m)



2075

TSS=M5

BSS

M4

2125

M3

15

10

5

0 m

TSS

BSS

mud    silt    v.f.s
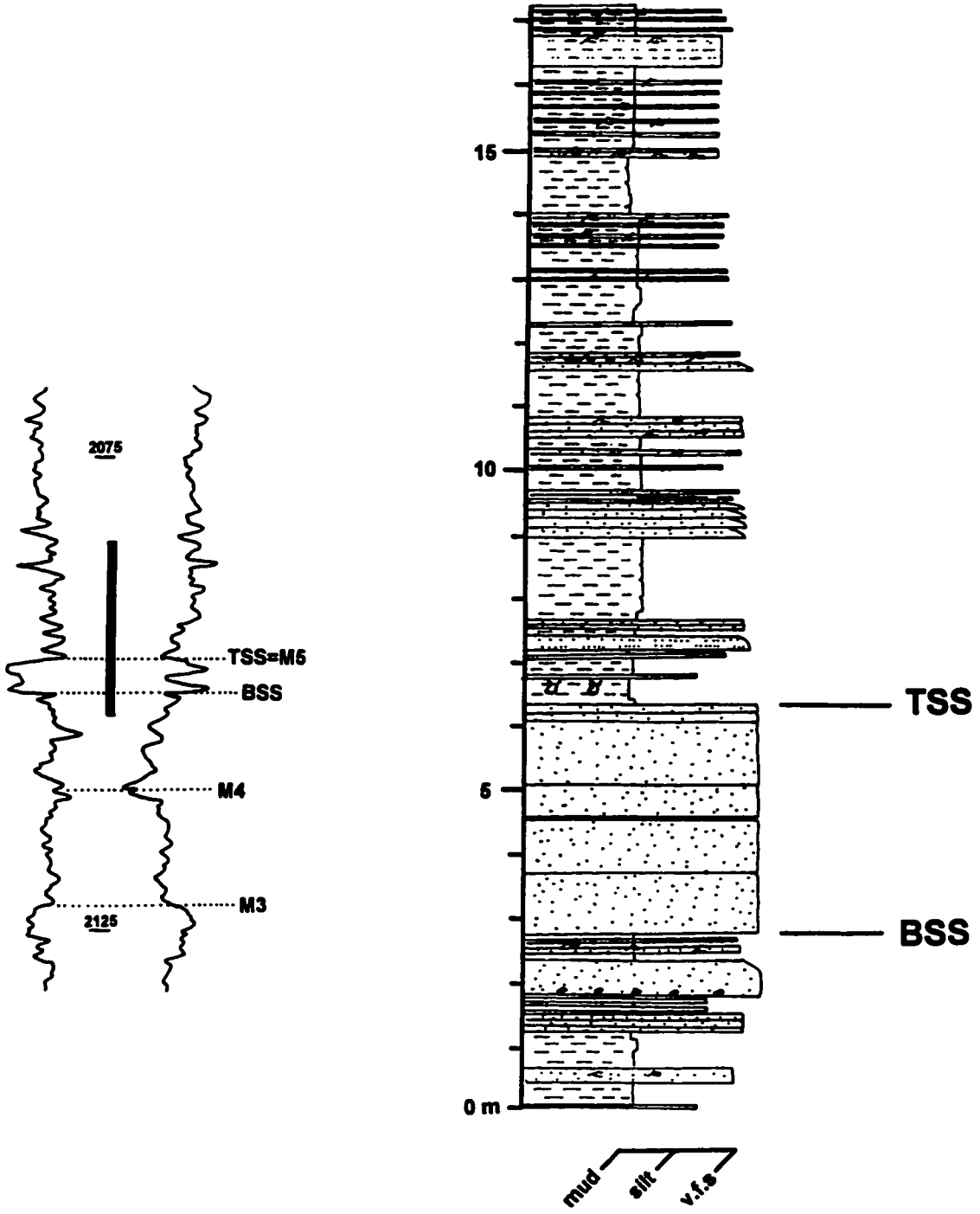
# Appendix A-16
## 14-23-74-8W6 (2144.0-2160.4 m)
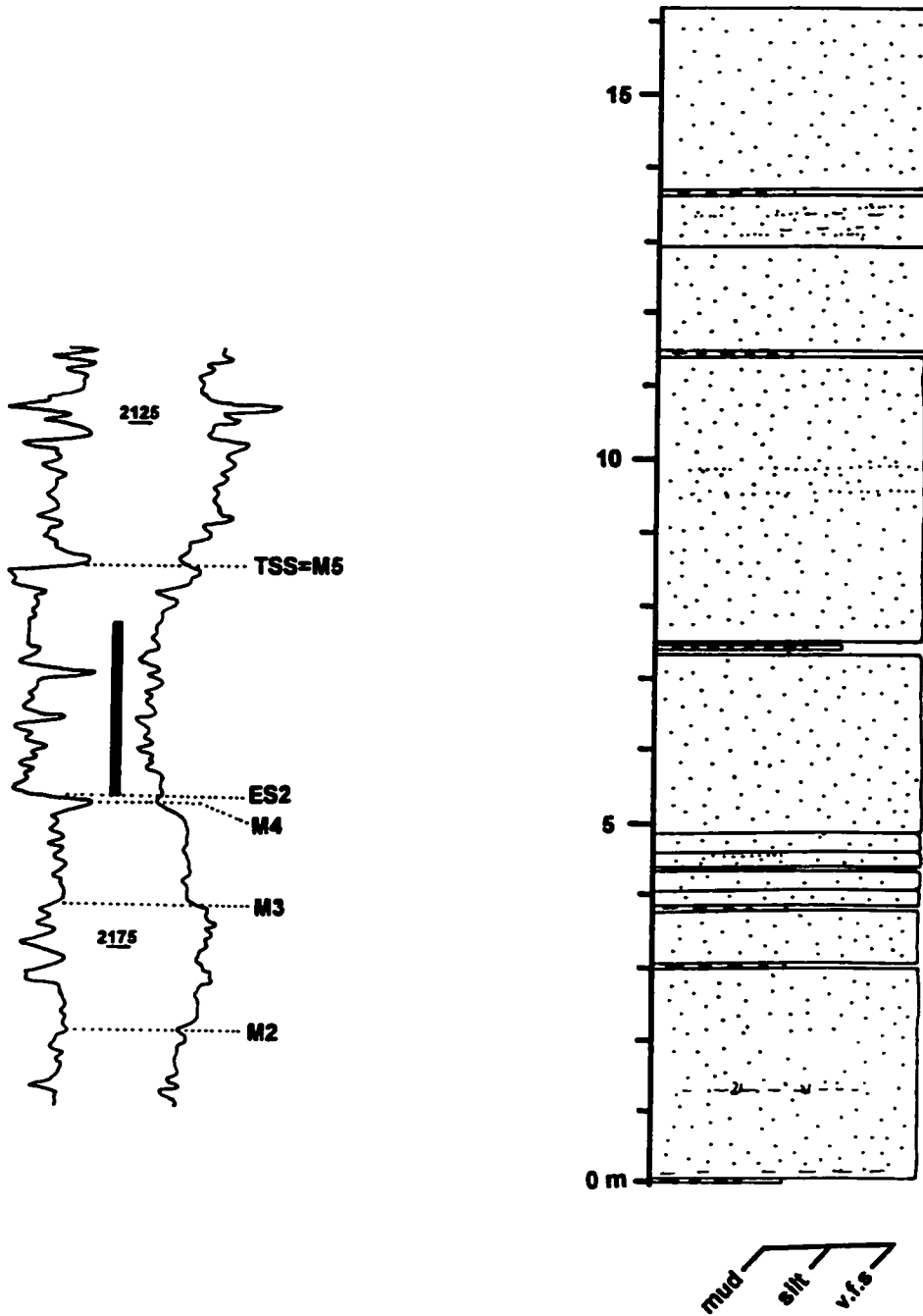
# Appendix A-17
## 16-27-74-8W6 (2141.0-2159.3 m)
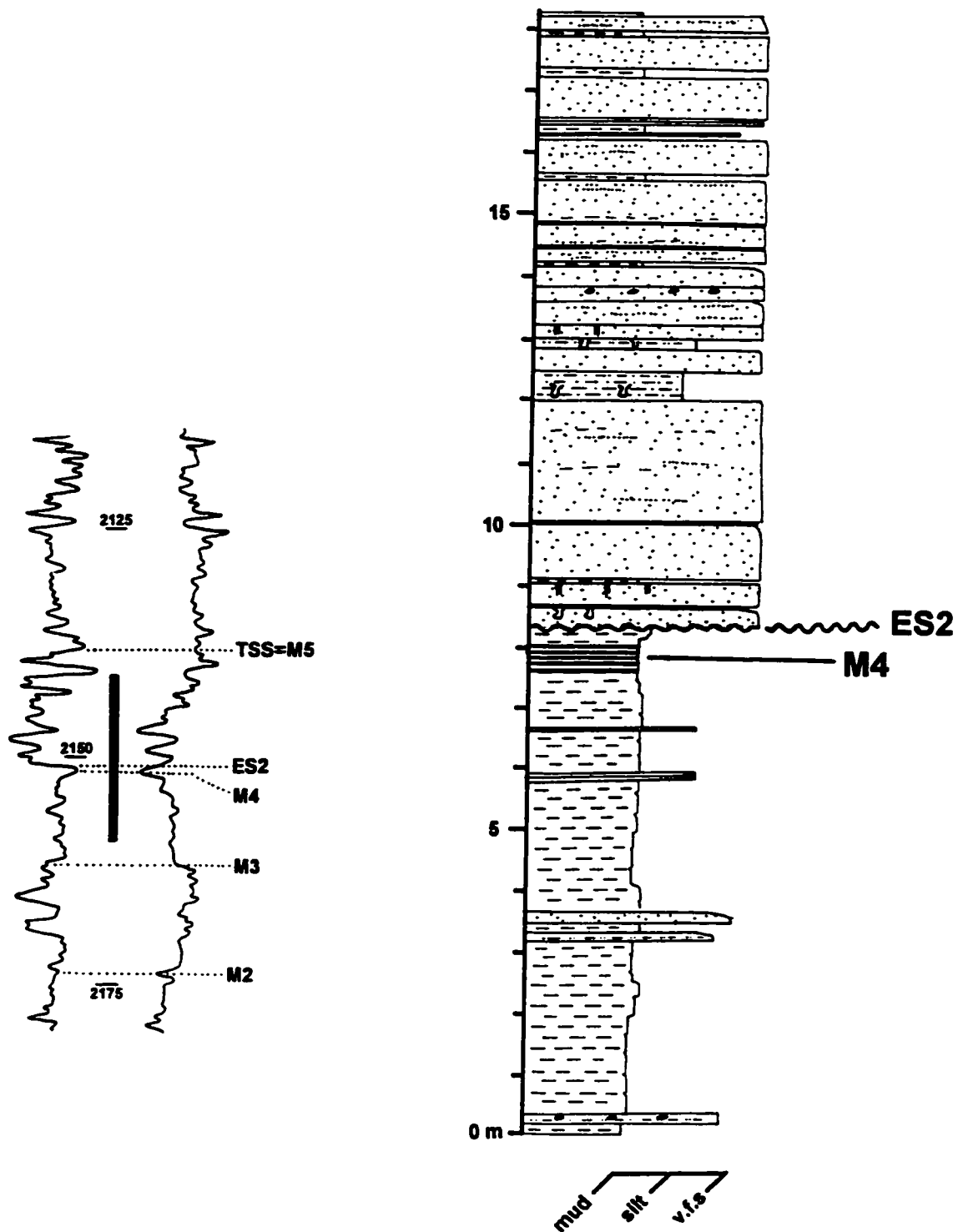
# Appendix A-18
## 14-7-75-8W6 (2176.3-2187.1 m)
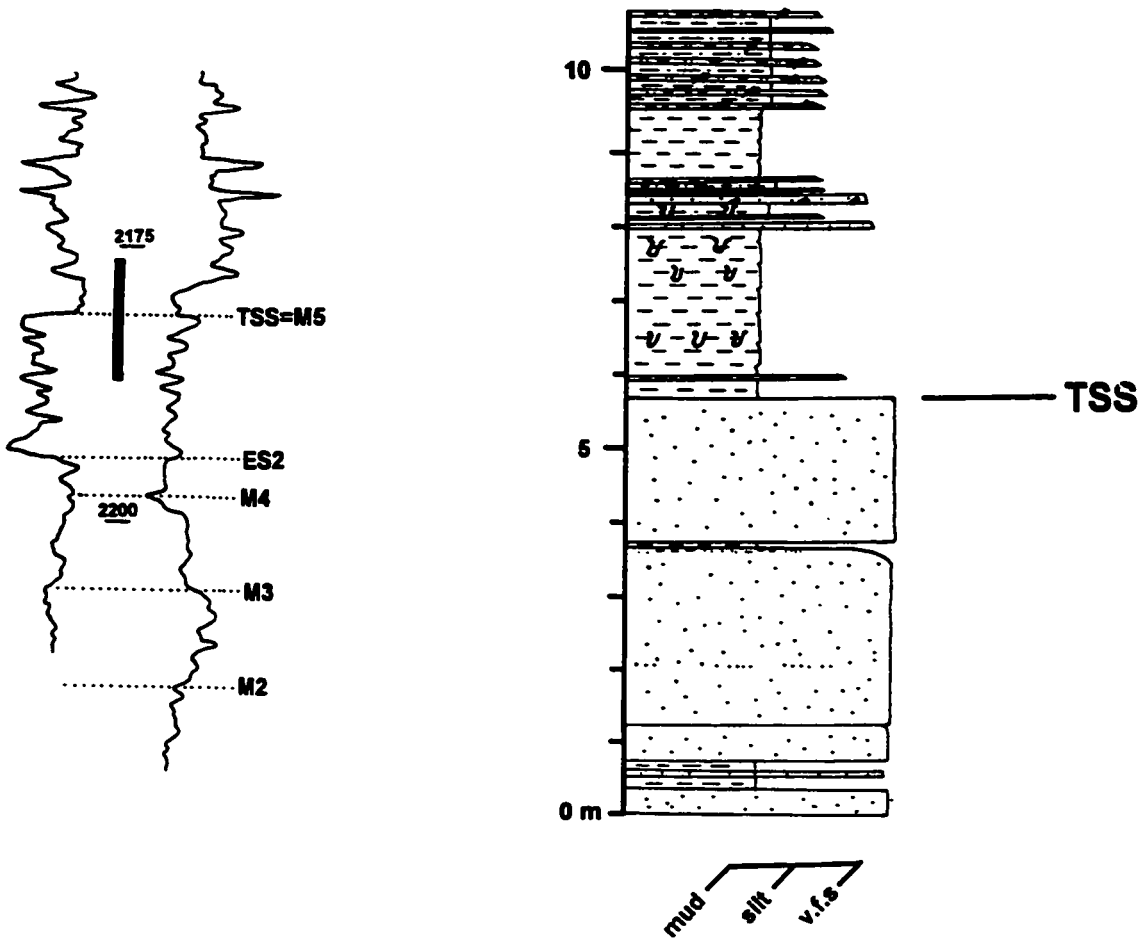
# Appendix A-19
## 6-9-75-8W6 (2139.8-2155.0 m)
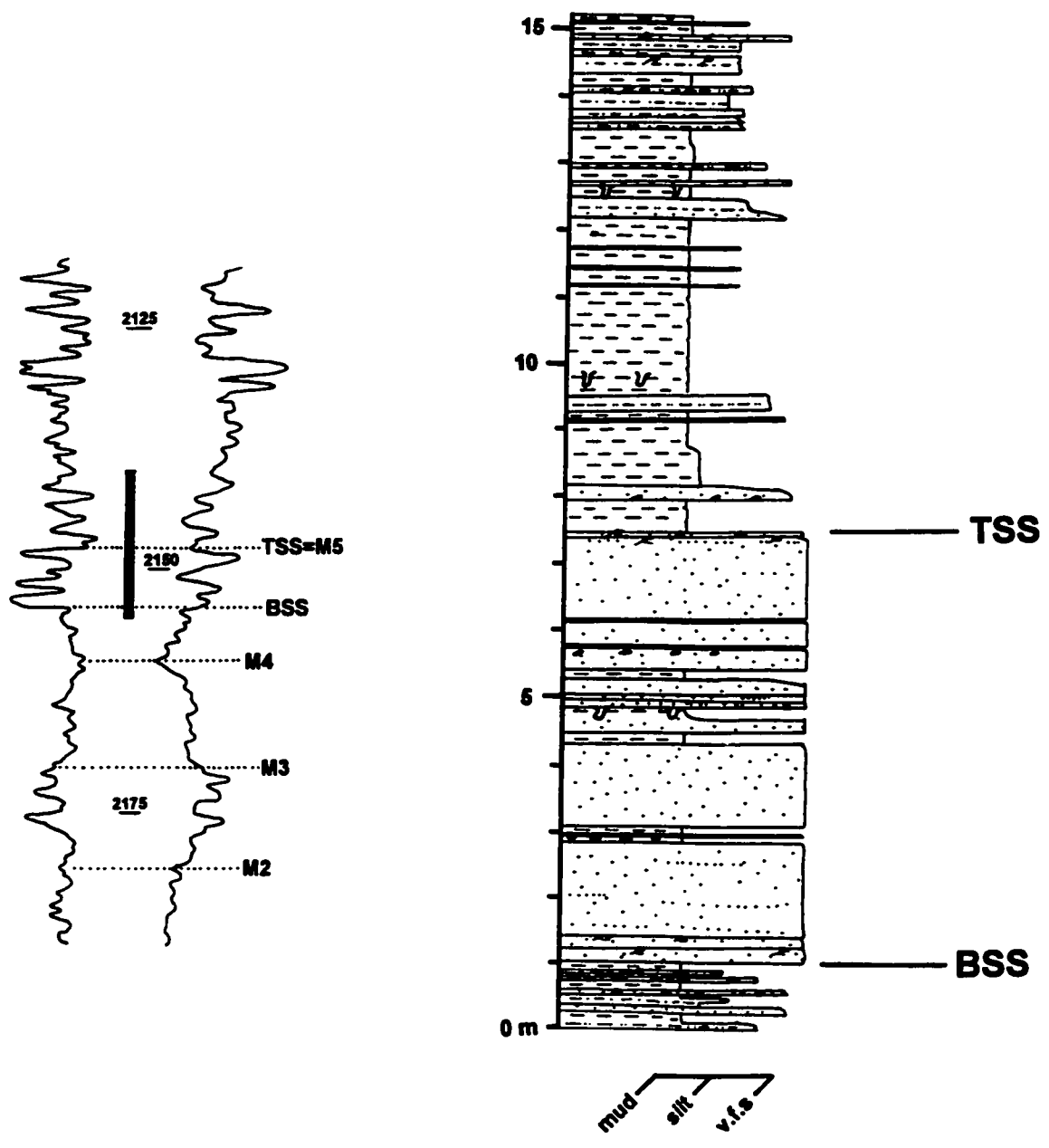
# Appendix A-20
## 14-17-75-8W6 (2160.0-2178.0 m)



TSS

BSS

M4

TSS=M5
BSS
M4
M3

2150

2175

15

10

5

0 m

mud    silt    v.f.s
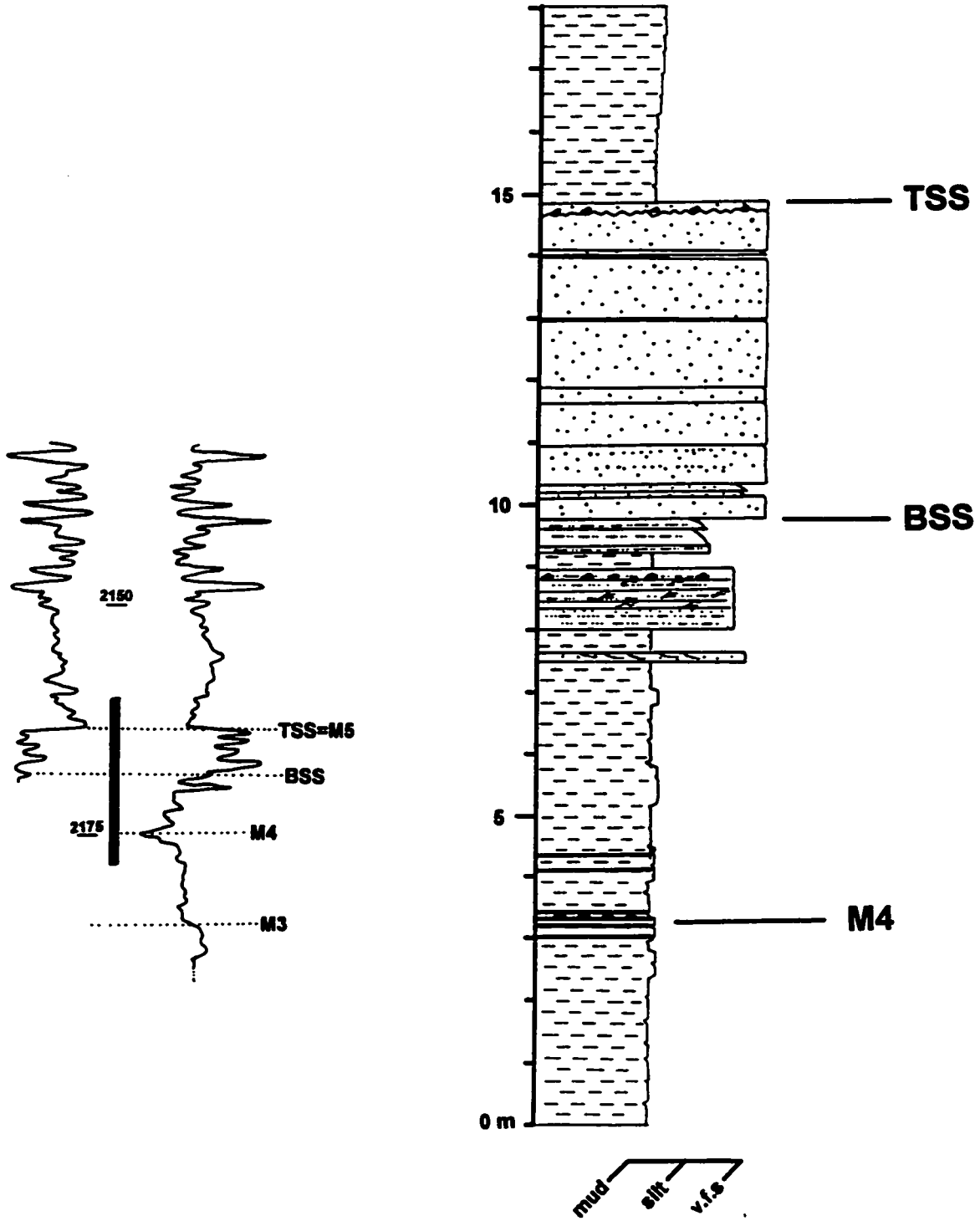
# Appendix A-21
## 8-19-75-8W6 (2217.0-2232.25 m)
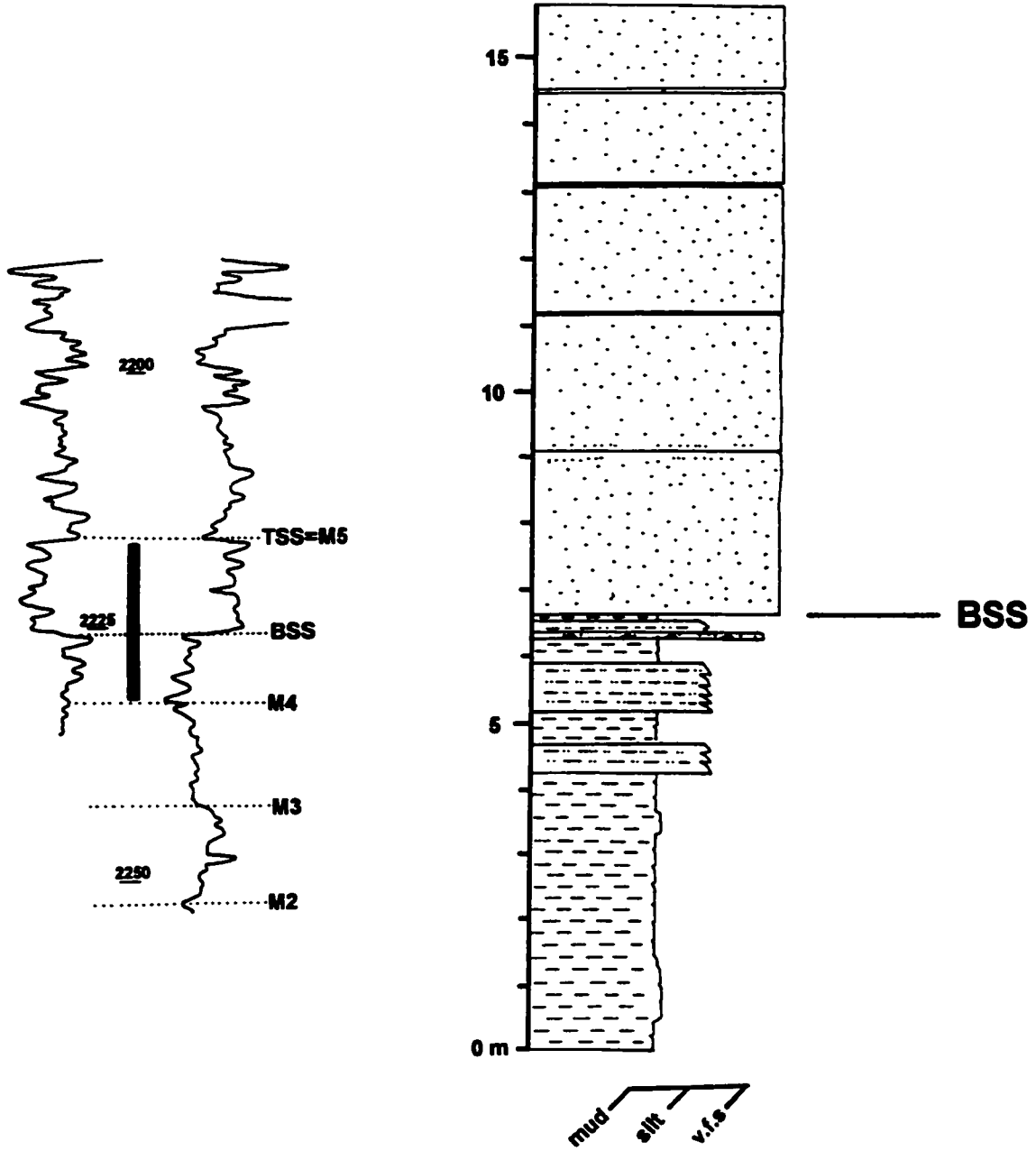
# Appendix A-22
## 12-22-75-8W6 (2172.0-2190.0 m)



M5

TSS

ES2

M5

TSS

ES2

M4

M3

2175

2200

15

10

5

0 m

mud    silt    v.f.s
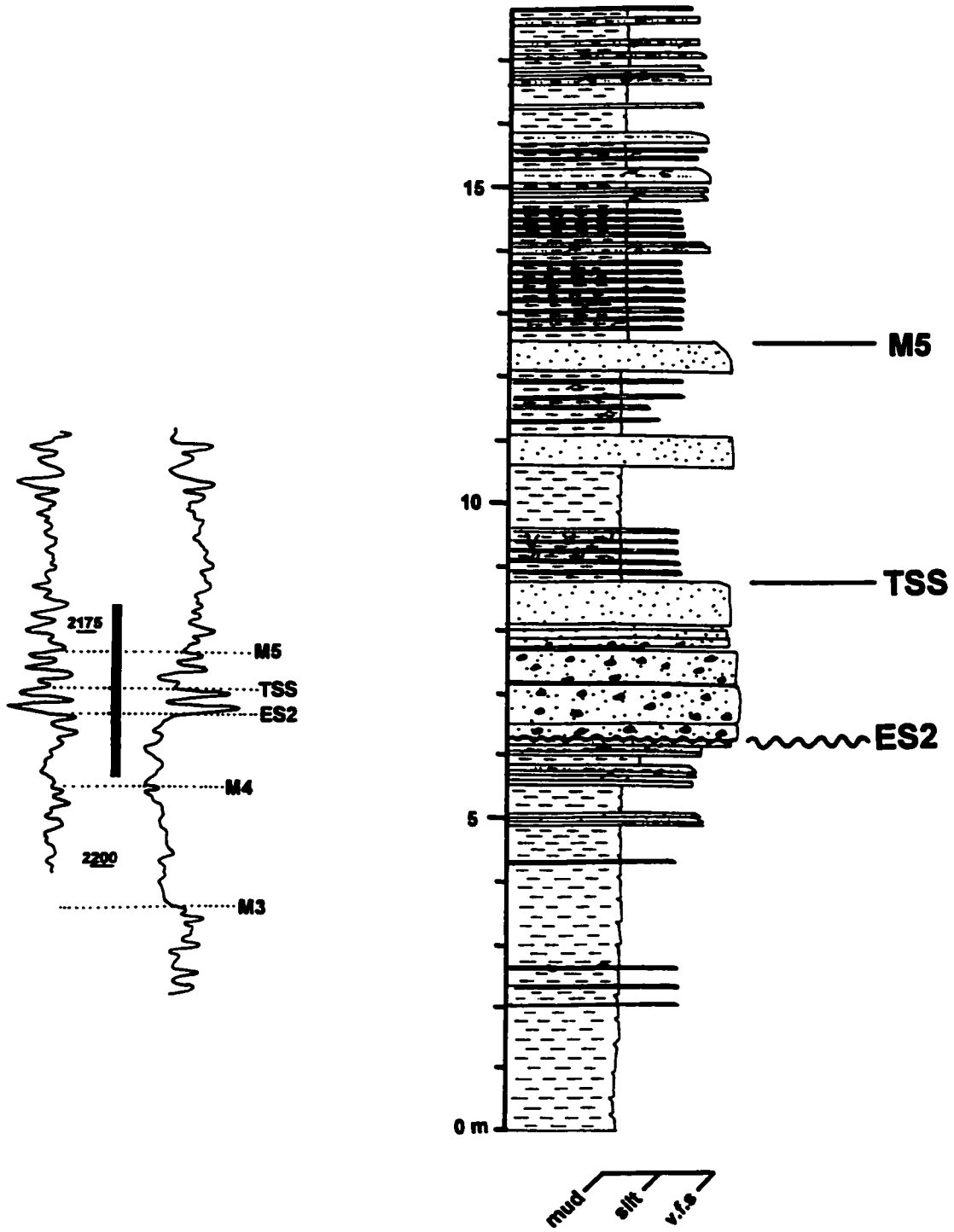
# Appendix A-23
## 6-25-75-8W6 (2161.0-2179.0 m)
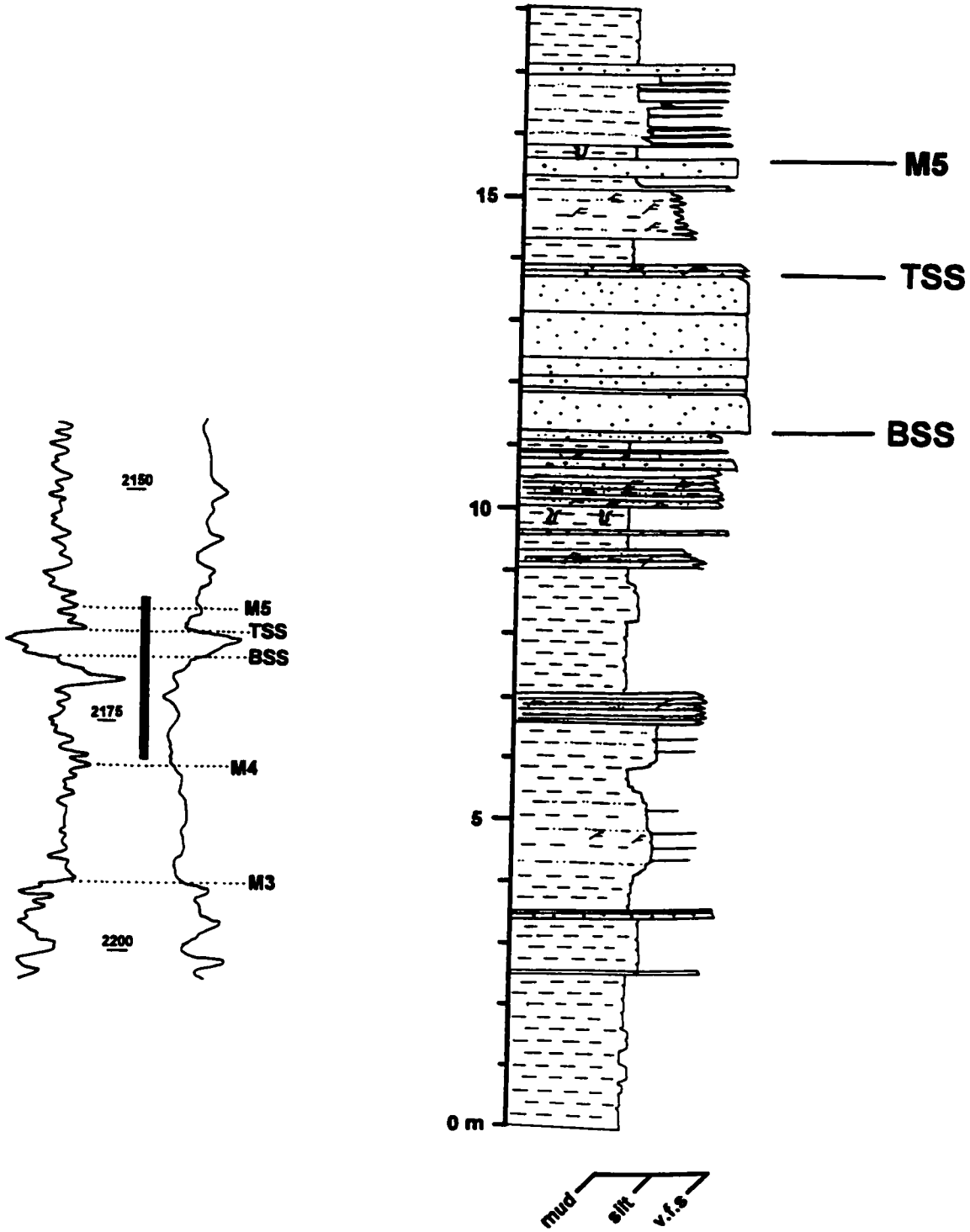
# Appendix A-24
## 6-11-75-9W6 (2274.4-2292.6 m)
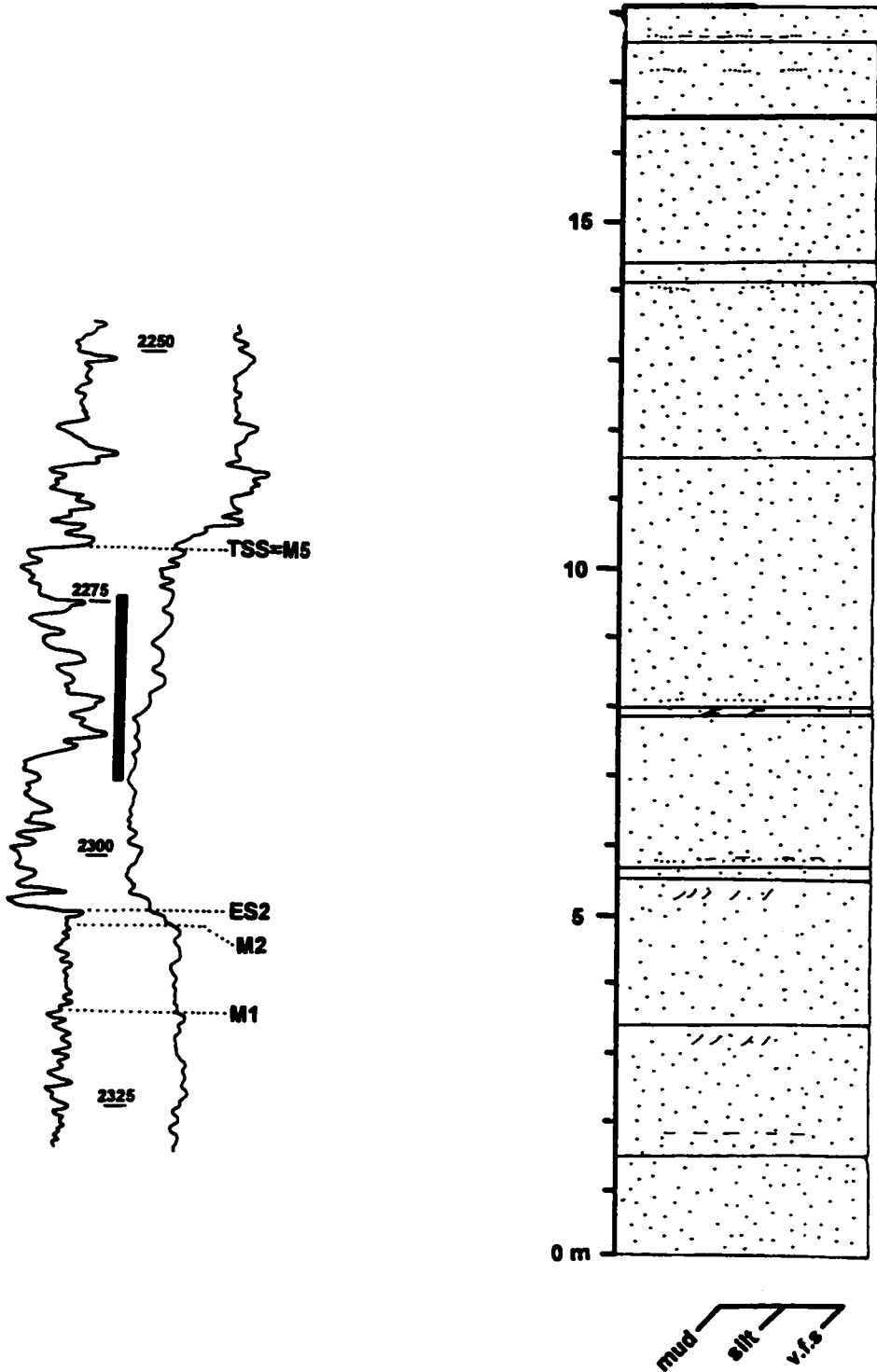
# Appendix A-25
## 12-17-75-9W6 (2255.5-2273.5 m)



2250

2275

2230

M5

M4

M3

M2

M1

M5

M4

15

10

5

0 m

mud  silt  v.f.s
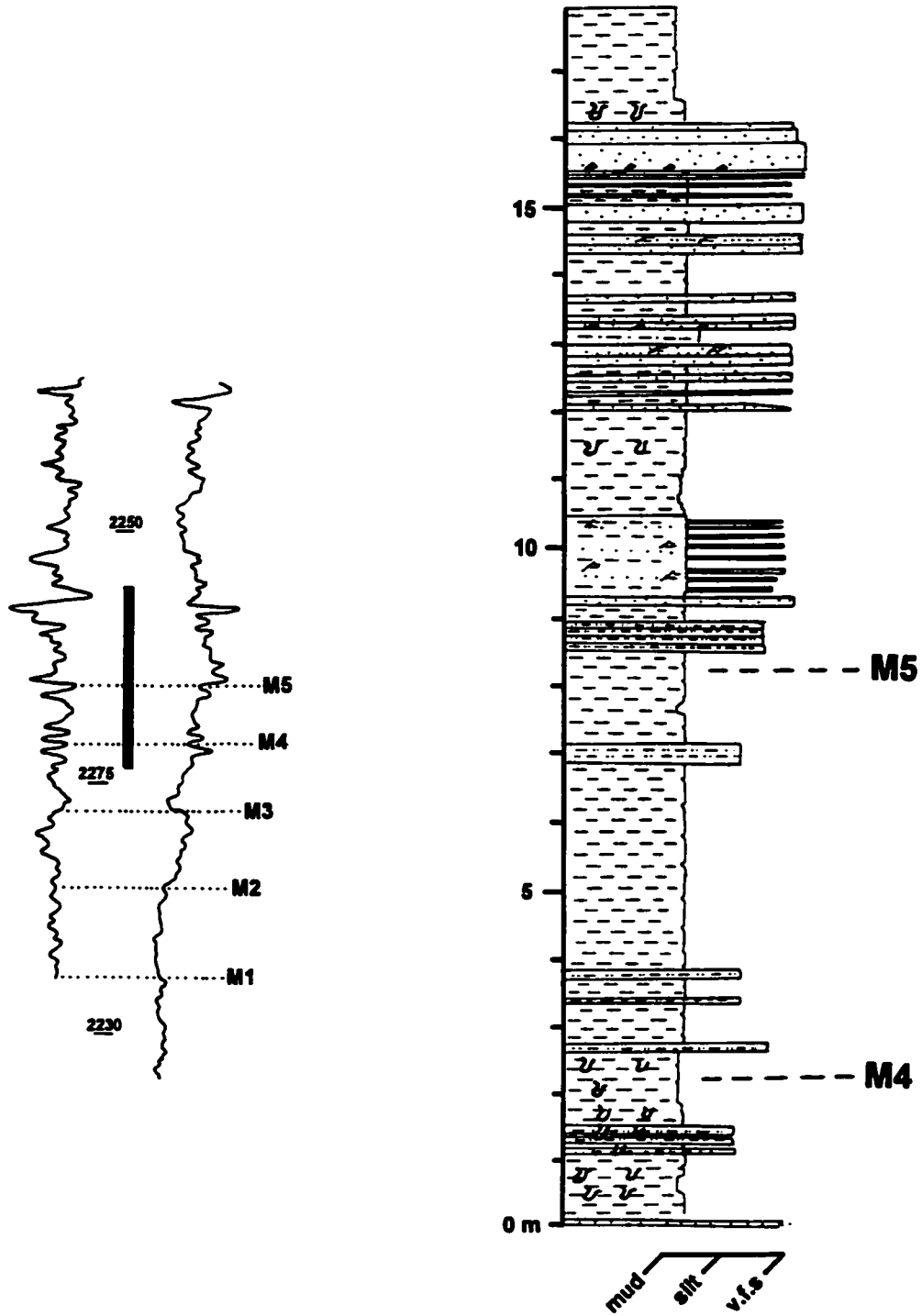
# Appendix A-26
## 8-24-75-9W6 (2212.0-2229.8 m)



15

2200

M5
TSS
ES2
M4

10

M3

M2

2250

M1

M5

TSS

5

ES2

M4

0 m

mud    silt    v.f.s
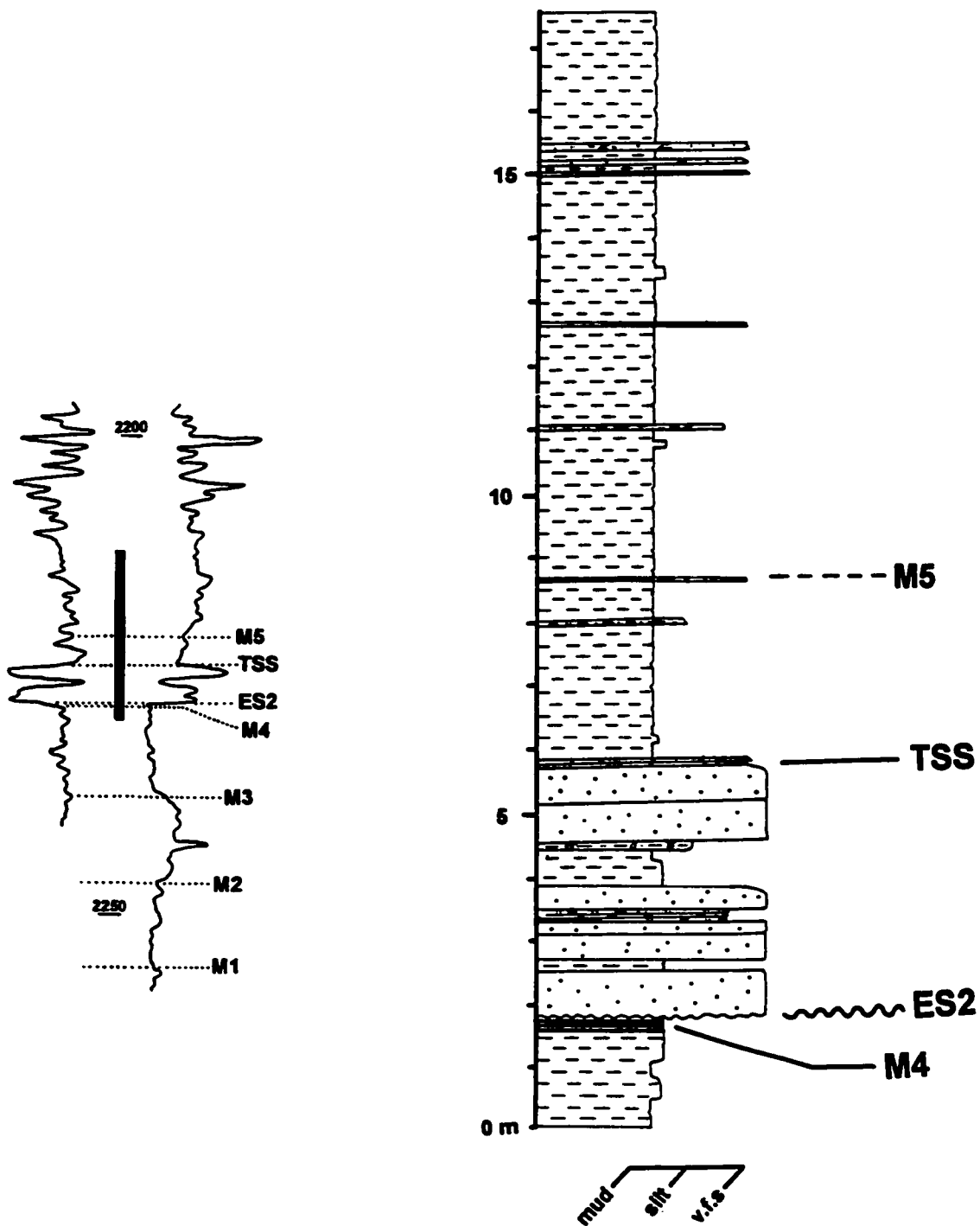
# Appendix A-27
## 6-26-75-9W6 (2182.5-2201.0 m)



BSS

TSS=M5

BSS

M4

M3

M2

M1

2175

2200

2225

M4

0 m

5

10

15

mud    silt    v.f.s
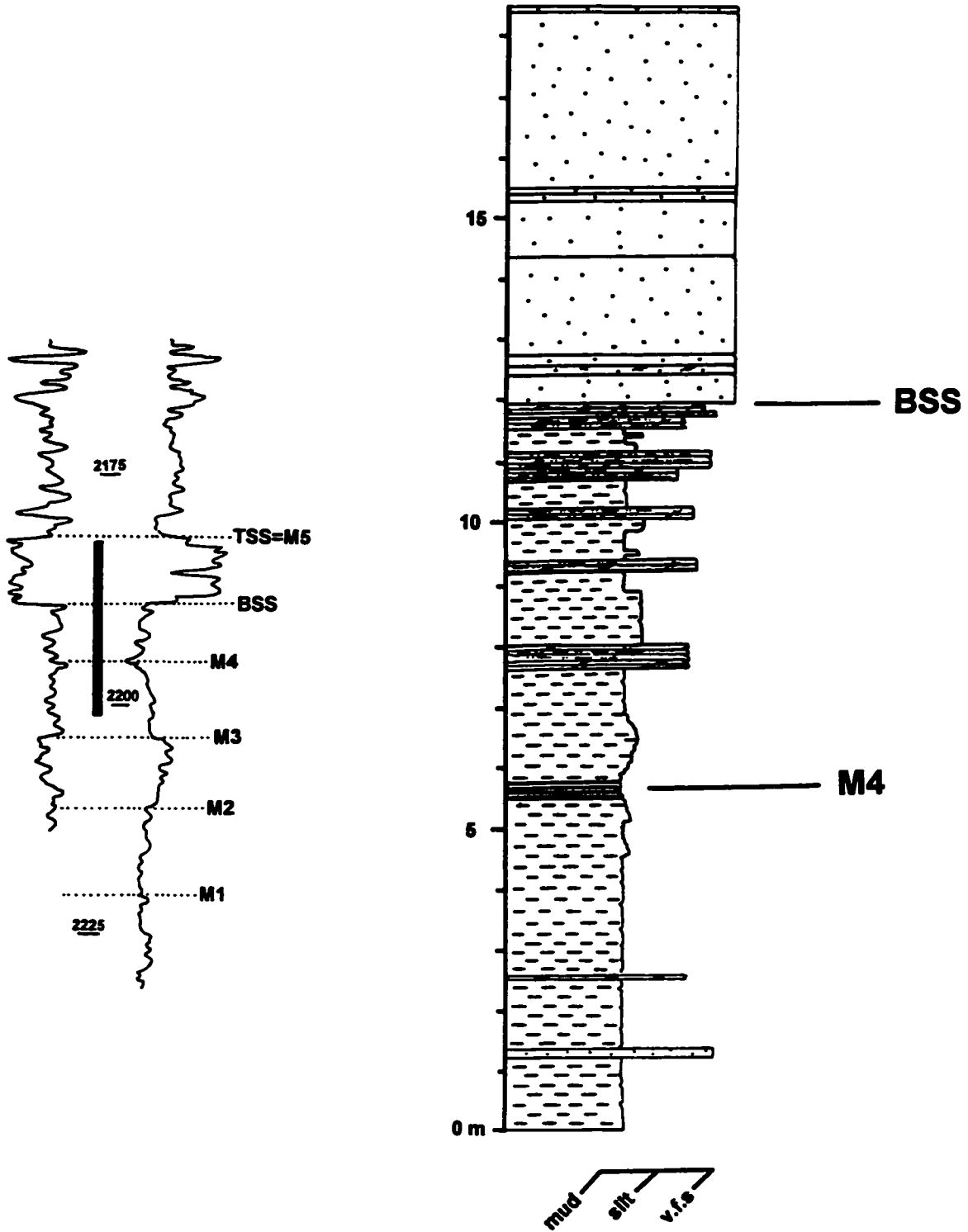
# Appendix A-28
## 6-27-75-9W6 (2221.0-2239.0 m)
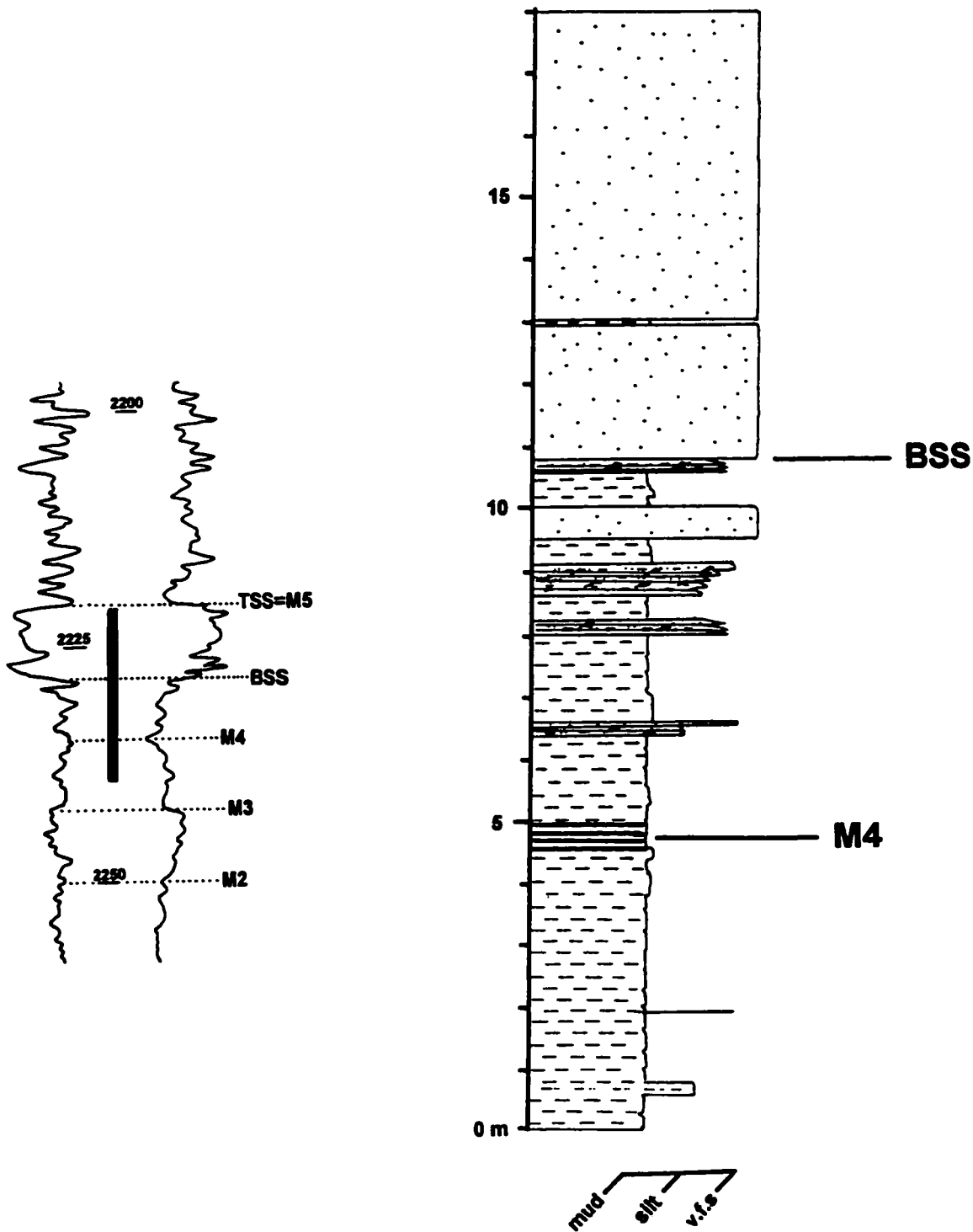
# Appendix A-29
## 15-28-75-9W6 (2221.2-2237.4 m)
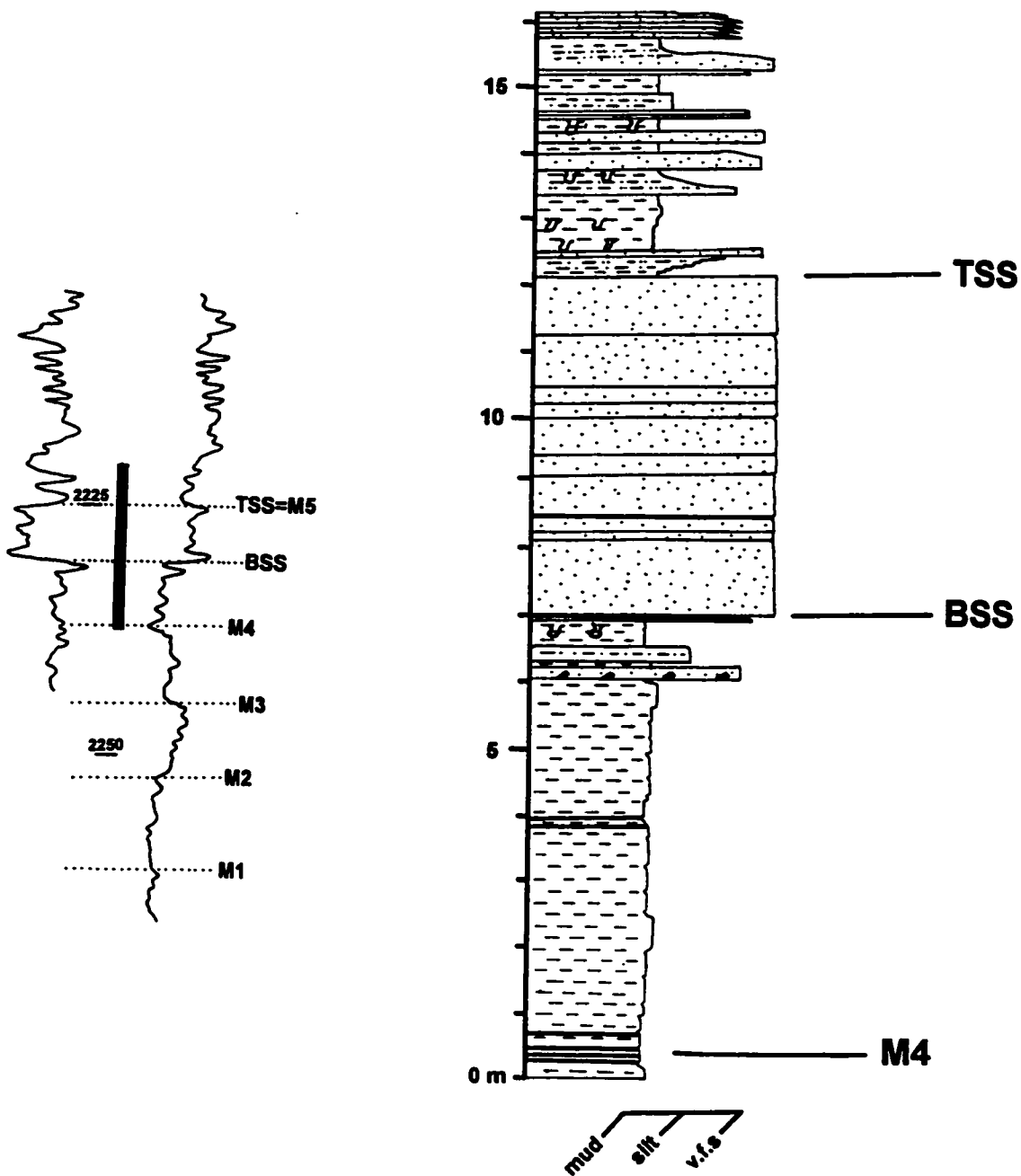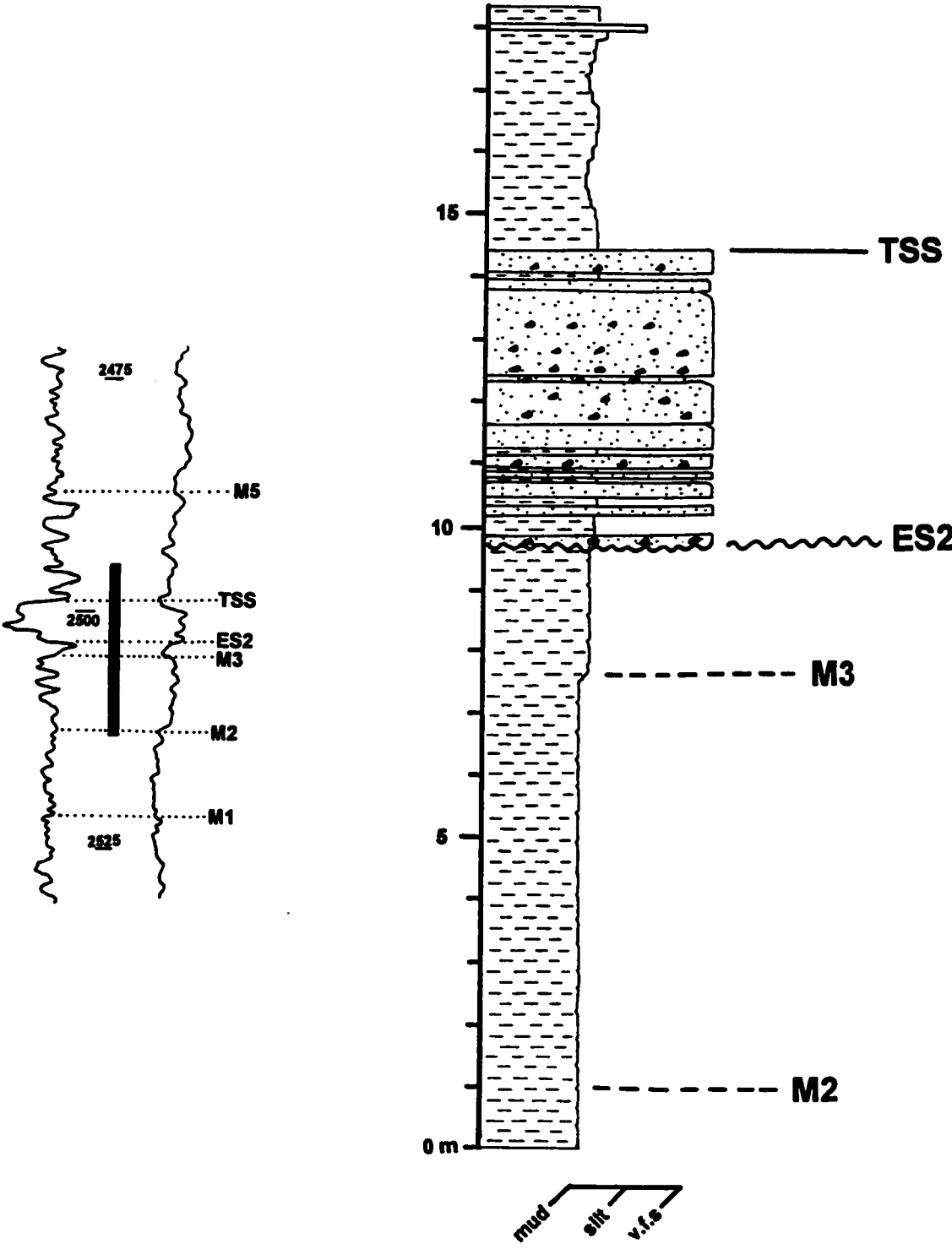
# Appendix A-30
## 6-1-76-9W6 (2136.3-2154.7 m)
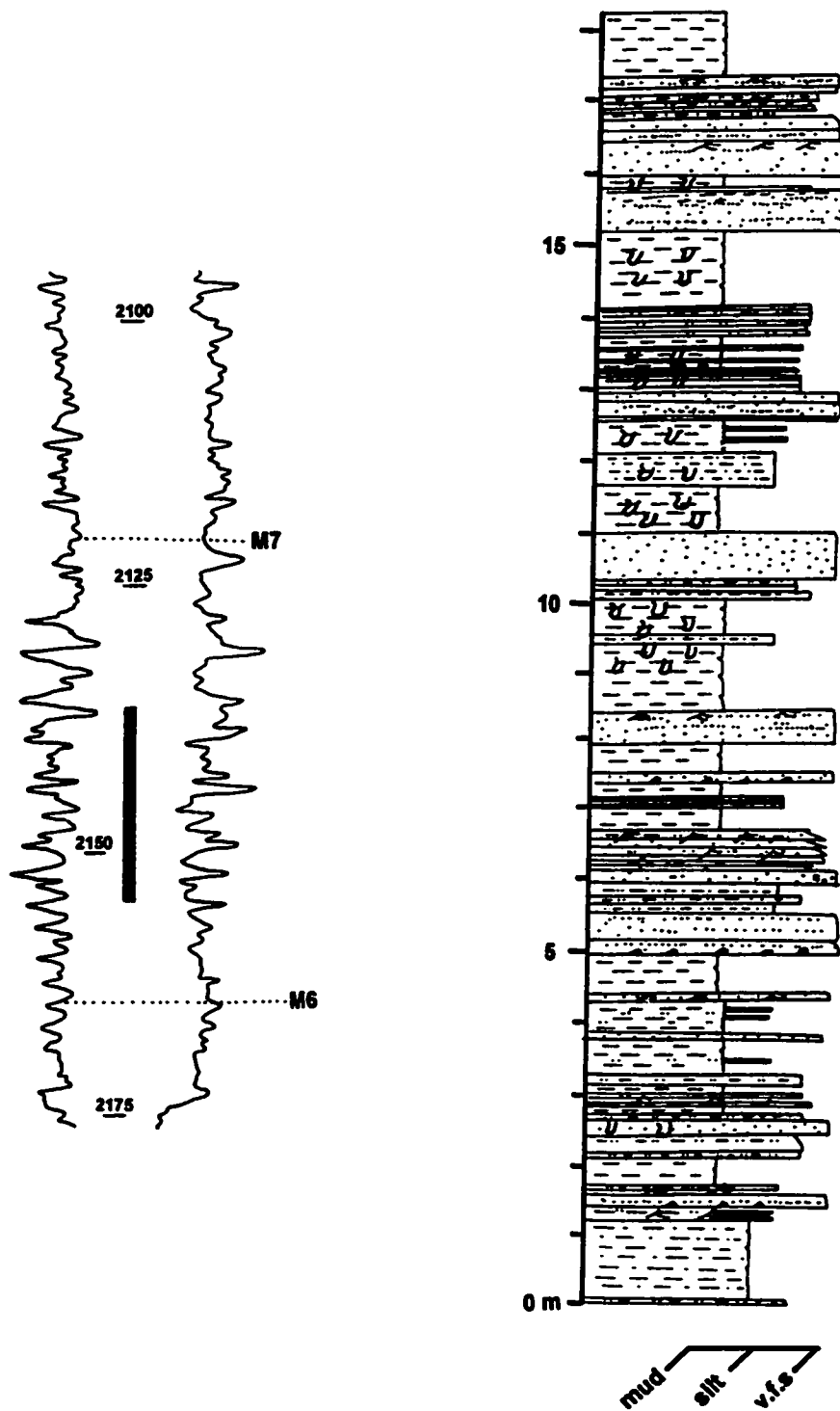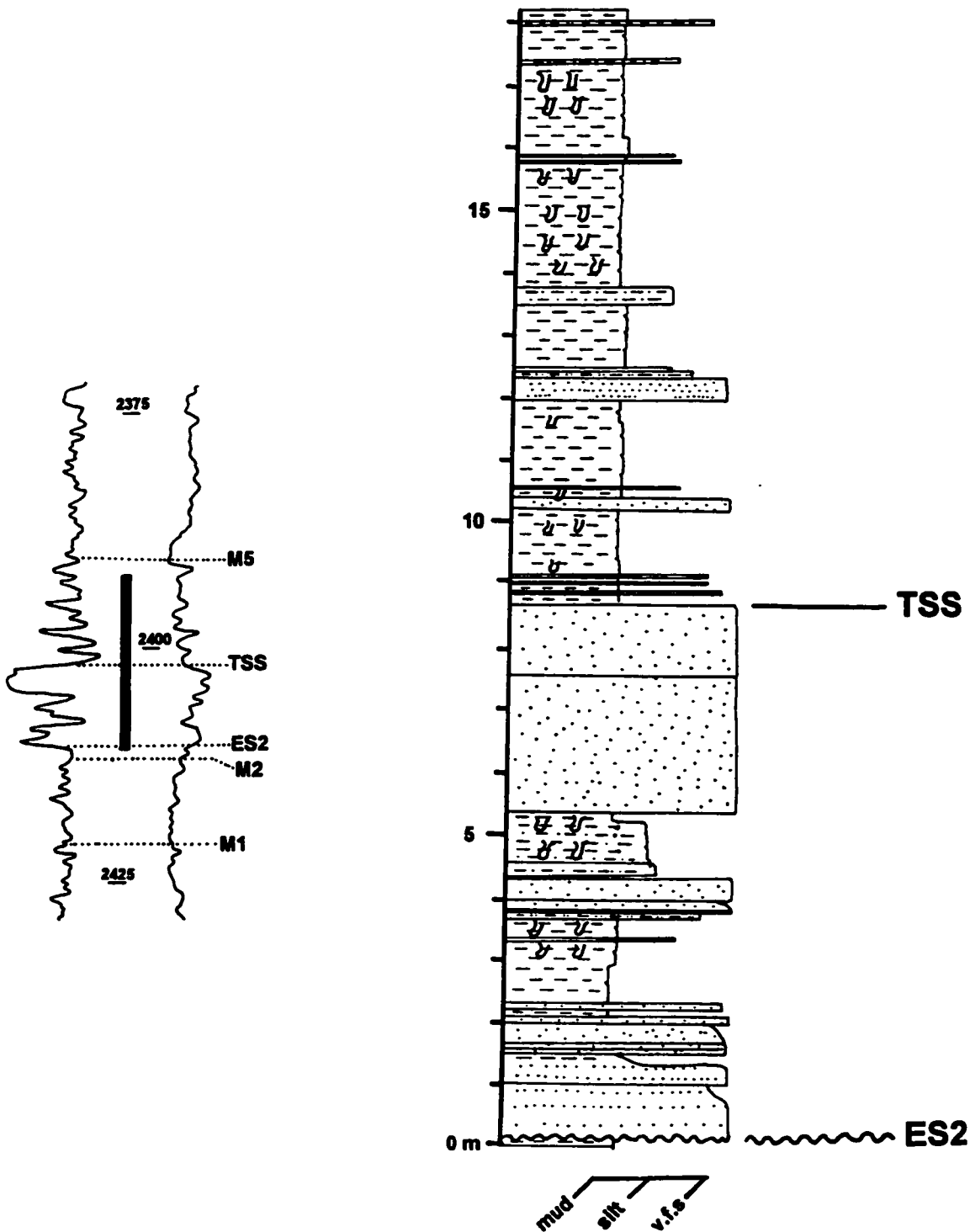
# Appendix A-31
## 14-13-74-10W6 (2341.5-2359.5 m)
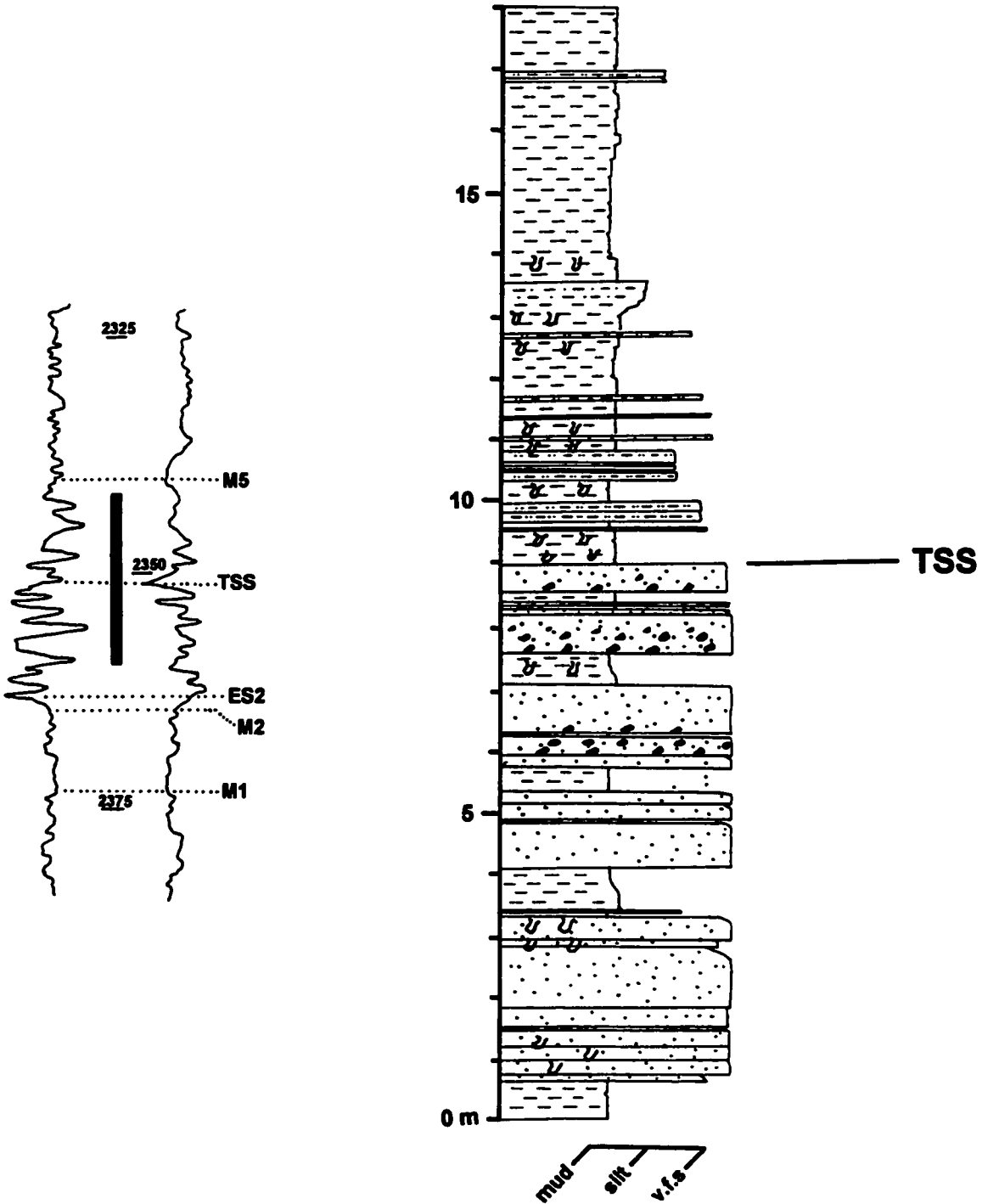
# Appendix A-32
## 14-19-74-10W6 (2495.0-2513.4 m)
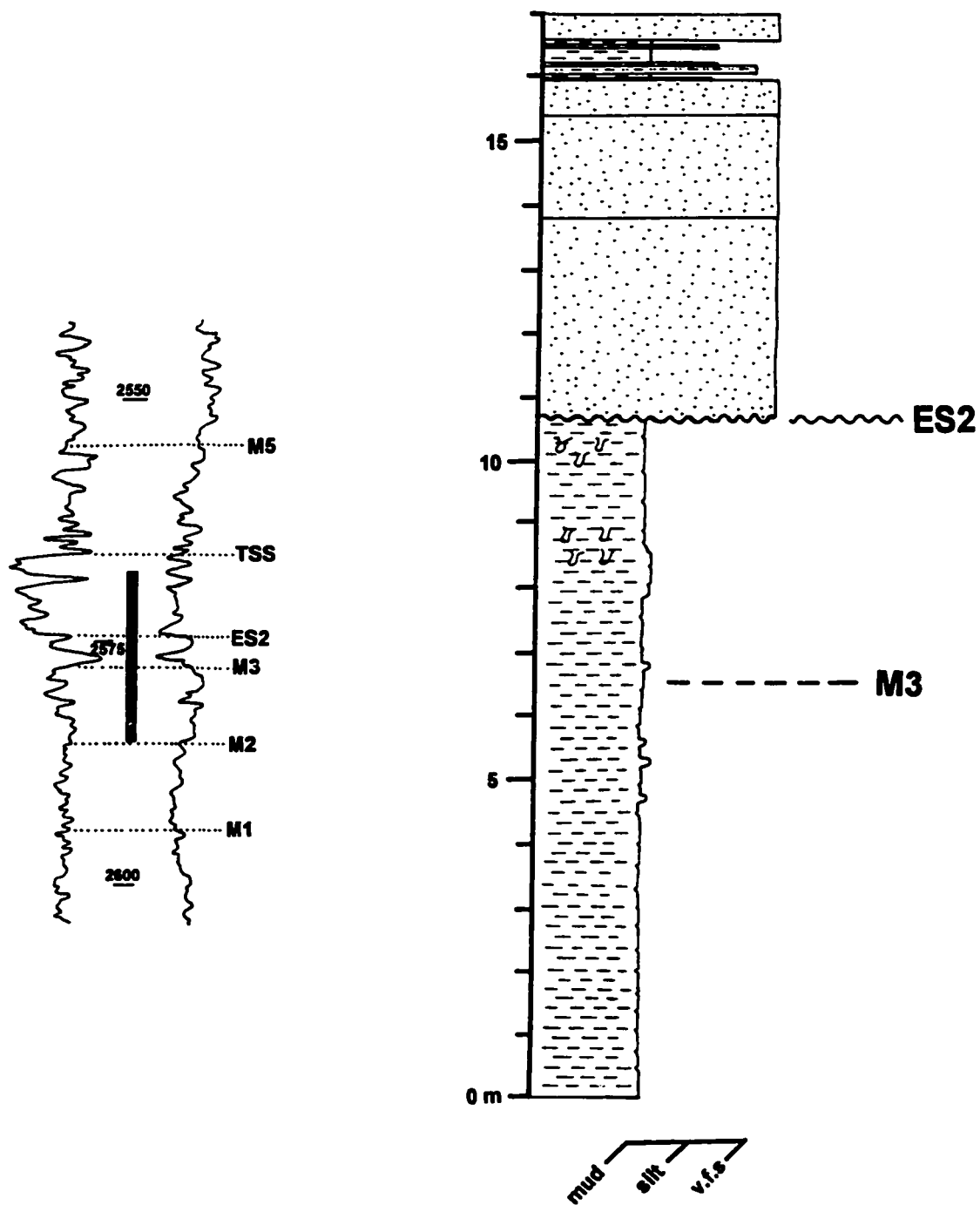


TSS

ES2

M3

M2

2475

M5

TSS
2500
ES2
M3

M2

M1
2525

15

10

5

0 m

mud   silt   v.f.s

# Appendix A-33
## 4-27-74-10W6 (2392.3-2410.5 m)



2375

M5

2400

TSS

ES2

M2

M1

2425

15

10

TSS

5

0 m
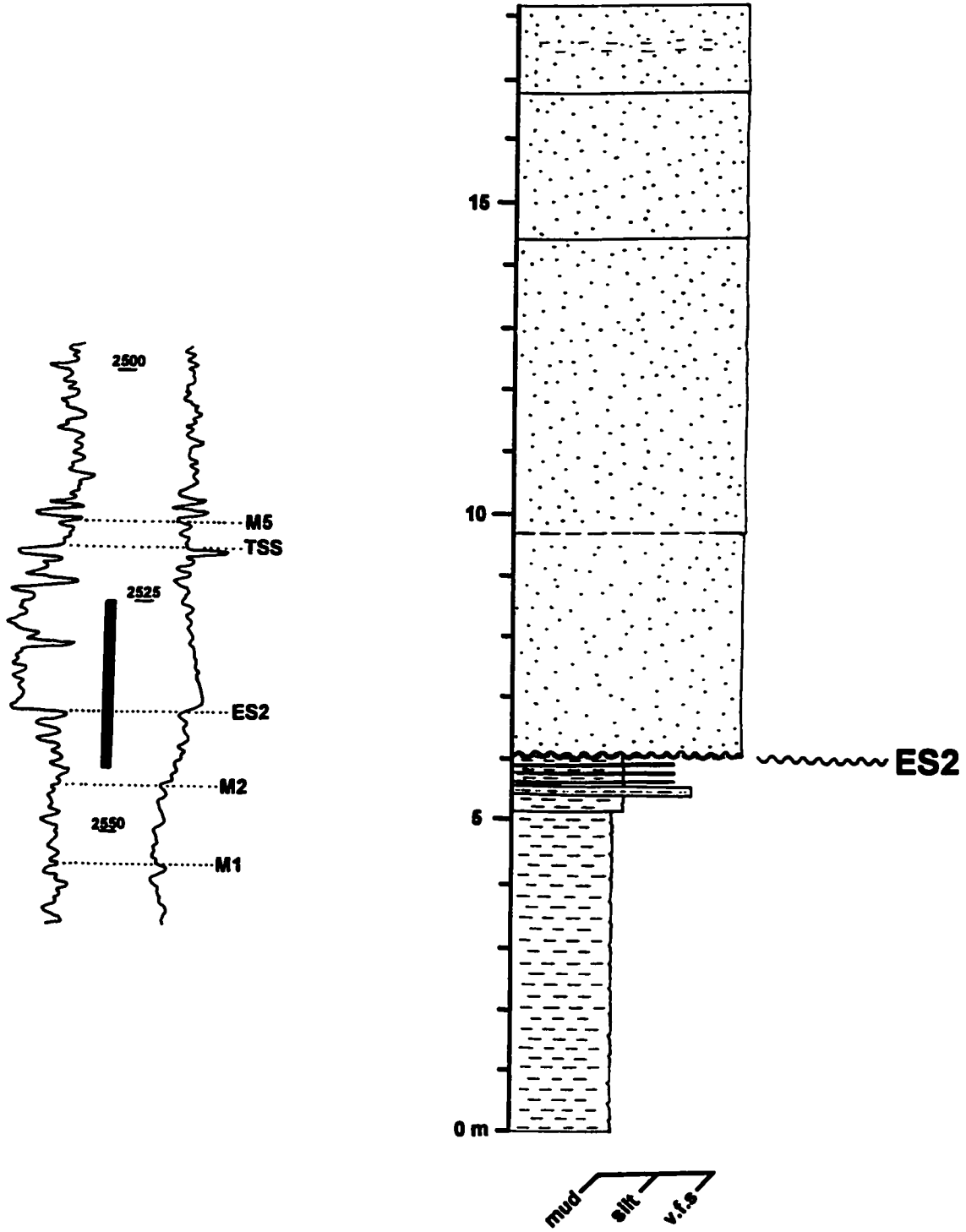
ES2

mud  silt  v.f.s

# Appendix A-34
## 2-27-74-11W6 (2568.0-2585.0 m)

# Appendix A-35
## 16-34-74-11W6 (2525.0-2543.2 m)

# Appendix A-36
## 14-33-76-11W6 (2412.0-2430.8 m)



M4

2400

M3

2425

M2

M1

2450

M2

15

10

5

0 m

mud    silt    v.f.s
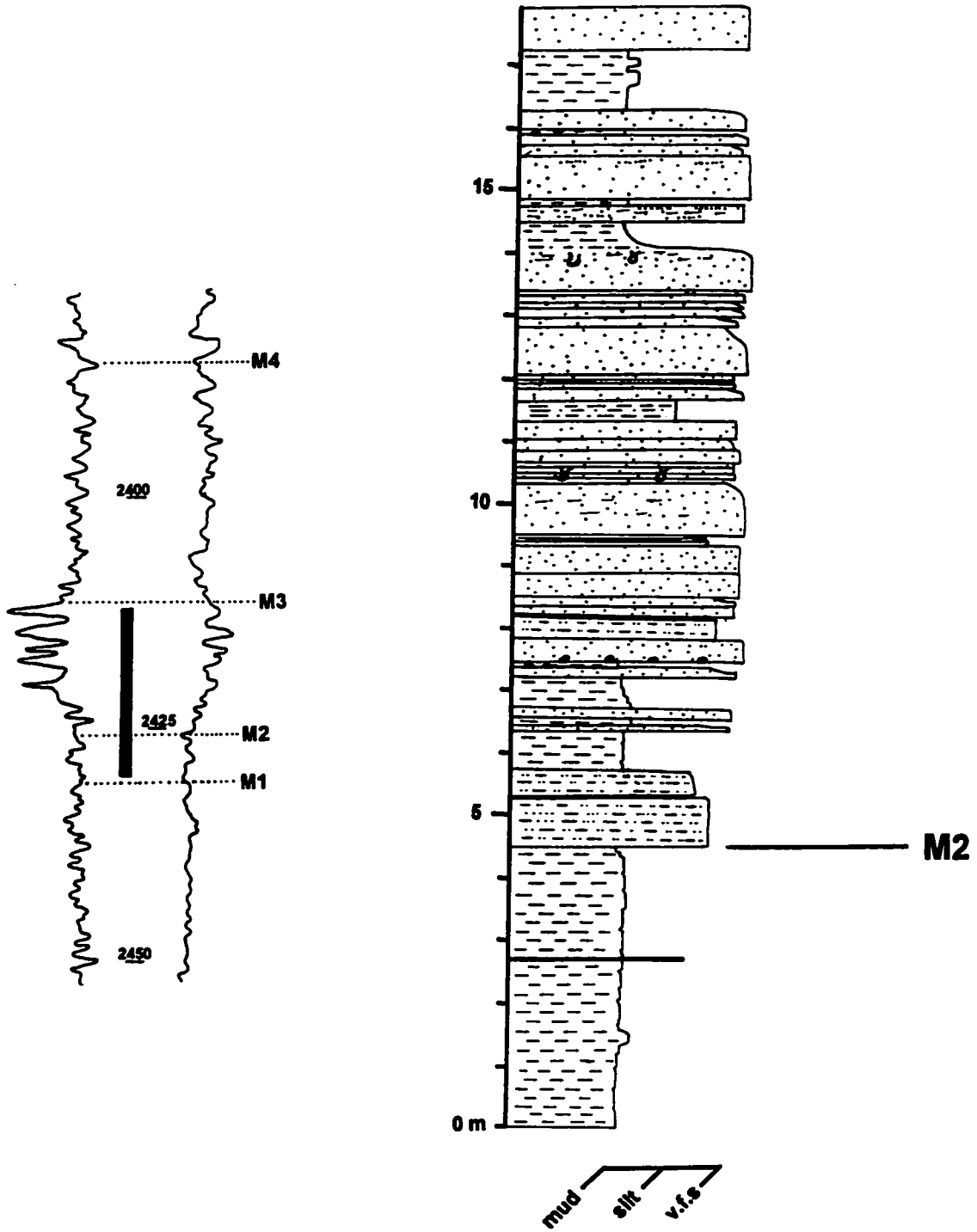
# Appendix A-37
## 6-14-77-11W6 (2188.4-2206.4 m)



M3

M4

2150

2175

M3

2200

M2

M1

M2

15

10

5

0 m

mud    silt    v.f.s
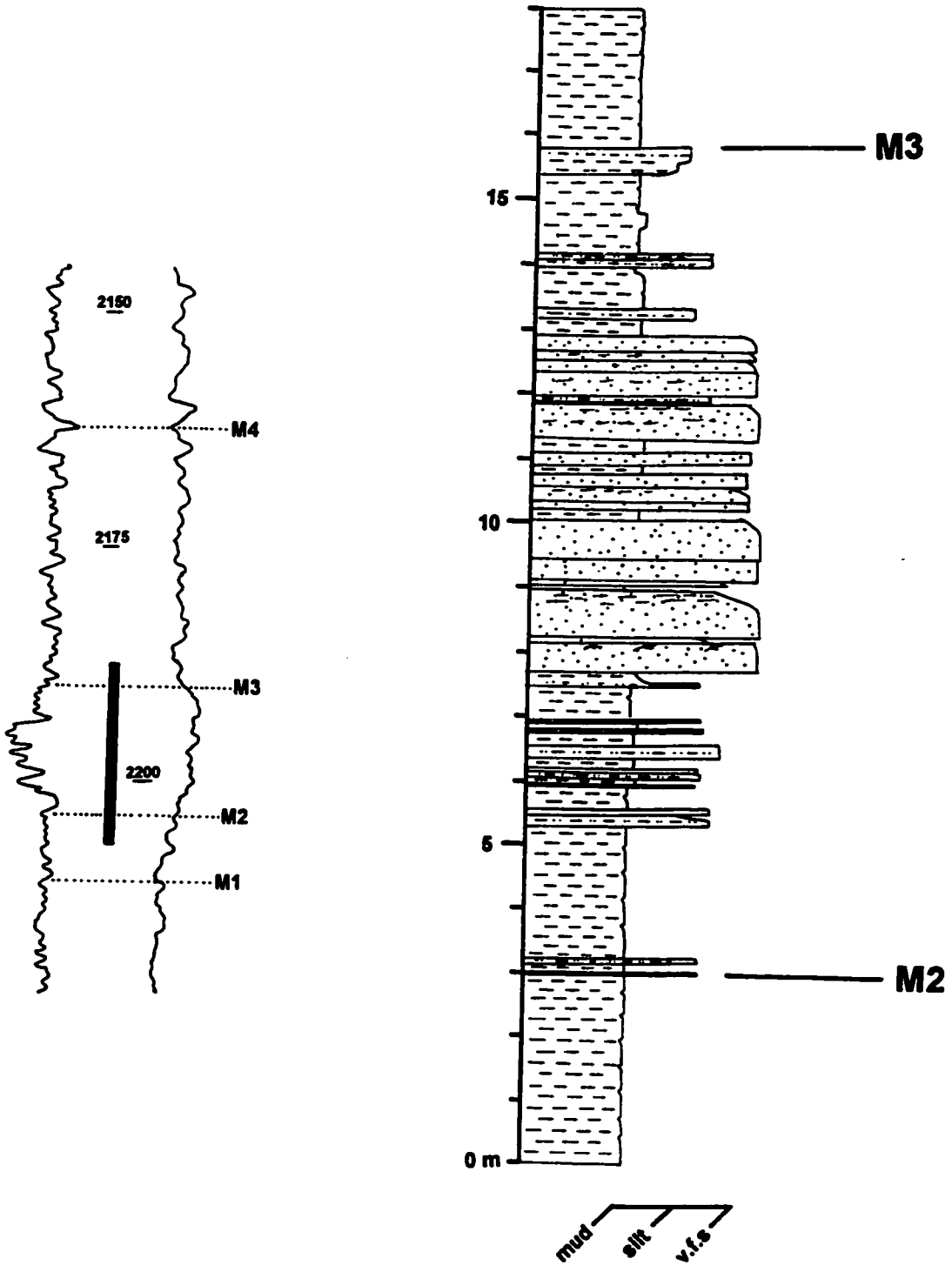
# Appendix A-38
## 6-15-77-11W6 (2214.2-2232.2 m)



M4

2200

M3

M2

M1

2225

15

M3

10

5

M2

0 m

mud  silt  v.f.s